Inaugural dissertation

for

obtaining the doctoral degree

of the

Combined Faculty of Mathematics, Engineering and Natural Sciences

of the

Ruprecht - Karls - University

Heidelberg

Presented by

M.Sc. Alessandra Boiti

born in: Tolmezzo (UD), Italy

Oral examination: 11-07-2024

Decoding Transcriptional Regulation in Response to Sunlight in Vertebrates

Referees: Prof. Dr. Nicholas S. Foulkes

Dr. Thomas Dickmeis

Acknowledgements

First and foremost, I would like to express my gratitude to my supervisor, Prof. Dr. Nicholas S. Foulkes. Thank you for giving me the opportunity to do my PhD in your lab. I started off during a pandemic with very limited lab and research experience, and your guidance, supervision, continued support, and trust through these four years have not only been crucial for the successful completion of my PhD but have also shaped me as a researcher. I am thankful for all the advice and insightful discussions for my projects, presentations, posters, and thesis, and especially for the continuous enthusiasm for our work.

I would like to thank Dr. Daniela Vallone for all the useful advice and help in troubleshooting, her strong technical knowledge and insightful comments, and for allowing me to teach and supervise Bachelor and Master students. I would also like to thank my TAC members, Dr. Thomas Dickmeis and Dr. Neil McKinnon, for the insightful discussions of my project and Dr. Sebastian Gornik (COS Heidelberg) for the precious help with the RNA-sequencing analyses.

I extend my gratitude to all my present and past lab members, Rima Siauciunaite, Yuhang Hong, Hongxiang Li, Yi Bi, Nathalie Geyer, Patrizia Birner, Leni Wagner, Carina Scheitle, and Lea Harrer, for welcoming me, teaching me techniques, sharing problems and solutions, and contributing to a relaxed and fun atmosphere in the lab. I especially would like to thank Hanna Weber and her work; I really enjoyed supervising you during your Master's thesis and becoming friends, sharing discussions, successes, and failures through our projects. I would also like to thank all the other friends and colleagues in IBCS-BIP for the fun lunches, Christmas parties,

and BBQs. Special thanks to Amer, for making this past stressful year much more fun, for supporting me, and for putting up with my endless complaining.

I would like to thank my family and all my friends: most of you have no idea of what exactly I have been doing for the past four years (nor will ever read this), but it does not stop you from supporting me. We often found even in the most different lives the problems we go through are very similar. To the ones who have started this journey with me, Chiara and Isa, I am so glad I shared this path with you, although I am the friend living 868km away. Sarah: thank you for always being my long-distance lab mate and closest friend in Germany, for your endless support and the adventures we shared.

Lastly, but most importantly, I would like to thank Marco: we barely knew each other when this journey started; in four years we went through two PhDs, got 517km closer, and are about to move to the other side of the world together. I could not have asked for a better companion through it all.

Contents

List of Figures **11**

List of Tables **15**

Abstract **17**

Zusammenfassung **19**

Abbreviations **21**

Publication **23**

1 Introduction **25**
1.1 Sunlight as a powerful environmental stimulus . . . 25
1.1.1 Light entrains the circadian clock . . . 26
1.1.2 The duality of light: damage and repair . . . 28
1.1.3 Mitochondria and heme . . . 30
1.2 Early pathways of light-mediated gene expression . . . 36
1.2.1 Extravisual photoreception . . . 36
1.2.2 Reactive Oxygen Species . . . 38
1.3 Fish models . . . 40
1.3.1 Zebrafish . . . 41
1.4 D-box mechanism . . . 44
1.4.1 Enhancers contribution to light-mediated gene expression . . . 47
1.5 Experimental Aims . . . 49

2 Methods **51**
2.1 Cell culture . . . 51
2.1.1 Light exposure experiments . . . 51
2.2 Zebrafish larvae experiments . . . 52
2.3 Gene expression analyses . . . 52
2.3.1 Total RNA extraction . . . 52
2.3.2 mRNA sequencing and analysis . . . 53
2.3.3 Reverse transcription . . . 54
2.3.4 Quantitative PCR . . . 55
2.3.5 mRNA stability assay . . . 55
2.4 Cavefish PAR-bZip and Nfil3 factors characterization and cloning . . . 56
2.4.1 Cavefish PAR factors 5' and 3' RACE PCR . . . 56
2.4.2 PAR-bZip factors cloning and mutations . . . 57
2.4.3 Plasmid DNA extraction . . . 59
2.4.4 Western Blot analysis . . . 59
2.5 Promoter bioinformatic analysis and cloning . . . 60
2.6 Cell transfection and bioluminescence assays . . . 61
2.7 Heme assays . . . 62
2.7.1 Oxalic acid assay for total heme quantification . . . 63

2.7.2 Regulatory heme HRP assay for free heme quantification 63
2.8 MTT assay 64
2.9 Statistical analysis 64

3 Results **65**
3.1 mRNA-sequencing experiments 65
3.1.1 Transcriptomic response to blue light in zebrafish cells 66
3.1.2 Zebrafish and cavefish cells - transcriptomic response to Blue light *de novo* analysis 73
3.1.3 Transcriptomic response to UV-C exposure 86
3.2 Confirmation of RNA-seq results 95
3.2.1 Blue light exposure upregulates the expression of mitochondria-related genes in zebrafish but not cavefish cells 96
3.2.2 UV-C irradiation upregulates the expression of mitochondria-related genes in zebrafish PAC2 cells 98
3.3 Blue light but not UV-C upregulates the expression of mitochondria-related genes in zebrafish larvae 100
3.4 Induction of mitochondria and heme-related genes by ROS treatment 104
3.5 Are mitochondria-related genes regulated via the D-box enhancer element? . . 105
3.5.1 Blue light-mediated expression of mitochondria and heme-related genes in zebrafish cells is dependent on *de novo* transcription 106
3.5.2 UV-C-mediated expression of mitochondria and heme-related genes in zebrafish cells is dependent on *de novo* transcription 107
3.5.3 No effect of clock entrainment on the expression of mitochondria and heme-related genes 108
3.6 Regulation of the mitochondria and heme-related genes via D-box enhancer elements 110
3.6.1 Transcription of *hebp2*, *abcb6a*, and *soul5* is light-regulated 113
3.6.2 Transcription of *hebp2* and *soul5* but not *abcb6a* is regulated by ROS . 116
3.7 Cloning the cavefish PAR bZip and Nfil3 transcription factors and alignment with the zebrafish orthologs 120
3.7.1 Western blots to check for expression of the factors in pCS2-MTK . . . 130
3.7.2 Functional assays: Testing the ability of the PAR factors and Nfil3 factors to activate the D-box 131
3.7.3 The N-terminal part of HLF-2 is important for the transactivation of hebp2-Luc 134
3.8 Changes to regulatory and total heme levels in zebrafish and cavefish cells . . . 136
3.8.1 Total heme levels in zebrafish cells and larvae, and cavefish cells are not affected by blue light 136
3.8.2 Total heme levels in zebrafish and cavefish cells are not affected by exposure to light and dark cycles 137
3.8.3 Regulatory heme levels in zebrafish and cavefish cells are not affected by exposure to light and dark cycles 138
3.9 Mitochondrial function in cells exposed to blue light 140

4 Discussion **141**
4.1 Blue light and UV-induced transcriptomes in zebrafish cells 142

4.2 The D-box: a wider mechanism of regulation in response to visible light, UV, and ROS . . . 144
4.2.1 Cavefish cells . . . 145
4.2.2 The role of ROS in light-induced gene expression . . . 146
4.2.3 PAR-bZip transcription factors involvement in D-box mediated gene expression . . . 147
4.3 Biological meaning of transcriptomic changes induced by sunlight in zebrafish 150
4.3.1 Adaptive mitochondrial responses to sunlight . . . 150
4.3.2 Heme: a connection to xenobiotic metabolism and oxidative stress regulation . . . 152
4.4 Conclusion . . . 155

5 References **157**

6 Supplementary tables **175**

List of Figures

1.1 The core circadian clock mechanism and its inputs and outputs 27
1.2 Visible and invisible light spectrum. 28
1.3 Mitochondrion (a) and Electron Transport Chain (b) structures. 31
1.4 Chemical structure of heme (left) and a scheme of its metabolism and transport within cells (right). 34
1.5 My two model species: zebrafish (*D. rerio* (left) and Somalian cavefish (*P. andruzzii* (right). 41
1.6 Mechanism of circadian clock entrainment and gene expression regulation via the D-box enhancer. 45
1.7 PAR-bZip and Nfil3 zebrafish protein structures. 46
1.8 Differences between the PAR-bZip and Nfil3 families of transcription factors in mammals and zebrafish. 47

2.1 mRNA-sequencing analysis pipeline. 54

3.1 Overview of the two mRNA-sequencing experiments. 66
3.2 Comparative analysis of samples of zebrafish cells exposed to 0-6 hours of blue light. 68
3.3 Differential expression analysis over time of blue light exposure compared to control in zebrafish cells. 69
3.4 Volcano plots highlighting DEGs over time of blue light exposure compared to control, in zebrafish cells. 69
3.5 Gene Ontology (GO) analysis of DEGs at 6 hours of blue light compared to DD control, in zebrafish cells. 71
3.6 Temporal expression patterns of DEGs during blue light exposure in zebrafish cells. 72
3.7 Heatmaps displaying temporal patterns of significantly upregulated genes in response to blue light, belonging to the category of clock and DNA damage repair (left) and the identified class of mitochondrial and heme-related genes (right). 73
3.8 Comparative analysis of samples of zebrafish cells (top) and cavefish cells (bottom) exposed to 0-6 hours of blue light. 75
3.9 Differential expression analysis over time of blue light exposure compared to control, in zebrafish (left) and cavefish (right) cells. 76
3.10 Volcano plots highlighting DEGs over time of blue light exposure compared to controls, in zebrafish cells. 77
3.11 Volcano plots highlighting DEGs over time of blue light exposure compared to control, in cavefish cells. 78
3.12 Gene Ontology (GO) analysis of DEGs at 6 hours of blue light compared to DD control, in zebrafish cells. 79
3.13 Gene Ontology (GO) analysis of DEGs at 6 hours of blue light compared to DD control, in cavefish cells. 80
3.14 Temporal expression patterns of DEGs during blue light exposure in zebrafish cells. 82

3.15 Temporal expression patterns of DEGs during blue light exposure in cavefish cells. . . . 83
3.16 Heatmaps displaying temporal patterns of significantly upregulated genes in response to blue light, belonging to the category of clock and DNA damage repair (left) and the identified class of mitochondrial and heme-related genes (right), in zebrafish cells. . . . 85
3.17 Heatmaps displaying temporal patterns in response to blue light of genes belonging to the category of clock and DNA damage repair (left) and the identified class of mitochondrial and heme-related genes (right) in cavefish cells. 86
3.18 Comparative analysis of samples of zebrafish cells (top) and cavefish cells (bottom) exposed to 20J/m^2 UV-C. . . . 88
3.19 Differential expression analysis following exposure to 20J/m^2 UV-C compared to control, in zebrafish (left) and cavefish (right) cells. . . . 89
3.20 Volcano plots highlighting DEGs following exposure to 20J/m^2 UV-C compared to 0h DD control, in zebrafish cells. . . . 90
3.21 Volcano plots highlighting DEGs following exposure to 20J/m^2 UV-C compared to 0h DD control, in cavefish cells. . . . 90
3.22 Gene Ontology (GO) analysis of DEGs 18 hours after exposure to 20J/m^2 UV-C, compared to 0h DD control, in zebrafish cells. . . . 92
3.23 Heatmaps displaying temporal patterns of response to 20J/m^2 UV-C of genes belonging to the category of clock and DNA damage repair (left) and the identified class of mitochondrial and heme-related genes (right) in zebrafish cells. . . . 93
3.24 Gene Ontology (GO) analysis of DEGs 18 hours after exposure to 20J/m^2 UV-C, compared to 0h DD control, in cavefish cells. . . . 94
3.25 Heatmaps displaying temporal patterns of response to 20J/m^2 UV-C of genes belonging to the category of clock and DNA damage repair (left) and the identified class of mitochondrial and heme-related genes (right) in cavefish cells. 95
3.26 Blue light-induced induction of mRNA expression of mitochondria and heme-related genes and *per2* following exposure of cells to blue light (468nm). 97
3.27 UV-C light-induced induction of mRNA expression of mitochondria and heme-related genes and *6-4 phr* in zebrafish cells. . . . 99
3.28 Blue light-induced induction of mRNA expression of mitochondria and heme-related genes and *per2* following exposure of zebrafish larvae to blue light (468nm). . . . 101
3.29 Light-induced induction of mRNA expression of mitochondria and heme-related genes and *6-4 phr* following irradiation of zebrafish larvae to 450J/m^2 UV-C. . . . 103
3.30 ROS-dependent induction of mRNA expression of mitochondria and heme-related genes following treatment with 300μM H_2O_2. . . . 105
3.31 Percentage of remaining mRNA levels of mitochondria and heme-related genes and *per2* following treatment with 5μg/mL Actinomycin-D and subsequent exposure to blue light or darkness in zebrafish cells. . . . 107
3.32 Percentage of remaining mRNA levels of mitochondria and heme-related genes and *6-4 phr* following treatment with 5μg/mL Actinomycin-D and subsequent exposure to UV-C or darkness in zebrafish cells. . . . 108
3.33 Expression of mitochondria and heme-related genes and the clock gene *per2* in zebrafish cells following circadian entrainment, in LD and DD conditions. . . . 110

3.34 Putative D-box and E-box sequences predicted in the zebrafish *hebp2* (A), *abcb6a* (B), and *soul5* (C) promoters. . . . 112
3.35 Sequence of the 142 bp fragment of the *hebp2* promoter inserted in the luciferase report vector. . . . 112
3.36 Sequence of the 269 bp fragment of the *abcb6a* promoter inserted in the luciferase report vector. . . . 112
3.37 Sequence of the 189 bp fragment of the *soul5* promoter inserted in the luciferase report vector. . . . 113
3.38 *In vivo* bioluminescence assay in zebrafish and cavefish cells transfected with zebrafish hebp2-Luc, soul5-Luc, and abcb6a-Luc. . . . 113
3.39 *In vivo* bioluminescence assay in zebrafish cells transfected with hebp2-Luc and its mutant constructs. . . . 114
3.40 *In vivo* bioluminescence assay in zebrafish cells transfected with hebp2-Luc and its mutant constructs. . . . 115
3.41 *In vitro* bioluminescence assay in zebrafish cells transfected with hebp2-Luc and mutant constructs, after 8 hours of exposure to blue light. . . . 115
3.42 *In vivo* bioluminescence assay in zebrafish cells transfected with hebp2-Luc, soul5-Luc, and abcb6a-Luc and treated with 1mM H_2O_2. . . . 116
3.43 *In vivo* bioluminescence assay in zebrafish cells transfected with hebp2-Luc and its mutant constructs and treated with 1mM H_2O_2. . . . 117
3.44 *In vivo* bioluminescence assay in zebrafish cells transfected with hebp2-Luc and its mutant constructs and treated with 1mM H_2O_2. . . . 118
3.45 Cotransfection of catalase (top) and a dominant-negative form of ERK (bottom) with hebp2-Luc, soul5-Luc, and xpc-Luc in zebrafish cells exposed to LD cycles. 120
3.46 The zebrafish *Nfil3-2a* sequence (up) and its two orthologs in cavefish. . . . 121
3.47 Alignment of zebrafish and cavefish TEF-1. . . . 122
3.48 Alignment of zebrafish and cavefish TEF-2. . . . 123
3.49 Alignment of zebrafish and cavefish DBP-1. . . . 123
3.50 Alignment of zebrafish and cavefish DBP-2. . . . 124
3.51 Alignment of zebrafish and cavefish HLF-1. . . . 124
3.52 Alignment of zebrafish and cavefish HLF-2. . . . 125
3.53 Alignment of zebrafish and cavefish Nfil3-1a. . . . 126
3.54 Alignment of zebrafish and cavefish Nfil3-1b. . . . 126
3.55 Alignment of zebrafish and cavefish Nfil3-2a. . . . 127
3.56 Alignment of zebrafish Nfil3-2a and cavefish Nfil3-2aX. . . . 128
3.57 Alignment of zebrafish and cavefish Nfil3-2b. . . . 129
3.58 Alignment of zebrafish and cavefish Nfil3-3a. . . . 130
3.59 Alignment of zebrafish and cavefish Nfil3-3b. . . . 130
3.60 Western blot of overexpression of zebrafish and cavefish PAR-bZip factors. . . . 131
3.61 Western blot of overexpression of zebrafish and cavefish Nfil3 factors. . . . 131
3.62 *In vitro* bioluminescence assay in zebrafish cells cotransfected with the 15xD-box$_{cry1a}$-Luc and the PAR and Nfil3 factors. . . . 132
3.63 *In vitro* bioluminescence assay in zebrafish (B) and cavefish (C) cells cotransfected with 15xD-box$_{cry1a}$-Luc and the PAR factors. . . . 133
3.64 *In vitro* bioluminescence assay in zebrafish (B) and cavefish (C) cells cotransfected with hebp2-Luc and the PAR factors. . . . 134
3.65 *In vitro* bioluminescence assay in zebrafish cells cotransfected with hebp2-Luc and the HLF2 hybrid factors. . . . 135

3.66 Total heme levels in zebrafish cells after exposure to blue light for up to 24 hours or darkness. 136
3.67 Total heme levels in zebrafish larvae during exposure to blue light or darkness. 137
3.68 Total heme levels in zebrafish PAC2 and cavefish EPA cells after exposure to LD cycles or darkness (DD). 138
3.69 Regulatory heme levels in zebrafish cells after exposure to LD cycles or darkness (DD). 139
3.70 Regulatory heme levels in zebrafish PAC2 and cavefish EPA cells after exposure to LD cycles or darkness (DD). 139
3.71 Metabolic activity assay of cells exposed to blue light (468nm) for up to 24 hours. 140

4.1 Schematic summary of the types of mitochondrial and heme genes upregulated in response to blue light and UV in zebrafish cells. 150

List of Tables

2.1 Primers used for real-time qPCR. 55
2.2 Primers used for the amplification of 5' and 3' ends of cavefish genes with RACE PCR. 57
2.3 Forward and reverse primers for TA cloning of cDNA sequences in pGEM-T Easy vector backbone. 58
2.4 Forward and reverse primers to amplify cDNA sequences from pGEM-T Easy vector and cloning into pCS2-MTK vector backbone. 58
2.5 Primers used to clone promoter constructs in luciferase reporter vector pGL3. . 60
2.6 Primers used to clone promoter constructs in luciferase reporter vector pTAL-pLUC from pGL3 vector. 60
2.7 Primers used for mutations to the D-box and E-box sequences zf *hebp2* promoter in pTAL-pLUC. 61

3.1 Alignment scores between zebrafish and cavefish PAR-bZip factors. 122
3.2 Alignment scores between zebrafish and cavefish Nfil3 factors. 125

S1 D-box and E-box predictions of mitochondrial and heme genes based on MotifViz analysis. 179
S2 Mitochondria and heme-related genes extracted from the Gene Ontology analysis for zebrafish cells exposed to 6 hours of blue light vs. nonexposed controls. 181
S3 ANOVA and Tukey HSD comparisons analyses for exposure to blue light of zebrafish PAC2 and cavefish EPA cells, and zebrafish larvae. 182
S4 ANOVA and Tukey HSD comparisons analyses for exposure to UV-C of zebrafish PAC2 cells and zebrafish larvae. 183
S5 ANOVA and Tukey HSD comparisons analyses for mRNA stability assays of zebrafish PAC2 cells following exposure to blue light and UV-C, and MTT assay. 184
S6 In vitro luciferase assays t-test analyses with Bonferroni corrections (adj p-val). 185

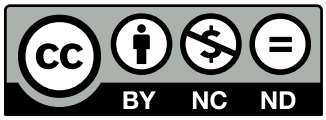

Abstract

Sunlight is a powerful environmental stimulus for most organisms, known to entrain their circadian clocks, activate their DNA repair systems, and impact various other physiological processes. Cells and tissues of zebrafish (*Danio rerio*) respond directly to light and the D-box enhancer element has previously been implicated in the subsequent regulation of various circadian and DNA repair genes. Additionally, the PAR-bZip and Nfil3 transcription factors have been identified as D-box regulators. However, the full extent of the transcriptional response to sunlight and its evolutionary nuances remains unclear. In the present study, the cellular light-mediated gene expression was explored in zebrafish and compared to that of the blind Somalian cavefish (*Phreatichthys andruzzii*), which evolved in perpetual darkness, and whose circadian clock and DNA repair mechanisms are not light-regulated. Two mRNA-sequencing experiments of zebrafish and cavefish cells exposed to blue light (468 nm) and to UV-C (20J/m^2) were performed. Gene ontology analyses of zebrafish cells exposed to blue light for 1 to 6 hours revealed the enrichment of genes related to mitochondrial structure and function, as well as heme biosynthesis, transport, and catabolism. The upregulation of these genes was also observed in 5 dpf zebrafish embryos exposed to blue light and in zebrafish cells 18 and 36 hours after exposure to UV-C. Their temporal profile of expression follows that of known D-box-regulated genes and is the result of *de novo* transcription. Bioinformatic, *in vitro*, and *in vivo* analyses supported the notion that in zebrafish the expression of these genes is regulated via D-box enhancer elements in their promoters. However, the upregulation of the mitochondrial and heme-related genes was absent in the cavefish cell line, highlighting the

evolutionary adaptability of light-sensing mechanisms. To gain insights into D-box-mediated gene expression and its evolution, the cavefish PAR-bZip and Nfil3 transcription factors were identified, and their function was compared with the zebrafish counterparts. The analyses revealed all PAR-bZip factors of both zebrafish and cavefish can activate transcription via the D-box enhancer element in both cell systems. The lower levels of activated transcription mediated by the cavefish factors suggests they might have been the target of evolution, either through mutation or alterations affecting their phosphorylation, binding efficiency, and/or cellular localization. The present findings expand the known landscape of light-mediated gene expression and identify the D-box as part of a broader mechanism extending beyond circadian clock entrainment and DNA repair. Despite the transcriptional changes in zebrafish cells, preliminary analyses reveal no significant changes in general mitochondrial function or heme levels. Nonetheless, the present study lays the groundwork for further investigation into the functional impact of the observed transcriptomic response, offering insights into its broader physiological implications.

Zusammenfassung

Sonnenlicht ist ein kraftvoller Umweltstimulus für die meisten Organismen, bekannt dafür, ihre circadianen Uhren zu synchronisieren, ihre DNA-Reparatursysteme zu aktivieren und verschiedene andere physiologische Prozesse zu beeinflussen. Zellen und Gewebe des Zebrafisches (*Danio rerio*) reagieren direkt auf Licht, und das D-Box-Enhancer-Element wurde bereits zuvor mit der anschließenden Regulation verschiedener circadianer und DNA-Reparaturgene in Verbindung gebracht. Darüber hinaus wurden die Transkriptionsfaktoren PAR-bZip und Nfil3 als D-Box-Regulatoren identifiziert. Jedoch bleibt das volle Ausmaß der transkriptionellen Reaktion auf Sonnenlicht und ihre evolutionären Nuancen unklar. In der vorliegenden Studie wurde die zelluläre lichtvermittelte Genexpression in Zebrafischen (D. rerio) untersucht und mit der des blinden somalischen Höhlenfisches (*Phreatichthys andruzzii)* verglichen, der sich in ständiger Dunkelheit evolvierte und dessen circadiane Uhr und DNA-Reparaturmechanismen nicht lichtreguliert sind. Es wurden zwei mRNA-Sequenzierungsversuche an Zebrafisch- und Höhlenfischzellen durchgeführt, welche blauem Licht (468 nm) und UV-C (20J/m2) ausgesetzt waren. Genontologieanalysen von Zebrafischzellen, die 1 bis 6 Stunden lang blauem Licht ausgesetzt waren, zeigten eine Anreicherung von Genen, die mit der mitochondrialen Struktur und Funktion sowie Häm-Biosynthese, -Transport und -Katabolismus in Zusammenhang stehen. Die Hochregulierung dieser Gene wurde auch bei 5 dpf alten Zebrafischembryonen nach Exposition gegenüber blauem Licht und bei Zebrafischzellen 18 und 36 Stunden nach Exposition gegenüber UV-C beobachtet. Ihr zeitliches Expressionsprofil folgt dem

bekannter D-Box-regulierter Gene und ist das Ergebnis einer *de-novo*-Transkription. Bioinformatische-, *in vitro*- und *in vivo*-Analysen unterstützten die Annahme, dass bei Zebrafischen die Expression dieser Gene über D-Box-Enhancer-Elemente in ihren Promotoren reguliert wird. Die Hochregulierung der mitochondrialen und Häm-bezogenen Gene war jedoch in der Höhlenfischzelllinie abwesend, was die evolutionäre Anpassungsfähigkeit von Lichtsensormechanismen verdeutlicht. Um Einblicke in die D-Box-vermittelte Genexpression und ihre Evolution zu gewinnen, wurden die PAR-bZip- und Nfil3-Transkriptionsfaktoren des Höhlenfisches identifiziert, und ihre Funktion wurde mit den Zebrafisch-Gegenstücken verglichen. Die Analysen ergaben, dass alle PAR-bZip-Faktoren sowohl bei Zebrafischen als auch bei Höhlenfischen die Transkription über das D-Box-Enhancer-Element in beiden Zellsystemen aktivieren können. Die geringeren Niveaus der aktivierten Transkription, vermittelt durch die Höhlenfischfaktoren, lassen darauf schließen, dass sie das Ziel der Evolution gewesen sein könnten, entweder durch Mutationen oder Veränderungen, die ihre Phosphorylierung, Bindungseffizienz und/oder zelluläre Lokalisation beeinträchtigen. Die vorliegenden Erkenntnisse erweitern das bekannte Bild der lichtvermittelten Genexpression und identifizieren die D-Box als Teil eines umfassenderen Mechanismus, der über die Synchronisierung der circadianen Uhr und die DNA-Reparatur hinausgeht. Trotz der transkriptionellen Veränderungen in Zebrafischzellen zeigen vorläufige Analysen keine signifikanten Veränderungen in der allgemeinen mitochondrialen Funktion oder des Hämspiegels. Dennoch legt die vorliegende Studie den Grundstein für weitere Untersuchungen des funktionellen Einflusses der beobachteten transkriptomischen Reaktion und bietet Einblicke in ihre umfassenden physiologischen Auswirkungen.

Abbreviations

ABCB6	ATP Binding Cassette subfamily B member 6
AhR	Aryl hydrocarbon Receptor
ANOVA	Analysis of Variance
ATP	Adenosine Triphosphate
BCA	Bicinchoninic Acid
BER	Base Excision Repair
BL	Blue light
BLVR	Biliverdin reductase
BMAL	Brain and Muscle ARNT-like protein
BP	Biological Process
bZip	Basic leucine Zipper domain
CC	Cellular Component
CLOCK	Circadian Locomotor Output Cycles Kaput
COX	Cytochrome Oxidase
CPDs	Cyclobutane Pyrimidine Dimers
CRE	cAMP Responsive Element
CRY	Cryptochrome
CPS	Counts Per Second
C-terminal	Carboxyl terminal
DD	Constant darkness
DDB2	DNA Damage Binding protein 2
DEGs	Differentially Expressed Genes
dH_2O	distilled water
DNA	Deoxyribonucleic Acid
dNTPs	Deoxynucleotide Triphosphates
DMSO	Dimethyl Sulfoxide
dpf	Days post-fertilization
D-box	D-box enhancer element
E4BP4	E4 Binding Protein 4
ERK	Extracellular signal-Regulated Kinase
ETC	Electron Transport Chain
E-box	E-box enhancer element
FAD	Flavin adenine dinucleotide
FECH	Ferrochelatase
FBS	Fetal Bovine Serum
FPKM	Fragments Per Kilobase per Million mapped reads
Fw	forward
GO	Gene Ontology
GPCR	G-Protein Coupled Receptor
h	Hours
H_2O_2	Hydrogen peroxide
HEBP2	Heme Binding Protein 2
HLF	Hepatic Leukemia Factor
HO	Heme Oxygenase
hpf	hours post-fertilization
HRP	Horseradish Peroxidase

JNK	c-Jun N-terminal Kinase
LB	Luria-Bertani Broth
LD	Light-Dark
M	Molar
MAPKs	Mitogen-Activated Protein Kinase
MF	Molecular Function
MKPs	MAPK Phosphatases
mL	Milliliter
mM	Millimolar
mRNA	Messenger RNA
MTT	3-(4,5-dimethylthiazol-2-yl)-2,5-diphenyltetrazolium bromide
NADH	Nicotinamide adenine dinucleotide
NADPH	Nicotinamide adenine dinucleotide phosphate
NER	Nucleotide Excision Repair
NFIL3	Nuclear Factor, Interleukin 3 regulated
ng	nanogram
NLS	Nuclear Localization Signal
nm	nanometer
NOXs	NADPH Oxidases
N-terminal	Amine-terminal
OCR	Oxygen Consumption Rate
ORF	Open Reading Frame
PAR	Proline-Acidic Rich
PBS	Phosphate Buffered Saline
PCA	Principal Component Analysis
PCR	Polymerase Chain Reaction
PER	Period
phr	Photolyase
pmol	Picomoles
PTU	phenylthiourea
QC	Quality Control
RACE	Rapid Amplification of cDNA Ends
RNA	Ribonucleic Acid
ROS	Reactive Oxygen Species
RPEs	Retinal Pigment Epithelium cells
RT-qPCR	Real-time quantitative PCR
Rv	Reverse
SCN	Suprachiasmatic Nucleus
SDS	Sodium Dodecyl Sulphate
SEM	Standard Error of the Mean
TBS	Tris Buffered Saline
TBS-T	TBS plus Tween-20
TEF	Thyrotroph Embryonic Factor
TMT	Teleost Multiple Tissue
TPM	Transcript Per Million
TSS	Transcription Start Site
TTFLs	Transcription-Translation negative Feedback Loops
Tukey HSD	Tukey Honestly Significant Difference
UV	Ultraviolet
μg	Microgram
μL	Microliter
μM	Micromolar
XPC	Xeroderma Pigmentosum, complementation group C
ZT	Zeitgeber

Publication

Hong, Y., **Boiti, A.**, Vallone, D. and Foulkes, N.S., 2024. Reactive Oxygen Species Signaling and Oxidative Stress: Transcriptional Regulation and Evolution. Antioxidants, 13(3), p.312.

1. Introduction

Sunlight is a powerful environmental stimulus for most species on Earth, from prokaryotic algae to highly complex organisms. It affects their circadian clock, DNA damage repair, and various other physiological processes at the cellular and system levels. Furthermore, light influences the organisms' behavioral patterns both through direct exposure and indirectly through its indirect effects on ecological systems. My project aims to unravel sunlight-responsive molecular pathways in vertebrates by investigating how light affects cell biology and by identifying the key transcriptional regulators of sunlight-induced gene expression.

1.1 Sunlight as a powerful environmental stimulus

Sunlight is a source of energy, enabling plants and algae to synthesize complex organic molecules such as glucose starting from water and carbon dioxide via photosynthesis. This process releases oxygen thereby creating a habitable environment for organisms on Earth. Moreover, sunlight is a source of heat which is vital for the maintenance of a thriving environment and for the survival of most species. The directionality of sun rays serves as an orientation compass for many vertebrate and invertebrate species [1], [2]. Sunlight also has essential roles at the organism and cellular level. Specifically, it is the most important zeitgeber (time giver), or stimulus that entrains the circadian clock of most species. This allows them to sense day-night and seasonal rhythms and to anticipate and adapt their physiology and behavior in anticipation of regular daily and seasonal environmental changes [3]. At the same time, sunlight exposure comes with the inherent risk of DNA damage, mostly caused by the short ultraviolet wavelengths [4]. Furthermore, the visible components of light have also been shown

to influence the metabolic and redox state of cells and to affect their survival [5]. To counteract this, many organisms have evolved protective mechanisms whereby upon light exposure, their cells upregulate the expression of genes involved in processes such as DNA damage repair [6], [7] and redox homeostasis [8].

1.1.1 Light entrains the circadian clock

Light is fundamentally important for biological timing. In many plants and animals, photoperiod sensing mechanisms work together with so-called circannual clocks to allow the measurement of day length and subsequent prediction of seasonal changes. This allows them to select the best times for reproduction and dormancy, depending on temperature, weather, and food availability over the year [9], [10]. Organisms have evolved to synchronize their metabolic, physiological, and behavioral activities with the day-night cycles, using both light and the entrainment of their circadian rhythms to optimize functions. This alignment ensures they adapt efficiently to daily challenges and thereby enhance their survival. The most studied internal clock system is the circadian clock, which is based on the 24-hour day and night cycles of the Earth [11]. At the molecular level, the circadian clock is a system of Transcription-Translation negative Feedback Loops (TTFLs), requiring approximately 24 hours to complete one cycle (Figure 1.1) [12]. The core clock mechanism in vertebrates is composed of two principal positive elements, the proteins CLOCK and BMAL, which drive the expression of the two main negative elements, period (PER) and cryptochrome (CRY). CLOCK and BMAL act as transcription factors controlling the expression of *per* and *cry*, as well as other clock genes, by binding to E-Box regulatory sequences found in their promoters. As their levels increase, PER and CRY proteins inhibit their own transcription by interfering with CLOCK and BMAL function at the E-Box sites. PER and CRY levels decrease, as does their inhibitory effect in the

nucleus, leaving the CLOCK-BMAL complex free to bind to and activate transcription from the E-box sites, thereby starting a new cycle. Through this core TTFL and additional regulatory mechanisms, the circadian clock is in principle self-sustaining and can function endogenously. However, in the absence of external cues, this rhythm tends to drift out of phase from the environmental day-night cycle [13]. To ensure proper synchronization with the external environment, the clock is reset daily by zeitgebers. The most important zeitgeber is light, but other stimuli such as UV, food intake, temperature, and Reactive Oxygen Species (ROS) can also entrain the clock [14]. The mechanism by which light and other signals affect the circadian clock is still not fully understood, but it seems to involve transcriptional regulatory pathways. The outputs of the circadian clock are numerous, ranging from physiological processes such as gene and hormonal regulation, cell cycle, and metabolism [15]–[17] to behavior e.g. sleep-wake cycles, locomotor activity, and feeding patterns [18], [19]. A variety of studies have linked disturbances in this timing mechanism, such as those resulting from night shifts and extensive use of artificial light, with increased risk of mental disorders, metabolism dysfunction, cancer, and cardiovascular disorders among others [20], [21].

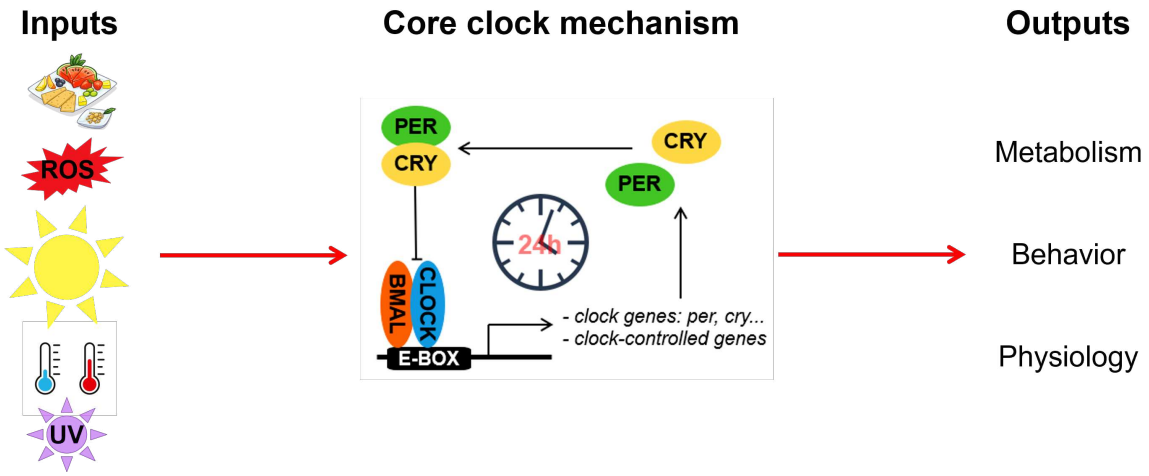

Figure 1.1. The core circadian clock mechanism and its inputs and outputs.

1.1.2 The duality of light: damage and repair

While sunlight has proven to be an important stimulus for organisms, it can also negatively influence them and especially their cells, by damaging macromolecules, e.g. DNA and proteins (Figure 1.2).

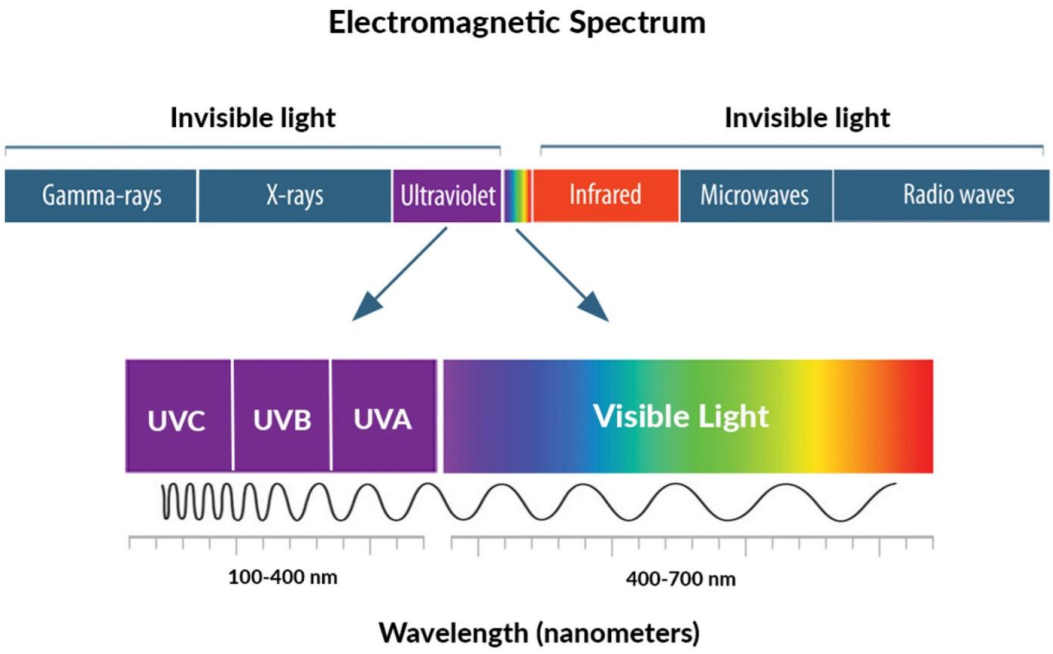

Figure 1.2. Visible and invisible light spectrum. Shorter wavelengths carry more energy. Figure taken from https://www.nei.nih.gov/ [22].

1.1.2.1 Effects of visible light on cells

Visible and infrared light (400-1000nm) can influence the metabolic and redox state of cells and affect their survival [5]. In fact, many proteins found in cells contain chromophores such as porphyrins and flavins, which can absorb and interact with light. For instance, Cytochrome Oxidase (COX), a mitochondrial enzyme crucial for the Electron Transport Chain (ETC) and ATP production, contains porphyrin. Flavoproteins, coenzymes containing flavins that are essential for various enzymatic reactions, have been linked to metabolism and oxidative stress

responses. Short wavelengths of light (400-520nm) interacting with these molecules generate ROS [23]. As we will see later, the resulting ROS can act as a crucial signaling molecule, but also negatively affect cells by impairing the ability of mitochondria to produce ATP and by damaging DNA. On the other hand, the long wavelengths of light (630nm-1000nm) appear to have a protective effect on cells, stimulating ATP synthesis [24] and reducing ROS levels [25]. Furthermore, a transcriptomic experiment using human fibroblasts by Song and colleagues [26] pointed to red light (628nm, 0.88J/cm^2) being protective of cells, via its effect on the expression of genes related to growth and proliferation, immune and inflammation responses, and energy metabolism, while apoptosis-related genes instead appear to be downregulated. Thus visible light offers both challenges and benefits to cells, influencing metabolic processes, redox states, and survival through complex interactions with chromophores.

1.1.2.2 UV-induced damage and repair

The ultraviolet (UV) components of light (<400nm), UV-A (320-400nm), UV-B (280-320nm), and UV-C (200-280nm) are the primary cause of cellular damage by sunlight [4]. Exposure of cells to these wavelengths introduces covalent modifications into their DNA structure, mutations that are heritable upon DNA replication. The major products of UV-B and UV-C radiation are 6-4 photoproducts and Cyclobutane Pyrimidine Dimers (CPDs), which can in turn actively interfere with cellular transcription and replication [27]. Furthermore, the absorption of UV by the side chains of certain amino acids can influence the structure and functions of proteins [28]. On the skin, DNA damage results from the effects of UV-B, and indirectly from UV-A via ROS production, akin to blue light [29], while UV-C is mostly absorbed by the Earth's ozone layer and atmosphere and so has very little effect under natural conditions. The term "photodermal aging" describes the structural and functional effects of these wavelengths

on macromolecules observable in the human skin through the aging process [30]. Therefore, organisms need to protect themselves from sunlight, which can otherwise lead to several pathologies, one of the most common being skin cancer [31]. One such mechanism of protection against UV-related damage is photoreactivation, which is present in most species but has been lost during the evolution of placental mammals [32]. Photoreactivation is driven by visible light and starts from the upregulation of a subset of DNA repair enzymes called photolyases [33]. The photolyases, specifically 6-4 phr and CPD phr accurately and efficiently reverse DNA lesions using energy harvested from visible light. Aside from photoreactivation, DNA damage is repaired via two other main mechanisms: Nucleotide Excision Repair (NER), and Base Excision Repair (BER) [4]. These repair mechanisms use energy from ATP to excise damaged nucleotides and replace them with newly synthesized DNA. Evidence from mammals shows that UV radiation induces the expression of *XPC* and *Neil1*, two important members of the NER mechanism that serve as damage recognition factors, as a protective strategy [34]. In this way, NER activity is increased upon the first exposure to sunlight and can thereby more efficiently combat the damage that accumulates during extended sunlight exposure.

1.1.3 Mitochondria and heme

Previous microarray studies performed on zebrafish larvae, cells, and hearts exposed to light identified the upregulation of genes involved in light signaling, oxidative stress responses, detoxification, DNA repair, heme metabolism, mitochondria, retinol-binding, as well as genes coding for transcription factors [35], [36]. Furthermore, transcriptomic comparisons on the Staghorn coral *Acropora cervicornis* during day and night times showed differential expression of circadian clock-related genes, genes related to mitochondria metabolism (ATP synthase and ETC components), and oxidative stress [37]. Another species of coral, *Euphyllia paradivisa*,

showed many genes involved in mitochondria organization are rhythmically expressed with a peak at dusk and trough at dawn in coral kept in LD conditions [38].

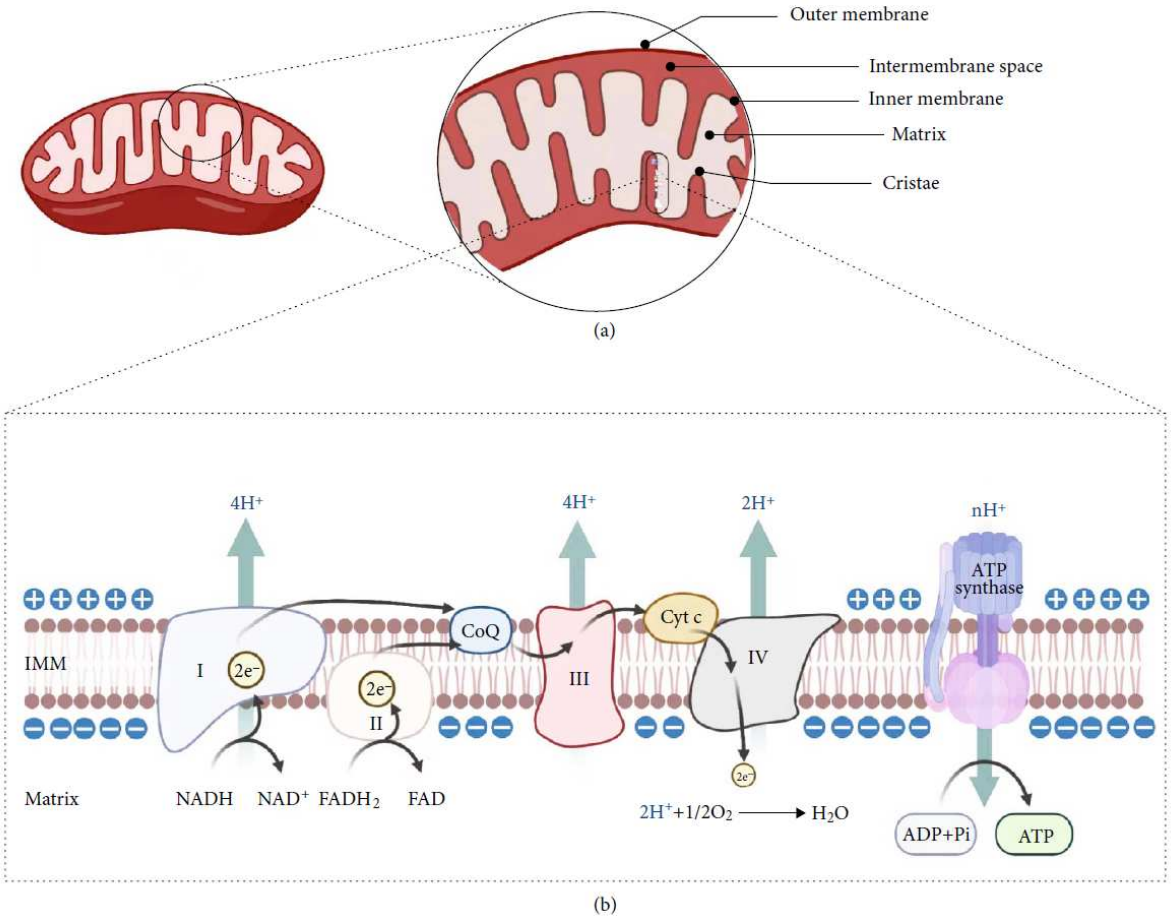

Figure 1.3. Mitochondrion (a) and Electron Transport Chain (b) structures. Mitochondria present an outer and an inner membrane. The inner membrane is folded in cristae which increase its surface area. The ETC is found in this membrane and is made of four main protein complexes. Complex I receives electrons from the carrier NADH, while Complex II receives them from $FADH_2$. The electrons are then transferred via Coenzyme Q to Complex III, then Cytochrome c, and finally to Complex IV where oxygen is reduced to H_2O. The movement of electrons through the ETC generates a proton gradient which drives the synthesis of ATP from ADP and inorganic phosphate (Pi) by ATP synthase. Scheme taken from Yuan and colleagues [39].

Mitochondria are abundant cellular organelles with a key role in the production of energy through oxidative respiration, where carbohydrates and lipids are converted into ATP, the main energy storage molecule. Mitochondria are highly dynamic and can be found both as separate organelles as well as in a tubular formation, structures resulting from fission and fusion processes that are tightly controlled [40]. Their morphology,

abundance, and function vary considerably across tissues, cell types, species, and cellular states. Dysfunctions of mitochondria have been linked with various diseases, such as cancer, diabetes, neurodegenerative disorders, and aging [40]. Mitochondria present two compartments, separated by an inner membrane where membrane-spanning complexes of the ETC are found (Figure 1.3). The inner mitochondrial membrane is folded into cristae to increase the surface area available to carry out oxidative phosphorylation and produce ATP. Here electrons are transferred to molecular oxygen via the four redox carrier complexes of the ETC, producing H_2O. This process inherently generates superoxides as all complexes leak single electrons to oxygen molecules, making mitochondria the main source of cellular ROS [41]. Furthermore, within the ETC there are many proteins containing flavins and porphyrins such as heme, chromophores which absorb light at maximas of 450nm and 400-410nm, respectively [23], [42] leading to the generation of ROS and damage to DNA and proteins. The effect of light on mitochondria has mostly been studied in Retinal Ganglion Cells (RGCs) and Retinal Pigment Epithelium (RPEs) of mammals due to their constant exposure to light and their role in visual photoreception. Osborne and colleagues [43] demonstrated that exposure of RGCs to constant blue light for 48 hours leads to a 20% loss in viability which is further enhanced when cells are stressed by serum deprivation. Together with another study on human RPEs [44], they pointed at mitochondria-generated ROS via the ETC complexes action to be responsible for the blue light-induced apoptosis. Inhibition of ETC by rotenone, depletion of key parts of the ETC, and mitochondria-targeted antioxidants all lead to a decrease in cell death from light exposure. Furthermore, mitochondria function and structure have been connected to the circadian clock. As reviewed by De Goede and colleagues [40], several knockouts of clock genes led to changes in dynamics, morphology, ATP production, and mitochondria-related gene expression in various cell types, and mitochondrial respiration, measured via Oxygen

Consumption Rate (OCR), has been reported as intrinsically rhythmic.

One key molecule synthesized within mitochondria is heme, an iron-containing tetrapyrrole generated through a series of enzymatic steps in the mitochondrial matrix [45]. Heme synthesis, transport, and degradation are tightly controlled (Figure 1.4). Most heme is bound to sensors and proteins that either transport it or use it for their enzymatic reactions, and it is degraded by Heme Oxygenase (HO). A small pool of regulatory heme (5-10% of the total) is free or bound to proteins with low affinity [46], [47]. Heme is best known for its role in oxygen binding and transport throughout the organism, however, it is a highly versatile molecule with numerous other functions spanning transcriptional and translational regulation, involvement in metabolic and signaling pathways, redox sensing, and detoxification of xenobiotic compounds [48], [49]. Within mitochondria, hemoproteins are important mediators of electron transport [50]. Therefore, heme levels within cells have to be tightly controlled. The pool of free, or labile, heme constituted by newly synthesized and unbound heme is a source of redox-active iron ions, which can react in the Fenton reaction with H_2O, thereby generating hydroxyl free radicals [51]. This excessive ROS production further increases pro-inflammatory molecules. Due to its hydrophilic and hydrophobic properties, heme molecules can intercalate in cell membranes, affecting membrane permeability, oxidizing the surrounding molecules, and increasing oxidative stress [52], [53]. On the other hand, the enzymes Ferrochelatase (FECH), biliverdin (BLVR), and HO, key players in the degradation of heme, producing bilirubin and biliverdin, are thought to be also important in antioxidant mechanisms as well [52]. Green light (490-580nm) in the rat retina was shown to induce HO-1, the rate-limiting enzyme for heme degradation, to protect cells from oxidative damage [54].

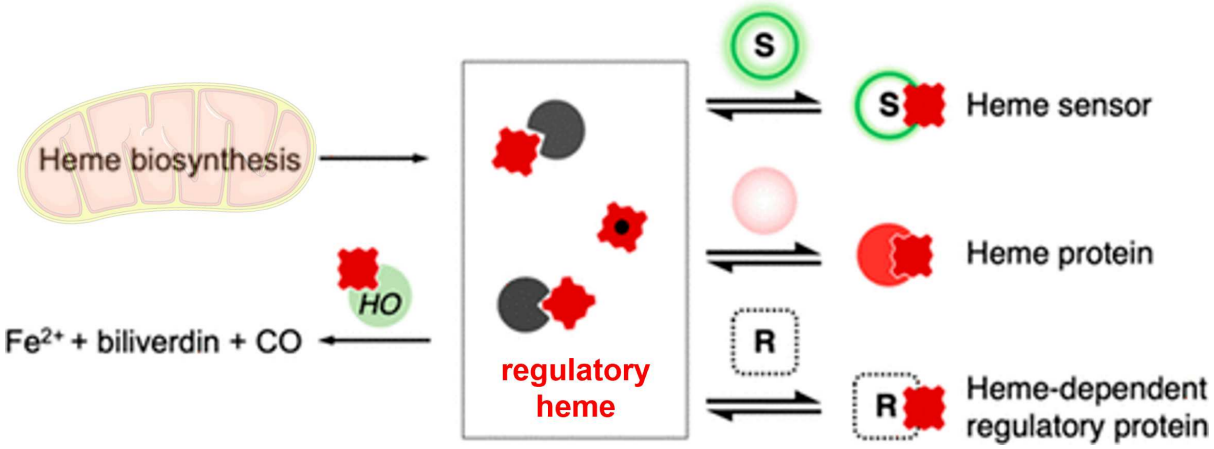

Figure 1.4. Chemical structure of heme (left) and a scheme of its metabolism and transport within cells (right). Heme has hydrophilic and hydrophobic regions. Its synthesis, transport, and degradation are tightly controlled. Most cellular heme is bound to sensors and proteins. A small pool of heme (5-10% of the total) is either free or bound to proteins with low affinity, and is referred to as regulatory heme. Figure adapted from Gallio and colleagues [46].

Heme has been suggested as a redox sensor linking oxidative stress to the circadian clock [50]. It binds and increases the activity of REV-ERB proteins, which are involved in the negative regulation of the TTFL by repressing the transcription of *bmal* [55], [56]. Heme can also bind to the PER and CRY proteins and thereby disrupt their ability to heterodimerize and regulate transcription. One study found heme to oscillate in a circadian manner, with peaks every 12h after serum shock in mouse 3T3 cells, and the addition of heme successfully entrained their circadian clocks [57]. ALAS1, the rate-limiting enzyme for heme biosynthesis, is also under circadian regulation [45].

1.1.3.1 *Abcb6a*, *hebp2*, *soul5*

The expression of a number of genes has been shown to be strongly regulated by light in zebrafish cells which are connected with mitochondria, heme binding or transport. These include the *abcb6a*, *hebp2*, and *soul5* genes. The zebrafish gene abcb6a codes for a protein belonging to the ATP-binding cassette, subfamily B. ABC transporters are found on various cellular membranes and are involved in the ATP-dependent efflux of diverse substrates. The

specific function in zebrafish is poorly understood however, mammalian studies identified ABCB6 as a mitochondrial porphyrin transporter [58] and proposed its involvement in the synthesis of heme [59]. As already discussed, porphyrin levels and location have to be tightly controlled, and since they cannot readily cross the membrane, mechanisms are in place to shuttle them where needed. ABCB6 is located in the outer mitochondrial membrane and on the plasma membrane, with a cytoplasmic nucleotide-binding site, necessary to catalyze the hydrolysis of ATP [60]. It is thought to have an antioxidant function, both by providing heme to catalase, for which it is a crucial co-factor, and by increasing catalase expression [61]. It was also identified as an important factor in porphyrias, as individuals with the disease tend to carry variant alleles of the *abcb6* gene, and its knock out in a mouse model of porphyria is characterized by damaging porphyrin levels in blood and liver cells [62]. Like many other ABC transporters, it has a role in mediating resistance against cytotoxic compounds, for instance exposure of mice to arsenic leads to ROS generation and increases *abcb6* expression as a protective measure to counter its effects [63]. In humans, mice, and zebrafish its transcription is influenced by the Aryl hydrocarbon Receptor (AhR), which has a central role in the response to xenobiotic insults ([64], [65].

HEPB/SOUL proteins are a family of proteins binding to heme and various other intermediaries [66]. Their roles are not yet completely understood, but they are thought to function as buffers, by binding newly synthesized heme before it is incorporated by hemoproteins, thereby preventing its aggregation and cytotoxic effects such as ROS generation [67]. In mice, HEBP2 has a high affinity for heme. However, the human ortholog has a mutation to the His42 residue which is thought to be essential for heme-binding properties, questioning this role in the species ([68], [69]. In mammals, fish, and birds, HEBP2 has been found in the retina and other photoreceptive tissues, such as the chicken pineal gland [70], [71]. In corals

kept in LD cycles, compared to those kept in DD, *hebp2* is among the rhythmic genes that are upregulated during the light period [37], [38]. Despite its uncertain connection to heme, HEBP2 can promote mitochondrial membrane permeability transition, leading to a loss of membrane potential and thus negatively affecting mitochondrial function [72], [73]. Furthermore, it binds the antiapoptotic protein Bcl-xL and promotes necrotic cell death under stress conditions [69], [73]. The heme-binding protein SOUL5 has been observed in zebrafish and medaka [71], [74] and not much is known about it. It is highly similar to HEBP2 and is predicted to function as a cytoplasmic protein with the ability to bind heme.

1.2 Early pathways of light-mediated gene expression

As we have seen, light can influence the circadian clock, DNA repair, oxidative responses, and other physiological functions. One of the main ways by which light acts on cells is by regulating the expression of genes involved in these processes. Two main pathways through which a light stimulus can be transduced to a cellular output have been studied extensively: photoreceptors and ROS.

1.2.1 Extravisual photoreception

Cells or structures that are sensitive to light to some degree are called photoreceptors [75]. Well-known and well-studied photoreceptors, for obvious reasons, are retinal cells in the eyes, which collect visual information and relay it to the brain for further processing. However, many other photoreceptors with non-visual functions have been found in and outside the retina. They are involved in the entrainment of the circadian clock and of sleep-wake cycles [75], as well as sexual maturation and reproduction [76], [77], and skin color changes [78], [79], among

others. Common photoreceptors are opsins, G-Protein Coupled Receptors (GPCRs) made of a protein with seven transmembrane domains containing a chromophore, usually retinol. When the chromophore absorbs photons, it activates the GPCR which leads to a biochemical cascade of events affecting a variety of cellular processes. Different opsins have different absorption spectra and different patterns of expression throughout the body, which also varies among different species. For instance, opsins are found in greater numbers and wider distribution in fish and birds compared to reptiles and amphibians [80]. Their location is thought to be related to their function [80]–[82]. Cryptochromes are also photoreceptors. These highly conserved flavoproteins are close relatives of the photolyase DNA damage repair enzymes and are thought to be involved in various processes, including circadian rhythms and phototaxis [83].

1.2.1.1 Opsins in fish

Fish possess a wide variety of opsins and some of these are also conserved in mammals [82]. In zebrafish 42 opsins (10 visual and 32 non-visual) have been identified, with differential patterns of expression across tissues. Many of these overlap with the expression of clock genes. Fernandes [84] demonstrated how larvae lacking eyes and the pineal gland retain their response to light, demonstrating that these two organs are not necessary for the regulation of the circadian clock and other light-related processes. Interestingly, Teleost Multiple Tissue opsin (TMT) and melanopsin have been implicated in the transduction of blue and light signals in fish cells [85] highlighting their potential roles in the response to light. Despite the wide distribution and diversity of opsins and their implications in light-dependent processes, the precise mechanisms that connect them to gene expression in fish remain largely unexplored.

1.2.2 Reactive Oxygen Species

The discovery of reactive oxygen species (ROS) in cells led to the identification of a variety of biological reactions in which ROS are involved, acting as regulators of cell physiology and pathology [86]. ROS are highly reactive molecules containing oxygen, including peroxides (H_2O_2), superoxide (O_2^-), hydroxyl radicals ($^{\bullet}OH$), and single oxygen ($_1O^2$) [87]. Within cells, they are primarily generated during the mitochondrial oxidative phosphorylation process as a byproduct of ATP production [41]. Complexes I and III, NADH-ubiquinone oxireductase and ubiquinol-cytochrome c oxireductase respectively, are significant contributors to ROS generation, especially of superoxide anions [88]. Other sources of ROS are NADPH Oxidases (NOXs), enzymes containing a flavocytochrome domain plus two heme molecules [89]. Superoxide anions produced by the ETC and NOXs are then converted into hydrogen peroxide, a less reactive ROS, either spontaneously or enzymatically by Superoxide Dismutase (SOD) [90]. ROS have the potential for both beneficial and detrimental effects within cells. ROS levels are strictly controlled via various scavengers and antioxidants, including the enzymes catalase, Glutathione Peroxidase (GPx), SOD, and peroxiredoxins (PRDX) [8], [41]. Under normal conditions, ROS serve as important signaling molecules in various physiological pathways [91]. High ROS concentrations, for instance resulting from light exposure, lead to oxidative stress, which is determined by an imbalance between ROS levels and the ability of cells to detoxify and counteract and repair the resulting damage [43], [87]. Indeed the free radicals can damage DNA, proteins, and lipids and put the cells at risk of death. Studies have connected ROS to various pathological conditions. For instance, they are involved in DNA mutations and genomic instability resulting in cancer and tumor growth [92]. ROS can also oxidize cysteine residues on proteins and enzymes, affecting their activity [93]. This process has been described for enzymes involved in signaling pathways that regulate cell proliferation, metabolism, and

cancer cell survival [94].

1.2.2.1 ROS as signaling molecules in light-induced gene expression

Since ROS production was detected in cells upon light exposure, ROS has been proposed to serve as a crucial signaling molecule mediating light-dependent changes in gene expression [95]–[98]. Consistently, catalase, an enzyme that breaks down H_2O_2, shows an antiphasic pattern of expression compared to the light-inducible clock genes *cry1a* and *per2* in fish, and light-dependent gene expression is inhibited by *catalase* overexpression, implicating ROS in the light transduction pathway [95]. Furthermore, Mitogen-Activated Protein Kinases (MAPKs), known to transmit extracellular signals to the nucleus via a phosphorylation cascade, can be activated by ROS [99]. In turn, MAPKs affect various cellular processes, such as proliferation, migration, inflammatory responses, and apoptosis [99]. Three levels of kinases (MAPKKKs, MAPKKs, MAPKs) are involved, as well as MAPK phosphatases (MKPs) which act as negative regulators. Ultimately MAPKs phosphorylate proteins such as transcription factors that can have a broad range of targets within the nucleus. There are three classes of MAPKs: extracellular signal-regulated kinases (ERKs), c-Jun N-terminal kinases (JNKs), and p38 mitogen-activated protein kinases (p38s) [100]. All of them have been implicated in the regulation of gene expression by light. Evidence for the involvement of ROS and MAPKs in light signal transduction comes from various studies in mammals and fish. In mammals, light-inducible genes in the hypothalamus, such as *per1* and *per2* possess cAMP response element (CRE) binding sites in their promoters, which are bound by the transcription factor CREB, following its phosphorylation by MAPKs [98], [101], [102]. In zebrafish cells, treatment with p38 inhibitors increases *per1* and *per2* expression in darkness, consistent with a positive role for p38 in light-induced gene expression [95], [103]. Similarly, JNK seems to act as

a positive element in this regard [104]. Studies also point to the involvement of ERK signaling in light-regulated gene expression but its specific role remains unclear as inhibition has been reported to both decrease [96], [103] and increase [104], [105] levels of clock and DNA repair genes during light exposure. However, there is evidence suggesting that ROS-independent pathways also coordinate light-induced gene expression, as cells show gene regulation in response to red light, which does not significantly increase ROS levels [105]–[107]. The intricate interplay between ROS and MAPK signaling in light-induced gene expression suggests the existence of a complex regulatory network, with studies in both mammals and fish revealing critical molecules in mediating these cellular responses to light.

1.3 Fish models

In most animals, light represents the key signal to synchronize their circadian clock with the environment [21]. However, the molecular basis of this entrainment is not yet fully understood. In mammals, the light stimulus is perceived via retinal ganglion cell photoreceptors and retinal opsins [108] and relayed to the Suprachiasmatic Nucleus (SCN) of the hypothalamus. The SCN is the master clock oscillator, which in turn entrains the clocks of the peripheral organs via systemic signals. In fish, as well as birds, reptiles, and amphibians, the pineal gland serves as a master clock regulator in the brain. However unlike mammals, cells and tissues of many fish species are also directly responsive to light, and their clocks can be entrained independently of the pineal gland [109]. As we have seen before, studies point to cell-membrane-spanning opsin photoreceptors [85], and to light-induced ROS generation [97] as possible mediators of these responses. Thus, cell lines derived from fish tissues can be used to study directly light-induced gene expression, making fish an invaluable tool for understanding the mechanisms of the

response to light and their evolution in different photic environments. In the present study, I focused on the zebrafish (*Danio rerio* and the Somalian cavefish (*Phreatichthys andruzzii* due to their intriguing and diverging cellular responses to light.

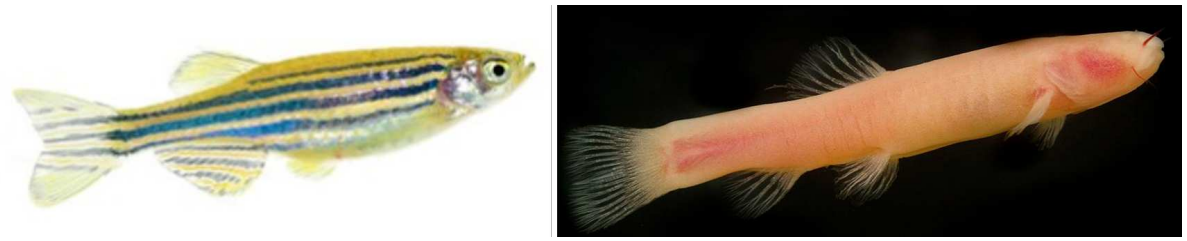

Figure 1.5. My two model species: zebrafish (*D. rerio* (left) and Somalian cavefish (*P. andruzzii* (right). The Somalian cavefish presents various troglomorphic features deriving from its evolution in constant darkness, such as the loss of eyes and pigmentation.

1.3.1 Zebrafish

The zebrafish *D. rerio* is a small, freshwater teleost fish belonging to the Cyprinidae family, native to South Asia (Figure 1.5, left). It became popular for research purposes, being a rather complex vertebrate with much in common with mammals from a biological point of view, and having advantageous characteristics over other vertebrate species (e.g. mice and rats). The most prominent features are their short generation time, rapid and easily observable embryonic development, suitability for high-throughput screening, and relatively easy genetic manipulation [110]–[112]. In 2013 the entire zebrafish genome was sequenced, revealing a homology of 70% with the human genome [113] and further enabling the use of precision tools for genome editing, rapid production of transgenic fish strains, as well as enhancement of genomic, transcriptomic, and proteomic studies. As such, zebrafish are widely used in genetic [114], drug discovery and development [110], developmental biology [115], and neurobiology [116] studies.

1.3.1.1 Light-mediated gene expression in zebrafish

As stated above, fish cells and tissues are directly responsive to light, and most of the studies on this mechanism and its connection to the circadian clock and DNA damage repair have been performed on zebrafish. Aside from its already mentioned important functions in many organisms, light is fundamentally important for the development and survival of zebrafish embryos [117], whose eggs are laid in the early morning and thus immediately exposed to light. Mechanisms are in place to prevent UV-dependent damage. On the one hand, gadusol, an endogenous sunscreen, is maternally inherited, persists in embryos and larvae up to 5dpf, and is then endogenously produced [118]. At the same time, the expression of photoreactivation enzymes for DNA repair, such as *6-4 phr*, is upregulated within 6 hpf to reverse UV-dependent damage [6], [117]. Light is also crucial in the early synchronization of circadian rhythms in a wavelength-dependent manner, and embryos grown in complete darkness do not develop a fully functional clock [119], [120]. Furthermore, light is necessary for synchronizing the S-phase in embryos, which occurs around 3 hours before the start of the night. After their successful entrainment by LD cycles, the S-phase rhythms are sustained under circadian clock control [121]. Embryos grown in DD instead show abnormal and arrhythmic S-phase. Finally, transcriptomic research identified various light-induced genes in zebrafish involved in circadian clock, light signaling, stress responses, DNA repair, heme metabolism, mitochondria, and binding to retinol [35], [36]. The upregulation of enzymes for detoxification and repair of oxidation and UV damage, as well as genes regulating metabolism, suggests a robust cellular response to sunlight in zebrafish.

1.3.1.2 The Somalian Cavefish, *P. andruzzii*

A key organism to study the response to light and its evolution alongside zebrafish is *Phreatichthys andruzzii*, a blind cyprinid cavefish from Somalia. *P. andruzzii* have evolved for more than 2 million years isolated in deep caves beneath the Somalian desert in an extreme environment characterized by constant darkness, constant temperature, and low food availability [122]. As a result, they present various troglomorphic features like the loss of eyes, pigmentation, and scales (Figure 1.5, right). Interestingly, their circadian clock is not responsive to light [85]. This is matched at the behavioral level by arrhythmic locomotor activity upon artificial exposure to LD cycles. However, they retain a functional clock which can be entrained by food delivery. This was determined both at the molecular level, with the rhythmic expression of clock genes in response to food, and at the behavioral level, as they show food anticipatory behavior [85]. Remarkably, the period of their entrained rhythm in cultured cells is infradian at around 43 hours per cycle and it decreases as temperatures increase, suggesting that the cavefish clock has also lost temperature compensation. Similarly to clock genes, light-directed DNA repair mechanisms are also not induced upon light exposure [7]. One of the reasons why *P. andruzzii* cells do not respond to light is found in the mutations of the TMT and melanopsin genes, which lead to premature stop codons and the absence of the site that covalently links to the chromophore retinaldehyde in the resulting proteins [85]. This negatively affects the photoreception of the short wavelengths of blue and green light. These characteristics and its evolutionary close relationship with *D. rerio*, (both are members of the Cyprinidae family), allow cavefish cells to be used as a "natural knock-out" for sunlight-regulated gene transcription. Studying and comparing the two organisms allows an understanding of the complexity and evolution of the cellular response to light as well as the identification of the key transcriptional regulatory elements that have served as the target for evolutionary adaptations in extreme photic

environments.

1.4 D-box mechanism

The precise mechanism by which light entrains the clock, activates DNA damage repair systems, and influences other physiological processes described above remains unclear. Because of their characteristic response to light, zebrafish and their cells were extensively used to explore the molecular mechanisms of light-dependent transcriptional regulation and their evolution. Studies done in my lab on the promoters of the light-induced clock genes *per2* and *cry1a* first revealed the presence of D-box enhancer sequences [123]. It was then demonstrated that these D-box sequences are both necessary and sufficient to induce gene expression upon exposure of zebrafish cells to light, UV, and ROS [7], [105], [123] (Figure 1.6). Subsequently, functional D-box enhancers were found in the promoters of light-induced DNA repair genes such as *6-4 phr* and *ddb2* [7]. Putative D-boxes were also predicted in a set of light-regulated genes in zebrafish, related to the circadian clock, DNA repair, stress responses, heme metabolism, mitochondria, and binding to retinol [36].

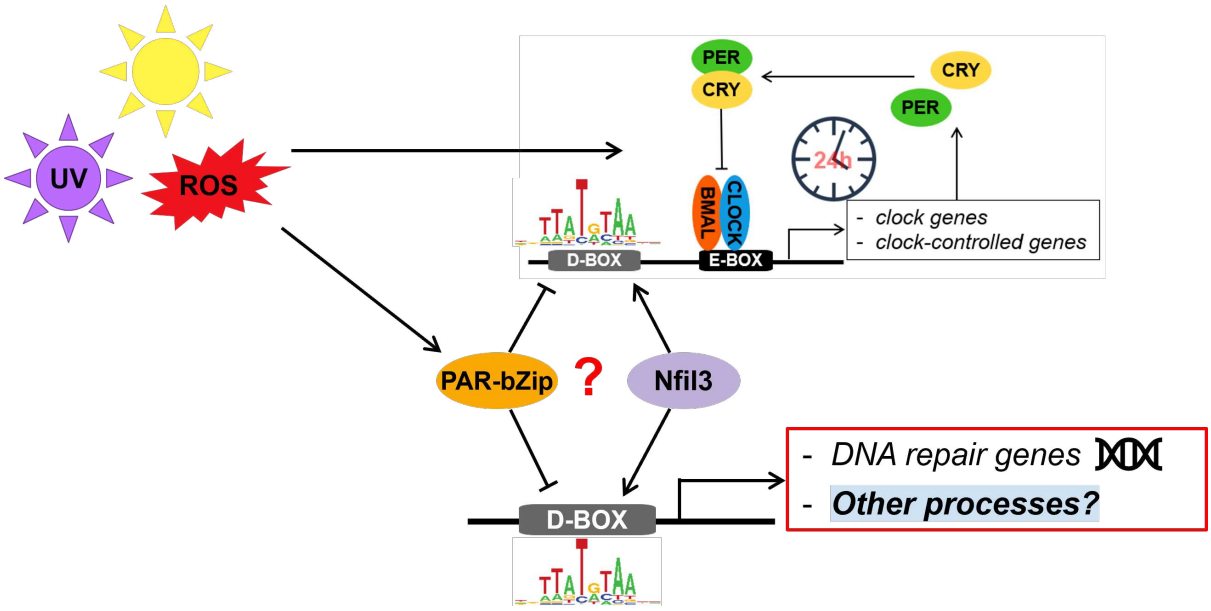

Figure 1.6. Mechanism of circadian clock entrainment and gene expression regulation via the D-box enhancer.

Mouse and human studies have previously identified a group of transcription factors of the PAR-bZip/Nfil3 family, which can bind to the D-box (also called PARRE, or PAR response element) to modulate gene expression [124]–[127]. There are four mammalian PAR-bZip/Nfil3 factors: the three proline-acidic rich (PAR) factors Thyrotroph Embryonic Factor (TEF), Hepatic Leukemia Factor (HLF), and D-box Binding Protein (DBP), and the Nuclear Factor, Interleukin 3 Regulated (Nfil3, also known as E4BP4). The PAR factors are transcriptional activators, enhancing gene expression via direct binding to the D-box, while Nfil3 is a repressor that competes with the PAR factors to inhibit gene expression. Due to genome duplication, in most teleosts there are 12 members in the PAR-bZip/Nfil3 family: two of each *TEF*, *HLF*, and *DBP*, and six *Nfil3* genes [123], [128]. Recently, based on phylogenetic and conserved syntenic analyses Sun and colleagues [129] postulated that *Nfil3-1* (E4BP4-1) is the ortholog of mammalian *Nfil3* and that together with *Nfil3-2* (E4BP4-2) and *Nfil3-3* (E4BP4-3) it is duplicated in teleosts. This resulted in the genes *Nfil3-1a*, *Nfil3-1b*, *Nfil3-2a*, *Nfil3-2b*, *Nfil3-3a*, and *Nfil3-3b*. Mammals have instead lost the *Nfil3-2* and *Nfil3-3* genes. The presence of

greater diversity within the PAR-bZip/Nfil3 family in fish indicates a potentially more complex regulatory system compared to mammals.

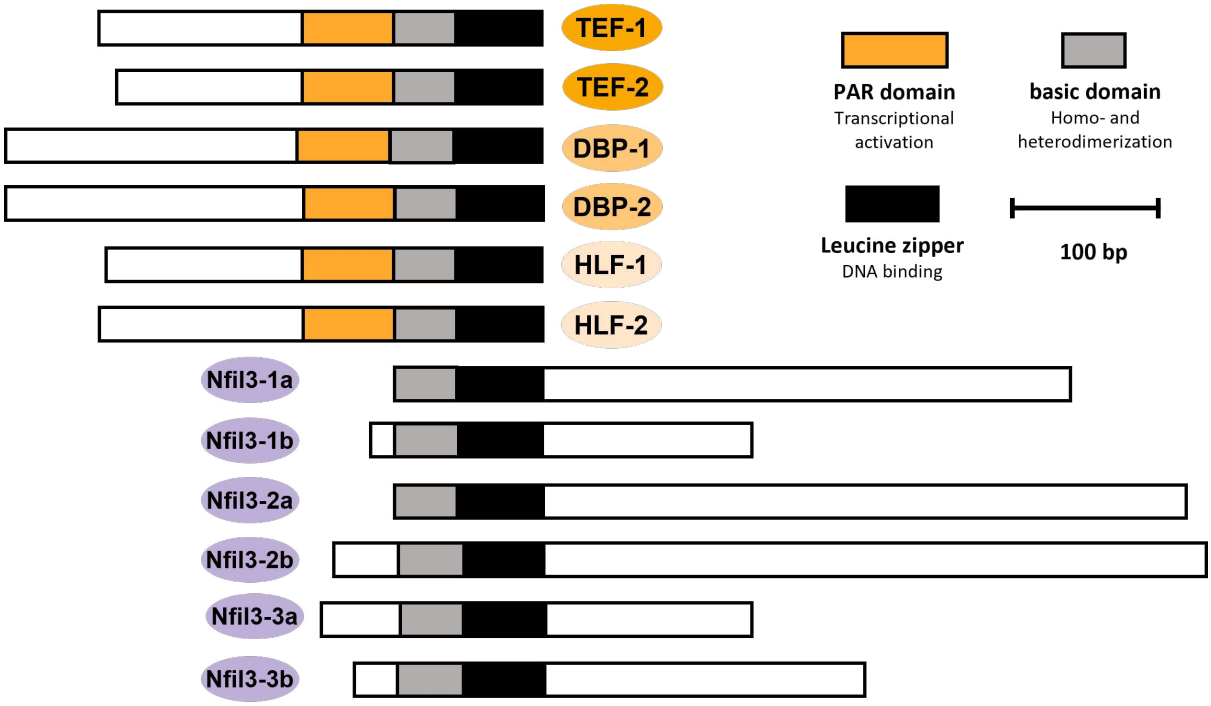

Figure 1.7. PAR-bZip and Nfil3 zebrafish protein structures. The PAR-bZip proteins TEF, DBP, and HLF contain the Proline Acidic Rich (PAR) domain, important for transactivation. All proteins contain the basic domain and the leucine zipper domain, important for homo- and hetero-dimerization, and for DNA binding.

These factors all share a basic DNA-binding domain, and a leucine zipper dimerization domain (bZip) and can homo- and hetero-dimerize to bind to the D-box site to enhance or repress gene transcription [130] (Figure 1.7). In fish, as we have seen, the D-box is part of the circadian clock input pathway, a key player in the entrainment of the clock in response to light signals. However, its role in mammals primarily involves the transcriptional regulation of clock output pathways. In fact, many of the PAR-bZip factors in mice have rhythmic expression, providing a link between the circadian clock and downstream factors [131], [132] (Figure 1.8). In mammals, conserved D-box sequences have been identified in the promoters of genes involved in circadian clock regulation [133], xenobiotic metabolism [132], thyroid hormone production [134], and glucose and lipid metabolism [135], [136] among others. These genes are under

circadian control in mammals, underscoring the evolutionary diversification of light response mechanisms among vertebrates, and the clock adopting the regulation of light-dependent gene expression in non-light-responsive organisms. The promoters of several zebrafish light-induced genes have been investigated in *P. andruzzii* to determine whether the loss of their expression was dependent on mutations or the absence of the D-boxes. However, many cavefish promoters retain functional D-boxes that can be activated by light in the context of zebrafish cells [7], [85], [137] indicating that the reason for the loss of light-dependent gene expression lies upstream within the pathway.

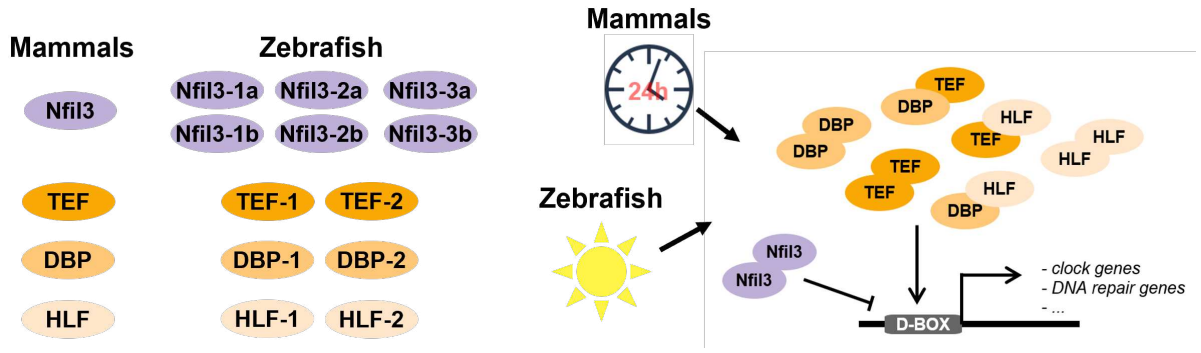

Figure 1.8. Differences between the PAR-bZip and Nfil3 families of transcription factors in mammals and zebrafish The PAR-bZip and Nfil3 proteins bind to the D-box enhancer sequence found on the promoter of various genes to influence their expression. In mammals, these transcription factors are circadian clock outputs, while in zebrafish they are part of the light signaling pathway that influences the circadian clock, among other processes.

1.4.1 Enhancers contribution to light-mediated gene expression

The E-box is the main element through which clock genes control circadian output. The two main positive elements of the TTFL, CLOCK, and BMAL, heterodimerize and bind to the E-box, activating the transcription of various genes. However, the presence of E-boxes close to D-boxes in many clock and DNA repair genes suggests a possible involvement of this enhancer in light-mediated regulation. For instance, mutation of the E-box of the *per2* promoter affects its activation by light [138]. Furthermore, a role in light-mediated gene

expression has been proposed for the AP-1 binding site [35]. The Activator Protein-1 (AP-1) complex is formed by heterodimers of the transcription factors families c-Fos and c-Jun and are involved in the response and regulation of ROS within cells. Based on mice studies within the light-inducibility of *per* and other light-responsive genes in the SCN neurons, the CRE site (cAMP response element) has also been proposed as a mediator of light-induced expression [98], [102]. However, work from my lab has found no role for the AP-1 site in the transactivation of the *cry1a* promoter [107]. CREB (CRE binding protein) is activated by phosphorylation in response to light, and in turn, transactivates the promoters of *per1* and *per2* independently of the E-box [98]. Finally, the E2F enhancer proved to be necessary for the induction of the DNA repair gene *ddb2* in *P. andruzzii* [137]. Interestingly this gene, contrary to most others, retains its light-inducibility in cavefish.

1.5 Experimental Aims

Sunlight-induced transcriptional changes have mostly been observed in circadian and DNA repair genes. However, the full extent of the transcriptional response to sunlight, its evolutionary trajectory, and the underlying regulatory mechanisms remain poorly understood. My project aims to unravel the cellular pathways of response to sunlight in vertebrates. Moreover, I wish to explore how these mechanisms evolve in response to long-term changes in lighting conditions, such as those experienced by the Somalian cavefish *P. andruzzii*. To do so, two main approaches are used. The first approach involves examining the transcriptomes of zebrafish and cavefish cells exposed to visible (blue, 468 nm) and ultraviolet light (20J/m^2 UV-C). This will provide a broad perspective of the effects of light on cell biology. One objective is to obtain a functional overview of the classes of genes regulated by light and in zebrafish cells and to get insights into potential regulatory mechanisms. Which gene classes are responsive to light, and what roles do they play in cellular functions? Do they represent protective mechanisms to counteract sunlight damage, as is the case for photoreactivation? In contrast, the Somalian cavefish model allows me to analyze how evolution in an aphotic environment has influenced these responses. Previous studies show these cavefish have lost several light-dependent functions, so do their cells retain any transcriptional response to light?

The second part of the project focuses on one known light-dependent regulatory mechanism, well studied in my lab: the D-box enhancer found in the promoters of light-regulated clock and DNA repair genes. This element has been demonstrated to be both necessary and sufficient for gene induction upon exposure to light, UV, and ROS. My study aims to further investigate the roles of the D-box and the twelve PAR-bZip and Nfil3 transcription factors in light-mediated gene expression. Does this element regulate other classes of genes in response to light and UV, among those identified by the transcriptomic studies? Do the PAR-bZip and Nfil3 transcription

factors, known regulators of the D-box, play a role in the loss of light-induced gene expression in the blind cavefish?

2. Methods

2.1 Cell culture

Zebrafish (PAC2) and cavefish (EPA) fibroblast cell lines derived from 24hpf embryos were cultured in Leibovitz L-15 medium (Gibco) that was supplemented with 15% (PAC2) or 20% (EPA) Fetal Bovine Serum (FBS, Gibco), 100U/mL penicillin, 100μg/mL streptomycin, and 50μg/mL gentamicin (Gibco) in an atmospheric CO_2, non-humidified incubator at 26°C [139]. Following washing with PBS (Gibco) and detachment with 0.25% Trypsin-EDTA (Gibco), confluent cell cultures were passaged every seven to ten days at a ratio of 1:6. For 96-well plates, 3x10^4 cells/well were seeded. For 24-well plates, 8x10^4 cells/well were seeded. For 6-well plates, 3x10^5 cells/well were seeded.

2.1.1 Light exposure experiments

PAC2 and EPA cells were kept in darkness for 48 hours to dampen the rhythmicity of clock-dependent gene expression and then exposed to up to 6 hours of blue light, or UV-C with recovery in darkness for up to 36 hours. The light sources used are:

- Tungsten white light source (20μW/cm^2)
- Monochromatic blue light emitting diodes (LED, Kopa, 468nm)
- Laboratorial UV light (Vetter GmBH, 254nm)

2.2 Zebrafish larvae experiments

Wildtype WIK zebrafish were maintained at 28°C in water circulation systems, under 12:12 light/dark conditions, and fed twice per day. Husbandry and experimental procedures were performed as described previously [7] following European Legislation for the Protection of Animals used for Scientific Purposes (Directive 2010/63/EU). Crossing was performed according to standard methods. For all experiments, zebrafish embryos were raised in complete darkness, in 28°C incubators in E3 medium, with the addition of 200μM 1-phenyl 2-thiourea (PTU) from 24 hpf onwards. They were exposed to up to 6 hours of blue light at 5dpf. For UV-C treatments, most of the medium was taken away, the larvae were exposed to 450J/m^2 UV-C, then the medium was returned and they were left to recover in darkness for up to 36 hours.

2.3 Gene expression analyses

2.3.1 Total RNA extraction

Cells and zebrafish embryos were collected in 400μL of TRIzol Reagent (ThermoFisher) and stored at -80°C overnight. Total RNA extraction was performed following the manufacturer's instructions. Briefly, the samples were thawed and homogenized by repeatedly forcing them through a 24G or 23G needle, for cells and embryos respectively. Chloroform (80μL) was added, then the samples were vortexed and centrifuged at 4°C and 12000rpm for 15 minutes to achieve phase separation. The clear supernatant was transferred to a new Eppendorf tube and 200μL of Isopropanol was added. After centrifugation, the resulting RNA pellet was washed twice with 75% ethanol, air-dried, and dissolved in 20μL of dH_2O. The total RNA concentration and purity were measured using the NanoDrop OneC (ThermoFisher) and an aliquot was used

for 1.5% agarose gel electrophoresis to check for integrity.

2.3.2 mRNA sequencing and analysis

To prepare samples for mRNA sequencing, zebrafish and cavefish cell samples were collected TRIzol reagent for RNA extraction following light exposure. The experiment was performed in triplicate. Total RNA was extracted as described above and 4μg of each sample was shipped to Novogene (UK) for mRNA sequencing and preliminary bioinformatic analysis. The company performed the sequencing on the Illumina platform as well as subsequent quality control (error rate distribution, GC-content distribution, and data filtering), mapping to the reference genome (for the *D. rerio* dataset), and gene expression quantitation. As there is no available reference genome for the cavefish *P. andruzzii*, *de novo* transcriptome analysis was performed in collaboration with Dr. Sebastian Gornik (COS). A detailed pipeline for the analysis is shown in Figure 2.1. The Trinity software [140] was used to assemble the short reads into full transcripts, which were then quantified and annotated via alignment of the transcripts and longest Open Reading Frame (ORF) against UniProt via Blast-X alignment. Domains were predicted via alignment in the PFAM database. Transcripts within the datasets were quantified and excluded based on the Transcript Per Million (TPM) cut-off of 5. Transcripts were quantified for each sample, and differential expression analysis was performed across all time points, considering transcripts with |logFoldChange| >= 2 and adjusted p-value < 0.001 to be Differentially Expressed Genes (DEGs). Finally, functional enrichment testing was performed via Gene Ontology (GO) analysis on 0h vs. 6h DEGs for blue light exposure samples, 0h vs. 18h, and 0h vs. 36h DEGs for UV-C exposure samples. DEGs were also clustered according to their temporal expression profiles.

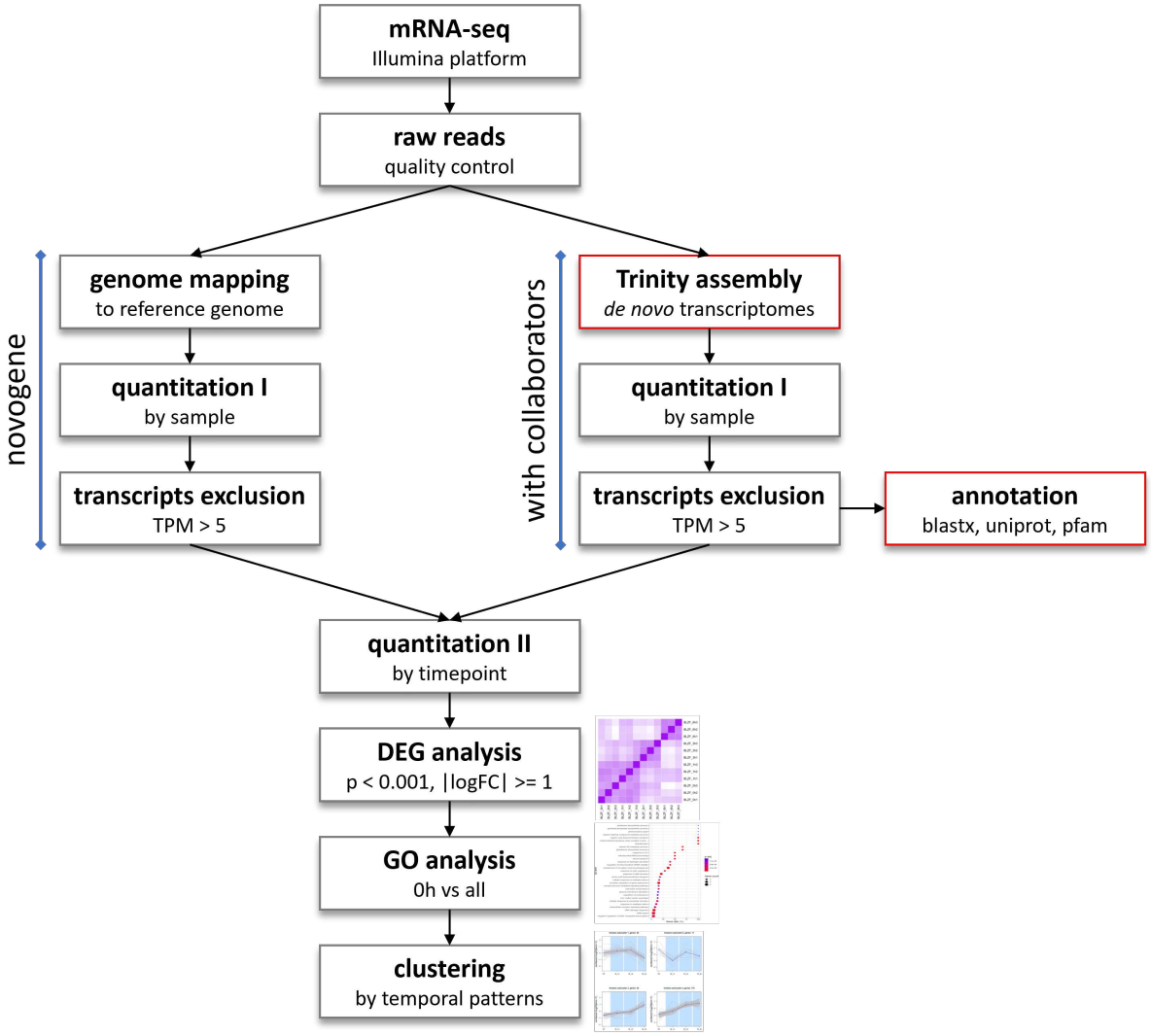

Figure 2.1. mRNA-sequencing analysis pipeline. *D. rerio* datasets, for which a reference genome is available, were subjected to standard transcriptome sequencing analysis (left) as well as *de novo* analysis (right). Cavefish *P. andruzzii* datasets were subjected to *de novo* analysis, as no available reference genome is available. Quantitation, DEG, GO, and clustering analyses and graphs were performed with R software.

2.3.3 Reverse transcription

Reverse transcription was performed starting from 1μg of total RNA. The RNA was incubated with 1U DNase (Promega) and 10U RNase inhibitor (Promega) at 37°C for 30 minutes, followed by the addition of DNase Stop Solution (Promega) and incubation at 65°C for 10 minutes. Random primers (200ng) were added and incubated at 70°C for 5 minutes. The RT reaction was performed with the RevertAid Reverse Transcription kit (ThermoFisher), with incubation

at 25°C for 10 minutes, followed by 60 minutes at 42°C and 15 minutes at 70°C. The resulting cDNA was diluted 1:10 and the quality of synthesis as well as loading was controlled by PCR using β-actin primers.

2.3.4 Quantitative PCR

SyBrGreen (Promega) master mix was used for quantitative PCR analysis in the Real-Time PCR ABI QuantStudio3 qPCR Cycler (ThermoFisher) according to the manufacturer's instructions. Briefly, 5μL of cDNA was mixed with 10μL of SyBr Green master mix, and 5μM forward and reverse primers were used for each reaction. Primers used are shown in Table 2.1. Data were analyzed according to the $2^{-\Delta\Delta CT}$ method and expression of β-actin was used for normalization.

Gene	Direction	Primer sequence 5'-3'
zf abcb6a	Fw	AAGACTTGAAGGTGACGCTG
zf abcb6a	Rv	CCATAGCGGCTGTACCAAAT
zf 6-4 phr	Fw	AATGGCAAGACTCCCATGAC
zf 6-4 phr	Rv	GTGGCCCTAAGGATGACGTA
zf actin	Fw	GATGAGGAAATCGCTGCCCT
zf actin	Rv	GTCCTTCTGTCCCATGCCAA
zf c-myc	Fw	GGCTAGCAACAATCACAGCA
zf c-myc	Rv	ATGCACTCTGTCGCCTTCTT
cf/zf per2	Fw	CCGCAAAGTTTCCTTCGTCA
cf/zf per2	Rv	CATTACTGCCCAGACTCCCA
cf abcb6a	Fw	GAGAGAAGCAGAGAGTTGCCA
cf abcb6a	Rv	CAAGAATCACATCGGCTCC
cf actin	Fw	GATGAGGAAATCGCTGCCCT
cf actin	Rv	GTCCTTCTGTCCCATGCCAA
cf hebp2	Fw	CCGCACTTACCACACAACAA
cf hebp2	Rv	CTTTCACAAGTGGGTCCAGC

Table 2.1. Primers used for real-time qPCR.

2.3.5 mRNA stability assay

To test whether the upregulation of our genes of interest following blue light exposure is due to *de novo* transcription or to post-transcriptional mechanisms, Actinomycin-D was used as an inhibitor of cellular transcription. After two days in darkness, PAC2 cells were treated with 5μg/mL Actinomycin-D (A1410, Sigma-Aldrich) and samples were collected in TRIzol

at regular intervals. cDNA was synthesized from total RNA and RT-qPCR was performed. The relative amount of mRNA present in the samples exposed to blue light and UV-C compared to the controls kept in darkness was used to calculate whether light exposure affected mRNA stability. All primers used are listed in Table 2.1.

2.4 Cavefish PAR-bZip and Nfil3 factors characterization and cloning

2.4.1 Cavefish PAR factors 5' and 3' RACE PCR

The genome of the cavefish *P. andruzzii* is not well characterized and the complete sequences of the PAR b-Zip transcription factors TEF-2, HLF-1, Nfil3-3a, and Nfil3-1b were unknown. Therefore, primers were designed based on the zebrafish mRNA sequences, after identifying regions that are highly conserved across various fish species. These small amplified segments were then sequenced and used to design primers for 5' and 3' Rapid Amplification of cDNA Ends (RACE) PCR (SMARTer RACE 5'/3' Kit, Takara Bio, USA) which was performed according to the manufacturer's instructions. All primers used are listed in Table 2.2. First-strand cDNA synthesis was performed starting from 1μg of total RNA extracted from cavefish cells. Two reactions were prepared, with 5'-CDS Primer A and 3'-CDS Primer A, to generate cDNA ready for the amplification of 5' and 3' ends, respectively. After the addition of the RNA, the reactions were incubated at 42°C for 90 minutes, followed by 10 minutes at 70°C. The resulting cDNA was used for PCR with the provided Universal Primer together with the 5'- and 3'- gene-specific primers, and incubated for 25 cycles at 94°C for 30 seconds, followed by 30 seconds at 68°C and 3 minutes at 72°C. A small aliquot of the amplification products was run on a 1% electrophoresis gel. If no clear bands could be seen, an additional reaction with nested

universal and gene-specific primers was performed to increase the specificity of the amplified ends. Multiple bands instead indicated multiple transcriptional start sites or the presence of different transcripts and variants. Subsequently, the amplified cDNA was purified with the NucleoSpin Gel and PCR Clean-Up Kit (Takara Bio, USA) and ligated to the pRACE vector using the In-Fusion HD Master Mix (Takara Bio, USA). After 15 minutes at 50°C, 2.5μL of each reaction was transformed into 50μL DH5alpha competent cells and plated on ampicillin agar plates. A library was created for each 3' and 5' end reaction and all resulting plasmids were sequenced (Microsynth Seqlab GmbH, Göttingen). The sequences of the cavefish genes were identified by combining the 5' and 3' ends and aligning the resulting sequence with the corresponding zebrafish mRNA sequence.

Gene	Amplification	Primer sequence 5'-3'
cf HLF-1	5' RACE	GATTACGCCAAGCTTGGCCAGAACGTTCTTACAGCGGCCG
cf HLF-1	3' RACE	GATTACGCCAAGCTTGAACCCCATGAAGCTGCCCTTTCACCA
cf HLF-1	5' RACE nested	GATTACGCCAAGCTTCCGGTTACTGCGATCCACCACTGAAGG
cf Nfil3-1b	5' RACE	GATTACGCCAAGCTTGCTTCACGCTTTGGCACCGCAACCT
cf Nfil3-1b	3' RACE	GATTACGCCAAGCTTCCTGCCCAAGGTGATGTTGCTGGGG
cf Nfil3-1b	5' RACE nested	GATTACGCCAAGCTTAGACGCCAAGACAGAGAGGCTTCCCAT
cf Nfil3-1b	3' RACE nested	GATTACGCCAAGCTTATGGGTGGTTTCTTCGTATCGCCACGG
cf TEF-2	5' RACE	GATTACGCCAAGCTTCAATCTGGTTCTCTTTCAGACGCCG
cf TEF-2	3' RACE	GATTACGCCAAGCTTCGGAGGAGATCGAGGTGAACGTGG
cf TEF-2	3' RACE nested	GATTACGCCAAGCTTCCCACAGATCTGGTCCTGTCCAGCGTT

Table 2.2. Primers used for the amplification of 5' and 3' ends of cavefish genes with RACE PCR.

2.4.2 PAR-bZip factors cloning and mutations

Once complete mRNA coding sequences were amplified, they were purified with a ReliaPrep® column (Promega) and cloned into pGEM-T Easy (Promega, storage vector). They were subsequently cloned for expression in eukaryotic cells into the CMV-promoter driven pCS2-MTK vector, for which the start codon was mutated and thereby the coding sequence was inserted in frame with a 5' 5x myc tag sequence (EQKLISEEDL) to ectopically express N-terminally tagged PAR-bZip proteins. cfTEF-1, cfDBP-1, cfHLF-1, cfHLF-2, cfNfil3-2a,

cfNfil3-3a, cfNfil3-1b, and cfNfil3-2b were PCR-amplified from EPA cDNA using primers listed in Table 2.3 and inserted int pGEM-T Easy via TA cloning. All factors were PCR-amplified from the pGEM-T Easy plasmids using a primer containing the mutated start codon and a restriction site, and either T7 or Sp6, depending on the orientation of the sequence (Table 2.4). They were then purified and ligated into the pCS2-MTK vector. The zebrafish PAR-bZip transcription factors had already been cloned in pCS2-MTK vectors [123].

Gene	Direction	Primer sequence 5'-3'
cf HLF-1	Fw	GCGATGGAGAAGATGGAGAAGA
cf HLF-1	Rv	GTTGGGGGCTCACAGAGGG
cf TEF-2	Fw	GATAATATCGCGCTAATGATGCCC
cf TEF-2	Rv	GAAGCGTGTCCCTCACAGTGAG
cf Nfil3-1b	Fw	TGAAAATGGAGTCTGCTTTC
cf Nfil3-1b	Rv	TCAATCTGACAAGTACACTGG
cf Nfil3-2a 1	Fw	AGGAGCAATGGAAAGTTTGAGC
cf Nfil3-2a 1	Rv	GGTTTCTTGGCGTTGTTGCT
cf Nfil3-2a 2	Fw	AGCACAATTTTGAGTCAGGT
cf Nfil3-2a 2	Rv	TTGTTTAGTCATGTCTCTTTTTACA
cf Nfil3-2b 1	Fw	TCTTTGGAGGAAAAAGCAGAAGC
cf Nfil3-2b 1	Rv	ACCTGCTCCATGTCCTCAAC
cf Nfil3-2b 2	Fw	ACCCCAAAGAAGCGTCATCC
cf Nfil3-2b 2	Rv	TCAATAGGATGGAAAGGTGACA
cf Nfil3-3a	Fw	CACACACTAACTCAAAGCATGAAGG
cf Nfil3-3a	Rv	GTGGGACAGATGATTTCAGTTCAC

Table 2.3. Forward and reverse primers for TA cloning of cDNA sequences in pGEM-T Easy vector backbone.

Gene	Direction	Primer sequence 5'-3'	Res. Site
cf DBP-1	Fw	CCTCCAAGCCAATTTCTCAG	StuI
cf DBP-1	Rv	CCTCAAAGATCTCCGTGGCGG	StuI
cf DBP-2	Fw + T7	CGCGAATTCACTAGTGATTTGTTGGCCAGG	EcoRI
cf HLF-2	Fw + T7	TAACGAATTCTTGTCTAGACAGCTC	EcoRI
cf TEF-1	Fw + Sp6	GGGAATTCGATTCTCGGACAAACTTGGAC	EcoRI
cf TEF-2	Fw + T7	CTAGTGAATTCATCGCGCTATTGATGCCC	EcoRI
cf Nfil3-1a	Fw + T7	CGCGAATTCACTAGTGATTTGCAAGCCA	EcoRI
cf Nfil3-1b	Fw	GAATTCGATTTGAAACTCGAGTCGCTTTC	XhoI
cf Nfil3-1b	Rv	GCGAATTCTCGAGTGATTTCAATCTGACAA	XhoI
cf Nfil3-2a	Fw + T7	GAATTCGATTAGGCCTCATTGGAAAGTTTG	StuI
cf Nfil3-2b	Fw + Sp6	CTTAAAAGGCCTATTTGGAAAGCCTAA	StuI
cf Nfil3-3a	Fw	CACACACTAACTCGAGGCTTGAAGGACC	XhoI
cf Nfil3-3a	Rv	GATTTGTGGCTCGAGATGATTTCAGTTCAC	XhoI
cf Nfil3-3b	Fw + Sp6	CGCGGGAATTCGATTTGTCTTTCACCA	EcoRI
sp6		TATTTAGGTGACACTATA	
T7		TAATACGACTCACTATAGGG	

Table 2.4. Forward and reverse primers to amplify cDNA sequences from pGEM-T Easy vector and cloning into pCS2-MTK vector backbone.

2.4.3 Plasmid DNA extraction

Minipreps and maxipreps were prepared using the Qiagen Kit, starting from 3mL or 100mL, respectively, of liquid cultures of bacteria grown overnight in Luria Bertani (LB) medium supplied with 100μg/ml ampicillin. The resulting plasmid DNA pellets were resuspended in distilled water, their purity and concentration measured with the NanoDrop, and sequenced to confirm insertion of the desired sequences and eventual mutations.

2.4.4 Western Blot analysis

PAC2 and EPA cells were seeded in 6-well plates and 1μg of the PAR-bZip and Nfil3 transcription factors was transfected. After 48 hours, the cells were washed with PBS, lysed in 200μL 1x Passive Lysis Buffer (Promega), collected in cold 1.5ml Eppendorf tubes, and stored at -80°C. Protein content was quantified using the BCA Protein Assay Kit (Pierce™, ThermoFisher), 20μg were diluted in Laemmli buffer containing 100mM DTT and boiled for 5 minutes. They were then loaded on 10% polyacrylamide-SDS gels and blotted on an Immobilon®-P PVDF membrane (Merck Millipore). After 1 hour at RT in blocking solution of TBS + 0.1% Tween-20 (Carl Roth) and 5% non-fat dry milk powder, the membranes were incubated in blocking solution containing 1:1000 primary antibody (Anti-Myc tag monoclonal antibody, Millipore) overnight, followed by one hour in the secondary antibody, diluted 1:7500 (Goat Anti-mouse polyclonal antibody, Cell Signaling). The chemoluminescent signal was detected using the Clarity Western ECL system (Bio-Rad). Following thorough washing, these steps were repeated with the b-actin primary antibody diluted 1:10000 and secondary antibody (Goat Anti-mouse polyclonal antibody) for normalization.

2.5 Promoter bioinformatic analysis and cloning

Promoter regions 1kb upstream of the Transcription Start Site (TSS) plus the 5' Untranslated Regions (UTR) of genes were retrieved using BioMart from Ensembl (GRCz11). Clover [141] was used to screen the promoters for putative D-box and E-box sequences. The promoters of zebrafish *hebp2*, *abcb6a*, and *soul5*, containing D-box-like and E-box-like motifs, were cloned into the pGL3Basic (Promega) luciferase expression vector, which does not contain a eukaryotic promoter sequence. The fragments were PCR-amplified from PAC2 genomic DNA using primers containing a HindIII restriction site and ligated into the HindIII-cut vector. All primers used are listed in Table 2.5. Smaller fragments of *hebp2* (144bp) and *soul5* (189bp) promoters were cloned into pTAL-pLUC, a modified version of the minimal promoter luciferase expression vector pLucMCS (Stratagene). All primers used are listed in Table 2.6.

Promoter	Direction	Primer sequence 5'-3'
zf abcb6a	Fw	GCATAAATAGATCAAAAAGCTTGATAGGTAACAG
zf abcb6a	Rv	GTCACCTTCAAGCTTTCGAGTGC
zf hebp2	Fw	GTTTTTTAAAGAAGGAAGCTTGTGTAATTTTC
zf hebp2	Rv	CTGTTGACAAGCTTAAAAGCAGAAAGC
zf soul5	Fw	CAGTCTGTAGTCAAAAGCTTGTGAATG
zf soul5	Rv	GAATTTTGTAAGCTTCAGGCTGAGCA

Table 2.5. Primers used to clone promoter constructs in luciferase reporter vector pGL3.

Promoter	Direction	Primer sequence 5'-3'
zf hebp2	Fw	TCGTCACAACCAATCGGTACCTTC
zf hebp2	Rv	CGCTGTTAAATAACGCTAGCGCTTAAG
zf soul5	Fw	AAGCAGGTACCGTGATTTTTTTCTTTTGTTAC
zf soul5	Rv	GCTTAGCTAGCAAGAGAGAGGAAACGTGTG

Table 2.6. Primers used to clone promoter constructs in luciferase reporter vector pTAL-pLUC from pGL3 vector.

Single D-box and E-box sequences of the *hebp2* promoter were mutated (4-7bp) using the Q5® Site-Directed Mutagenesis kit (Promega), to completely scramble the enhancer sequence and insert a restriction enzyme site to easily identify mutants. The enhancer sequences were mutated (bold) as follows:

- D-Box 1 mutation: AGTGATGTAACAT → AG**C**GA**C**GT**CG**CAT (AatII site)
- D-Box 2 mutation: CGTTACTTAAG → CG**C**G**A**G**C**T**CC**G (SacI site)
- D-Box 3 mutation: GTTATTTAAC → G**C**G**A**G**T**A**CT**C (ScaI site)
- E-Box mutation: GCGCGTGTGT → **CAGGATCCGA** (BamHI site)

The primers used for site-directed mutagenesis can be found in Table 2.7. Due to the closeness between the second and third D-box sequences, new primer pairs were necessary for the second round of mutations to match the mutated sequences.

Mutation	Direction	Primer sequence 5'-3'
D-box 1 mut	Fw	TCGCATGAAAACACGGAAGTAGTCCTGTC
D-box 1 mut	Rv	CGTCGCTCCCATGCGAAGGCTCCG
D-box 2 mut	Fw	CTCCGCGTAGAGTTATTTAACAGCG
D-box 2 mut 2	Fw	CTCCGCGTAGAGCGAGTACTCAG
D-box 2 mut	Rv	CTCGCGCTGACAGGACTACTTCCG
D-box 3 mut	Fw	TACTCAGCGAAACTGTATATTCTC
D-box 3 mut 2	Fw	TACTCAGCGAAACTGTATATTCTCTATCTAAGCGTTATAACAC
D-box 3 mut	Rv	CTCGCTCTACGCTTAAGTAACGC
D-box 3 mut 2	Rv	CTCGCTCTACGCGGAGCTCGCGC

Table 2.7. Primers used for mutations to the D-box and E-box sequences zf *hebp2* promoter in pTAL-pLUC.

2.6 Cell transfection and bioluminescence assays

Transfection was performed 24 hours after seeding, using FuGene HD (Promega) according to the manufacturer's instructions. For *in vivo* experiments, 25-100ng of the luciferase reporter plasmid containing the promoter of interest was transfected in each well of a 96-well plate. After 24 hours 0.5mM D-Luciferin Firefly, potassium salt (L-8220, Biosynth) was added to the culture medium, and bioluminescence was measured automatically using a Topcount NXT counter (Perkin Elmer). Cells were either exposed to 12:12h light:dark cycles, or kept in darkness and treated with 1mM hydrogen peroxide 24 hours after a D-luciferin medium change.

Data was analyzed using the Microsoft Excel macro "Import and Analysis" (S. Kay, Scripps Research Institute) and plotted with R software. For *in vitro* experiments, cells were seeded in a 24-well plate and transfected with 50-200ng of the luciferase reporter vector, 50ng of the β-galactosidase expression vector (pcDNA3.1/myc-His/lacZ, Invitrogen), and 1ng of the pCS2-MTK expression vector containing the transcription factor of interest. After 48 hours in complete darkness, the cells were lysed using Firefly Lysis Buffer (0.1M Tris acetate pH 7.5, 2mM EDTA, 1% Triton X-100). The cell lysates were used for luciferase assay using the Luciferase Assay System kit (Promega) and luciferase activity was measured using a VICTOR Multilabel Plate Reader (Perkin Elmer). The β-galactosidase assay served as normalization for transfection efficiency.

2.7 Heme assays

Cells were seeded in 6-well plates. Following one wash in PBS, cells were collected via trypsinization (125μL Trypsin stock solution and 500μL PBS), followed by centrifugation at 4000xg for 5 minutes. After removing the supernatant, pellets were stored at -80°C until use. Before use, pellets were lysed in 100μL PBS + 0.1% Triton X 100 (Carl Roth) + 0.1% Protease inhibitors (P8340, Sigma-Aldrich), sonicated for 10s at a low setting, and centrifuged at 12000xg for 5 minutes, at 4°C to remove cell debris. Protein quantification was performed with Pierce BCA assay according to the manufacturer's instructions. Hemin (Sigma-Aldrich) solutions were freshly prepared in 100% DMSO for the oxalic acid assay and in 0.1N NaOH for the regulatory heme assay. Concentrations were measured using a millimolar extinction coefficient of 180 at 400nm for DMSO and 58.4 at 385nm for NaOH.

2.7.1 Oxalic acid assay for total heme quantification

For quantification of total heme in cells, a slightly modified version of the protocols from Sassa [142] and Sinclair [143] was used. Briefly, cell lysates (10μg) were mixed with 500μL 2M oxalic acid (Sigma-Aldrich) and split in half. One half was heated at 95°C for 30 minutes to allow removal of the iron ion from heme, resulting in protoporphyrin IX, a fluorescent molecule. The other half was kept in darkness at RT and served as a control for the presence of endogenous protoporphyrin IX. The fluorescence of samples as well as heme standards (0nm-2μM in DMSO) was measured with a spectrophotometer (SpectraMax iD3, USA) with excitation at 400nm and emission at 620nm. The values of unheated samples were subtracted from heated ones and the standard curve was used to quantify heme. Zebrafish embryos (10 per sample) were collected at 5dpf and washed with PBS before the addition of 500μL 2M oxalic acid.

2.7.2 Regulatory heme HRP assay for free heme quantification

For quantification of free heme, the RH assay protocol by Atamna and colleagues [47] was used. Briefly, 10mg of the enzyme Horseradish Peroxidase (holo-HRP, 150U/mg, Sigma-Aldrich) was inactivated via two acid-acetone treatments leading to the removal of heme. The resulting apo-HRP was resuspended in PBS and the concentration was determined using a molar extinction coefficient of 20000 at 280nm before dilution to 50μM and storage at -20°C. Cell lysates (10μg protein) and heme standards (0-2.5nmol in 0.1N NaOH) were diluted to 100μL with PBS and 5μM apo-HRP. After 10 minutes at 4°C to allow reconstitution to the active enzyme holo-HRP by binding to heme, the activity of holo-HRP was measured by mixing 10μL of each sample with 200μL TMB solution (1-Step TMB Elisa Substrate Solution, ThermoFisher), and the absorbance was measured at 652nm.

2.8 MTT assay

Cell viability and metabolic activity were measured with the MTT (3-(4,5-dimethylthiazol-2-yl)-2,5-diphenyltetrazolium bromide, Sigma-Aldrich) assay. Cells were seeded in 96-well plates and exposed to light the next day or kept in darkness. At each time point, cells were washed once with PBS and incubated for four hours in darkness with 0.5mg/mL MTT in L-15 medium. After medium removal, 200μL 100% DMSO was added and incubated for five minutes in darkness in oscillation. Absorbance at 590nm was measured with the SpectraMax iD3 spectrophotometer.

2.9 Statistical analysis

Data analysis and graphs were made using R software and InkScape. All results are expressed as means $\pm$ Standard Error of the Mean (SEM). ANOVA with multiple comparisons post-hoc tests (Tukey HSD) or t-tests with Bonferroni corrections were used to determine significance. Values of $p<0.05$ were considered statistically significant, and values of $p<0.05$, $p<0.001$, $p<0.001$ are represented in graphs by *, **, ***, respectively. Detailed statistical information can be found in the Supplementary tables.

3. Results

3.1 mRNA-sequencing experiments

As a first step, my goal was to define the light- and UV-induced transcriptome in the zebrafish and cavefish cell lines. In conventional mRNA-sequencing analysis, the short reads (150bp) produced by Illumina sequencing are aligned to a reference genome and quantified. However, contrary to *D. rerio*, no annotated genome is available for the cavefish *P. andruzzii*. The use of *de novo* analysis was therefore required for the cavefish datasets. In collaboration with Dr. Sebastian Gornik (COS, Heidelberg), Trinity software was used to reconstruct full transcripts, or "pseudo-genes", from the short reads. The resulting transcripts and the amino acid sequences translated from the longest Open Reading Frames (ORFs) were used for annotation, by aligning them to the UniProt database. Domains were identified via alignment to the pFAM database. For quantification purposes, raw reads were aligned to the transcripts. The *de novo* annotation led to a confident annotation of 39.5% of the transcripts for the zebrafish transcriptome and 43.5% for the cavefish transcriptome. To ensure the validity and reliability of the *de novo* analysis for the cavefish dataset and to allow for direct comparison of the two species, a dual approach was used. Both conventional and *de novo* analyses were performed on the zebrafish dataset and the results were compared. The cavefish dataset was then directly compared to the zebrafish *de novo* data.

I carried out two mRNA-sequencing experiments to characterize and compare the transcriptomic response of zebrafish PAC2 and cavefish EPA embryonic cell lines after exposure to sunlight (Figure 3.1). The sunlight stimulus was deconstructed into two parts. For the visible spectrum, blue light (468nm) was chosen, as it has been shown to be important

for organisms to synchronize their clocks [104] and is among the preferred wavelengths for photoreactivation [144], [145]. UV-C was chosen as a major environmental stressor. Although under natural conditions only very limited levels of UV-C reach the Earth's surface, UV-C irradiation is commonly used as a strong signal in laboratory experiments designed to test the general effects of UV radiation. Both stimuli have previously been shown to lead to the strong upregulation of various circadian clock and DNA damage repair genes [146].

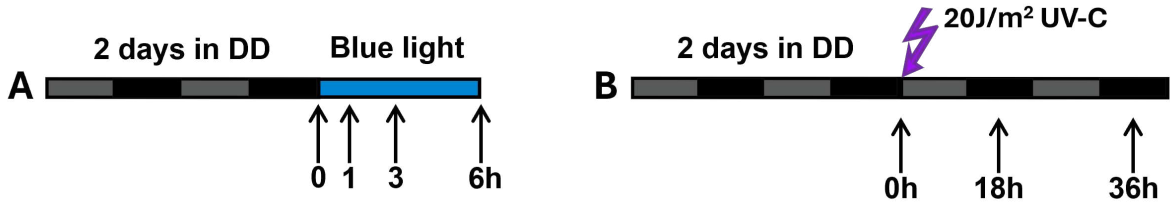

Figure 3.1. Overview of the two mRNA-sequencing experiments. A) Blue light exposure experiment. Zebrafish and cavefish cells were maintained in constant darkness (DD) for 48 hours, then exposed to blue light (468nm) for up to six hours. Samples were collected at four time points: nonexposed (0 hours) and after 1, 3, and 6 hours of blue light exposure. **B) UV-C exposure experiment.** Zebrafish and cavefish cells were maintained in constant darkness for 48 hours, then exposed to a 20J/m^2 UV-C pulse followed by 36 hours in darkness. Samples were harvested at three time points: nonexposed (0 hours), 18, and 36 hours after UV-C irradiation. The experiment was performed three times independently.

3.1.1 Transcriptomic response to blue light in zebrafish cells

For the blue light exposure mRNA-sequencing experiment zebrafish PAC2 and cavefish EPA cells were seeded and kept in darkness for two consecutive days to dampen circadian clock-dependent gene expression. They were then exposed to up to 6 hours of blue light (468nm). Samples were collected in TRIzol before treatment (0h) and after 1, 3, and 6 hours. These time points were selected based on previous studies that have characterized the dynamics of light-induced gene transcription related to the circadian clock and DNA repair pathways [7], [107]. The experiment was performed in triplicate. After total RNA extraction, samples were sent for sequencing by Novogene, which also performed quality control (QC) of the raw reads, alignment to the genome, and quantification for the zebrafish dataset. Raw reads were used for

de novo analysis of both zebrafish and cavefish datasets. mRNA transcripts were quantified and Differentially Expressed Genes (DEGs) were identified across all time points (p.adj < 0.001 & |logFoldChange| > 1). These genes were used for further analyses and characterization of the transcriptional response to blue light of zebrafish and cavefish cells.

To assess the variability and reproducibility of biological replicates, Principal Component Analysis (PCA) was performed to visualize the overall expression patterns and identify clusters of samples based on their differential expression profiles. The plot in Figure 3.2 (left panel) illustrates the PCA results, where each dot represents one sample. The first two principal components (PC1 and PC2) explain most of the variance, 51% and 38%, respectively. The biological triplicates cluster tightly together, a sign of high similarity between them and the reproducibility of the experiment. The samples clustered in three main groups, correctly reflecting the different time points. The 0 and 1-hour samples are not too dissimilar from each other. Samples of 3 and 6 hours are distinctly separated from this cluster along the y-axis and x-axis, respectively, highlighting differences in gene expression profiles due to blue light treatment. The correlation matrix (Figure 3.2, right panel) also reveals a high correlation between the biological replicates and overall similarity between the control (0h) and 1 hour of blue light. There is a low correlation between 3 and 6 hours of treatment and between each group and the 0 and 1-hour samples. Both plots suggest consistent gene expression profiles within triplicates throughout blue light exposure and strong changes in gene expression after 3 and 6 hours of the treatment.

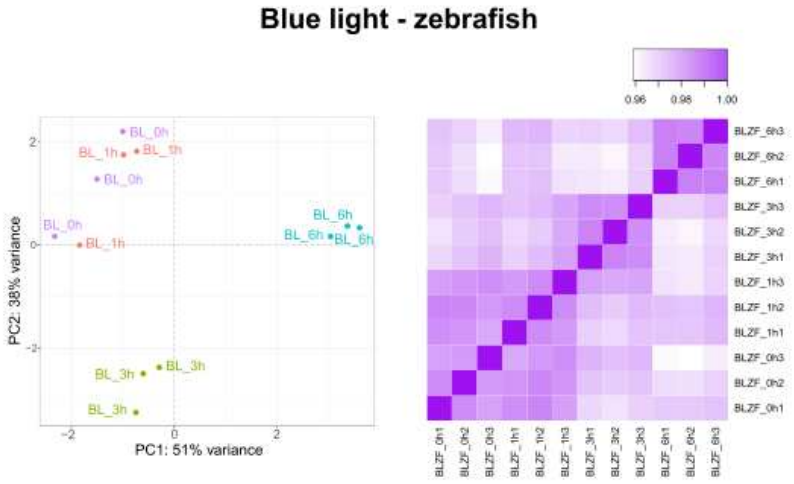

Figure 3.2. Comparative analysis of samples of zebrafish cells exposed to 0-6 hours of blue light. PCA plot (left) demonstrates the distribution of sample replicates. The x-axis represents the first principal component PC1, capturing 51% of the variance, and the y-axis represents PC2, accounting for 38% of the variance. The correlation matrix (right) illustrates Spearman correlation coefficients between all pairs of sample replicates.

I identified differentially expressed genes as having a |logFoldChange| > 1 and p.adj < 0.001, adjusted for multiple comparisons. A total of 331 genes were differentially expressed in zebrafish cells at either 1, 3, or 6 hours of blue light exposure compared to the control kept in darkness. Figure 3.3 illustrates the amounts of DEGs at each time point. After 1 hour of exposure, there is a minimal transcriptomic response (five upregulated and seven downregulated genes), while at 3 and 6 hours many more significantly upregulated genes are identified (135 and 273 respectively). Downregulated genes remain low (14 and 19) at these time points. Volcano plots of the DEGs at different time points further reveal the magnitude of changes in gene expression levels in response to blue light (Figure 3.4). At 1 hour of exposure, very few genes are significantly up- and down-regulated (y-axis) and with low magnitude (x-axis, log fold changes between -3 and 3). On the other hand, various genes are strongly regulated after 3 and 6 hours of exposure. Among the most strongly expressed genes are clock-related genes *per2*, *cry1a*, *lonrf1*, and *lonrf1l*, as well as DNA-repair genes *xpc* and *6-4 phr*. These genes are known to be upregulated in response to light. *Per1b*, a clock-related gene, is instead downregulated at 6

hours, consistent with its decreased expression levels during the daytime compared to darkness [147].

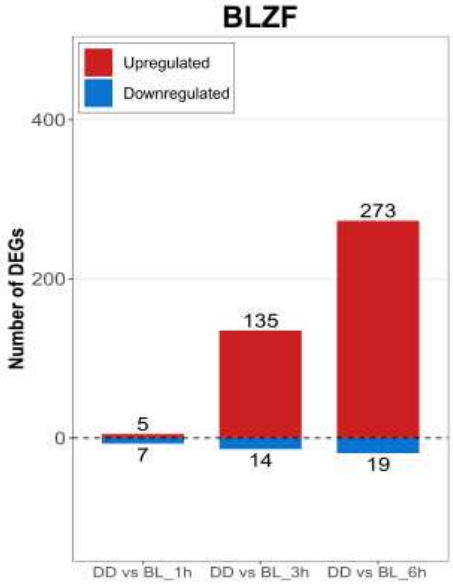

Figure 3.3. Differential expression analysis over time of blue light exposure compared to control in zebrafish cells. Bars represent the numbers of DEGs (p-adj < 0.001, |logFoldChange| > 1) at 1, 3, and 6 hours of blue light (BL) compared to DD controls. Red bars indicate upregulated genes and blue bars indicate downregulated genes.

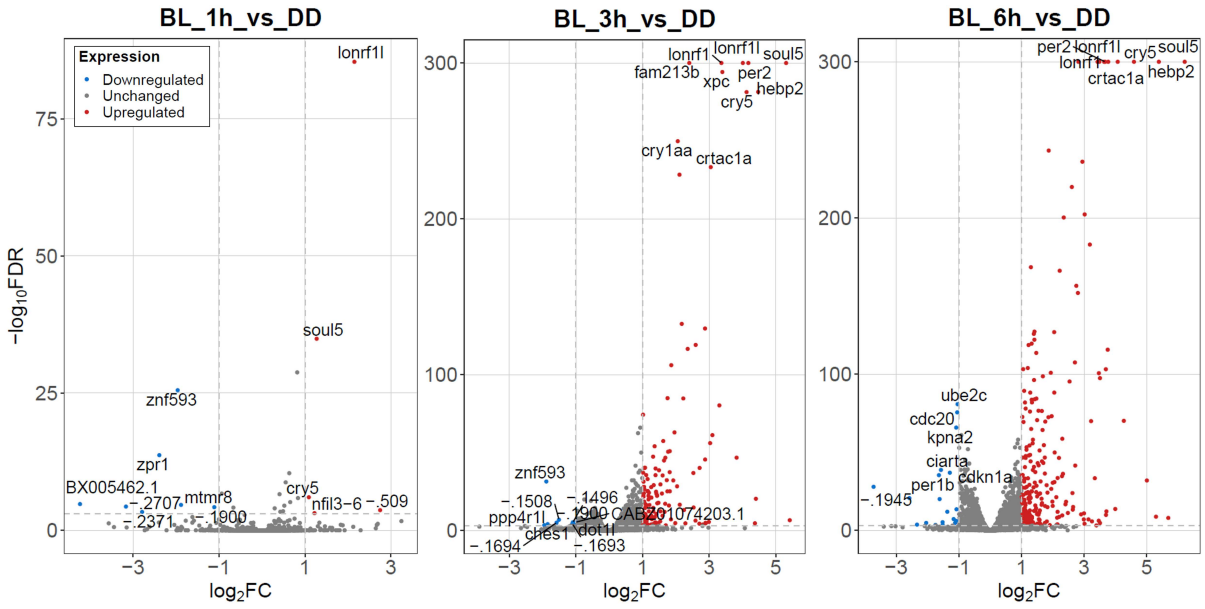

Figure 3.4. Volcano plots highlighting DEGs over time of blue light exposure compared to control, in zebrafish cells. The x-axis displays the $\log_2$ fold change ($\log_2$FC) which indicates the magnitude of change in expression. The y-axis reflects statistical significance of the differential expression, shown by the $\log_{10}$ of the p-value adjusted for multiple comparisons (False Discovery Rate, FDR). Upregulated genes are shown in red, downregulated genes in blue, and unchanged genes in grey. The most strongly regulated genes are labeled.

3.1.1.1 Functional characterization of DEGs after blue light exposure in zebrafish cells

Gene Ontology (GO) analysis was performed on the DEGs upregulated at 6 hours compared to the control (Table S2). Besides the expected circadian clock and DNA repair genes, the analysis revealed significant enrichment of 63 genes related to mitochondria structure and function, as well as to heme biosynthesis and metabolism (Figure 3.5). A total of 700 genes significantly regulated between any time point were identified. The DEGs were clustered using the unsupervised k-means method, according to their temporal expression patterns throughout exposure to blue light (Figure 3.6). Clusters 4, 5, and 6 show significantly upregulated genes across time points with varying degrees of change, and Cluster 2, accounting for most of the DEGs, represents genes upregulated at 6 hours only. Cluster 1 shows genes downregulated at 6 hours, and Cluster 3 groups the few genes with a general trend of downregulation. Upon closer inspection, I found the mitochondrial and heme-related zebrafish genes belong to the same clusters as the 18 identified clock and DNA repair genes (Clusters 4 and 5) and are similarly upregulated at 3 and 6 hours (Figure 3.7). The zebrafish genes *abcb6a*, *hebp2*, and *soul5*, highlighted in red in the heatmap, were selected to represent the class of mitochondria and heme-related genes in further experiments aimed to explore the transcriptional control mechanisms operating on this class of genes.

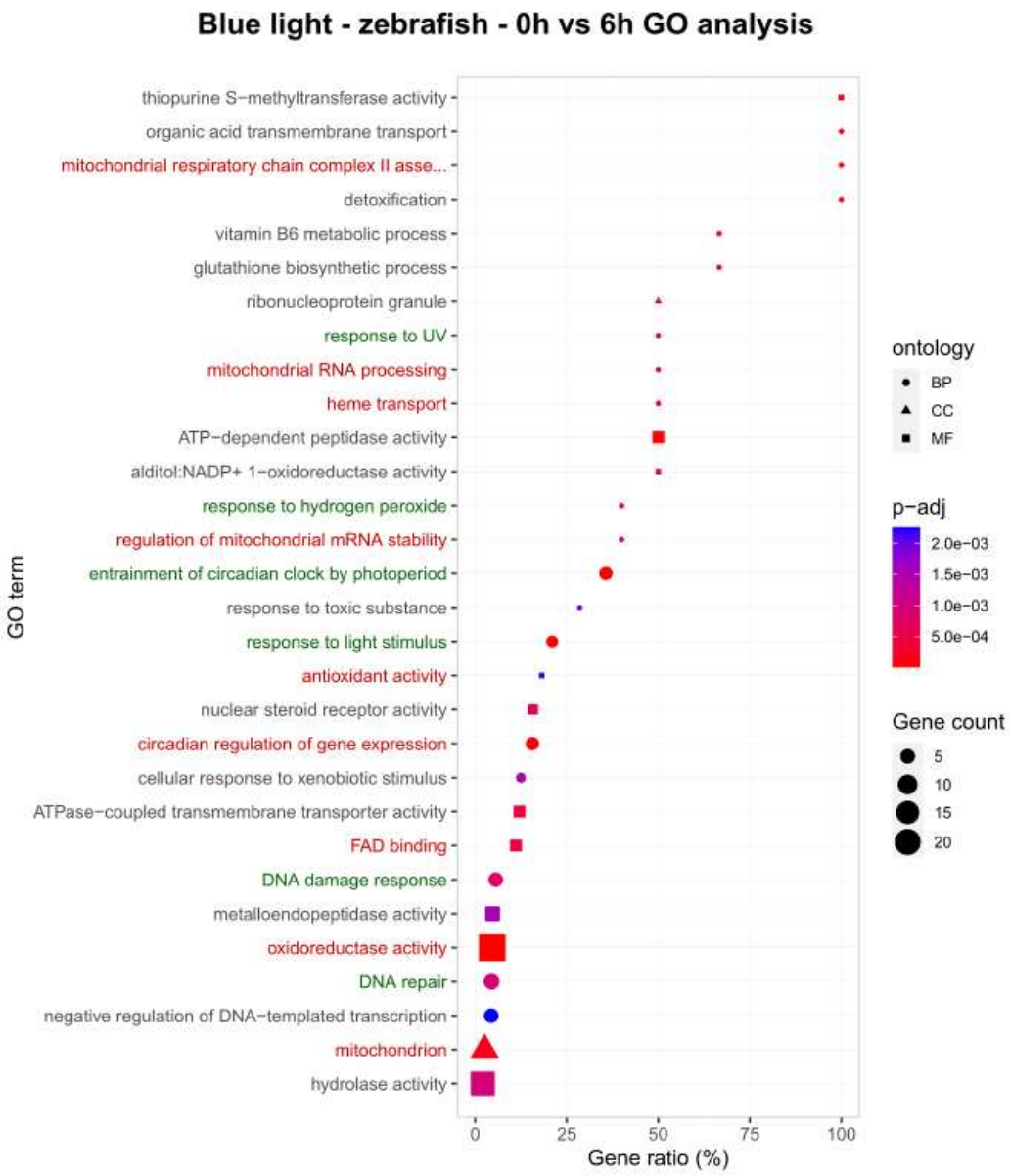

Figure 3.5. Gene Ontology (GO) analysis of DEGs at 6 hours of blue light compared to DD control, in zebrafish cells. The chart summarizes the enriched GO terms across the ontologies Biological Process (BP), Cellular Component (CC), and Molecular Function (MF). Only the 30 most significantly enriched terms are listed on the y-axis, the x-axis indicates the percentage of upregulated genes within their specific category. The size of the shapes indicates the number of upregulated genes for each category, and the shape indicates the ontology. The color indicates the adjusted p-value (p-adj) in a gradient from blue (highest p-value) to red (lowest p-value).

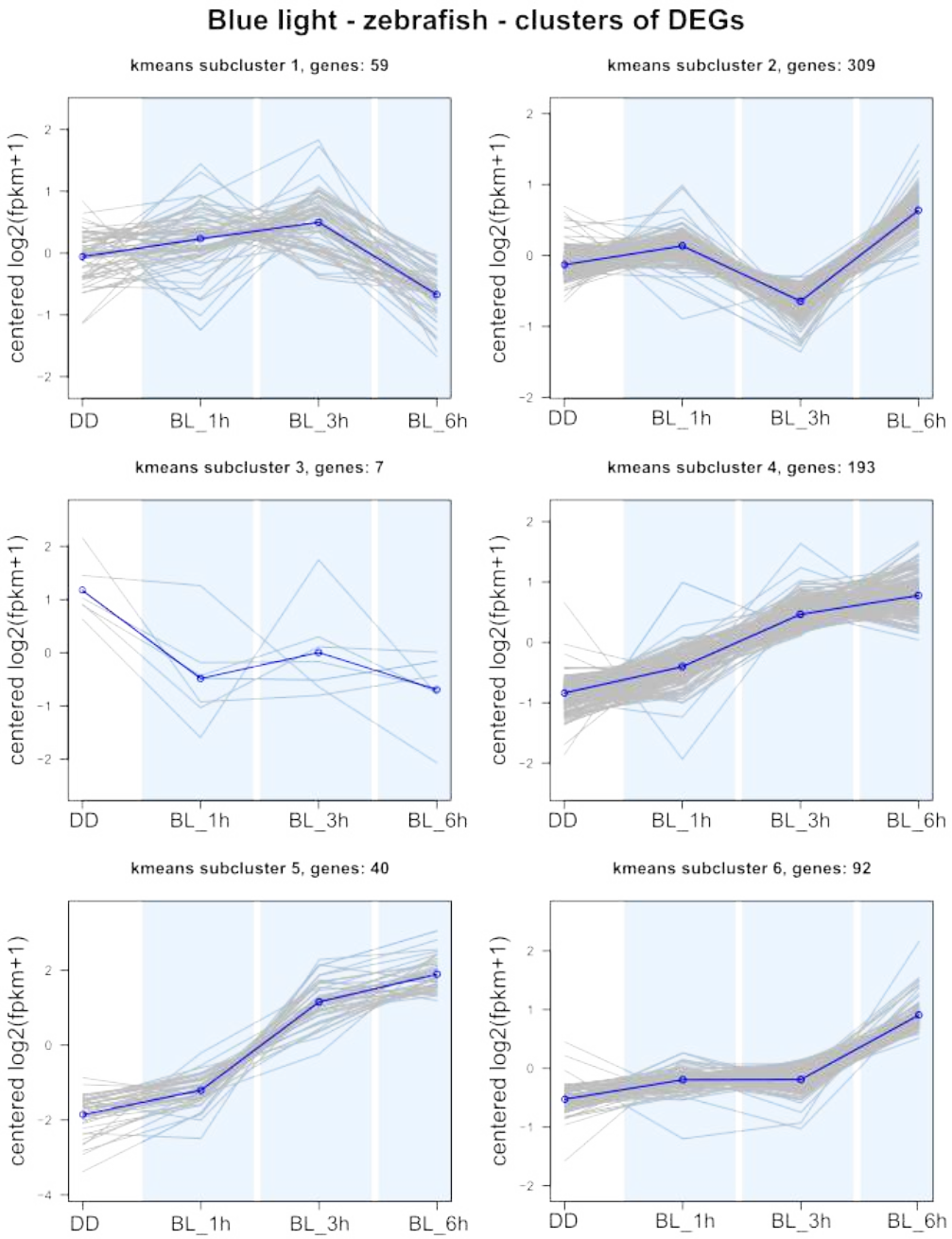

Figure 3.6. Temporal expression patterns of DEGs during blue light exposure in zebrafish cells. Significant DEGs were clustered using the unsupervised k-means clustering method, according to their temporal expression patterns throughout blue light exposure. The y-axis represents centered $\log_2$-transformed expression levels (normalized Fragments Per Kilobase per Million mapped reads, FPKM) while the x-axis represents time of blue light exposure. Individual genes are plotted in grey lines, while the blue line indicates the overall mean expression profile of the cluster.

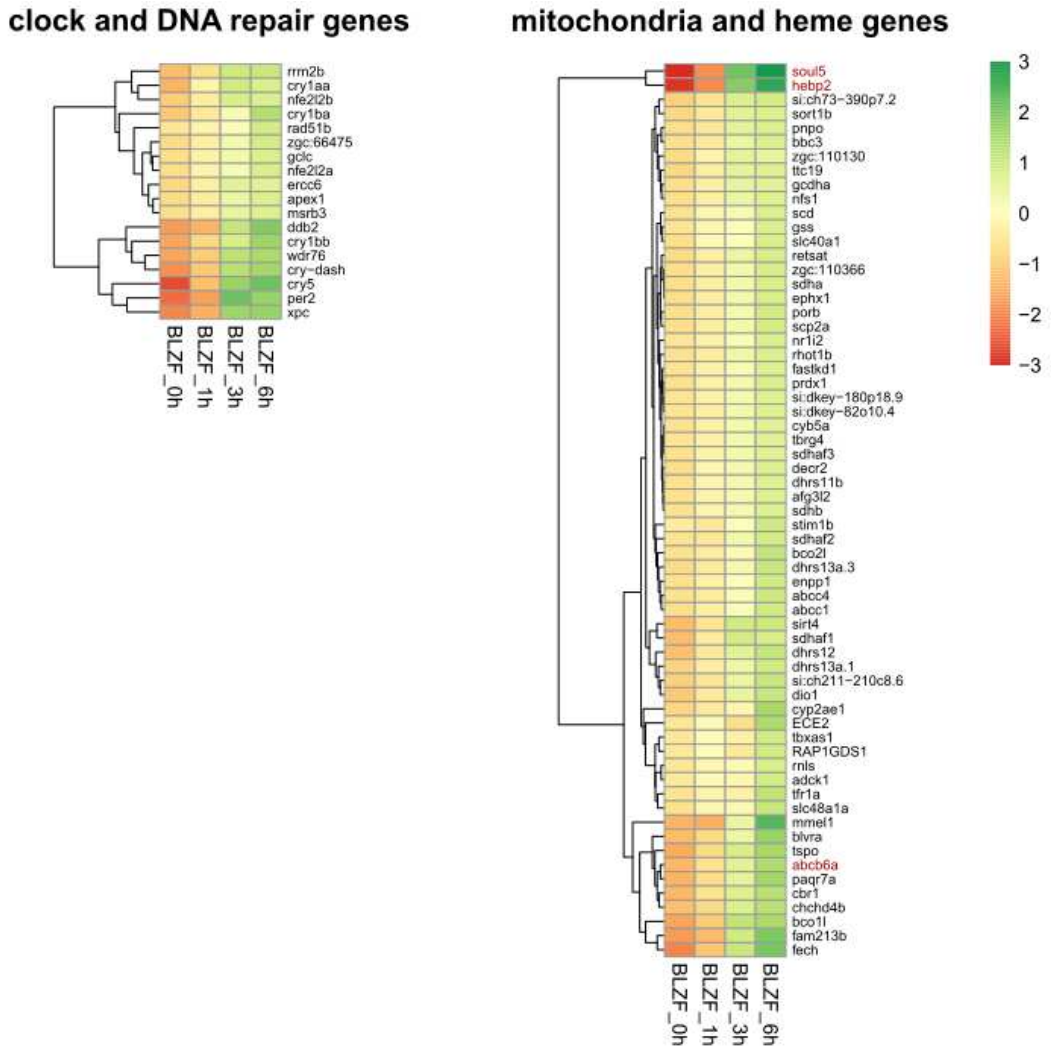

Figure 3.7. Heatmaps displaying temporal patterns of significantly upregulated genes in response to blue light, belonging to the category of clock and DNA damage repair (left) and the identified class of mitochondrial and heme-related genes (right). The color scale represents $\log_2$-transformed expression values, with red indicating downregulation and green upregulation across the different time points (y-axis). Each row represents an individual gene and the dendrogram illustrates hierarchical clustering based on strength and expression profile. The two groups show similar expression patterns of upregulation in response to blue light. Genes of interest are shown in red (right).

3.1.2 Zebrafish and cavefish cells - transcriptomic response to Blue light *de novo* analysis

I analyzed the zebrafish and cavefish datasets resulting from the *de novo* RNA-sequencing protocol in the same way as the original zebrafish dataset. To assess the variability and reproducibility of biological replicates PCA was performed to visualize the overall expression patterns and identify clusters of samples based on their differential expression profiles. The

plot in Figure 3.8 (left panel) illustrates the PCA results for zebrafish cells, where each dot represents one sample. The first two principal components PC1 and PC2 explain 31% and 13% of the variance, respectively. The biological triplicates cluster tightly together, a sign of high similarity between them and an indication of the reproducibility of the experiment. Overall the samples clustered in three main groups, correctly reflecting the different time points. The 0 and 1-hour samples are not too dissimilar from each other. Samples of 3 and 6 hours are distinctly separated from this cluster along the y-axis and x-axis, highlighting differences in gene expression profiles due to blue light treatment. The correlation matrix (Figure 3.8, right panel) also reveals a high correlation between the biological replicates and overall similarity between the control (0h) and 1 hour of blue light. There is a low correlation between 3 and 6 hours of treatment and between each group and the 0 and 1-hour samples. Both plots suggest consistent gene expression profiles within triplicates throughout blue light exposure and strong changes in gene expression after 3 and 6 hours of the treatment. Furthermore, they reveal similar results to the zebrafish data analyzed with the standard RNA-sequencing pipeline, thus ensuring the validity and reliability of the *de novo* analysis for the cavefish dataset. The PCA for the cavefish dataset already reveals some differences in the response of these cells to light compared to zebrafish cells. The first principal component PC1 captures 15% of the variance, while PC2 accounts for 12% of the variance. Replicates of each timepoint tend to cluster together, indicating similarity between triplicates and the reproducibility of the experiment. Modest correlation within triplicates across different time points and low correlation between time points are observed. The correlation matrix (right) shows a generally higher correlation across all samples and no clear differences across time points. Both graphs indicate a generally lower strength of the response to blue light in cavefish cells compared to zebrafish cells.

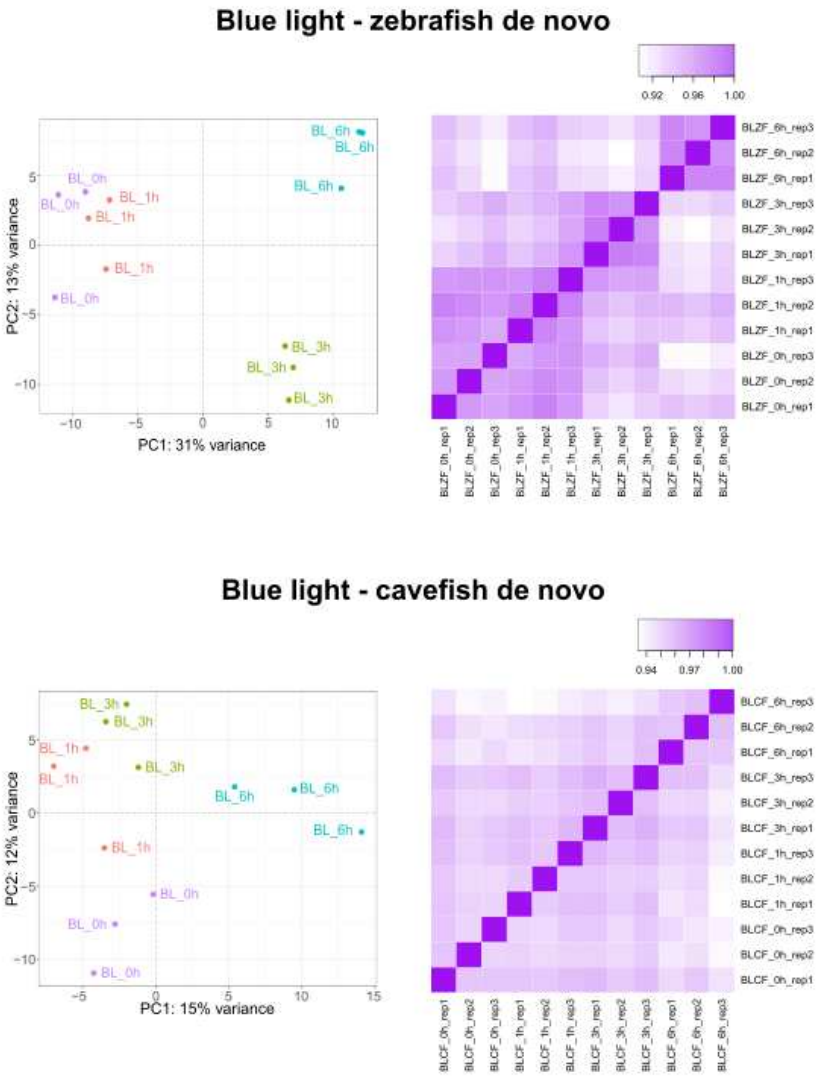

Figure 3.8. Comparative analysis of samples of zebrafish cells (top) and cavefish cells (bottom) exposed to 0-6 hours of blue light. PCA plot (left) demonstrates the distribution of sample replicates while the correlation matrix (right) illustrates Spearman correlation coefficients between all pairs of sample replicates. **Zebrafish (top):** The first principal component PC1 (x-axis) captures 31% of the variance, while PC2 (y-axis) accounts for 13% of the variance. **Cavefish (bottom):** The first principal component PC1 (x-axis) captures 15% of the variance, while PC2 (y-axis) accounts for 12% of the variance.

I identified differentially expressed genes as having a |logFoldChange| > 1 and p.adj < 0.001, adjusted for multiple comparisons. A total of 607 genes were differentially expressed in zebrafish cells at either 1, 3, or 6 hours of blue light exposure compared to the control kept in darkness. In comparison, only 278 genes were differentially expressed in the cavefish cells. Figure 3.9 illustrates the amounts of DEGs at each time point in zebrafish (left) and

cavefish (right) samples. After 1 hour of exposure, zebrafish cells have a low transcriptomic response (29 upregulated and 21 downregulated transcripts), while at 3 and 6 hours, many more significantly upregulated transcripts are identified (211 and 411 genes, respectively). There are fewer downregulated genes (67 and 61 genes) at these time points. Overall, the response of zebrafish cells to blue light is mostly characterized by the upregulation of genes. In comparison, fewer DEGs are identified at all time points in cavefish cells (Figure 3.9, right). Only 36 and 26 genes are upregulated and downregulated, respectively, after 1 hour of exposure. Upregulated genes double after 3 hours of exposure (67 genes) and again after 6 hours (136 genes). On the other hand, the numbers of DEGs remain low at both time points (25 and 49 genes, respectively). Overall, the magnitude of transcriptional changes occurring in cavefish cells is much smaller than in zebrafish cells.

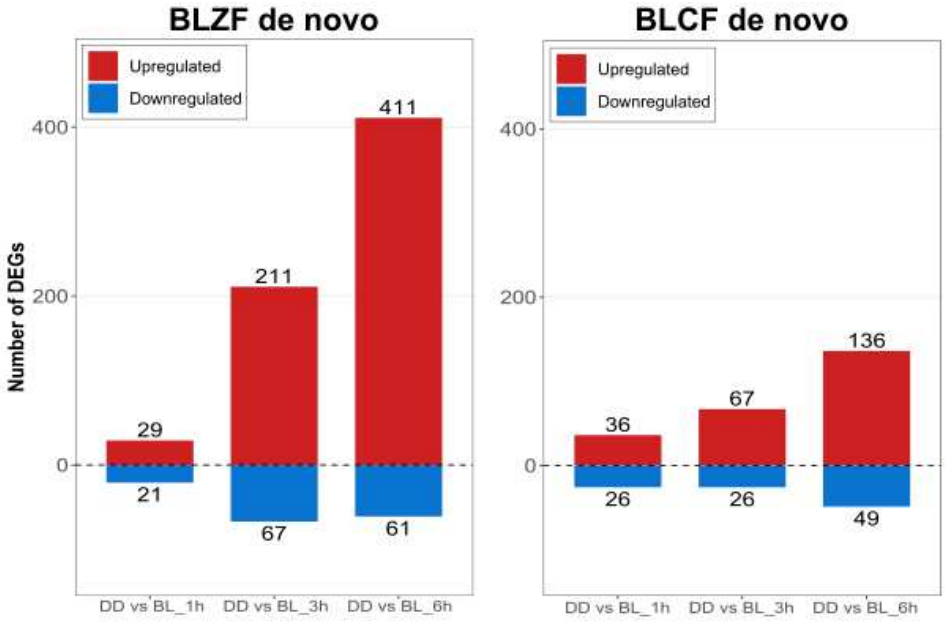

Figure 3.9. Differential expression analysis over time of blue light exposure compared to control, in zebrafish (left) and cavefish (right) cells. Bars represent the numbers of DEGs (p-adj < 0.001, |logFoldChange| > 1) at 1, 3, and 6 hours of blue light (BL) compared to DD control. Red bars indicate upregulated genes and blue bars indicate downregulated genes.

Volcano plots of the zebrafish DEGs at different time points further reveal the magnitude of changes in gene expression levels in response to blue light (Figure 3.10). Overall, there is

a clear trend of upregulation of gene expression over time. At 1 hour of exposure, few genes are significantly up- and down-regulated (y-axis) but the magnitude of change is high (x-axis, log fold changes between -11 and 11). Many genes are strongly regulated after 3 and 6 hours of exposure, and among the most strongly upregulated genes are clock-related genes *per2*, *cry1*, and *lonrf1*, as well as the gene *hebp2*, which were also identified by the previous analysis. Instead, there is no upregulation of such genes in cavefish cells, as expected (Figure 3.11).

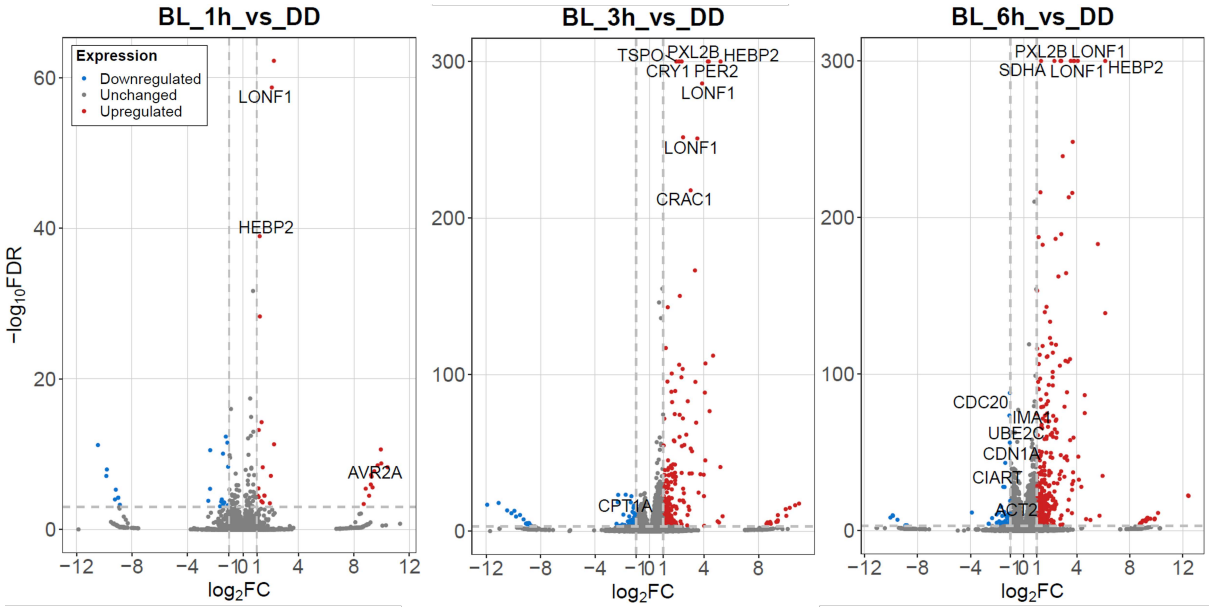

Figure 3.10. Volcano plots highlighting DEGs over time of blue light exposure compared to controls, in zebrafish cells. The x-axis displays the $\log_2$ fold change ($\log_2$FC) which indicates the magnitude of change in expression. The y-axis reflects statistical significance of the differential expression, shown by the $\log_{10}$ of the p-value adjusted for multiple comparisons (False Discovery Rate, FDR). Upregulated genes are shown in red, downregulated genes in blue, and unchanged genes in grey. The most strongly regulated genes are labeled.

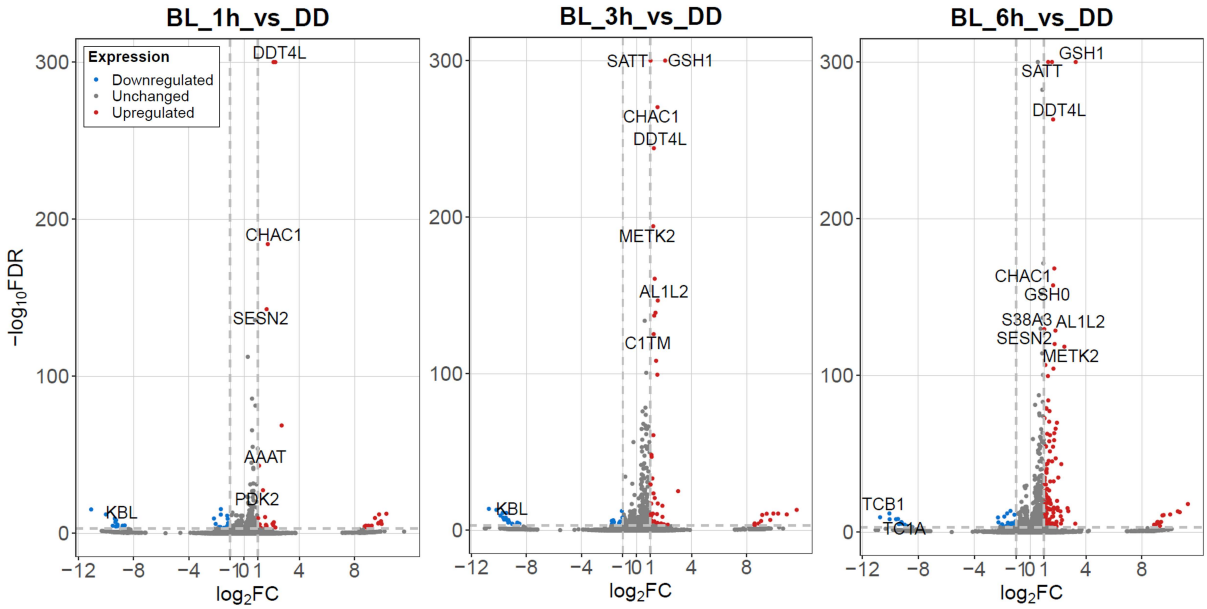

Figure 3.11. Volcano plots highlighting DEGs over time of blue light exposure compared to control, in cavefish cells. The x-axis displays the $\log_2$ fold change ($\log_2$FC) which indicates the magnitude of change in expression. The y-axis reflects statistical significance of the differential expression, shown by the $\log_{10}$ of the p-value adjusted for multiple comparisons (False Discovery Rate, FDR). Upregulated genes are shown in red, downregulated genes in blue, and unchanged genes in grey. The most strongly regulated genes are labeled.

3.1.2.1 Functional characterization of DEGs after blue light exposure in zebrafish and cavefish cells

Gene Ontology (GO) analysis was performed on the zebrafish DEGs upregulated at 6 hours compared to the control. As I reported previously, the analysis revealed a significant enrichment of genes related to clock and DNA repair, and more interestingly, to mitochondria structure and function, as well as heme biosynthesis and metabolism (Figure 3.12). The GO analysis reveals similar results to the zebrafish data analyzed with the standard RNA-sequencing pipeline, thus ensuring the validity and reliability of the *de novo* transcript construction and subsequent annotation for both datasets.

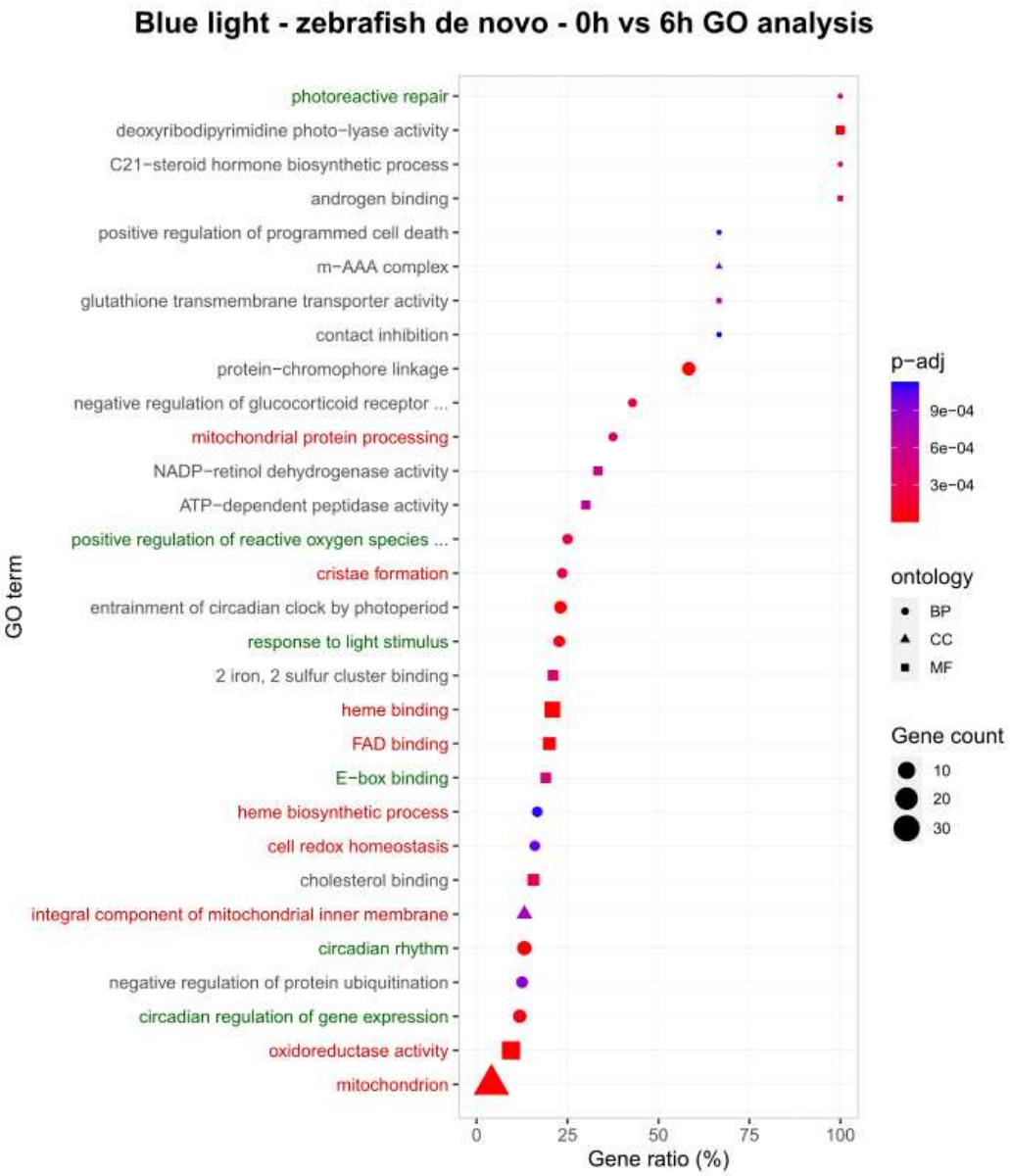

Figure 3.12. Gene Ontology (GO) analysis of DEGs at 6 hours of blue light compared to DD control, in zebrafish cells. The chart summarizes the enriched GO terms across the ontologies Biological Process (BP), Cellular Component (CC), and Molecular Function (MF). The 30 most significantly enriched terms are listed on the y-axis, the x-axis indicates the percentage of upregulated genes within their specific category. The size of the shapes indicates the number of upregulated genes for each category, and the shape indicates the ontology. The color indicates the adjusted p-value (p-adj) in a gradient from blue (highest p-value) to red (lowest p-value).

Gene Ontology (GO) analysis was performed on the cavefish DEGs upregulated at 6 hours compared to the control (Figure 3.13). The GO analysis reveals no enrichment of genes related to the circadian clock and to DNA repair mechanisms, in line with the loss of these responses to light by *P. andruzzii*. Furthermore, no enrichment of genes connected to mitochondria and

heme was detected. Cavefish cells, however, still responded to light with the upregulation of genes related to oxidative stress, in agreement with the reported increases in ROS levels upon blue light exposure.

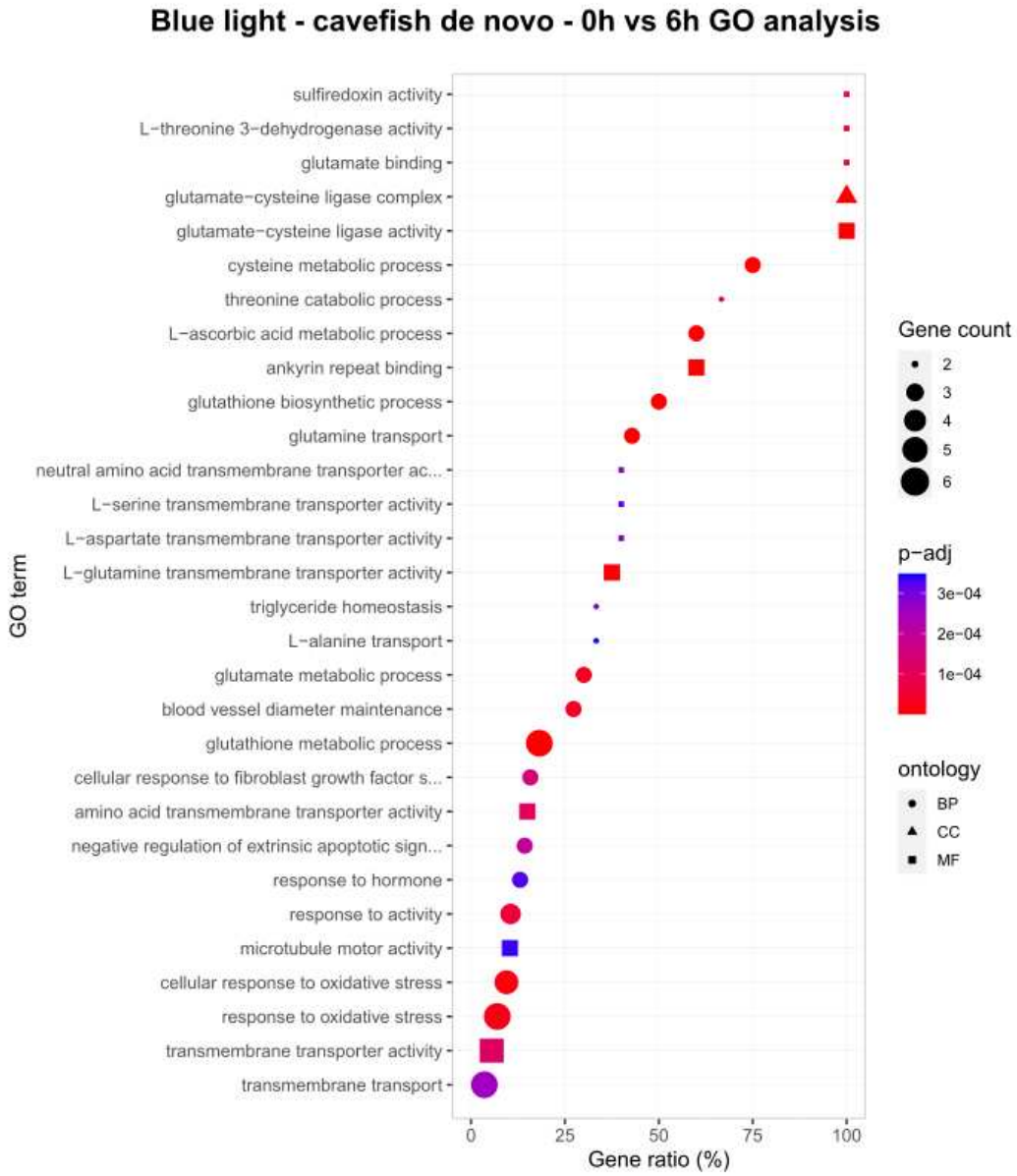

Figure 3.13. Gene Ontology (GO) analysis of DEGs at 6 hours of blue light compared to DD control, in cavefish cells. The chart summarizes the enriched GO terms across the ontologies Biological Process (BP), Cellular Component (CC), and Molecular Function (MF). The 30 most significantly enriched terms are listed on the y-axis, the x-axis indicates the percentage of upregulated genes within their specific category. The size of the shapes indicates the number of upregulated genes for each category, and the shape indicates the ontology. The color indicates the adjusted p-value (p-adj) in a gradient from blue (highest p-value) to red (lowest p-value).

A total of 1197 genes in the zebrafish dataset were significantly regulated between any time

point. On the other hand, only 460 DEGs were identified in the cavefish dataset. Significant DEGs were clustered using the unsupervised k-means method, according to their temporal expression patterns throughout exposure to blue light in zebrafish (Figure 3.14) and cavefish cells (Figure 3.15). The DEGs of the zebrafish dataset were divided into four clusters of upregulated genes (Clusters 1, 3, 4, and 5) and two clusters of downregulated genes (Clusters 2 and 6). Cluster 1 includes genes upregulated only after 6 hours of exposure, while genes upregulated after 1 hour are in Cluster 3. Clusters 4 and 5 represent genes upregulated across time points but with different magnitudes of change. Finally, Cluster 2 and 6 include genes downregulated at 3 and 6 hours, respectively.

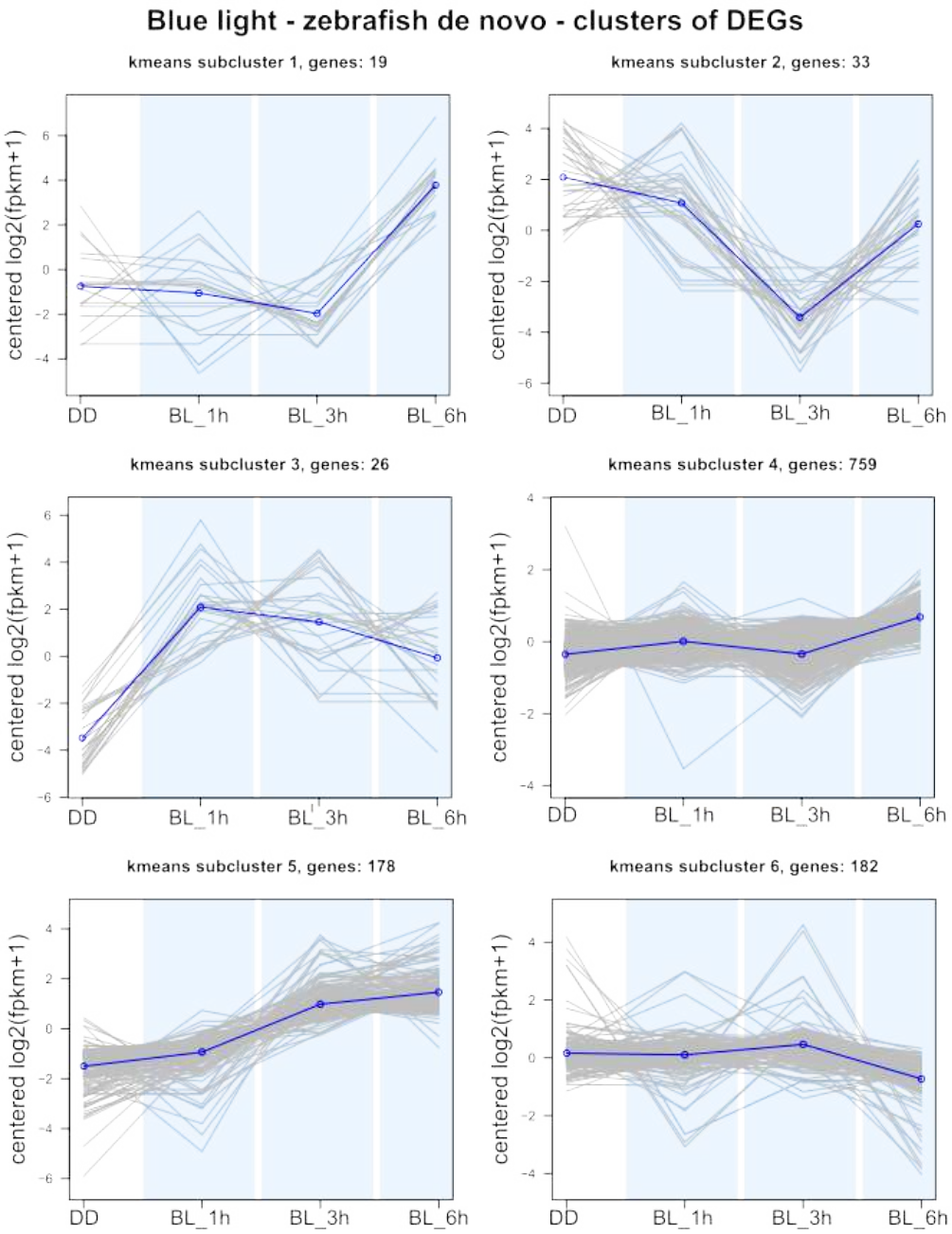

Figure 3.14. Temporal expression patterns of DEGs during blue light exposure in zebrafish cells. Significant DEGs were clustered using the unsupervised k-means clustering method, according to their temporal expression patterns throughout blue light exposure. The y-axis represents centered $\log_2$-transformed expression levels (normalized Fragments Per Kilobase per Million mapped reads, FPKM) while the x-axis represents time of blue light exposure. Individual genes are plotted in gray lines, while the blue line indicates the overall mean expression profile of the cluster.

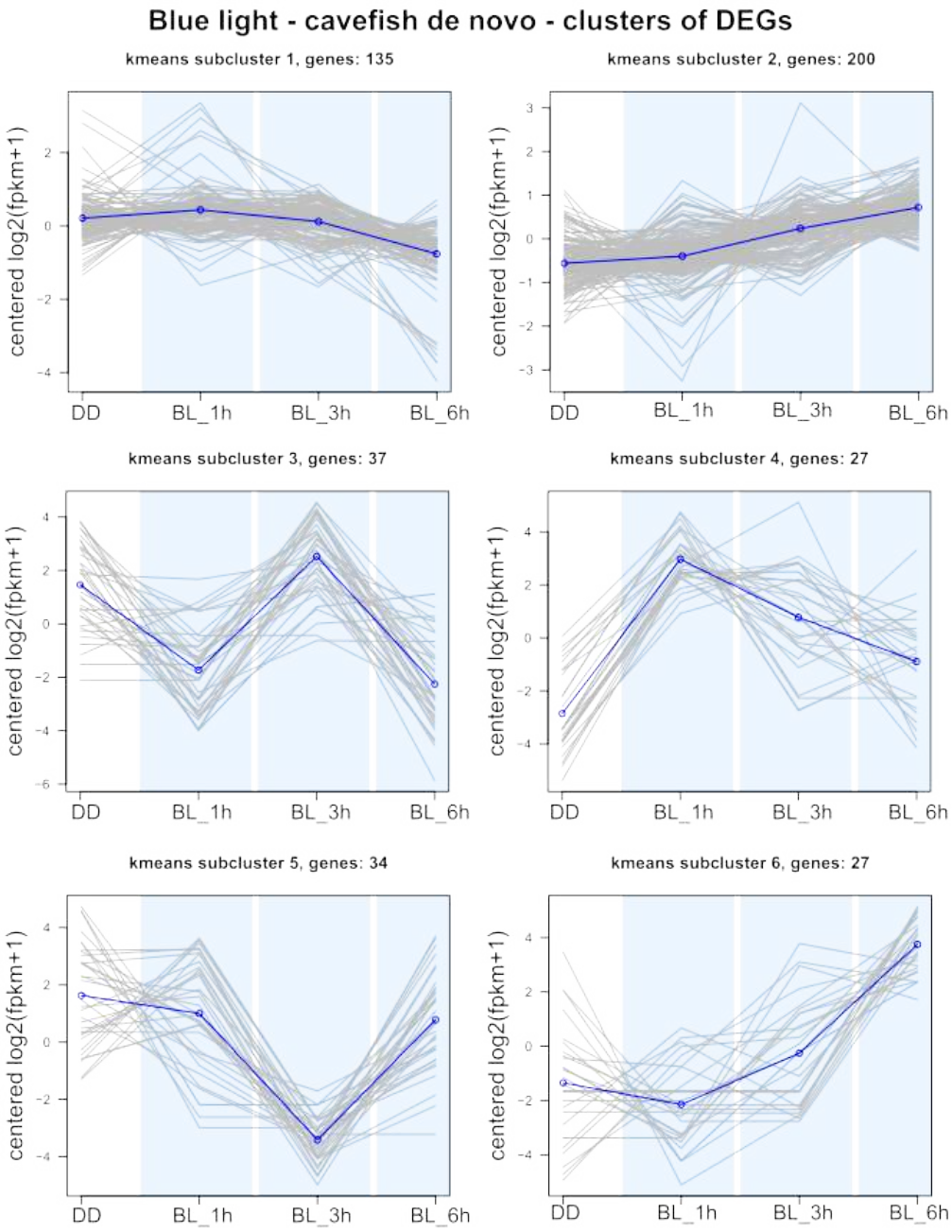

Figure 3.15. Temporal expression patterns of DEGs during blue light exposure in cavefish cells. Significant DEGs were clustered using the unsupervised k-means clustering method, according to their temporal expression patterns throughout blue light exposure. The y-axis represents centered $\log_2$-transformed expression levels (normalized Fragments Per Kilobase per Million mapped reads, FPKM) while the x-axis represents time of blue light exposure. Individual genes are plotted in gray lines, while the blue line indicates the overall mean expression profile of the cluster.

The mitochondrial and heme-related zebrafish genes identified in the original dataset were again found to belong to the same clusters as the clock and DNA repair genes (Clusters 4 and 5) and are similarly upregulated at 3 and 6 hours (Figure 3.16). The zebrafish genes *abcb6a*,

hebp2, and *soul5* are highlighted in red in the heatmap and show similar expression patterns as in the original analysis. *Soul5* here is identified as "HEBP2_HUMAN^SOUL" by the *de novo* analysis, as there is no corresponding ortholog in mammals and the *D. rerio* gene is not present in the UniProt database used for the annotation. The sequence was extracted from the *de novo* transcript file and compared to the zebrafish *soul5* to confirm its identity. Some of these genes were also successfully identified in the cavefish dataset and are shown in the heatmap of Figure 3.17. However, only two cavefish orthologs are significantly upregulated upon exposure to blue light: *abcb6a* and *ppm1k*. Similarly, out of the clock and DNA repair genes, only *ddb2* is upregulated, in line with previous research [137].

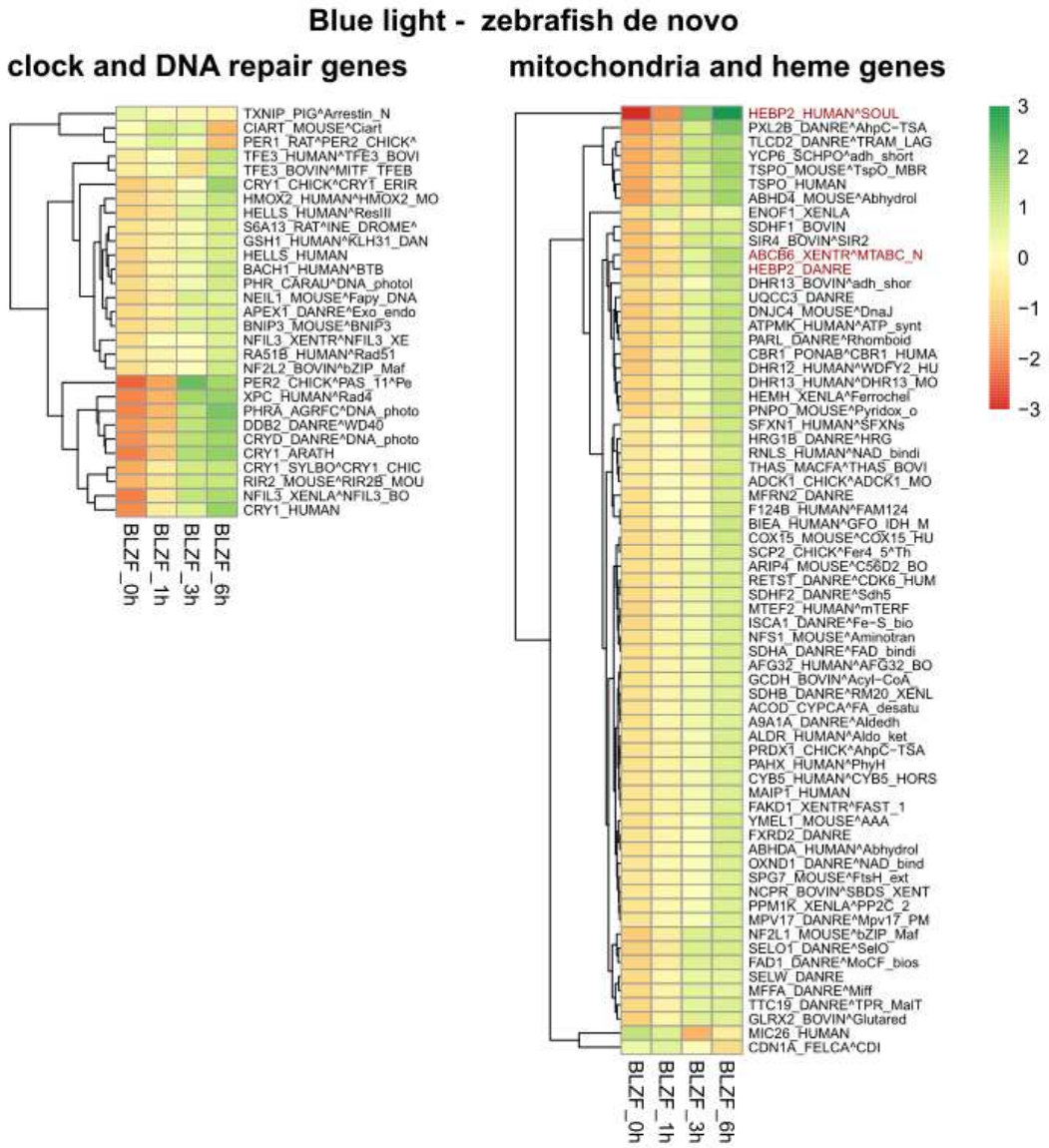

Figure 3.16. Heatmaps displaying temporal patterns of significantly upregulated genes in response to blue light, belonging to the category of clock and DNA damage repair (left) and the identified class of mitochondrial and heme-related genes (right), in zebrafish cells. The color scale represents $\log_2$-transformed expression values, with red indicating downregulation and green upregulation across the different time points (y-axis). Each row represents an individual gene and the dendrogram illustrates hierarchical clustering based on strength and expression profile. The two groups show similar expression patterns of upregulation in response to blue light. Genes of interest are shown in red (right).

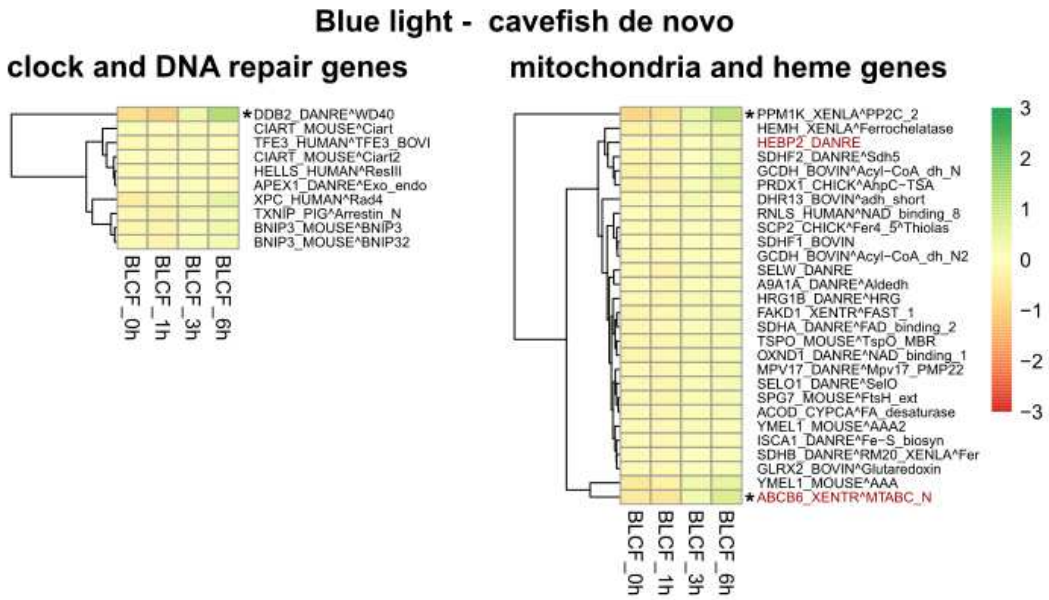

Figure 3.17. Heatmaps displaying temporal patterns in response to blue light of genes belonging to the category of clock and DNA damage repair (left) and the identified class of mitochondrial and heme-related genes (right) in cavefish cells. The color scale represents $\log_2$-transformed expression values, with red indicating downregulation and green upregulation across the different time points (y-axis). Each row represents an individual gene and the dendrogram illustrates hierarchical clustering based on strength and expression profile. Genes of interest are shown in red (right). The heatmaps focus on the cavefish orthologs of the zebrafish genes identified as significantly regulated by blue light. Significantly differentially expressed genes are indicated by *. Due to the *de novo* analysis, some zebrafish genes do not have identified orthologs in the cavefish dataset.

3.1.3 Transcriptomic response to UV-C exposure

The same analyses were repeated for zebrafish and cavefish cell line samples exposed to 20J/m^2 of UV-C light. To assess the variability and reproducibility of biological replicates, a PCA was performed to visualize the overall expression patterns and identify clusters of samples based on their differential expression profiles. The plot in Figure 3.18 (left panel) illustrates the PCA results for zebrafish cells, where each dot represents one sample. The first two principal components PC1 and PC2 explain 66% and 8% of the variance, respectively. The biological triplicates cluster tightly together, a sign of high similarity between them and the reproducibility of the experiment. Overall, the samples clustered in three main groups, correctly reflecting the different time points. Samples of 18 and 36 hours post-exposure are distinctly separated

from the nonexposed control, highlighting differences in gene expression profiles due to UV-C exposure. The correlation matrix (Figure 3.18, right panel) also reveals a high correlation between the three biological replicates and overall similarity between samples 18 and 36 after UV-C exposure, both of which have quite low correlation with the nonexposed control instead. Overall, both plots suggest consistent gene expression profiles within biological replicates and strong changes in gene expression following 20J/m^2 UV-C. The PCA and correlation matrix derived from the cavefish dataset show similar results (Figure 3.18, bottom). The first principal component PC1 captures 61% of the variance, while PC2 accounts for 12% of the variance. Replicates of each time point tend to cluster together, indicating similarity between triplicates and the reproducibility of the experiment. Modest correlation within triplicates across different time points and low correlation between time points are observed. The correlation matrix (right) shows moderate correlation within replicates at all time points and overall similarity between samples 18 and 36 after UV-C treatment, both of which have quite low correlation with the nonexposed control instead.

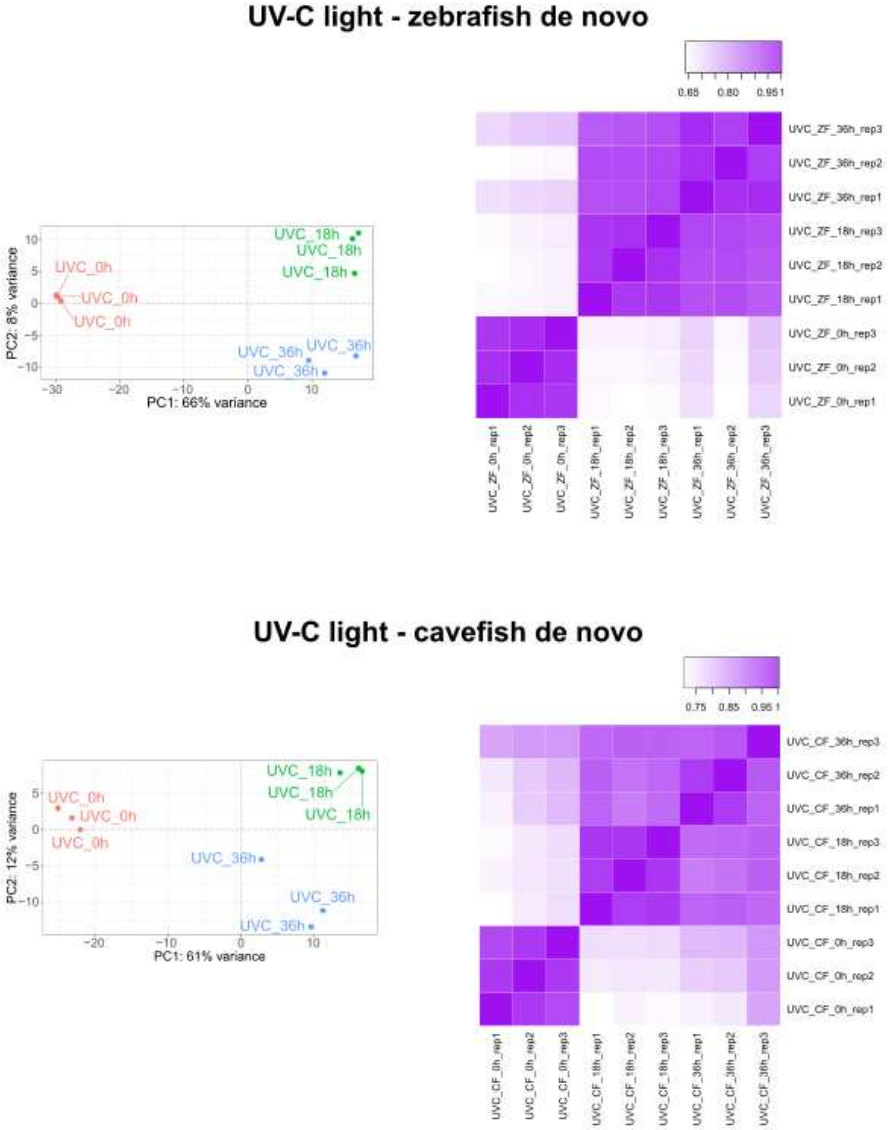

Figure 3.18. Comparative analysis of samples of zebrafish cells (top) and cavefish cells (bottom) exposed to 20J/m^2 UV-C. PCA plot (left) demonstrates the distribution of sample replicates while the correlation matrix (right) illustrates Spearman correlation coefficients between all pairs of sample replicates. **Zebrafish (top):** The first principal component PC1 (x-axis) captures 66% of the variance, while PC2 (y-axis) accounts for 8% of the variance. **Cavefish (bottom):** The first principal component PC1 (x-axis) captures 61% of the variance, while PC2 (y-axis) accounts for 12% of the variance.

I identified differentially expressed genes as having a |logFoldChange| > 1 and p.adj < 0.001, adjusted for multiple comparisons. A total of 9354 genes were differentially expressed in zebrafish cells between 18 and 36 hours after the UV-C treatment compared to the non-treated control. In comparison, 5052 genes were differentially expressed in the cavefish cells. Figure 3.19 illustrates the amounts of DEGs at each time point in zebrafish (left) and cavefish (right)

samples. Eighteen hours after the UV-C treatment, zebrafish cells have a high transcriptomic response (3710 upregulated and 4309 downregulated transcripts), while after 36 hours fewer genes are significantly regulated (2540 and 3864 genes respectively). Overall, there is a tendency for downregulation of gene expression following UV-C exposure (Figure 3.20). In comparison, fewer DEGs are identified at both time points in cavefish cells (Figure 3.19, right). Only 1490 and 2913 genes are upregulated and downregulated respectively 18 hours after the treatment, and even fewer genes are regulated after 36 hours (1080 upregulated and 1536 downregulated genes). Similarly to exposure to blue light, the magnitude of transcriptional changes occurring in cavefish cells is smaller than in zebrafish cells following UV-C (Figure 3.21). However, the response of both cell types is much stronger following UV-C treatment than during blue light exposure, due to the difference in cytotoxicity posed by the two wavelengths and to the different time courses analyzed.

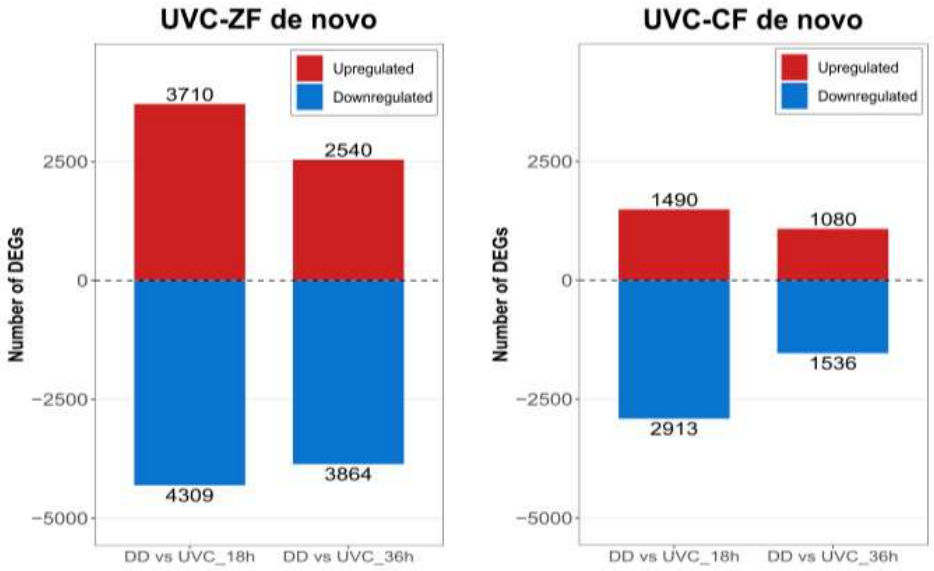

Figure 3.19. Differential expression analysis following exposure to 20J/m^2 UV-C compared to control, in zebrafish (left) and cavefish (right) cells. Bars represent the numbers of DEGs (p-adj < 0.001, |logFoldChange| > 1) at 18 and 36 hours after 20J/m^2 UV-C light (UVC) compared to 0h DD control. Red bars indicate upregulated genes and blue bars indicate downregulated genes.

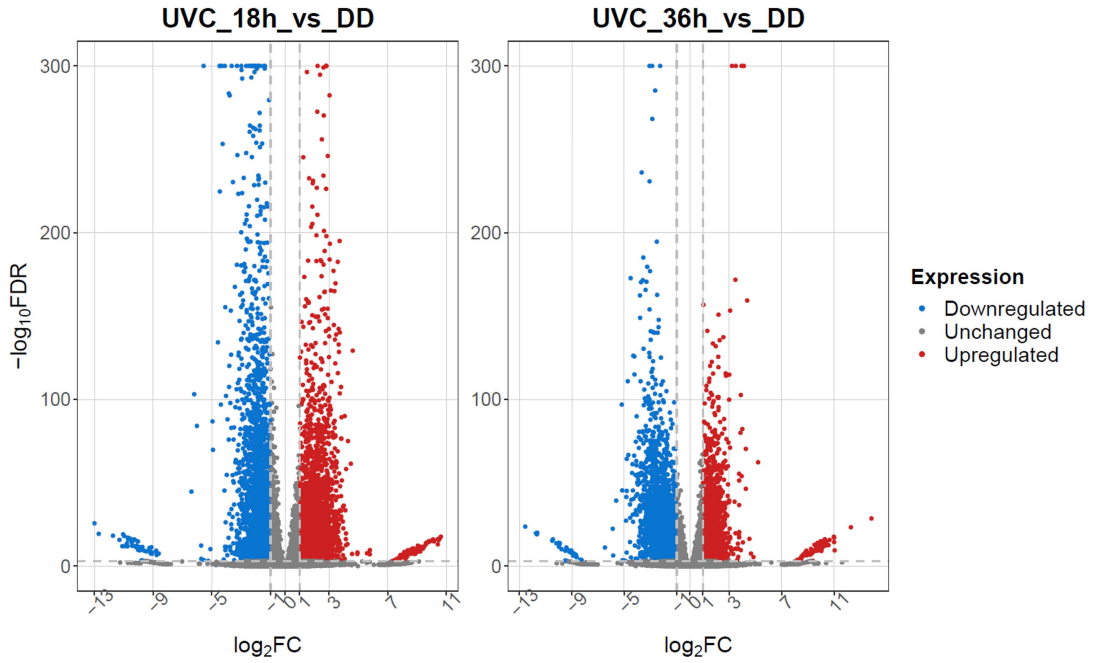

Figure 3.20. Volcano plots highlighting DEGs following exposure to 20J/m^2 UV-C compared to 0h DD control, in zebrafish cells. The x-axis displays the $\log_2$ fold change ($\log_2$FC) which indicates the magnitude of change in expression. The y-axis reflects statistical significance of the differential expression, shown by the $\log_{10}$ of the p-value adjusted for multiple comparisons (False Discovery Rate, FDR). Upregulated genes are shown in red, downregulated genes in blue, and unchanged genes in grey. The most strongly regulated genes are labeled.

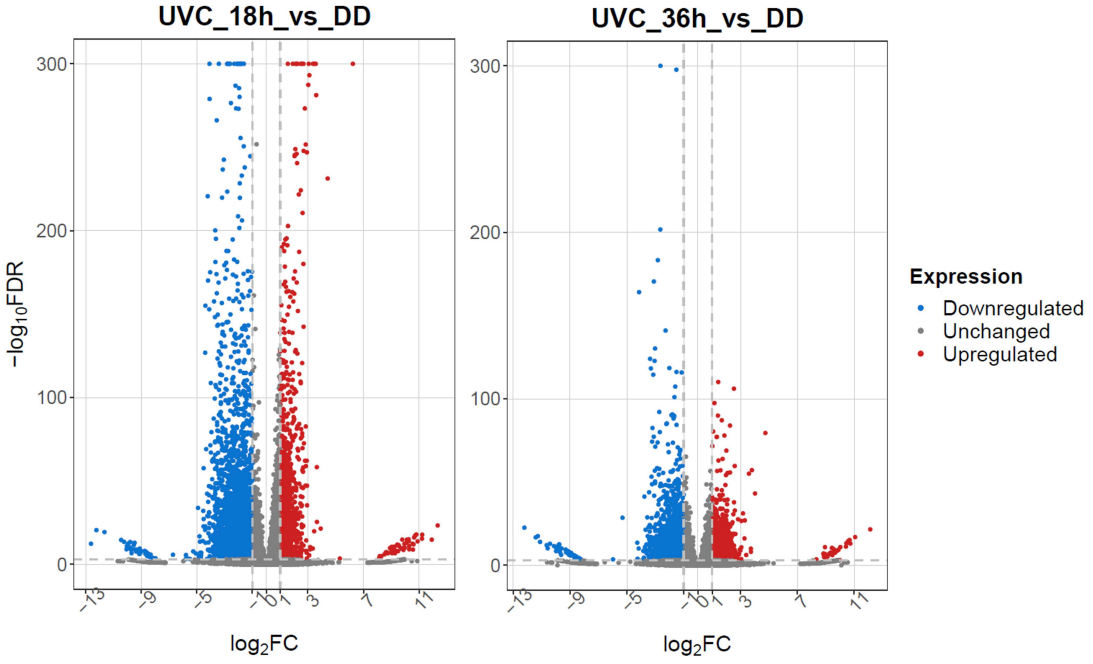

Figure 3.21. Volcano plots highlighting DEGs following exposure to 20J/m^2 UV-C compared to 0h DD control, in cavefish cells. The x-axis displays the $\log_2$ fold change ($\log_2$FC) which indicates the magnitude of change in expression. The y-axis reflects statistical significance of the differential expression, shown by the $\log_{10}$ of the p-value adjusted for multiple comparisons (False Discovery Rate, FDR). Upregulated genes are shown in red, downregulated genes in blue, and unchanged genes in grey. The most strongly regulated genes are labeled.

3.1.3.1 Functional characterization of DEGs after UV-C exposure in zebrafish and cavefish cells

Samples of cells collected 18 hours after 20J/m^2 UV-C exposure showed the greatest transcriptomic changes compared to nonexposed controls and were thus chosen for further GO analysis. In the zebrafish dataset, the analysis revealed a significant enrichment of genes related to circadian rhythms, as well as to cellular structural organization, signaling, protein modifications, and mRNA translation, among many others (Figure 3.22). Contrary to cells exposed to blue light, enrichment of genes related to mitochondria and heme is not highly relevant in the dataset, likely due to the high stress inflicted on cells by UV-C. Nevertheless, upon closer inspection, many of these genes are also upregulated in response to UV-C treatment, as can be seen in the heatmap of Figure 3.23. Among these are also *abcb6a*, *hebp2*, and *soul5*.

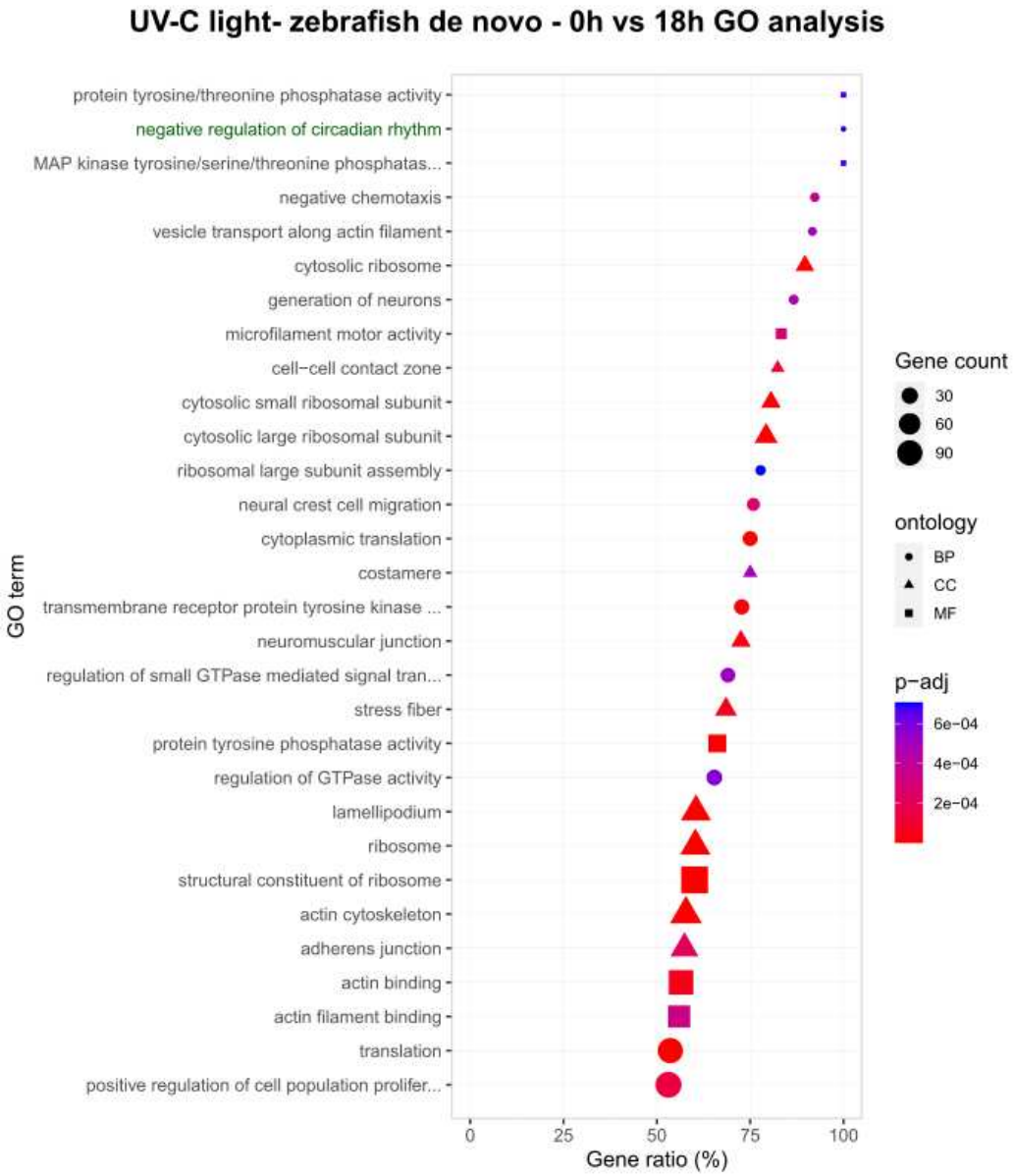

Figure 3.22. Gene Ontology (GO) analysis of DEGs 18 hours after exposure to 20J/m^2 UV-C, compared to 0h DD control, in zebrafish cells. The chart summarizes the enriched GO terms across the ontologies Biological Process (BP), Cellular Component (CC), and Molecular Function (MF). The 30 most significantly enriched terms are listed on the y-axis, the x-axis indicates the percentage of upregulated genes within their specific category. The size of the shapes indicates the number of upregulated genes for each category, and the shape indicates the ontology. The color indicates the adjusted p-value (p-adj) in a gradient from blue (highest p-value) to red (lowest p-value).

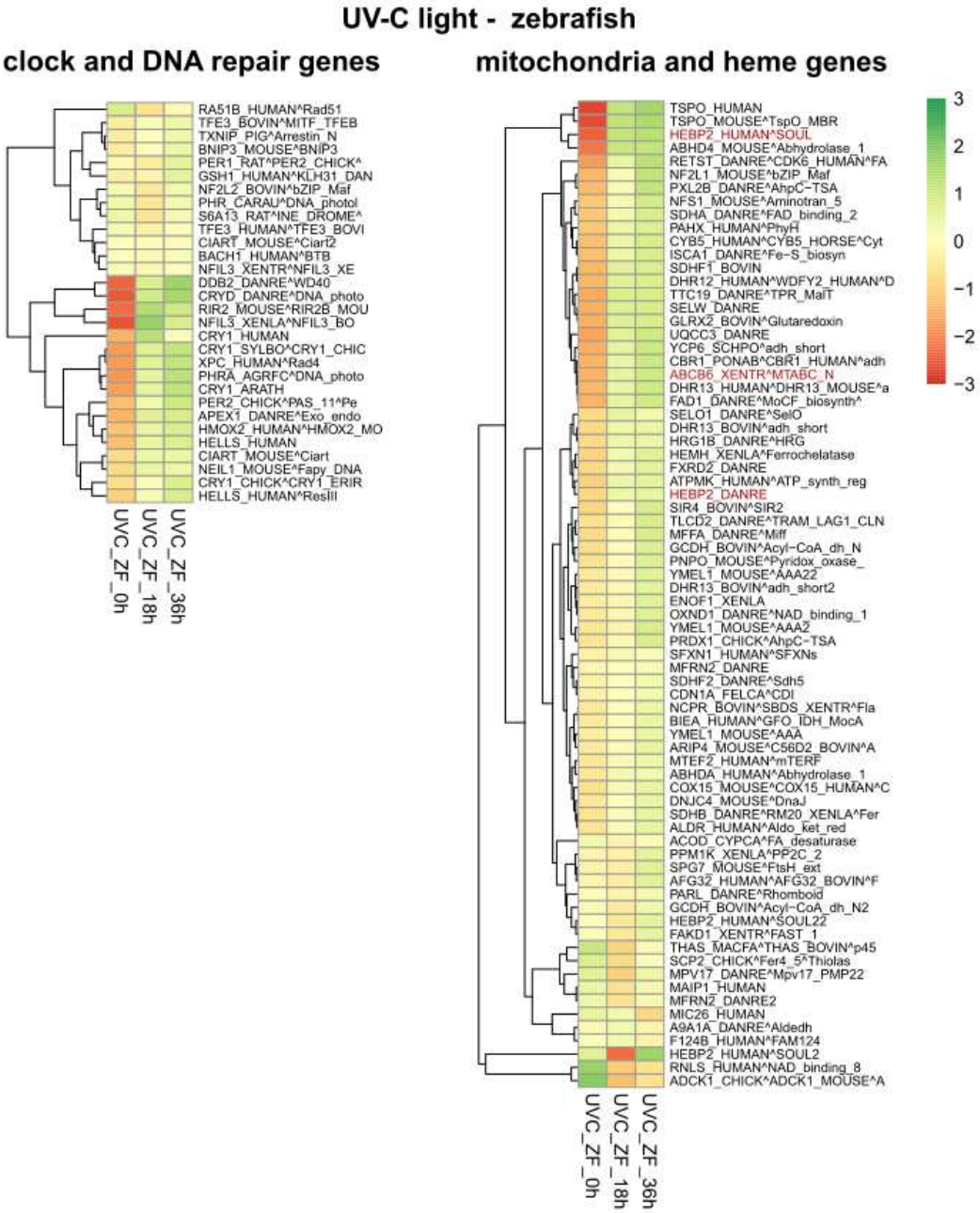

Figure 3.23. Heatmaps displaying temporal patterns of response to 20J/m^2 UV-C of genes belonging to the category of clock and DNA damage repair (left) and the identified class of mitochondrial and heme-related genes (right) in zebrafish cells. The color scale represents $\log_2$-transformed expression values, with red indicating downregulation and green upregulation across the different time points (y-axis). Each row represents an individual gene and the dendrogram illustrates hierarchical clustering based on strength and expression profile. Genes of interest are shown in red (right). The heatmaps focus on the zebrafish genes identified as significantly upregulated by blue light.

Similarly to zebrafish cells, the GO analysis of cavefish cells 18 hours after exposure to UV-C revealed significant transcriptomic changes related to cellular structural organization, as well as intracellular and extracellular signaling, among others (Figure 3.24). As expected, there

is no significant enrichment of clock and DNA repair genes, although *ddb2* is upregulated. Eleven of the previously identified mitochondria and heme genes are regulated in response to UV-C, as can be seen in the heatmap (Figure 3.25).

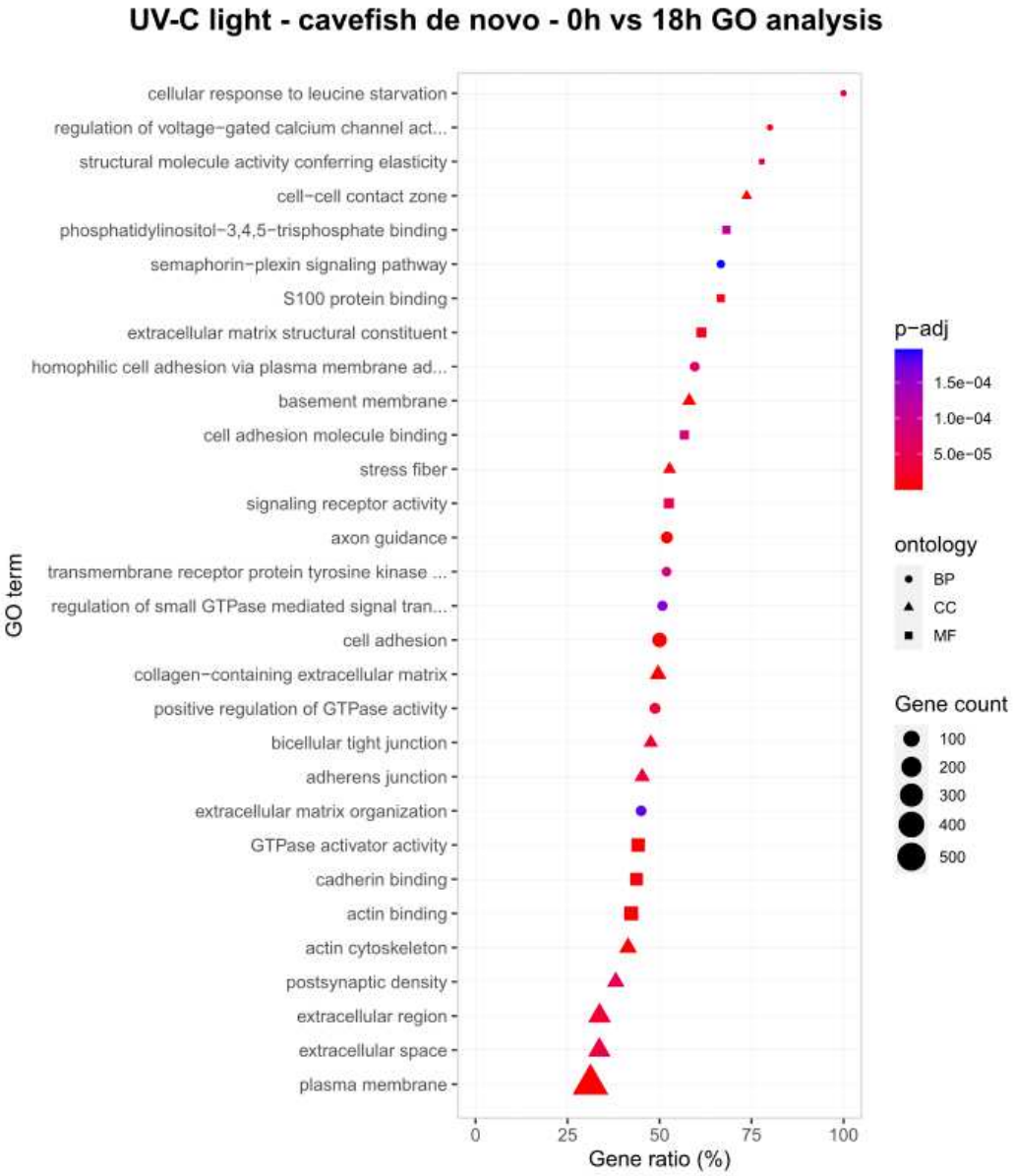

Figure 3.24. Gene Ontology (GO) analysis of DEGs 18 hours after exposure to 20J/m^2 UV-C, compared to 0h DD control, in cavefish cells. The chart summarizes the enriched GO terms across the ontologies Biological Process (BP), Cellular Component (CC), and Molecular Function (MF). The 30 most significantly enriched terms are listed on the y-axis, the x-axis indicates the percentage of upregulated genes within their specific category. The size of the shapes indicates the number of upregulated genes for each category, and the shape indicates the ontology. The color indicates the adjusted p-value (p-adj) in a gradient from blue (highest p-value) to red (lowest p-value).

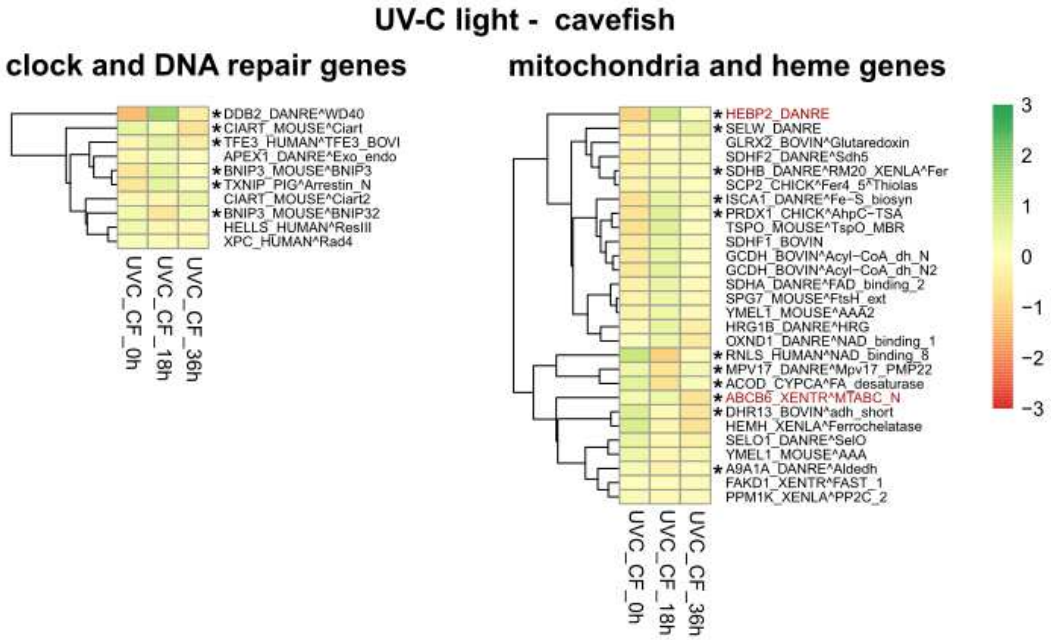

Figure 3.25. Heatmaps displaying temporal patterns of response to 20J/m^2 UV-C of genes belonging to the category of clock and DNA damage repair (left) and the identified class of mitochondrial and heme-related genes (right) in cavefish cells. The color scale represents $\log_2$-transformed expression values, with red indicating downregulation and green upregulation across the different time points (y-axis). Each row represents an individual gene and the dendrogram illustrates hierarchical clustering based on strength and expression profile. Genes of interest are shown in red (right). The heatmaps focus on the cavefish orthologs of the zebrafish genes identified as significantly regulated by blue light. Significantly differentially expressed genes are indicated by *. Due to the *de novo* analysis, some zebrafish genes do not have identified orthologs in the cavefish dataset.

3.2 Confirmation of RNA-seq results

The mRNA-sequencing experiments gave a broad overview of the response of zebrafish and cavefish cells to sunlight, both its visible and ultraviolet components. Consistent with previous studies [36], exposure of zebrafish cells to blue light and UV-C led to the expression of genes related to the circadian clock, like *per2* and *cry1a*, principal negative regulatory elements within the core clock mechanism [12]. These are known to be directly light-induced via the enhancer function of the D-box regulatory sequences found in their promoters [117], [123]. Genes involved in DNA damage repair, such as *6-4 photolyase* (*6-4 phr*), which harvests

energy from light to repair DNA lesions [33] were also significantly induced in response to light exposure. The D-box enhancer elements have been shown to be fundamental for the light-mediated induction of this class of genes in my lab. In comparison, most of these genes are not significantly induced in *P. andruzzii* cells, consistent with the theory that evolution in complete darkness fundamentally affected the organism's response to light at a cellular level [7], [85]. Interestingly, the transcriptome analyses in zebrafish cells highlighted the light-dependent regulation of another important subset of genes, namely those involved in mitochondria structure and function, as well as heme biosynthesis and metabolism. This response was completely absent in cavefish cells, reminiscent of the D-box-regulated genes related to circadian clock and DNA repair mechanisms. To further confirm these results, I chose three genes of interest *abcb6a*, *hebp2*, and *soul5* for real-time qPCR analysis (RT-qPCR), based on their strong induction in response to visible and ultraviolet light, as well as their suspected functions in the response to mitochondrial functions, heme metabolism, and oxidative stress. In the RT-qPCR experiments, mRNA expression of *per2* and *6-4 phr* (also known as *cry5*), two genes well documented to be strongly upregulated in response to blue light and UV-C exposure respectively, were measured to serve as positive controls.

3.2.1 Blue light exposure upregulates the expression of mitochondria-related genes in zebrafish but not cavefish cells

I repeated the blue light exposure experiment with both cell lines to test whether the mRNA-sequencing results could be replicated. The RT-qPCR analysis of genes *hebp2* and *soul5* confirms their strong upregulation in zebrafish (light grey bars) but not cavefish (grey bars) cells following 3 and 6 hours of blue light exposure (Figure 3.26), similar to the clock gene *per2*. *Abcb6a* instead partially retains its induction in cavefish cells and its fold induction at 3 and 6 hours in zebrafish cells is lower than those of the other genes (4 to 6-fold compared to

20 to 120-fold). The results are consistent with the transcriptome data and point to a partial loss of visible-light-induced expression of mitochondria and heme-related genes in *P. andruzzii*.

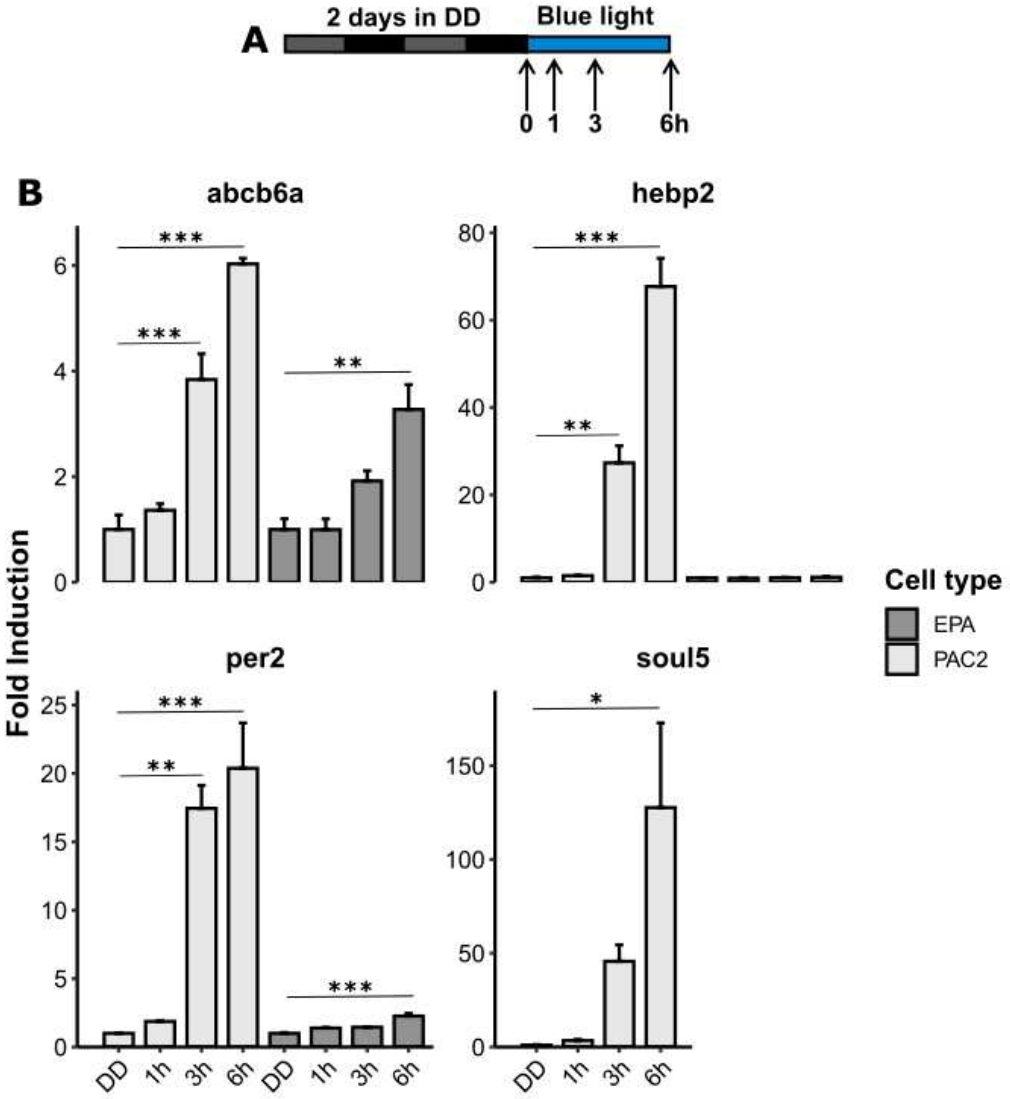

Figure 3.26. Blue light-induced induction of mRNA expression of mitochondria and heme-related genes and *per2* following exposure of cells to blue light (468nm). A) experimental scheme: cells were kept in darkness for two consecutive days in medium without phenol red, then exposed to 468nm LED blue light. **B)** RT-qPCR analysis of *abcb6a*, *hebp2*, and *soul5*, three mitochondria and heme-related genes, and *per2*, in zebrafish PAC2 (dark grey) and cavefish EPA (light grey) cells during 6 hours of blue light exposure (x-axis). Fold induction of mRNA expression compared with DD control samples kept in darkness is plotted on the y-axis as mean ± SEM (N=3 independent replicates). Expression levels in zebrafish and cavefish cells are compared via ANOVA followed by Tukey's HSD post-hoc multiple comparison tests against the DD control. Detailed statistical analysis can be found in Table (Table S3). $p<0.5$, $p<0.01$, $p<0.001$ are represented by *, **, and *** respectively.

3.2.2 UV-C irradiation upregulates the expression of mitochondria-related genes in zebrafish PAC2 cells

Next, I repeated the UV-C light exposure experiment in zebrafish PAC2 cells to confirm and strengthen the mRNA-sequencing results. Cells were kept in complete darkness for two days before 20J/m^2 UV-C irradiation and then maintained in complete darkness for up to 36 hours. These time points were selected for sampling based on documented changes in mRNA expression observed for genes involved in DNA repair responses [7]. Control samples were not exposed to UV-C, to account for endogenous changes in gene expression in the cell cultures over the following 36 hours which might result from progressive increases in cell density. The RT-qPCR analysis of the genes *abcb6a*, *hebp2*, and *soul5* confirms their strong upregulation in zebrafish cells 36 hours after UV-C exposure (violet bars), compared to the 0h control, and to the 36 hours untreated control (black bars) like the known DNA damage repair gene *6-4 phr* (Figure 3.27). *Hebp2* and *abcb6a* are also significantly induced 18 hours after the UV-C treatment. A time-dependent increase in the mRNA expression of these genes is also detected in the untreated samples (black bars), albeit attenuated compared to the treated samples. The results are consistent with the transcriptome data and further clarify the response to UV-C exposure from the intrinsic variation of the expression of the transcripts over time.

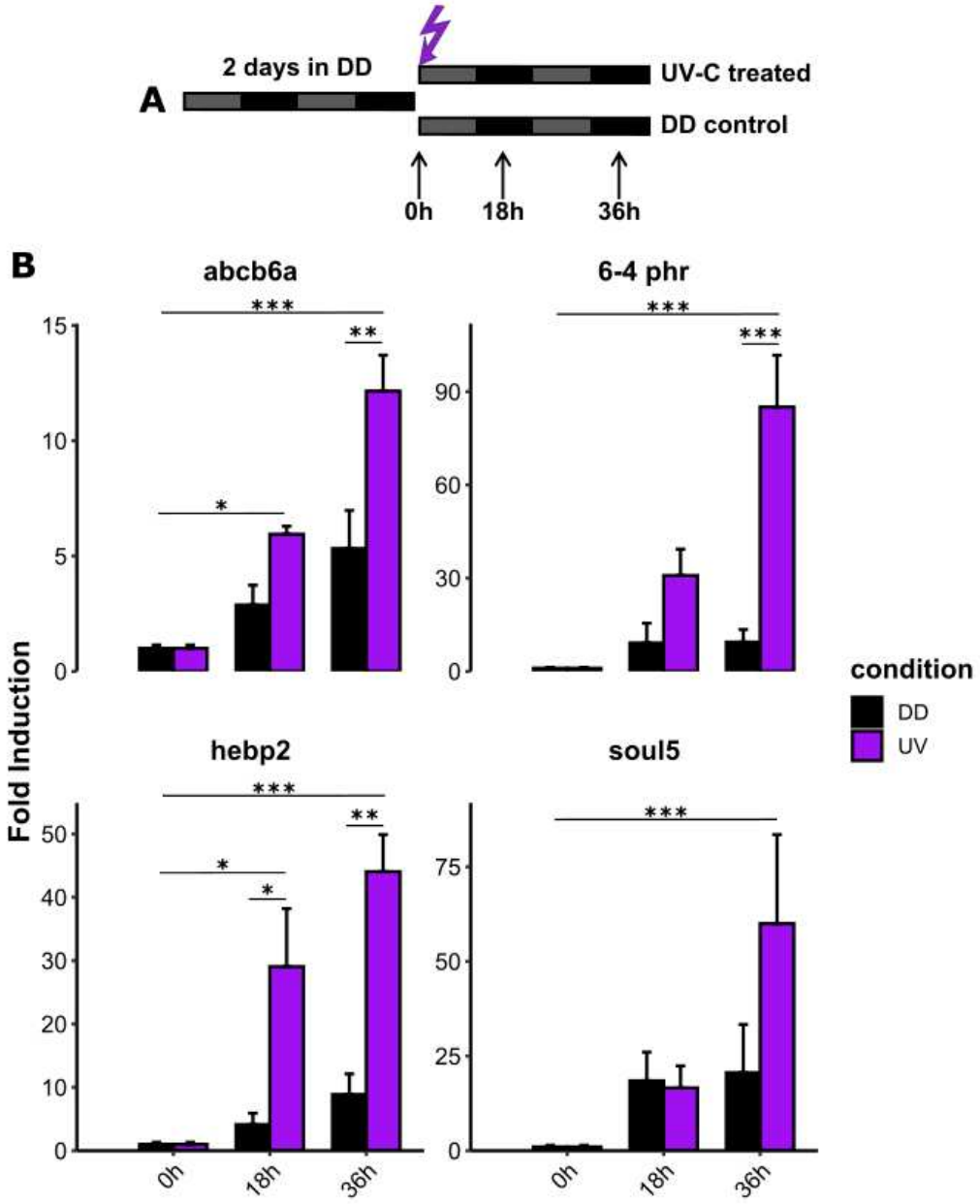

Figure 3.27. UV-C light-induced induction of mRNA expression of mitochondria and heme-related genes and *6-4 phr* in zebrafish cells. A) experimental scheme: cells were kept in darkness for two consecutive days in medium without phenol red, exposed to 20J/m^2 UV-C light after briefly removing the medium, and left to recover in darkness. **B)** RT-qPCR analysis of *abcb6a*, *hebp2*, and *soul5*, three mitochondria and heme-related genes, and *6-4 phr*, in zebrafish PAC2 cells following UV-C irradiation or untreated controls kept in darkness (x-axis). Fold induction of mRNA expression against the 0h control kept in darkness is plotted on the y-axis as mean ± SEM (N=3 independent replicates). Expression levels in zebrafish across time and treatment are compared via two-way ANOVA followed by Tukey's HSD post-hoc multiple comparison tests against the respective DD control. Detailed statistical analysis can be found in Table S4. $p<0.5$, $p<0.01$, $p<0.001$ are represented by *, **, and *** respectively.

3.3 Blue light but not UV-C upregulates the expression of mitochondria-related genes in zebrafish larvae

To explore whether the observed light-induced changes in gene expression in the zebrafish embryonic cell line was not a cell culture artifact and indeed represented an *in vivo*, organism-wide gene expression response, I extended the investigation of the response to both blue light and UV-C irradiation to zebrafish larvae. This has been previously reported for the circadian clock and DNA damage repair genes [36]. Mirroring the experiment performed in cells, zebrafish larvae were grown in complete darkness until the fourth or fifth day, to ensure the absence of clock-dependent rhythmic gene expression. Treatment with PTU was performed starting from 1dpf, to inhibit melanin production and maximize the penetration of light into the deep tissues of the animal. On the fifth day, as in the cell culture experiments, I exposed the larvae to blue light for up to 6 hours. Figure 3.28 depicts the results of the RT-qPCR analysis of *abcb6a*, *per2*, *hebp2*, and *soul5*. All genes are significantly upregulated in response to blue light at 6 hours, successfully mirroring the results seen in PAC2 cells. *Abcb6a* and *per2* are also significantly upregulated after 3 hours.

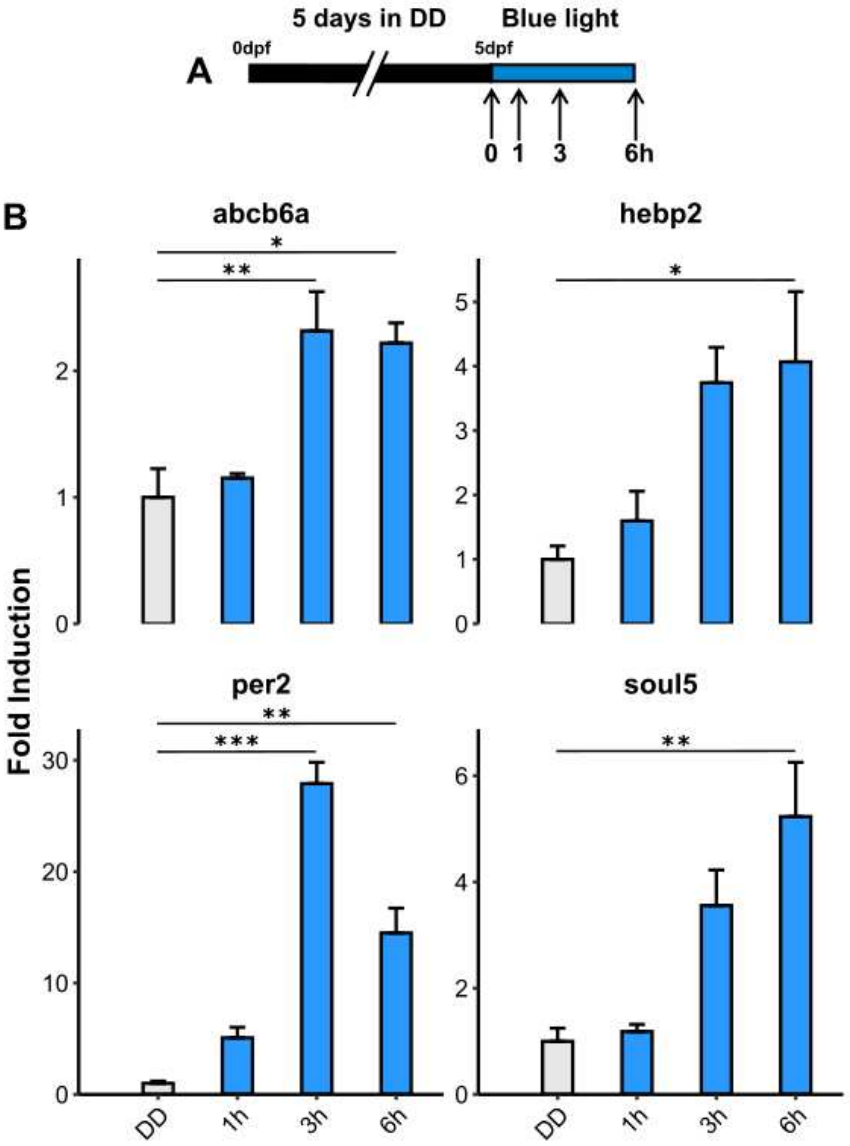

Figure 3.28. Blue light-induced induction of mRNA expression of mitochondria and heme-related genes and *per2* following exposure of zebrafish larvae to blue light (468nm). A) experimental scheme: zebrafish larvae were raised in darkness until 5dpf and treated with PTU at 1dpf to inhibit melanin production and allow light to penetrate deeper into the tissue. They were then exposed to 468nm LED blue light. **B)** RT-qPCR analysis of *abcb6a*, *hebp2*, and *soul5*, three mitochondria and heme-related genes, and *per2*, in zebrafish larvae during 6 hours of blue light exposure (x-axis). Fold induction of mRNA expression (blue bars) against DD control kept in darkness (grey bars) is plotted on the y-axis as mean ± SEM (N=3 independent replicates). Expression levels across time points are compared via ANOVA followed by Tukey's HSD post-hoc multiple comparison tests against the DD control. Detailed statistical analysis can be found in Table S3. $p<0.5$, $p<0.01$, $p<0.001$ are represented by *, **, and *** respectively.

After 3.5 days, as for the cell culture experiments, the larvae were irradiated with 450J/m^2 UV-C, and then were left to recover in complete darkness. Samples were taken at 0, 18, and 36 hours for both UV-C treated and untreated larvae. ANOVAs reveal a significant effect of

time points on the expression of *hebp2*, *abcb6a*, and *soul5* ($p<0.05$) but not of *6-4 phr*, and no significant effect of UV-C treatment (Figure 3.29). Therefore, my results for whole larvae do not entirely reflect the results obtained with the PAC2 cell line.

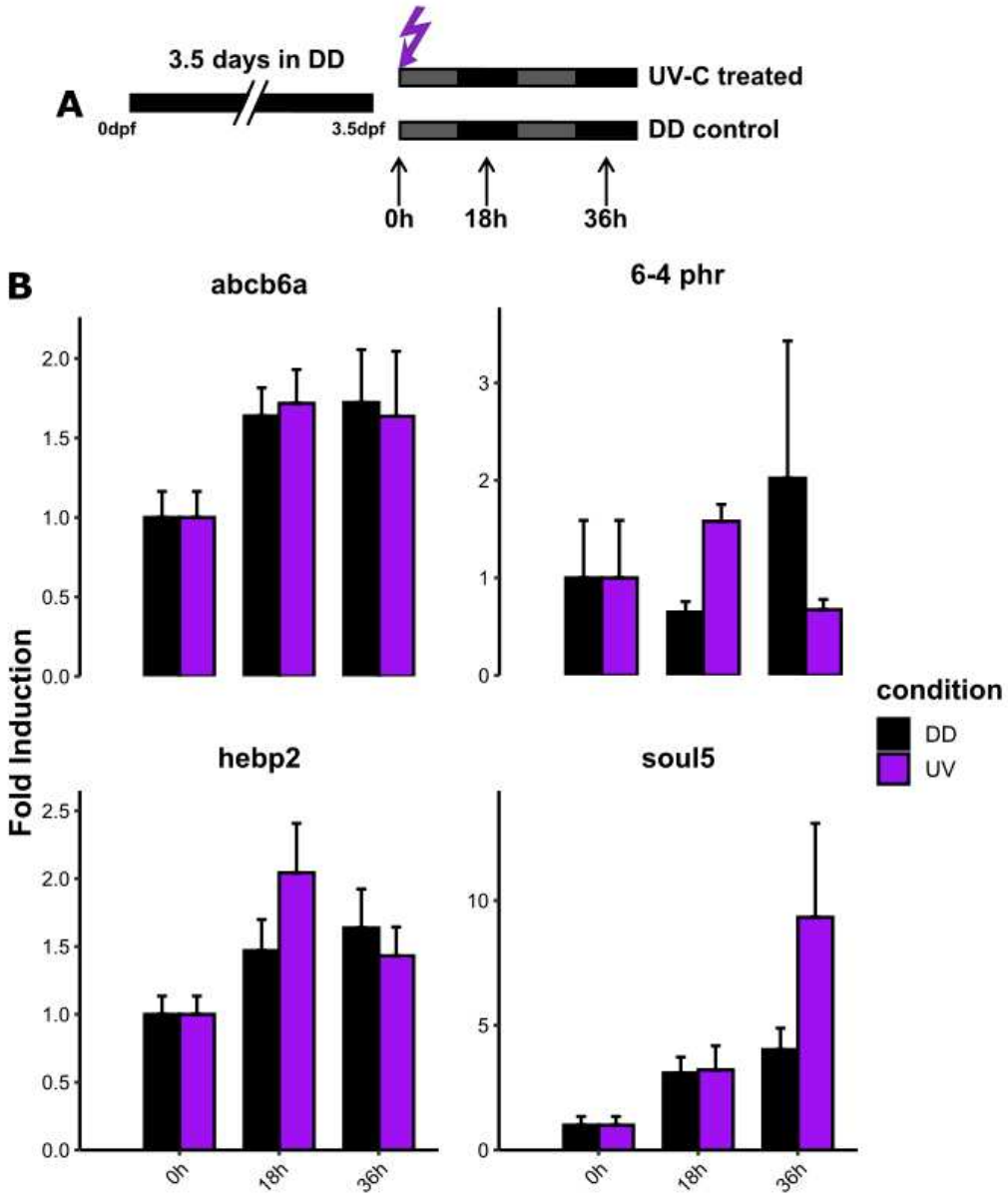

Figure 3.29. Light-induced induction of mRNA expression of mitochondria and heme-related genes and *6-4 phr* following irradiation of zebrafish larvae to 450J/m^2 UV-C. A) experimental scheme: zebrafish larvae were raised in darkness until 3.5dpf and treated with PTU from 1dpf to inhibit melanin production and allow light to penetrate deeper into the tissue. They were then exposed to 450J/m^2 UV-C light after removing most of the medium. The medium was then added back and larvae were kept in darkness. **B)** RT-qPCR analysis of *abcb6a*, *hebp2*, and *soul5*, three mitochondria and heme-related genes, and *6-4 phr*, in zebrafish larvae after 18 and 36 hours of UV-C exposure (x-axis). Fold induction of mRNA expression (violet bars) against 0h control kept in darkness (black bars) is plotted on the y-axis as mean ± SEM (N=3 independent replicates). Expression levels across time and treatment are compared via two-way ANOVA followed by Tukey's HSD post-hoc multiple comparison tests against the respective darkness control. Detailed statistical analysis can be found in Table S4. $p<0.5$, $p<0.01$, $p<0.001$ are represented by *, **, and *** respectively.

Overall, my data supports the presence of a global effect of visible light, but not ultraviolet light, on whole larvae which is not limited to the PAC2 cell line. However, the observed

induction of all genes is within a range of 2 to 30-fold in larvae exposed to blue light, values which are generally lower than in the zebrafish cell line. The finding could be due to tissue-specific differences in the strength of response to light, either due to the amount of light received within the structure of the larvae, or due to their intrinsic properties and functions. The discrepancy seen between larvae and PAC2 following UV-C irradiation could be attributed to the complex response of the entire organism to this stressful and damaging light insult, which could mask or diminish the expression of the studied genes. Furthermore, larvae have been shown to synthesize gadusol *de novo* [118], a UV-protective sunscreen compound that could reduce the expression of DNA damage repair and other genes known to be induced by UV-C in cell lines.

3.4 Induction of mitochondria and heme-related genes by ROS treatment

Visible light exposure has been shown to induce the levels of ROS in zebrafish cells and the D-box enhancer element is known to be activated by ROS, making it one of the ways how visible light activates the D-box. ROS treatment significantly upregulates the expression of the D-box-controlled circadian clock and DNA damage repair genes in PAC2 cells. A mRNA-sequencing experiment of zebrafish and cavefish cells exposed to 300μM hydrogen peroxide for 3 and 6 hours was previously done in my lab. The mitochondria-related genes *abcb6a*, *hebp2*, and *soul5* were significantly upregulated in response to ROS in zebrafish but not cavefish cells (data from my lab). To further confirm these results, PAC2 cells were exposed to ROS to check for effects on the expression of these genes, and a RT-qPCR analysis was performed. Indeed, 300μM hydrogen peroxide treatment leads to upregulation of *abcb6a*,

hebp2, and *soul5* expression after 3, 6, and 9 hours (Figure 3.30).

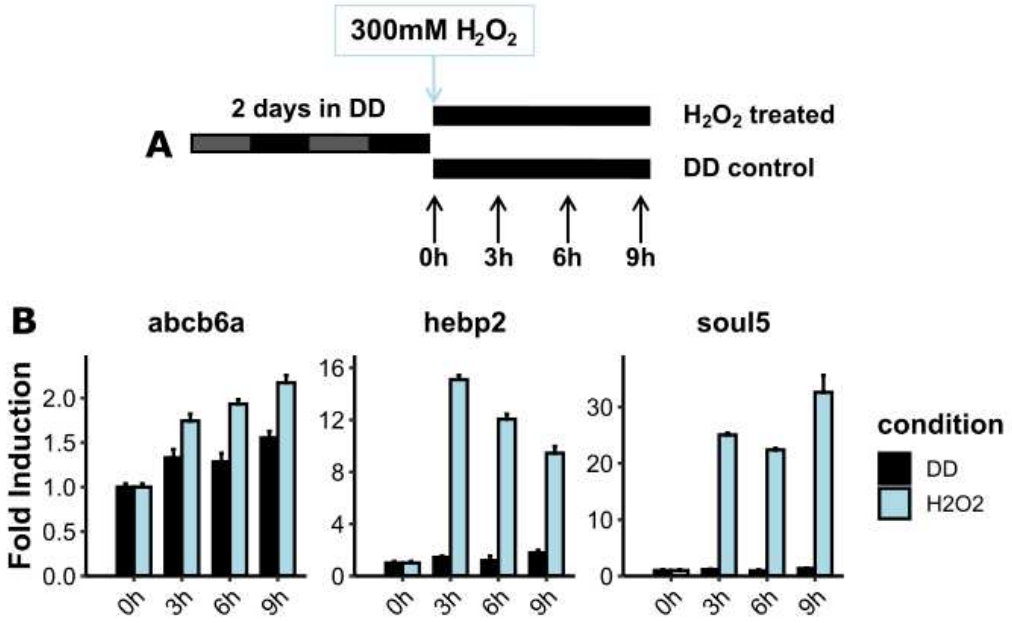

Figure 3.30. ROS-dependent induction of mRNA expression of mitochondria and heme-related genes following treatment with 300μM H_2O_2. A) experimental scheme: cells were kept in darkness for two consecutive days in medium without phenol red, then exposed to 300μM H_2O_2 or PBS (DD control) and kept in darkness until collection. **B)** RT-qPCR analysis of *abcb6a*, *hebp2*, and *soul5*, three mitochondria and heme-related genes, during 9h of ROS exposure (x-axis). Fold induction of mRNA expression compared with DD controls kept in darkness is plotted on the y-axis as mean ± SEM.

3.5 Are mitochondria-related genes regulated via the D-box enhancer element?

Both the transcriptomic and real-time qPCR gene expression analyses reveal a class of genes related to mitochondria structure and function and heme biosynthesis and metabolism are induced by visible and ultraviolet light. Previous experiments done in my lab also demonstrated the ROS-induced expression of these genes. Furthermore, the pattern of induction of these genes in response to blue and ultraviolet light is similar to that of the class of light-responsive circadian clock and DNA repair genes. The induction of the latter is mediated by light via the activation of multiple D-box enhancer elements found in their promoters. Therefore I hypothesized that

the mitochondria-related genes identified in the previous analysis are regulated by light via the same mechanism. However, this hypothesis is valid only if the measured upregulation of mRNA results from a directly light-mediated increase in transcription of the genes, and not from changes in the mRNA stability. Furthermore, the upregulation has to be independent of the circadian control of gene expression.

3.5.1 Blue light-mediated expression of mitochondria and heme-related genes in zebrafish cells is dependent on *de novo* transcription

To answer the first question, cells were treated with 5μg/mL Actinomycin-D, a compound that inhibits *de novo* gene transcription, mRNA expression levels were measured in cells maintained in blue light (BL) and darkness (DD), for up to 6 hours (Figure 3.31). Actinomicyn-D significantly decreases the levels of mRNA of *c-myc*, a gene with a very high mRNA turnover [148], as well as of *abcb6a*, *hebp2*, *soul5*, and *per2*. However, there is no significant difference in the amount of mRNA of these genes between the two conditions. Only *c-myc* is significantly affected by actinomycin-D in both blue light and DD ($p<0.001$). This indicates that the increased expression of these genes seen under blue light is solely the result of their transcriptional activation, which possibly involves the D-box enhancer.

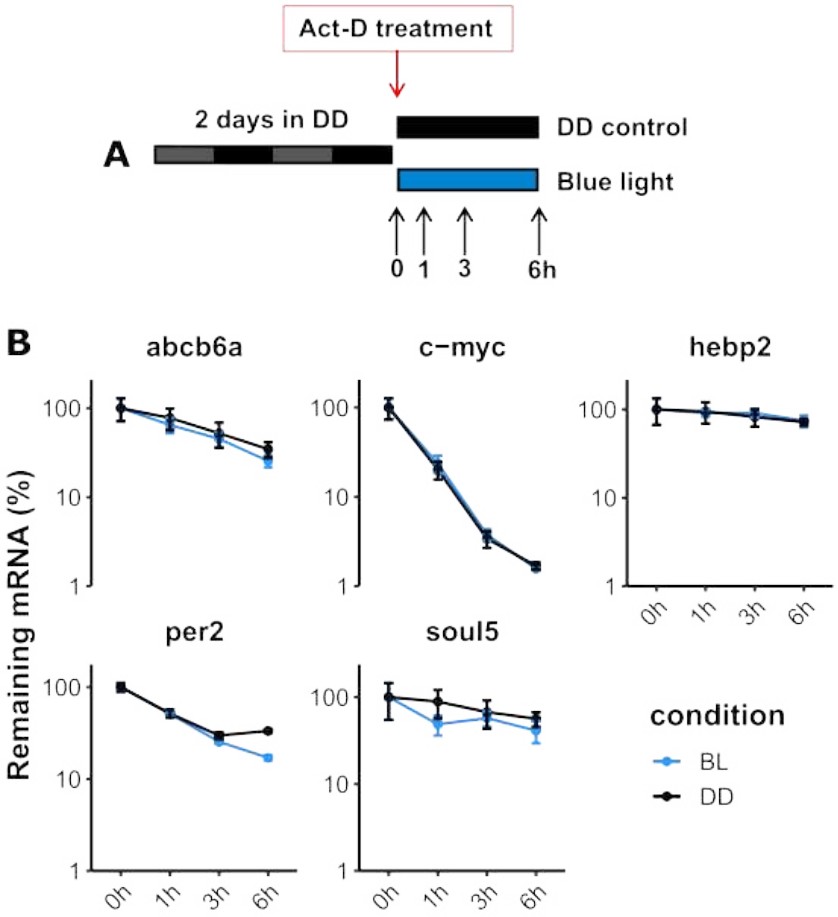

Figure 3.31. Percentage of remaining mRNA levels of mitochondria and heme-related genes and *per2* following treatment with 5μg/mL Actinomycin-D and subsequent exposure to blue light or darkness in zebrafish cells. **A)** experimental scheme: PAC2 cells were kept in darkness for two consecutive days in medium without phenol red, then treated with 5μg/mL Actinomycin-D and exposed to 468nm LED blue light or kept in darkness. **B)** RT-qPCR analysis of *abcb6a*, *hebp2*, and *soul5*, three mitochondria and heme-related genes, and *per2*, under blue light (blue) and in darkness (black). *c-myc* expression is measured to confirm the success of Actinomycin-D treatment. Data is plotted as the percentage of remaining mRNA compared to cells not treated with actinomycin-D (0h) on the y-axis as mean ± SEM (N=3 independent replicates). Expression levels in the two lighting conditions and across time points are compared via two-way ANOVA. Detailed statistical analysis can be found in Table S5.

3.5.2 UV-C-mediated expression of mitochondria and heme-related genes in zebrafish cells is dependent on *de novo* transcription

I repeated the experiment with UV-C exposure. In this case, cells were irradiated with 20J/m^2 UV-C, treated with Actinomycin-D 24 hours after UV-C exposure to inhibit transcription, and harvested at different time points (between 24 and 32 hours following exposure). Control samples (DD) were not exposed to UV-C. The results in Figure 3.32 show that Actinomycin-D

successfully dampens any light-mediated induction of *abcb6a*, *hebp2*, *soul5*, and *6-4 phr*.

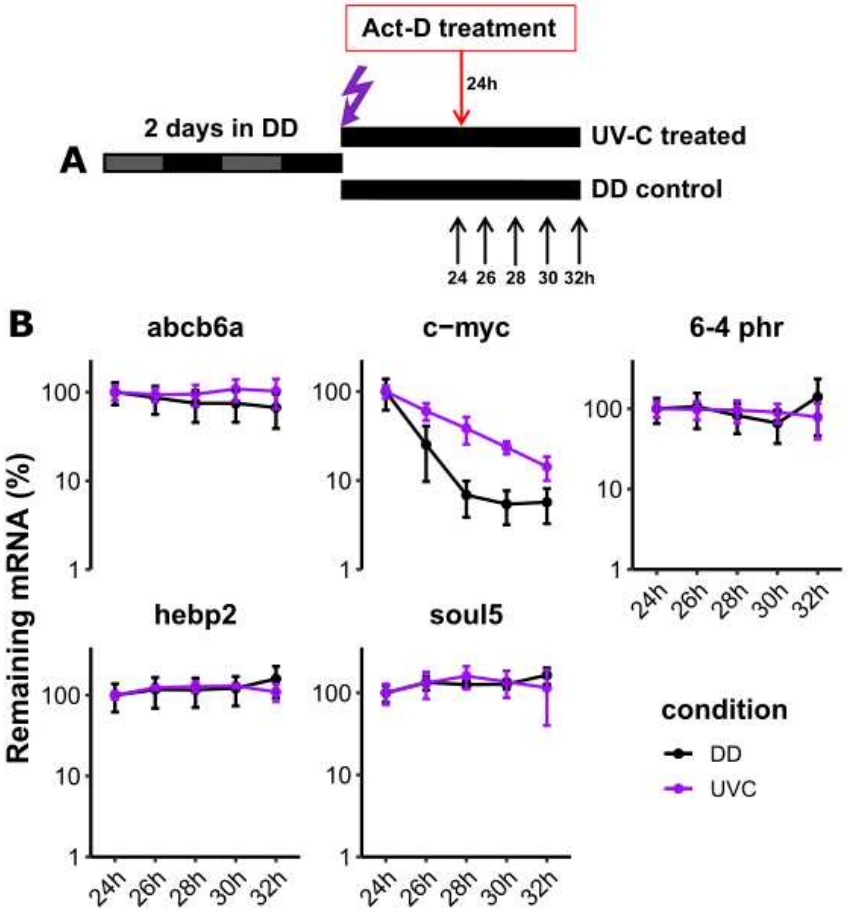

Figure 3.32. Percentage of remaining mRNA levels of mitochondria and heme-related genes and *6-4 phr* following treatment with 5μg/mL Actinomycin-D and subsequent exposure to UV-C or darkness in zebrafish cells. A) experimental scheme: cells were kept in darkness for two consecutive days in medium without phenol red, then irradiated with 20J/m^2 UV-C or kept in darkness, and treated with 5μg/mL Actinomycin-D after 24 hours. Samples were then taken every two hours up to 32 hours. **B)** RT-qPCR analysis of *abcb6a*, *hebp2*, and *soul5*, three mitochondria and heme-related genes, and *6-4 phr*, following UV-C irradiation (violet) and in darkness (black). *c-myc* expression is measured to confirm the success of Actinomycin-D treatment. Data is plotted as the percentage of remaining mRNA compared to cells not treated with actinomycin-D (24h) on the y-axis as mean ± SEM (N=3 independent replicates). Expression levels in the two lighting conditions and across time points are compared via two-way ANOVA. Detailed statistical analysis can be found in Table S5.

3.5.3 No effect of clock entrainment on the expression of mitochondria and heme-related genes

The regulation of clock and DNA repair genes is not only light-mediated. The expression of many of these genes is also dependent on circadian rhythms, which are indirectly affected by light. Clock-controlled gene expression is known to result from the regulation of E-box

enhancer elements found in promoters of clock and clock-controlled genes. These elements are bound by the proteins CLOCK and BMAL, the two main positive elements of the molecular clock mechanism [12]. It is therefore important to investigate the possibly complex regulation of mitochondria and heme-related genes by light via direct and indirect mechanisms. To do so, PAC2 cells were entrained for five consecutive days in 12h:12h light-dark cycles and gene expression was measured over the next day. A control group was instead transferred to complete darkness after entrainment to check for persistent gene expression oscillations in the absence of light. Typical clock-regulated genes, such as *per1b*, show a decrease in expression during the light period, and an increase in the dark period, which persists in the absence of light-dark cycles (DD) when the clock has been entrained, albeit with a lower amplitude of change (Figure 3.33). *Per2*, exclusively under the transcriptional control of D-box enhancer elements, shows upregulation in the light period, which is absent during the subjective light period in constant darkness. *Abcb6a*, *hebp2*, and *soul5* behave as *per2* and are only induced upon light exposure, indicating no circadian clock-dependent oscillations.

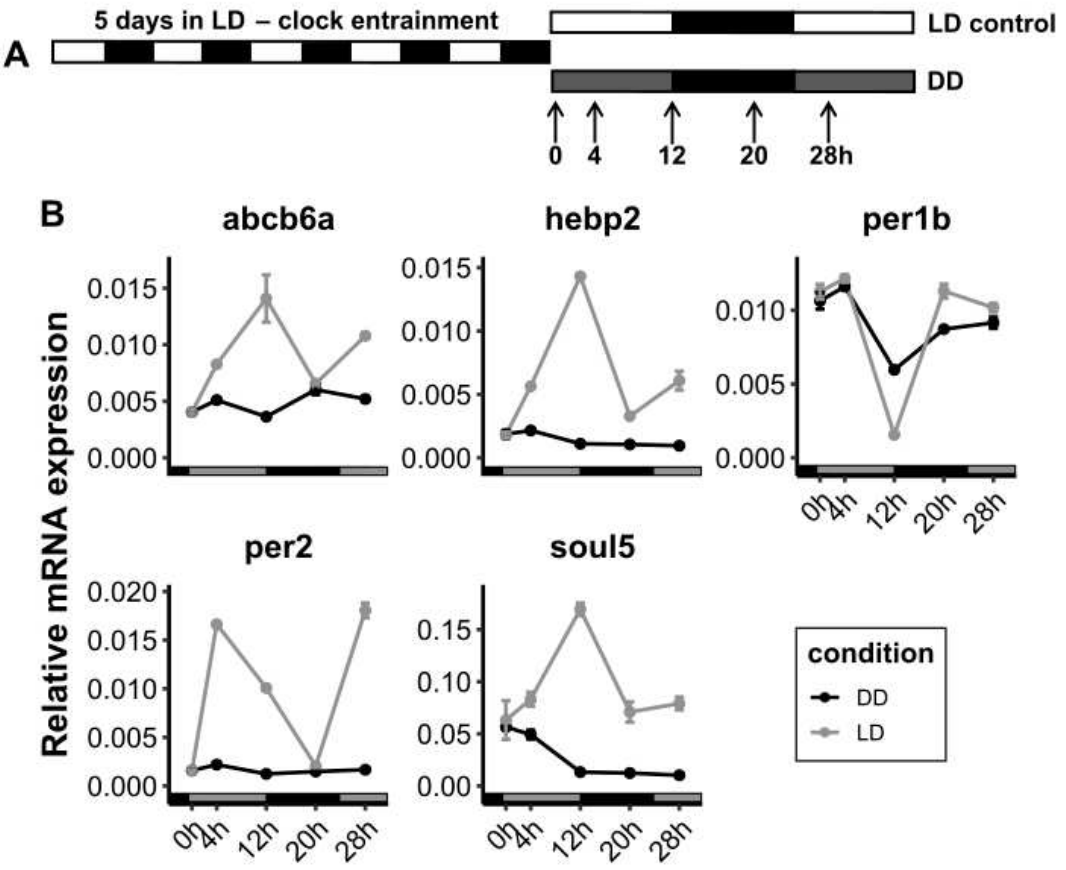

Figure 3.33. Expression of mitochondria and heme-related genes and the clock gene *per2* in zebrafish cells following circadian entrainment, in LD and DD conditions. A) experimental scheme: cells were entrained for five consecutive days in 12h:12h light-dark cycles (LD) in medium without phenol red, then kept in LD or put in complete darkness (DD). Samples were taken until 28 hours after the switch. **B)** RT-qPCR analysis of *abcb6a*, *hebp2*, and *soul5*, three mitochondria and heme-related genes, as well as *per2*, a light-regulated clock gene, and *per1b*, a solely clock-regulated gene. Relative mRNA expression of cells kept in LD or DD at different time points (x-axis) is plotted on the y-axis as mean ± SEM.

3.6 Regulation of the mitochondria and heme-related genes via D-box enhancer elements

So far my results have shown that the genes of interest *abcb6a*, *hebp2*, and *soul5* are regulated by visible and ultraviolet light as well as ROS, similarly to known D-box controlled genes like *per2* and *6-4 phr*. The upregulation is the result of transcriptional increases and is independent of circadian clock entrainment, both characteristics that point to the D-box enhancer as being

responsible for transcriptional regulation. To test this prediction bioinformatic, *in vivo*, and *in vitro* promoter analyses were performed. Firstly, the Clover software [141] was used to predict D-box and E-box sequences in the 5' untranslated region as well as 1kb upstream of the Transcription Start Site (TSS) of all mitochondria and heme-related genes identified within the RNA-sequencing analysis. D-box sequences were predicted in 70% of the genes, while E-box sequences in 48% of the genes. A table with the results of the promoter analysis for all mitochondria and heme-related genes can be found in the supplementary table (Table S1). The promoters schemes of the genes of interest *abcb6a*, *hebp2*, and *soul5*, containing the putative D-box and E-box sequences, are in Figure 3.34. Figures 3.35-3.37 display the sequences of the three promoters with D-boxes and E-boxes highlighted in blue and yellow, respectively. Three putative D-box and one E-box sequence were identified within the *hebp2* and the *soul5* promoters, while three D-box and two E-box sequences were identified in the *abcb6a* promoter. The predictions are consistent with the upregulation of these genes in response to visible and ultraviolet light, as well as ROS, seen in the previous experiments being the result of transcriptional activation via the D-box enhancer element. The presence of E-box-like sequences also suggests possible circadian regulation.

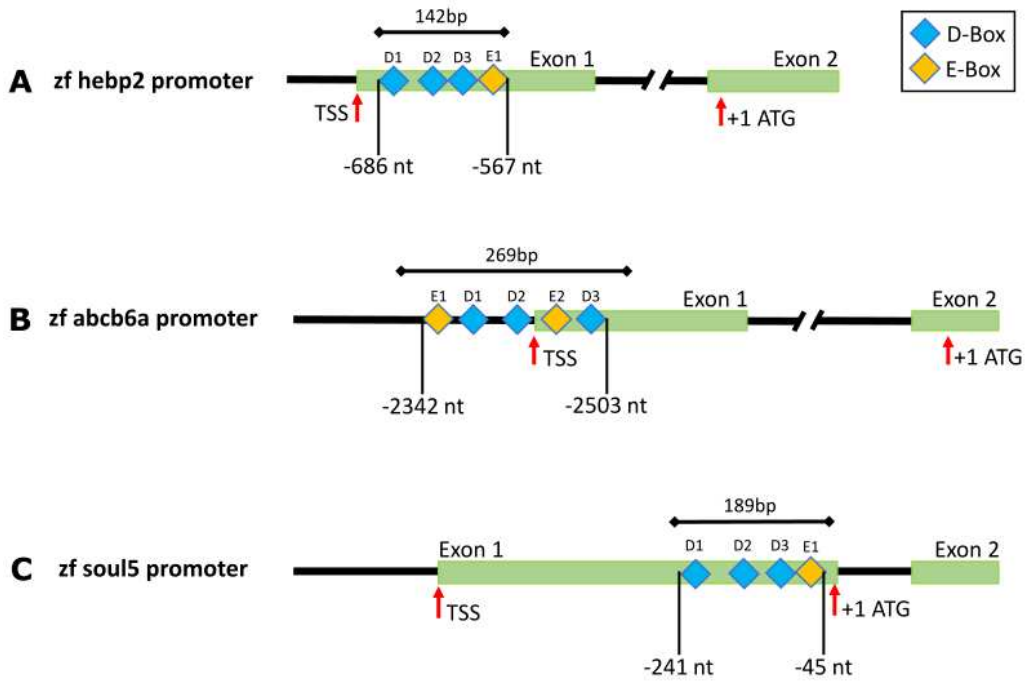

Figure 3.34. Putative D-box and E-box sequences predicted in the zebrafish *hebp2* (A), *abcb6a* (B), and *soul5* (C) promoters. D-box (orange) and E-box (blue) enhancer sequences were predicted by Clover software within 1kb of the TSS plus the 5' UTR of our mitochondrial and heme-related genes of interest. Exons, TSS, and ATG positions, as well as the distance (in nucleotides) of the first and last enhancer from the ATG, are indicated in the schemes. The upper bars indicate the sequences cloned into luciferase reporter vectors and their respective lengths.

```
5'   CTTCGCATGGGAGTGATGTAACATGAAAACACGGAAGTAGTCCTGTCAGCGTTACTTAAGCGTAGAGTTATTTAACAGCGAAACTGTATA
     ||||||||||||||||||||||||||||||||||||||||||||||||||||||||||||||||||||||||||||||||||||||||||| 90
3'   GAAGCGTACCCTCACTACATTGTACTTTTGTGCCTTCATCAGGACAGTCGCAATGAATTCGCATCTCAATAAATTGTCGCTTTGACATAT

     TTCTCTATCTAAGCGTTATAACACACCCGTGCGCGTGTGTGTGTTGGGCGAA   3'
     ||||||||||||||||||||||||||||||||||||||||||||||||||||   142
     AAGAGATAGATTCGCAATATTGTGTGGGCACGCGCACACACACAACCCGCTT   5'
```

Figure 3.35. Sequence of the 142 bp fragment of the *hebp2* promoter inserted in the luciferase report vector. Putative E-box sites are in orange and D-box sites are in blue.

```
5'   GATTGGACCAACCATACGTGCGCTGAGAAAAGTAACACTGCCCACGTCAGTAACCGTGACGTTTCAACTTTAAAACACAAAGCACTAGGA
     ||||||||||||||||||||||||||||||||||||||||||||||||||||||||||||||||||||||||||||||||||||||||||| 90
3'   CTAACCTGGTTGGTATGCACGCGACTCTTTTCATTGTGACGGGTGCAGTCATTGGCACTGCAAAGTTGAAATTTTGTGTTTCGTGATCCT

     CCATGAAGATTCTTGTCTTTCCCCGGTGTTATTGTATAAGTCATGGATGATGGAGTTGTACGGCGTGAGTTTATGACTGCAAGGGCACAC
     ||||||||||||||||||||||||||||||||||||||||||||||||||||||||||||||||||||||||||||||||||||||||||| 180
     GGTACTTCTAAGAACAGAAAGGGGCCACAATAACATATTCAGTACCTACTACCTCAACATGCCGCACTCAAATACTGACGTTCCCGTGTG

     AGCAAACGCAGACGTTTTGAATGATTTAACATCGCTGGAATAATCATAATTCATCTGAAGGGATAGTTATTGAAGGACGCACTCGAAAG   3'
     ||||||||||||||||||||||||||||||||||||||||||||||||||||||||||||||||||||||||||||||||||||||||||   269
     TCGTTTGCGTCTGCAAAACTTACTAAATTGTAGCGACCTTATTAGTATTAAGTAGACTTCCCTATCAATAACTTCCTGCGTGAGCTTTC   5'
```

Figure 3.36. Sequence of the 269 bp fragment of the *abcb6a* promoter inserted in the luciferase report vector. Putative E-box sites are in orange and D-box sites are in blue.

Figure 3.37. Sequence of the 189 bp fragment of the *soul5* promoter inserted in the luciferase report vector. Putative E-box sites are in orange and D-box sites are in blue.

3.6.1 Transcription of *hebp2*, *abcb6a*, and *soul5* is light-regulated

To determine whether these promoters are light-regulated, I cloned small fragments encompassing all elements into luciferase reporter vectors, hereafter referred to as abcb6a-Luc, hebp2-Luc, and soul5-Luc. I transfected the reporters in PAC2 and EPA cells (Figure 3.38) and tested them in *in vivo* bioluminescence assays in darkness (DD) and light:dark cycles (LD) to check for light and clock-regulated activation of transcription. All three demonstrate robust light-induced bioluminescence in PAC2, but not EPA, mirroring the endogenous mRNA expressions of these genes, as well as the promoters of the *cry1a* and *per2* genes [107].

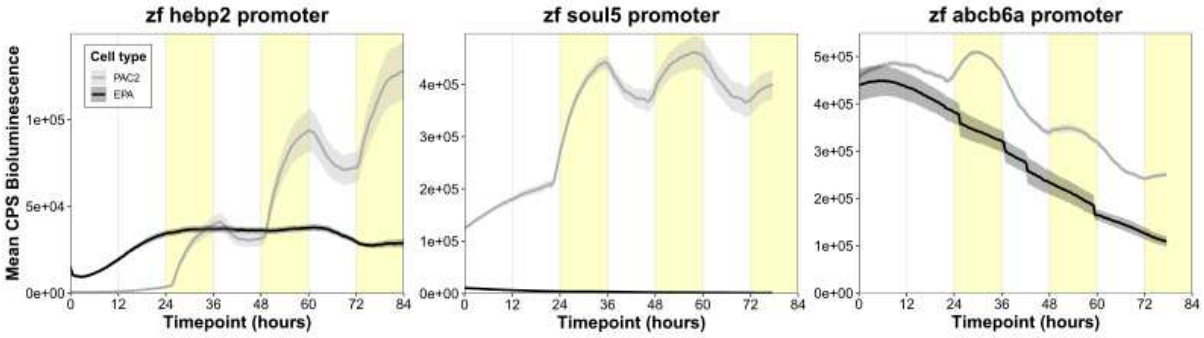

Figure 3.38. *In vivo* bioluminescence assay in zebrafish and cavefish cells transfected with zebrafish hebp2-Luc, soul5-Luc, and abcb6a-Luc. Real-time bioluminescence assay of zebrafish PAC2 (grey) and cavefish EPA (black) cells transfected with the luciferase reporters hebp2-Luc, soul5-Luc, and abcb6a-Luc exposed to 24 hours of darkness followed by LD cycles. Means of bioluminescence (CPS, N=8 wells) are plotted on the y-axis, with SEM indicated by shading, and time (hours) is on the x-axis. Lights-on periods are indicated by the yellow boxes.

3.6.1.1 Contribution of D-boxes and E-box to hebp2-Luc induction by light

To determine whether the responsiveness to light is dependent on the identified D-box and E-box sequences, I chose the hebp2-Luc promoter for further analyses. In the first round of site-directed mutagenesis, the synergic interaction and contribution of each enhancer within the promoter were tested. I prepared four constructs where each of the enhancer sequences was mutated by changes to 4-6 nucleotides, and they were transiently transfected in PAC2 cells (Figure 3.39). All retained light-induced bioluminescence, albeit with a lower amplitude compared to the non-mutated hebp2-Luc reporter, suggesting each of them significantly contributes to the promoter's response to light.

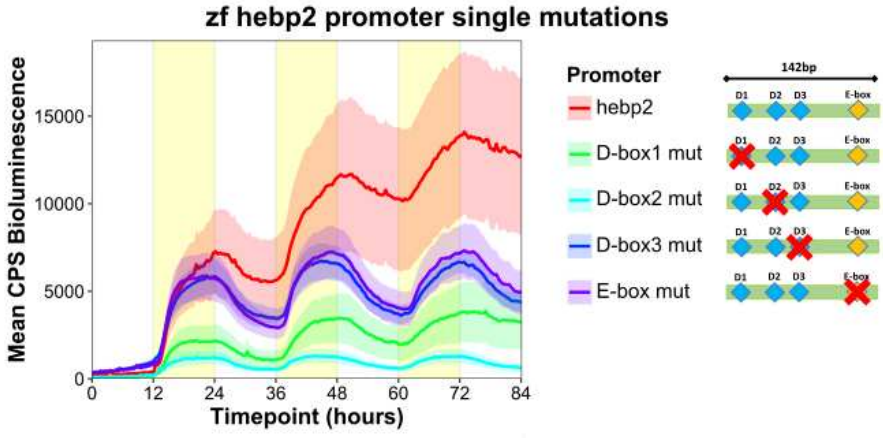

Figure 3.39. *In vivo* bioluminescence assay in zebrafish cells transfected with hebp2-Luc and its mutant constructs. Representative N=3 real-time bioluminescence assays of zebrafish cells transfected with the luciferase reporter hebp2-luc and constructs with single element mutations, exposed to LD cycles. Means of bioluminescence (CPS, N=6 wells) are plotted on the y-axis, with SEM indicated by shading, and time (hours) is on the x-axis. Lights-on periods are indicated by the yellow boxes.

I created subsequent constructs by site-directed mutagenesis of all but one enhancer sequence to investigate the contribution of single D-boxes and E-boxes to the light-induced expression of hebp2-Luc. I also prepared a construct with mutations to all enhancers. Upon transfection in PAC2 cells and exposure to LD cycles, the reporters showed minimal expression in response to light, indicating single D-boxes are not enough to convey the induction (Figure

3.40). Upon mutation of all enhancers (pink line) light-dependent expression is completely absent. The *in vitro* luciferase assay of PAC2 cells transfected with these reporters and exposed to blue light for eight hours also revealed minimal activation of the mutated promoters compared to the intact hebp2-Luc (Figure 3.41).

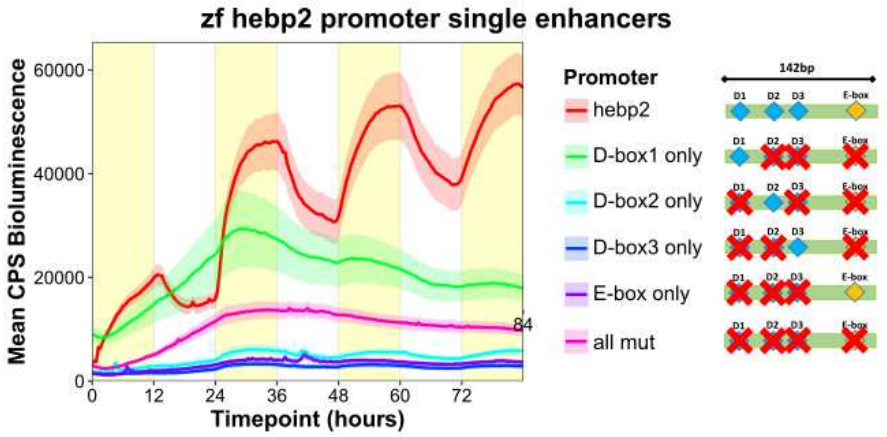

Figure 3.40. ***In vivo*** **bioluminescence assay in zebrafish cells transfected with hebp2-Luc and its mutant constructs.** Representative of N=3 real-time bioluminescence assays of zebrafish cells transfected with the luciferase reporter hebp2-Luc and constructs with mutations to all but one element, exposed to LD cycles. Means of bioluminescence (CPS, N=6 wells) are plotted on the y-axis, with SEM indicated by shading, and time (hours) is on the x-axis. Lights-on periods are indicated by the yellow boxes.

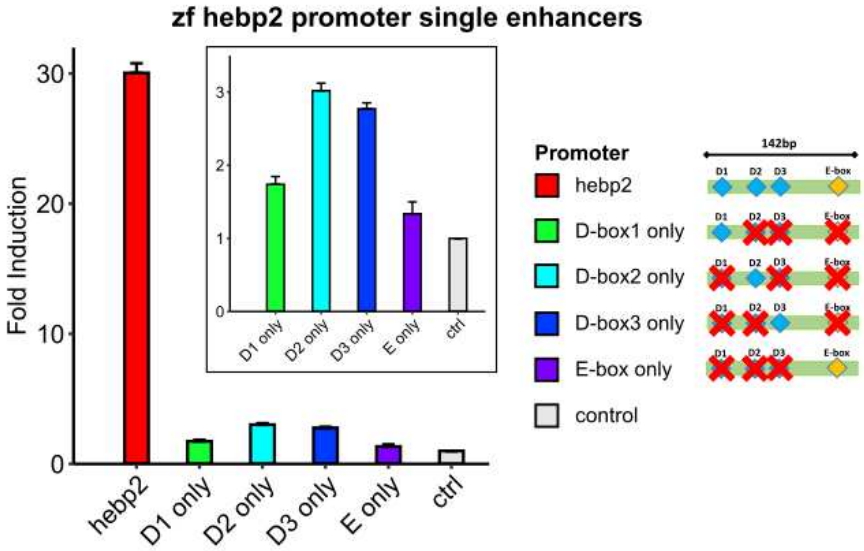

Figure 3.41. ***In vitro*** **bioluminescence assay in zebrafish cells transfected with hebp2-Luc and mutant constructs, after 8 hours of exposure to blue light.** Zebrafish cells were transfected with the luciferase reporter hebp2-Luc and constructs with mutations to all but one element, exposed to 8 hours of blue light. Fold inductions of relative bioluminescence compared to controls kept in darkness, $\pm$ SEM (N=2) are plotted on the y-axis, and time (hours) is on the x-axis. The β–galactosidase assay was used to normalize for transfection efficiency.

From the *in vivo* and *in vitro* luciferase assays it is clear that the induction of hebp2-Luc by light is dependent on the activation of the identified D-box and E-box sequences and that a synergistic effect between all enhancers grants *hebp2* its light-induced expression.

3.6.2 Transcription of *hebp2* and *soul5* but not *abcb6a* is regulated by ROS

The D-box is known to be responsible for the induction of clock genes like *per2* and *cry1a* in response to oxidative stress. Thus, the subsequent analysis aimed to evaluate the activation of abcb6a-Luc, hebp2-Luc, and soul5-Luc upon exposure to ROS. The luciferase reporter constructs were transiently transfected in PAC2 cells, followed by treatment with 1mM H_2O_2 in darkness. The hebp2-Luc and soul5-Luc reporters were induced (light blue line) with a peak around 3.5 hours after the treatment, compared to untreated controls (grey line) (Figure 3.42). Abcb6a-Luc instead did not show a clear ROS-dependent activation, although an overall increase in bioluminescence was seen at all time points.

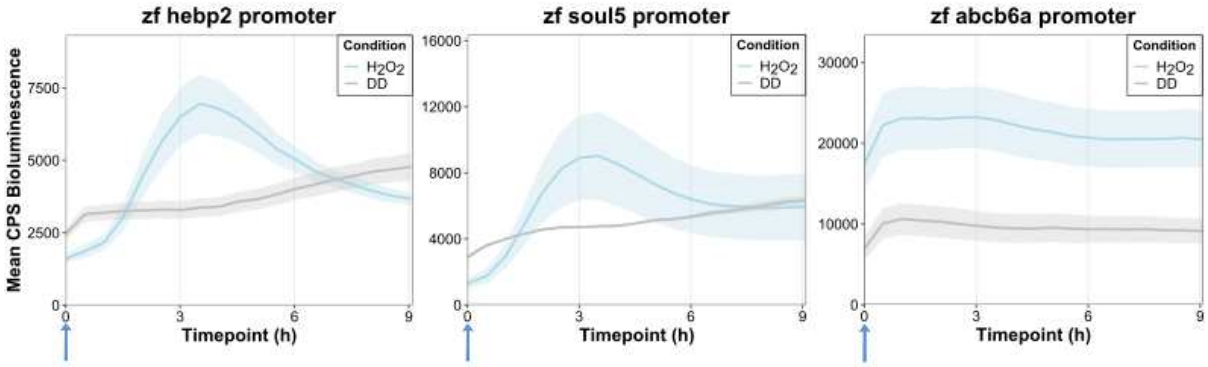

Figure 3.42. ***In vivo*** **bioluminescence assay in zebrafish cells transfected with hebp2-Luc, soul5-Luc, and abcb6a-Luc and treated with 1mM H_2O_2.** Representative of N=3 real-time bioluminescence assays of zebrafish cells transfected with the luciferase reporters hebp2-Luc, soul5-Luc, and abcb6a-Luc following 1mM H_2O_2 treatment (blue arrow) in darkness (DD). Treated wells are plotted in light blue, and unexposed controls in grey. Means of bioluminescence (CPS, N=4 wells) are plotted on the y-axis, with SEM indicated by shading, and time (hours) is on the x-axis.

3.6.2.1 Contribution of D-boxes and E-box to hebp2-Luc ROS-mediated induction

The contribution of single D-box and E-box sequences within the *hebp2* promoter was tested in response to ROS. The mutations to one of the four enhancers in hebp2-Luc are not sufficient to abolish the activation of the promoter in response to 1mM hydrogen peroxide treatment (Figure 3.43). On the other hand, single D-box and E-box enhancers are not enough to produce detectable activation (Figure 3.44), further suggesting the need for a synergistic effect of multiple enhancers to provide a robust light and ROS-dependent activation of *hebp2*.

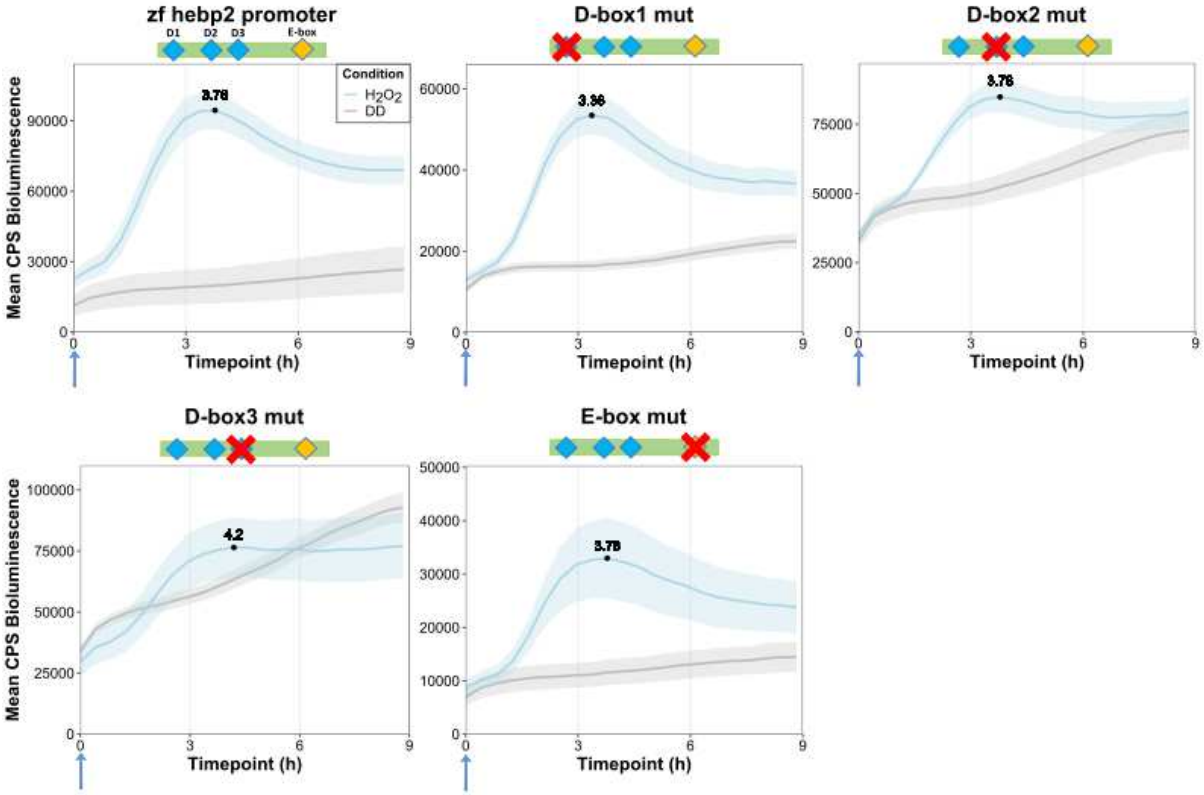

Figure 3.43. *In vivo* bioluminescence assay in zebrafish cells transfected with hebp2-Luc and its mutant constructs and treated with 1mM H_2O_2. Representative of N=3 real-time bioluminescence assays of zebrafish cells transfected with the luciferase reporter hebp2-Luc and its mutant constructs following 1mM H_2O_2 treatment (blue arrow) in darkness (DD). Treated wells are plotted in light blue, and nonexposed controls in grey. Means of bioluminescence (CPS, N=4 wells) are plotted on the y-axis, with SEM indicated by shading, and time (hours) is on the x-axis.

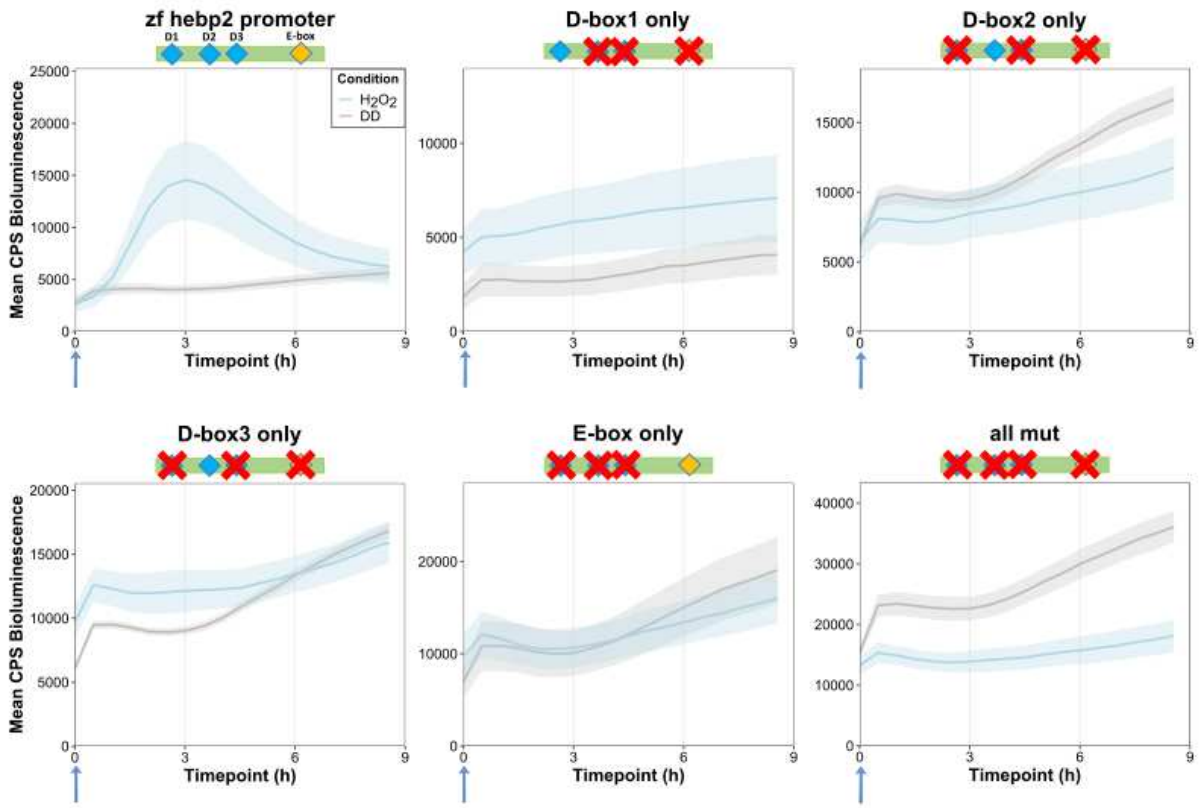

Figure 3.44. ***In vivo*** **bioluminescence assay in zebrafish cells transfected with hebp2-Luc and its mutant constructs and treated with 1mM H_2O_2.** Real-time bioluminescence assay of zebrafish cells transfected with the luciferase reporter hebp2-Luc and its mutant constructs following 1mM H_2O_2 treatment (blue arrow) in darkness (DD). Treated wells are plotted in light blue, and unexposed controls in grey. Means of bioluminescence (CPS, N=4 wells) are plotted on the y-axis, with SEM indicated by shading, and time (hours) is on the x-axis.

3.6.2.2 Is the activation of the *hebp2* and *soul5* promoters by ROS dose-dependent?

ROS is pivotal for the activation of D-box enhancer elements and previous results have implicated the MAPK signaling pathway, activated by oxidative stress, in light-mediated gene expression. Specifically, blue light has been shown to increase ROS levels within PAC2 cells, which in turn downregulate the ERK signaling pathway and increase the JNK and p38 stress kinase signaling pathway, and thereby leads to the activation of the D-box [105]. Does the expression of *hebp2* and *soul5* during light exposure also rely on the production of ROS in PAC2 cells? I used two experimental approaches to address this question. On the one hand, the

overexpression of catalase, an enzyme that catalyzes the break-down of H_2O_2 into water and oxygen, was used to dampen ROS increases in cells during light exposure. When hebp2-Luc and soul5-Luc were cotransfected with a catalase expression construct, bioluminescence measured *in vivo* over LD cycles was decreased compared to controls without catalase overexpression similarly to xpc-Luc (Figure 3.45, top). In the other approach, the overexpression of a dominant-negative form of ERK1 (dn-ERK) was previously reported to downregulate ERK signaling thus boosting the activation of the D-box. However, when hebp2-Luc and soul5-Luc were cotransfected with the dn-ERK, a bioluminescence increase was only seen in cells transfected with the soul5-Luc reporter (Figure 3.45, bottom). Overall the results point to ROS and ERK being possibly important players in the pathway of activation of the *hebp2* and *soul5* promoters in response to light, however, their activation does not solely rely on ROS and ERK.

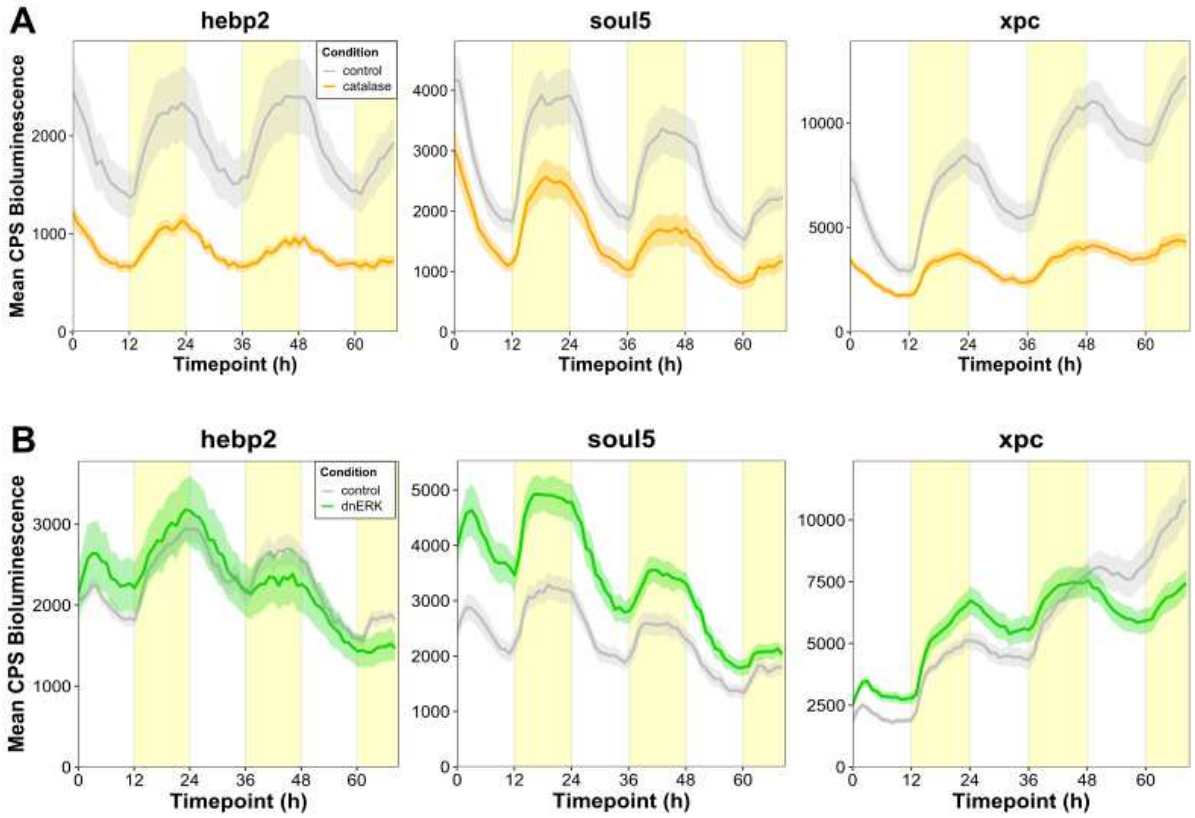

Figure 3.45. Cotransfection of catalase (top) and a dominant-negative form of ERK (bottom) with hebp2-Luc, soul5-Luc, and xpc-Luc in zebrafish cells exposed to LD cycles. Real-time bioluminescence assay of zebrafish cells cotransfected with the luciferase reporters hebp2-Luc, soul5-Luc, and xpc-Luc, and 100ng catalase expression vector (top, orange lines) or 100ng dominant-negative ERK (dn-ERK) expression vector (bottom, green lines). Cells are exposed for three days to 12h:12h light-dark cycles. Controls cotransfected with 100ng GFP expression vector instead of catalase or dn-ERK are plotted in grey. Means of bioluminescence (CPS, N=8 wells) are plotted on the y-axis, with SEM indicated by shading, and time (hours) is on the x-axis. Lights-on periods are indicated by the yellow boxes.

3.7 Cloning the cavefish PAR bZip and Nfil3 transcription factors and alignment with the zebrafish orthologs

Considering the ability of the PAR-bZip and Nfil3 transcription factors to bind and regulate transcription from the D-Box enhancer, they can be regarded as key candidates for contributing to the loss of light-induced gene expression in *P. andruzzii*. Evolutionary mutations and adaptations of these factors could contribute, at least in part, to the loss of D-Box activation

seen in cavefish. For this reason, all the sequences of cavefish PAR-bZip and Nfil3 transcription factors were successfully amplified by RT-qPCR and cloned in pGEM-T Easy as well as in the pCS2-MTK expression vector. Each of the zebrafish factors had one ortholog in cavefish. The gene *Nfil3-2a* presented two transcript variants: a full-length form (WT) sharing homology with the full-length zebrafish ortholog, and a mutant form (*Nfil3-2aX*) carrying a 145bp deletion in the middle, leading to a premature stop codon (Figure 6.1). The resulting Nfil3-2aX protein is made of 371 amino acids, while the NFil3-2a WT has 536 amino acids.

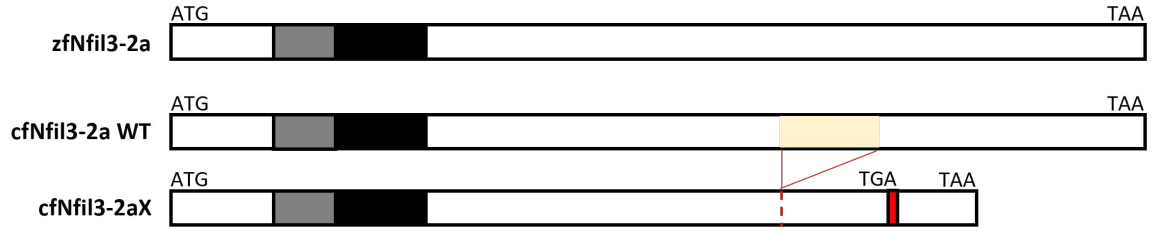

Figure 3.46. The zebrafish *Nfil3-2a* sequence (up) and its two orthologs in cavefish. The yellow box indicates the deletion of 145 bp in **Nfil3-2aX**. The red box indicates the premature stop codon created by the mutation.

Subsequently, I aligned the amino acid sequences of the zebrafish and cavefish factors. Homology scores for the PAR-bZip proteins are reported in Table 3.1. The C-terminal portion of the PAR-bZip proteins, which contains the PAR, basic, and leucine zipper domains, is mostly conserved in both species. The N-terminal sequences show the least homology. Among the PAR-bZip factors, DBP-1 and DBP-2 are the most conserved, with 93.7% and 93.3% homology, respectively, followed by HLF-2 (87.7%) and HLF-1 (86.7%). The least conserved are TEF-1 and TEF-2 (82.1% and 77.4%). The proline residues within the PAR domain and the isoleucine, leucines, and cysteine residues within the leucine zipper domain are all conserved across the two species, as they are in mouse factors [128]. Figures 3.47 - 3.52 show the alignments of each zebrafish and cavefish PAR-bZip protein.

Comparison	Amino acid similarity	Score	Gap frequency	GenBank accession n
TEF-1	82.1%	1261	1%	PP750800
TEF-2	77.4%	1147	3.2%	PP750801
DBP-1	93.7%	1776	1.4%	PP750802
DBP-2	93.3%	1805	1.1%	PP750803
HLF-1	86.7%	1303	2.7%	PP750804
HLF-2	87.7%	1340	3.3%	PP750805

Table 3.1. Alignment scores between zebrafish and cavefish PAR-bZip factors. Protein sequences were aligned with EXPASY protein alignment tool (https://web.expasy.org/sim/).

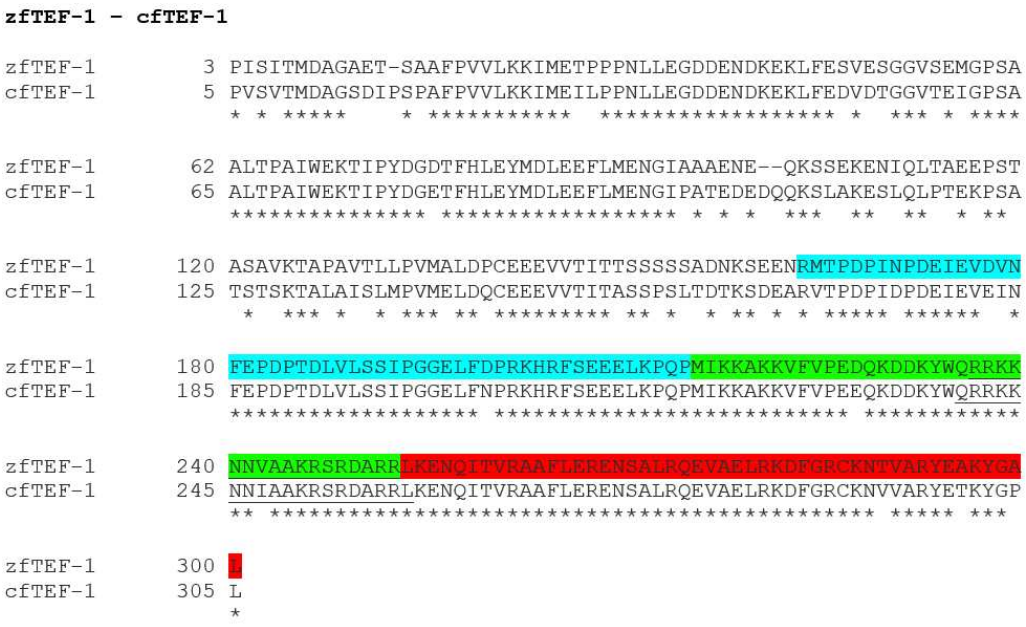

Figure 3.47. Alignment of zebrafish and cavefish TEF-1. The PAR domain is highlighted in light blue, the basic domain in green, and the leucine zipper in red. The predicted nuclear localization sequence is underlined.

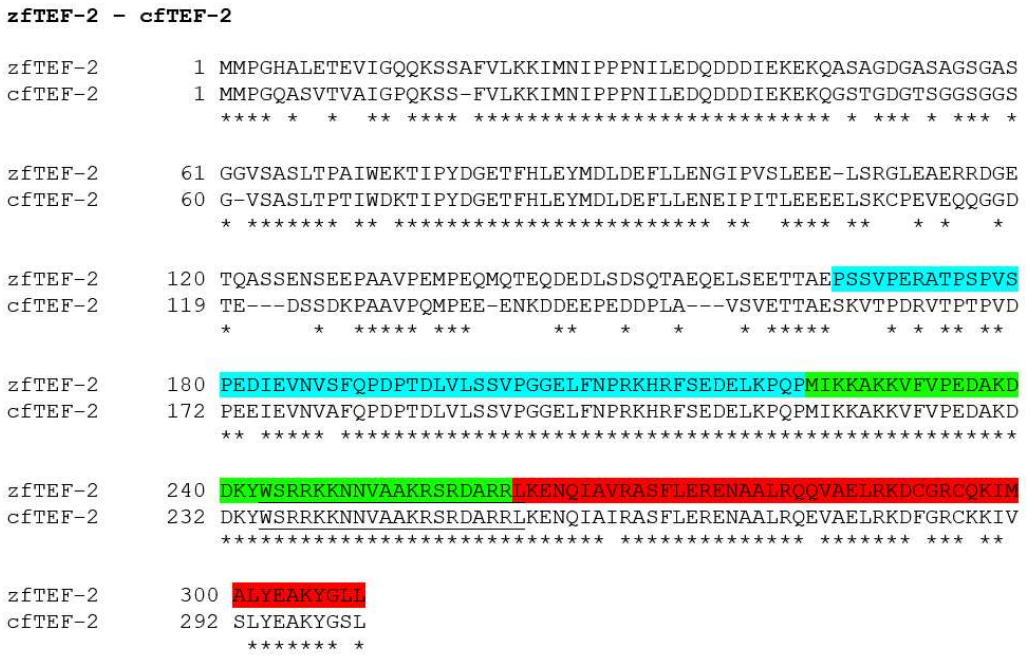

Figure 3.48. Alignment of zebrafish and cavefish TEF-2. The PAR domain is highlighted in light blue, the basic domain in green, and the leucine zipper in red. The predicted nuclear localization sequence is underlined.

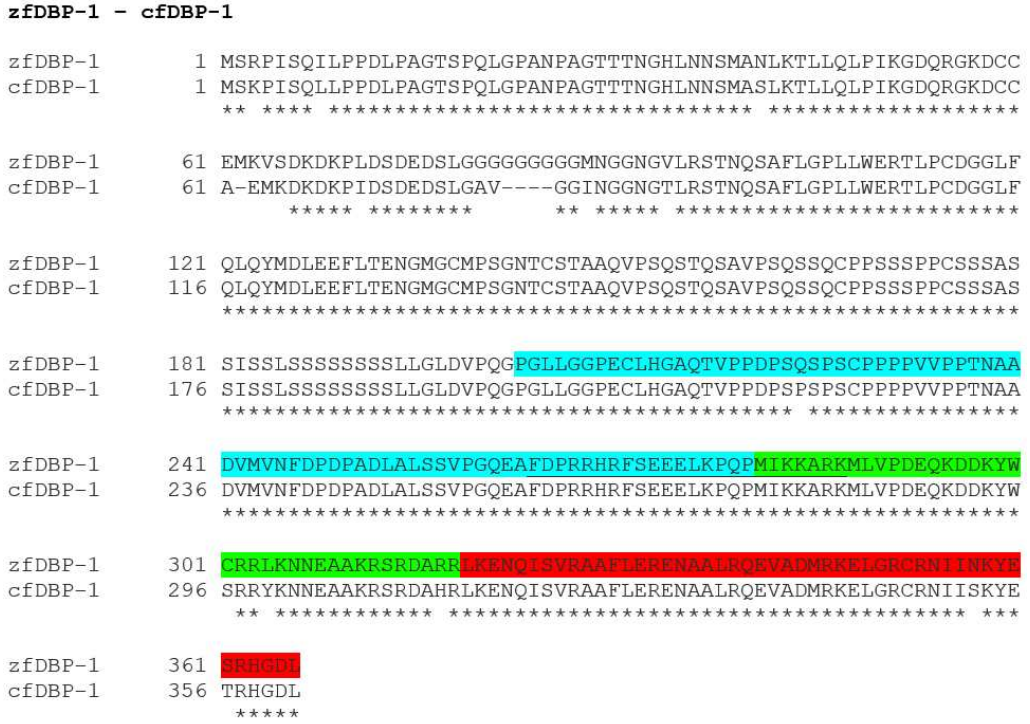

Figure 3.49. Alignment of zebrafish and cavefish DBP-1. The PAR domain is highlighted in light blue, the basic domain in green, and the leucine zipper in red. The predicted nuclear localization sequence is underlined.

zfDBP-2 – cfDBP-2

```
zfDBP-2       1 MARPLSQLLPPDLPSAGASPQFGNSSQAGVTHNGGHLNSTGNLKSLLQLPVKCDQRVKDC
cfDBP-2       1 MARPLSQLLPPDLPSAGASPQFGNSSQAGVSLNGGHLNSSTNLKSLLQLPVKGDQRGKDC
                ****************************  *******  *********** *** ***

zfDBP-2      61 GEMKGKERLDIDEDSLGRCPLRNGCSNGLVTDSNGAGTGSFSNNSNNNNSFLGPLLWERT
cfDBP-2      61 TEMKGKDRLDIDEDSLGRCPLRNGCSNGLV-DSNGAGTGSFSNG--NNNSFLGPLLWERT
                 ***** ********************** ************   **************

zfDBP-2     121 LPCDGGLFQLQYMDLEEFLTENGMSSMHNTSNSTSAQIPSQSSQSAVPNQGSQCLPTSPP
cfDBP-2     118 LPCDGGLFQLQYMDLEEFLTENGMSSMHSTSNSTSAQIPSQSSQSAVPNQGSQCLPTSPP
                ************************** ******************************

zfDBP-2     181 HCSSSSSPTSATASS-PSLLGLDMHTPQSMMGSTDCLHGTPPGSLEPTPSPSSTTCPPLP
cfDBP-2     178 HCSSSSSPTAATASSSPSLLGLDMHTPQSMMGTGDCLHGTPPGSLEPTPSPSSTTCPPLP
                ********* ***** ***************  *************************

zfDBP-2     240 TPPATNCNELLAPFDPDPADVALSSVPGQEAFDPRRHHFSDEDLKPQPMIKKARKMLVPE
cfDBP-2     238 TPPIANCNDMLAPFDPDPADVALSSVPGQEAFDPRRHRFSEEELKPQPMIKKARKMLVPD
                ***  ***  ************************** ** * ****************

zfDBP-2     300 DLKDEKYWSRRCKNNEAAKRSRDARRLKENQISVRAAFLERENAALRQEVADMRKELGRC
cfDBP-2     298 DLKDEKYWSRRCKNNEAAKRSRDARRLKENQISVRAAFLERENAALRQEVADMRKELGRC
                ************************************************************

zfDBP-2     360 RNILNKYESHHLDQ
cfDBP-2     358 RNILNKYESHHLDQ
                **************
```

Figure 3.50. Alignment of zebrafish and cavefish DBP-2. The PAR domain is highlighted in light blue, the basic domain in green, and the leucine zipper in red. The predicted nuclear localization sequence is underlined.

zfHLF-1 – cfHLF-1

```
zfHLF-1       2 EKMSRPLPINATFLPPTHGVLKSLLENPMKLPFHHDE--GFGKEKEKEKKLEDDASTLNT
cfHLF-1       3 EKMSRPLPINSAFLPPTHGVLKSLLENPMKLPFHHDEVKGFGKDKEKEKKLEEDGGPLNA
                **********  *************************  **** ******** *   **

zfHLF-1      60 PQSAFLGPTLWDKTLPYNADNFQLEYMDLEEFLLENNIPANPQSEQSQPSQP-----PLQ
cfHLF-1      63 PQSAFLGPTLWDKTLPYDGDNFQLEYMDLEEFLLENNIPANPASEQSQPSQQQQPQQPQQ
                *****************  ********************** ********      * *

zfHLF-1     115 PPSAPPTPSVVDLSNRDNSSSHNGMVAQNCLQNPTRPGLPASRDTPSPIDPDSIQVPLAY
cfHLF-1     123 PPSTPPTPSVVDRSNRTAPSVHSAIVGQNCLQSPNRAGL-TSRDTPSPIDPDTIQVPVRY
                *** ******** ***   * *   * ***** * * **  *********** ****  *

zfHLF-1     175 EPDPADLALSSVPGQEIFDPRKRKFSAEELKPQPMIKKARKVFIPEDLKDDRYWARRRKN
cfHLF-1     182 EPDPADLALSSVPGQEIFDPRKRKFSAEELKPQPMIKKARKVFIPEDLKDDRYWARRRKN
                ************************************************************

zfHLF-1     235 NIAAKRSRDARRLKENQIAIRAGFLEKENAALRAEVADLRKELGRCKNVLAKYEARHGPL
cfHLF-1     242 NIAAKRSRDARRLKENQIAIRAGFLEKENHALRQEVADLRKELGRCKNVLAKYEARHGPL
                ************************** *** ************************
```

Figure 3.51. Alignment of zebrafish and cavefish HLF-1. The PAR domain is highlighted in light blue, the basic domain in green, and the leucine zipper in red. The predicted nuclear localization sequence is underlined.

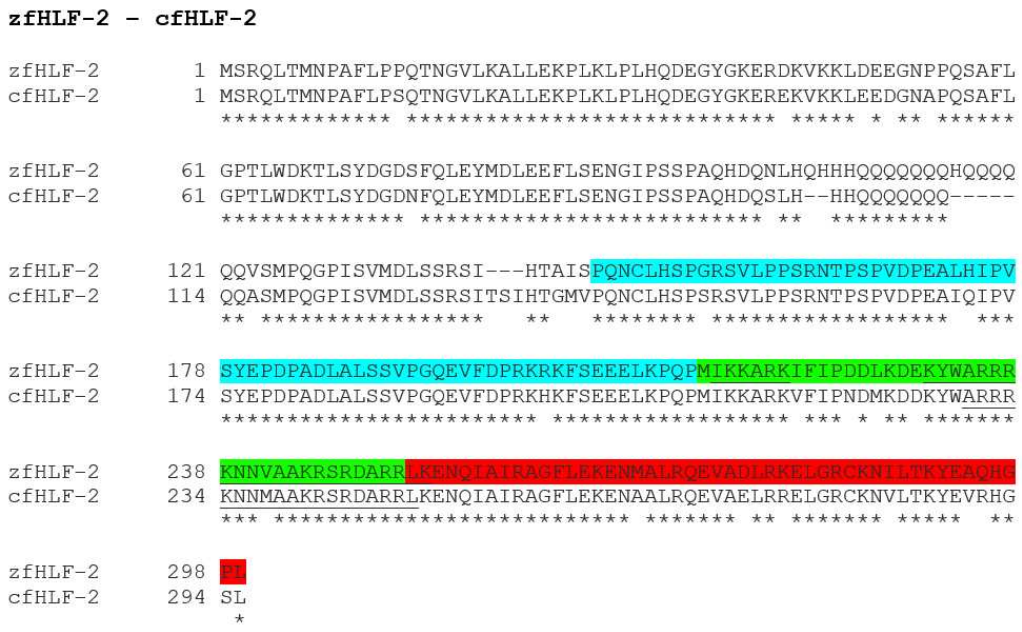

Figure 3.52. Alignment of zebrafish and cavefish HLF-2. The PAR domain is highlighted in light blue, the basic domain in green, and the leucine zipper in red. The predicted nuclear localization sequence is underlined.

Similarly to the PAR factors, the basic and leucine zipper domains found in the N-terminal regions of the Nfil3 proteins are highly conserved in zebrafish and cavefish and the main differences lie downstream in the C-terminal part. Homology scores for the Nfil3 proteins are reported in Table 3.2. Among them, Nfil3-1a is the most conserved (85.5%), followed by Nfil3-2b (83.9%), Nfil3-1b (82%), Nfil3-3b (81.2%), and the least conserved is Nfil3-3a (56.6%). The cavefish full-length Nfil3-2a WT shares 77.2% homology with the zebrafish Nfil3-2a, and the Nfil3-2aX has a 74.2% homology with the zebrafish factor, until its premature truncation. Figures 3.53 - 3.59 show the alignments of each zebrafish and cavefish Nfil3 protein.

Comparison	Amino acid similarity	Score	Gap frequency	GenBank accession n
Nfil3-1a	85.5%	1962	2.2%	PP750806
Nfil3-1b	82%	1119	0%	PP750810
Nfil3-2a WT	77.2%	2023	2.2%	PP750807
Nfil3-2aX (mut)	74.2%	1253	2.9%	PP750808
Nfil3-2b	83.9%	2450	3.7%	PP750811
Nfil3-3a	56.6%	662	10.4%	PP750809
Nfil3-3b	81.2%	1406	3.4%	PP750812

Table 3.2. Alignment scores between zebrafish and cavefish Nfil3 factors. Protein sequences were aligned with EXPASY protein alignment tool (https://web.expasy.org/sim/).

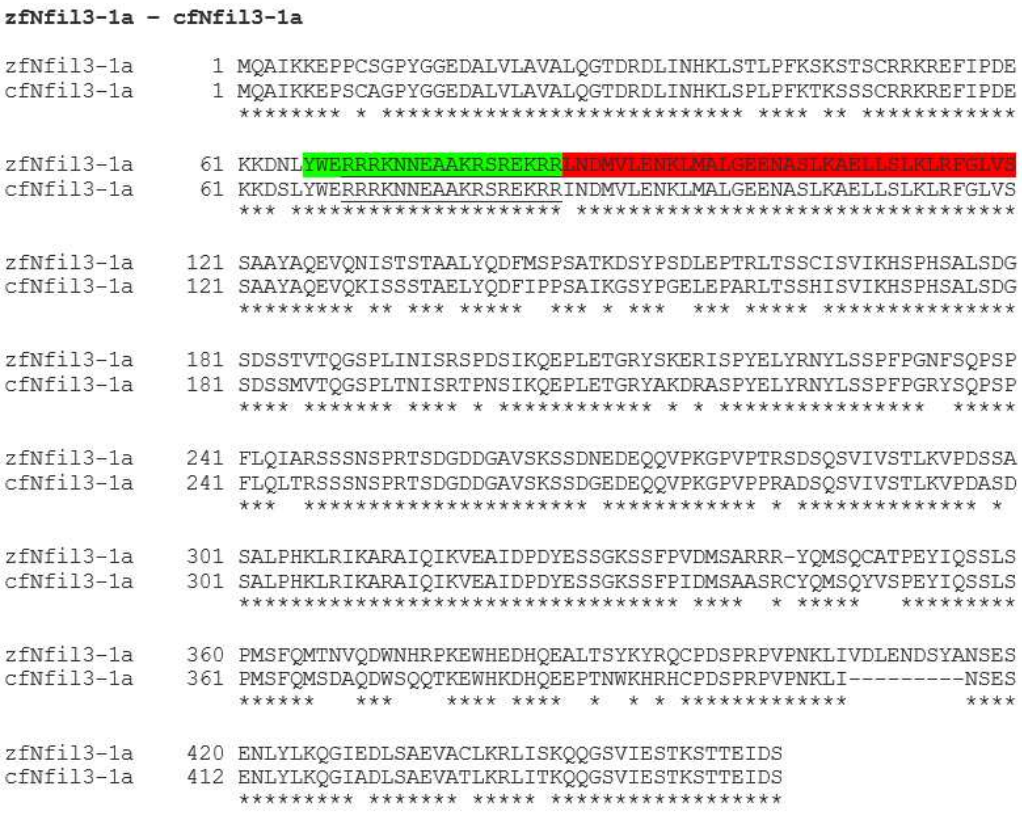

Figure 3.53. Alignment of zebrafish and cavefish Nfil3-1a. The basic domain in green and the leucine zipper in red. The predicted nuclear localization sequence is underlined.

Figure 3.54. Alignment of zebrafish and cavefish Nfil3-1b. The basic domain in green and the leucine zipper in red. The predicted nuclear localization sequence is underlined.

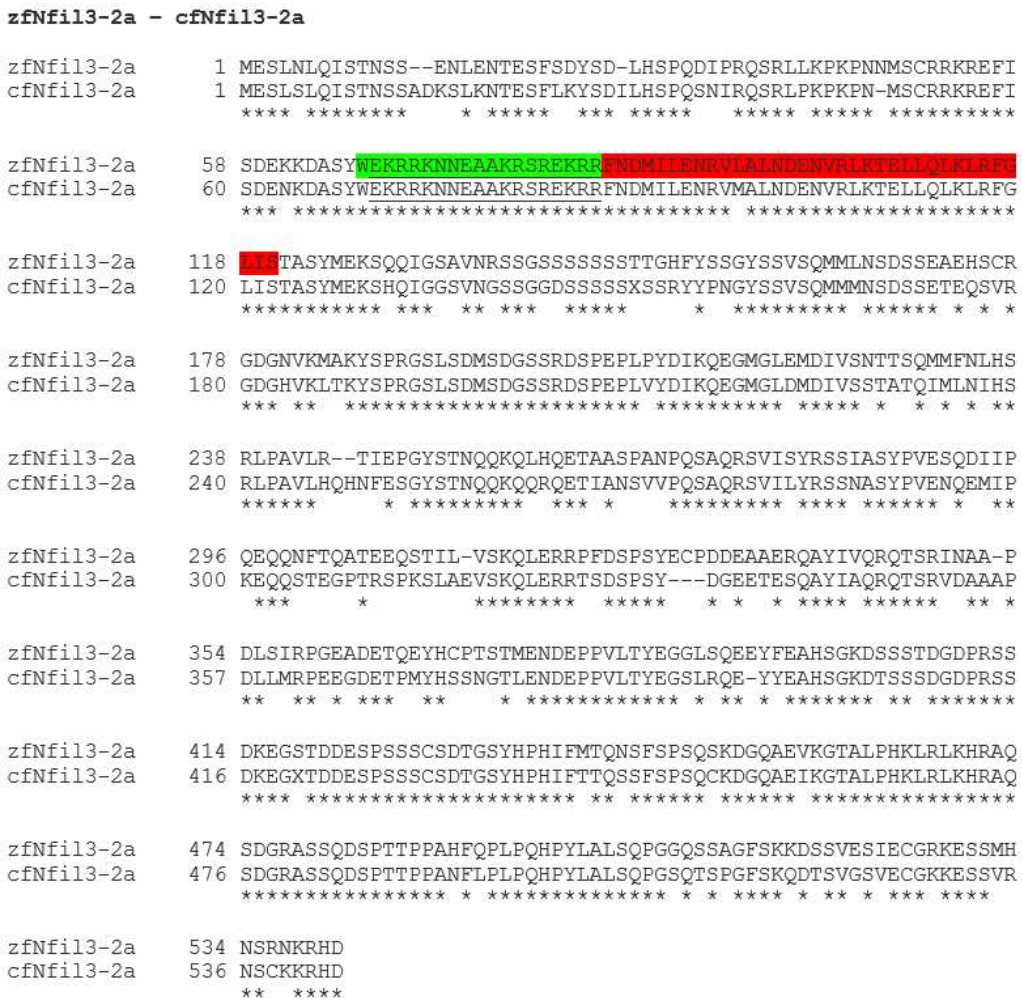

Figure 3.55. Alignment of zebrafish and cavefish Nfil3-2a. The basic domain in green and the leucine zipper in red. The predicted nuclear localization sequence is underlined.

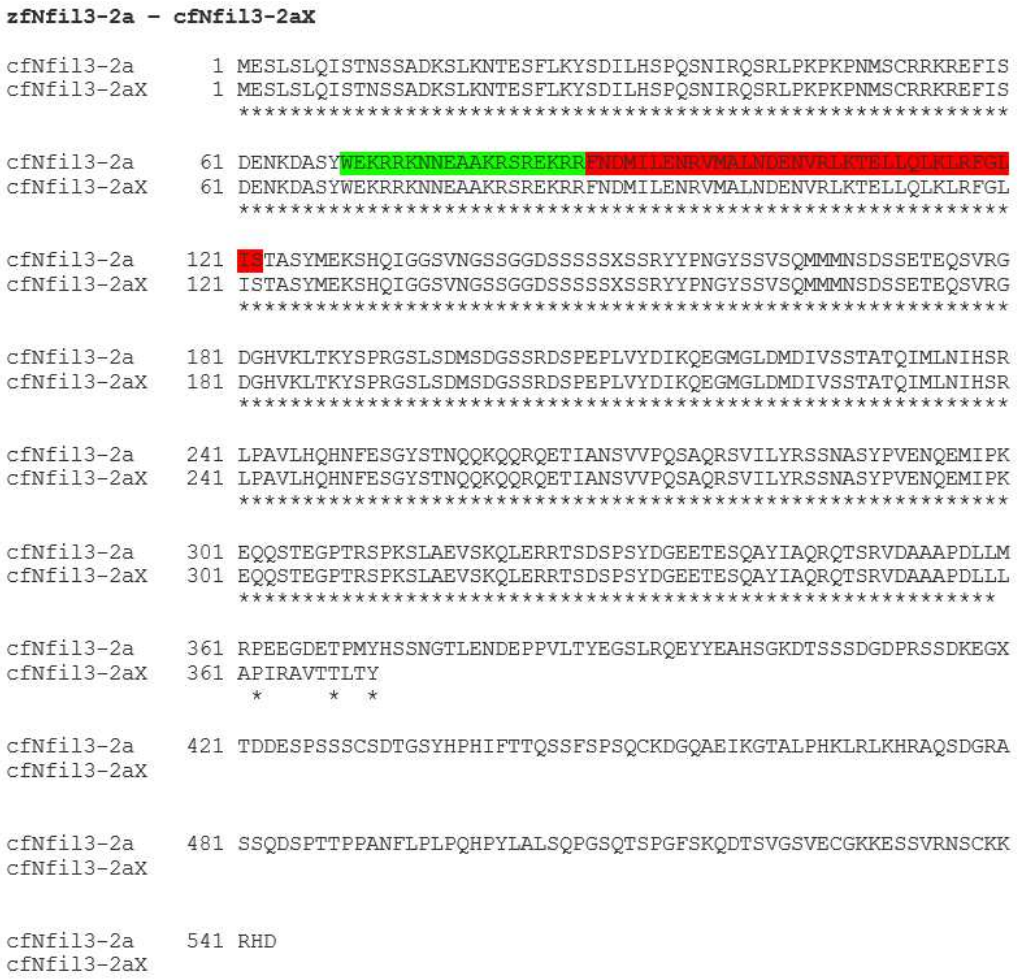

Figure 3.56. Alignment of zebrafish Nfil3-2a and cavefish Nfil3-2a. The basic domain in green and the leucine zipper in red. The predicted nuclear localization sequence is underlined.

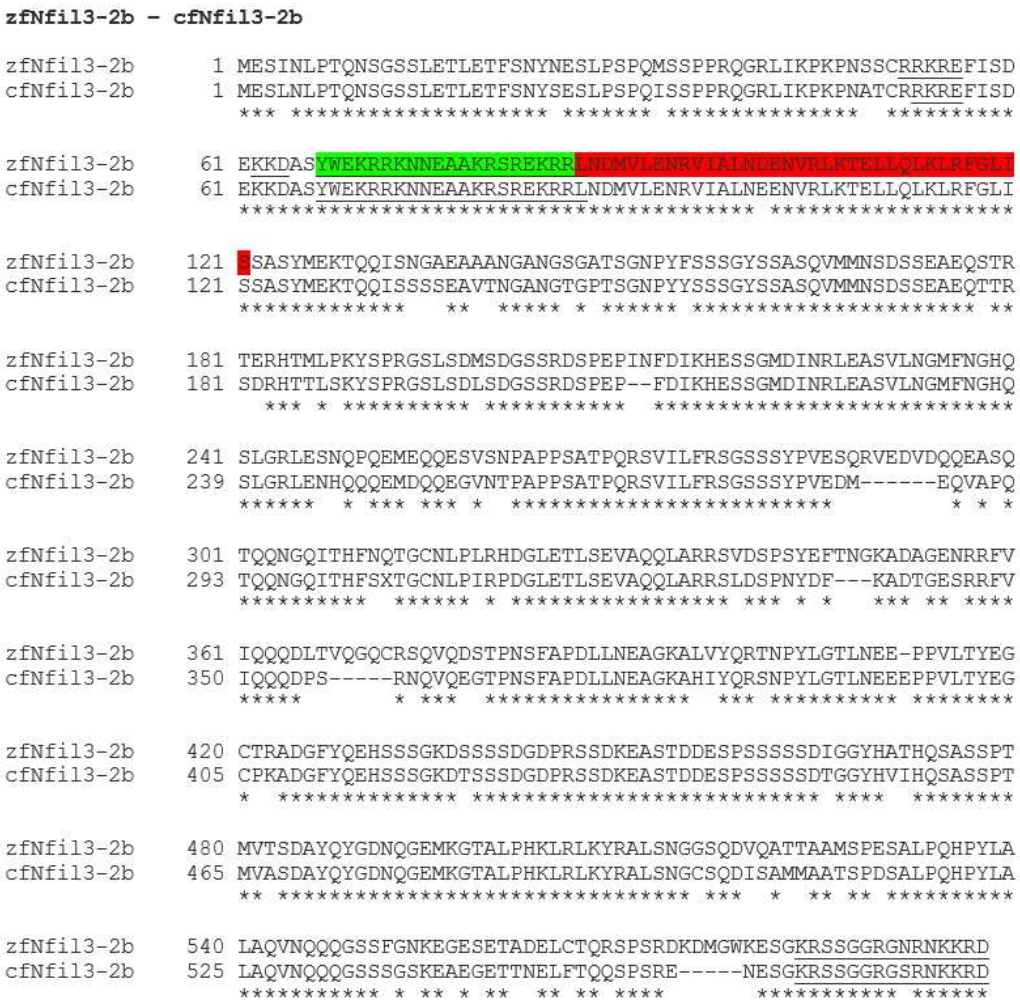

Figure 3.57. Alignment of zebrafish and cavefish Nfil3-2b. The basic domain in green and the leucine zipper in red. The predicted nuclear localization sequence is underlined.

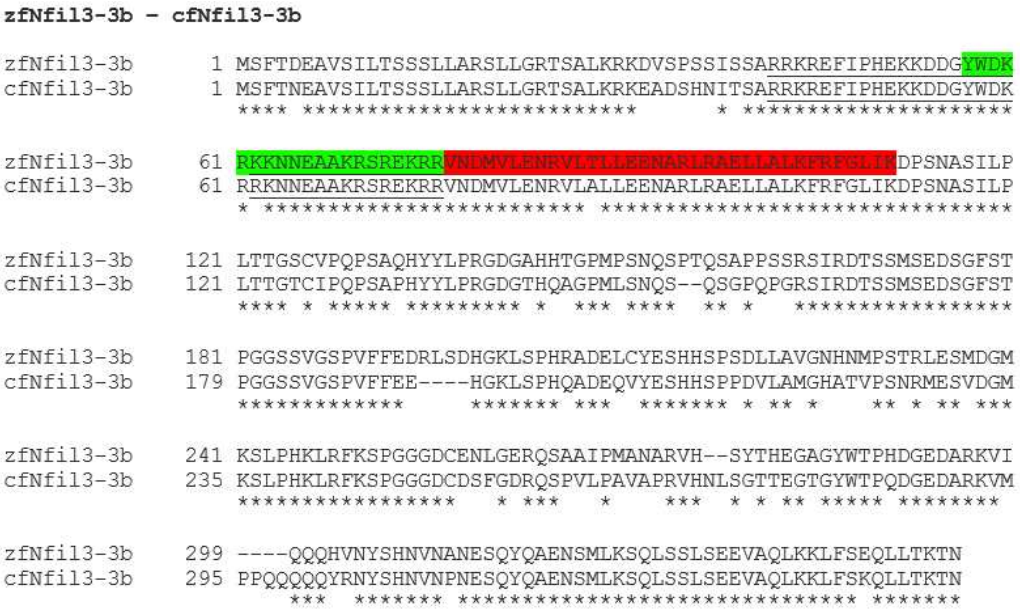

Figure 3.58. Alignment of zebrafish and cavefish Nfil3-3a. The basic domain in green and the leucine zipper in red. The predicted nuclear localization sequence is underlined.

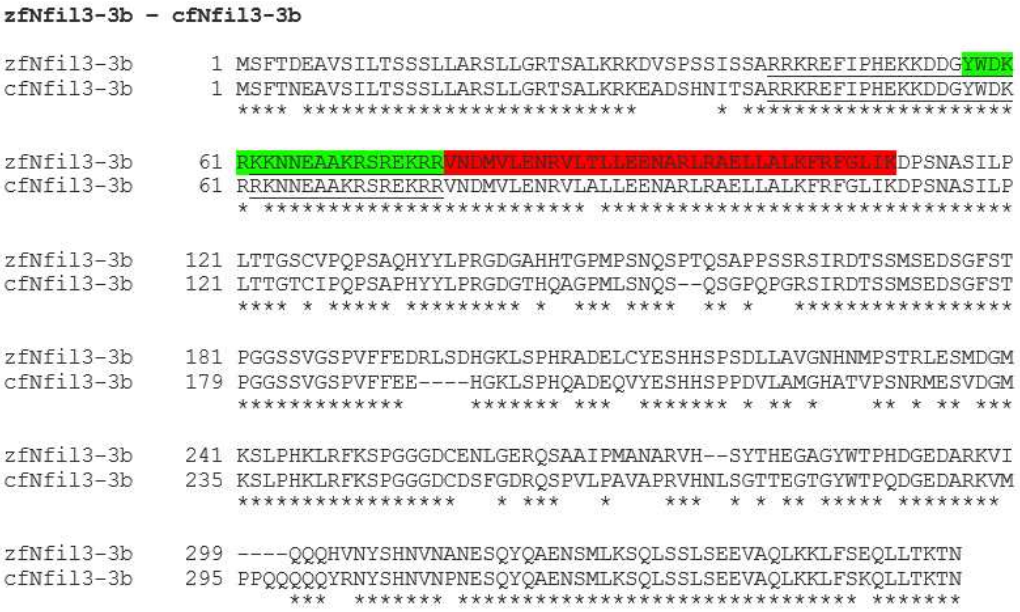

Figure 3.59. Alignment of zebrafish and cavefish Nfil3-3b. The basic domain in green and the leucine zipper in red. The predicted nuclear localization sequence is underlined.

3.7.1 Western blots to check for expression of the factors in pCS2-MTK

The PAR-bZip and Nfil3 factors were cloned in the pCS2-MTK vector, which contains a 5' 5x MYC tag sequence allowing for expression of N-terminally tagged proteins. The plasmids were

transiently transfected in zebrafish PAC2 cells and their expression was confirmed via western blotting (Figure 3.60 for PAR-bZip factors, Figure 3.61 for Nfil3 factors).

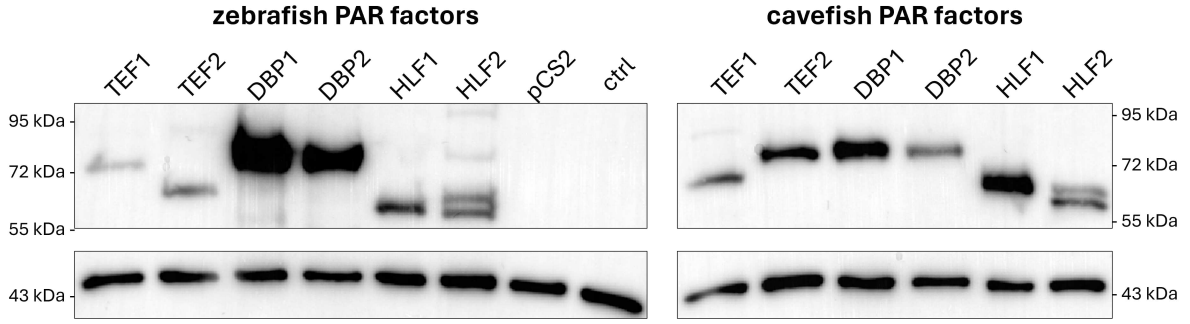

Figure 3.60. Western blot of overexpression of zebrafish and cavefish PAR-bZip factors. PAC2 cells were transiently transfected with 1μg of the expression vectors, which contain a 5x MYC tag at the N-terminal of the proteins (upper bands). The cells were lysed after 48 hours and a western blot was performed to detect protein expression. β–actin (lower bands) expression is used as loading control.

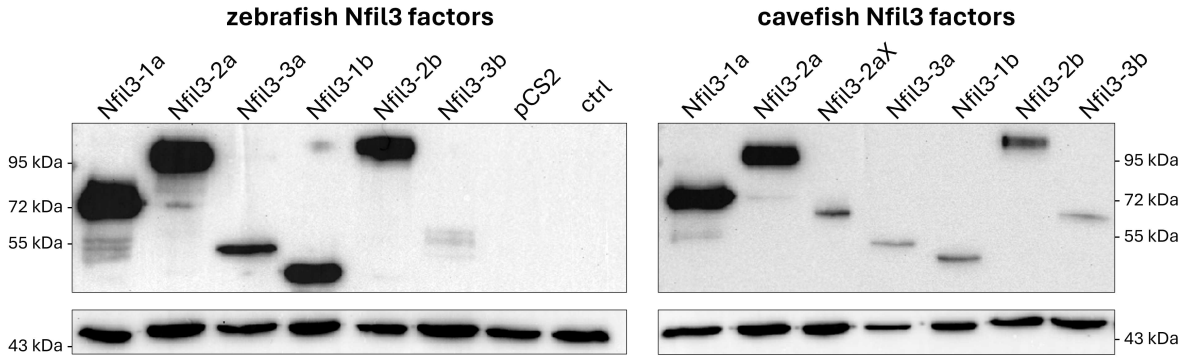

Figure 3.61. Western blot of overexpression of zebrafish and cavefish Nfil3 factors. PAC2 cells were transiently transfected with 1μg of the expression vectors, which contain a 5x MYC tag at the N-terminal of the proteins (upper bands). The cells were lysed after 48 hours and a western blot was performed to detect protein expression. β–actin (lower bands) expression is used as loading control.

3.7.2 Functional assays: Testing the ability of the PAR factors and Nfil3 factors to activate the D-box

The PAR-bZip and Nfil3 family of transcription factors bind to and regulate transcription via the D-box, as demonstrated in mammals [127], [149] and zebrafish [128]. Do genetic changes in these factors in any way account for the significant changes in light and ROS-induced gene expression in the cavefish? While the cavefish proteins present no obvious truncations, various non-conservative amino acid substitutions could potentially affect their structure, function,

and interaction with the D-box. Thus, their functional roles were investigated using *in vitro* luciferase reporter assays. Firstly, they were tested with a reporter vector containing a heterologous promoter consisting of 15 tandemly repeated copies of the cry1a D-box sequence cloned upstream of a minimal promoter driving the expression of luciferase, hereafter called 15xD-box$_{cry1a}$-Luc. The reporter was cotransfected with 1ng of the expression vectors of each of the transcription factors in zebrafish PAC2 cells, which were then lysed after 48 hours in darkness. All the PAR factors except DBP-1 successfully activate the 15xD-box$_{cry1a}$-Luc and the zebrafish orthologs lead to a stronger activation than the cavefish counterparts (Figure 3.62). The TEF-2 and DBP-2 of both species exhibit the strongest activation. On the other hand, the Nfil3 factors do not activate the D-Box reporter, consistent with the previous reports of Nfil3 being a repressor in mammals [127]. One exception is the cavefish factor Nfil3-2b, which leads to a 32-fold increase in activation.

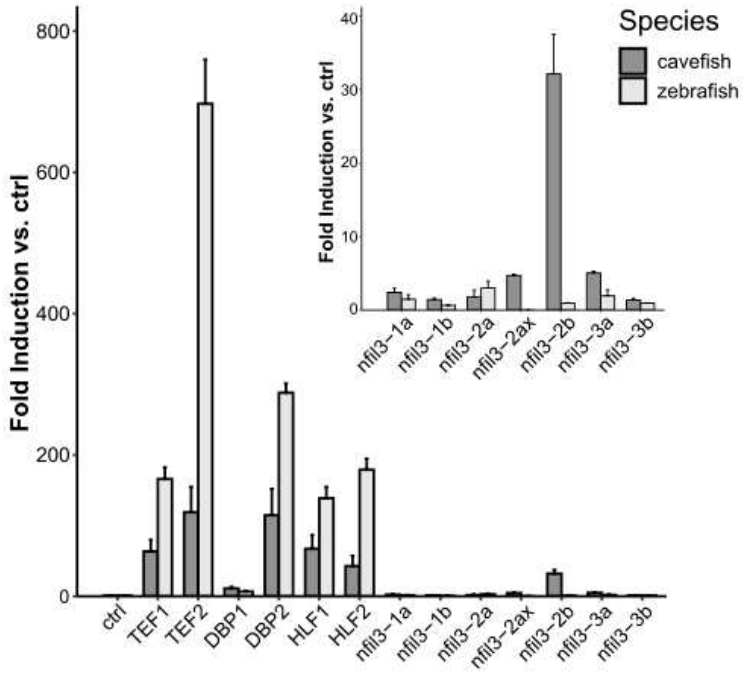

Figure 3.62. *In vitro* bioluminescence assay in zebrafish cells cotransfected with 15xD-box$_{cry1a}$-Luc and the PAR and Nfil3 factors. Zebrafish PAC2 cells were cotransfected with 200ng of 15xD-box$_{cry1a}$-Luc reporter and 1ng of the 6 zebrafish and 6 cavefish PAR and Nfil3 factors expression vectors (x-axis) and kept in darkness for 48 hours before lysis. Fold inductions of relative bioluminescence compared to the control condition, $\pm$ SEM are plotted on the y-axis. The β–galactosidase assay was used to normalize for transfection efficiency.

The assay was repeated in cavefish EPA cells for the PAR factors (Figure 3.63). The factors activate transcription similarly in both PAC2 and EPA cells, confirming there is nothing abnormal in the cavefish cell transcriptional regulatory machinery that could account for the loss of D-box-mediated gene expression. However, cotransfection of the cavefish factors in both cell types leads to weaker activation of the 15xD-box$_{cry1a}$-Luc, which poses the possibility of a mutation common to all cavefish factors or within upstream signaling pathways interacting with them and affecting their overall ability to activate the D-box.

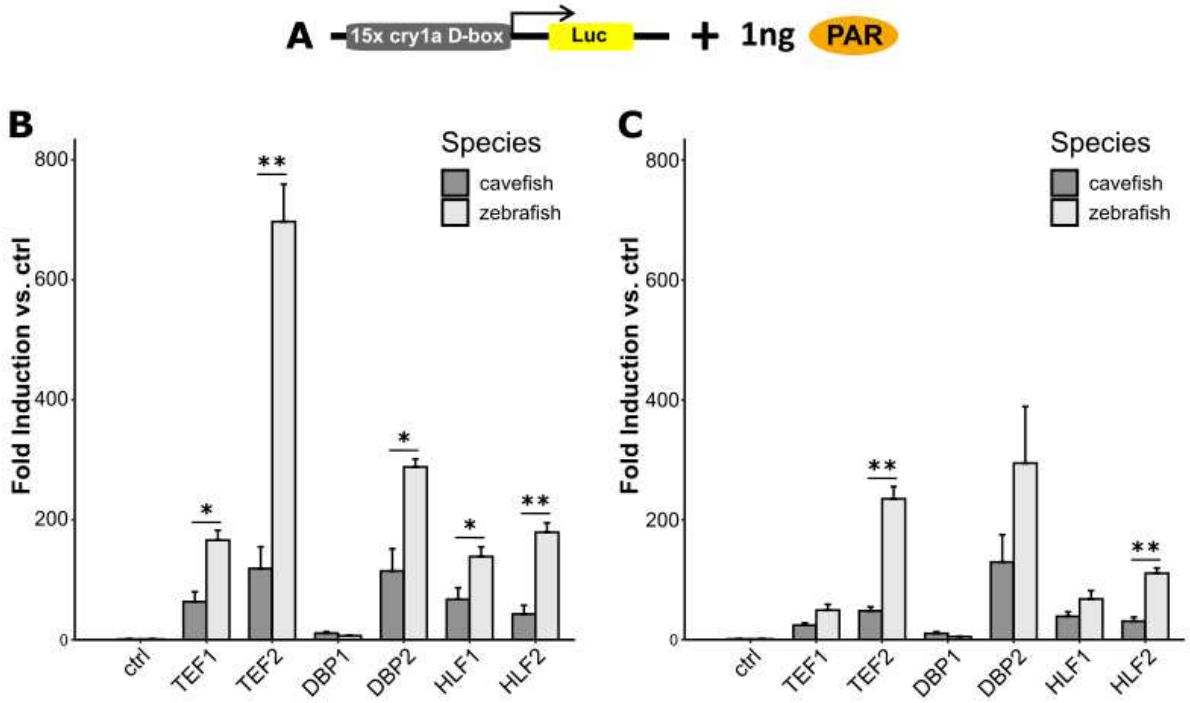

Figure 3.63. ***In vitro*** **bioluminescence assay in zebrafish (B) and cavefish (C) cells cotransfected with 15xD-box$_{cry1a}$-Luc and the PAR factors. A)** scheme of the 15xD-box$_{cry1a}$-Luc luciferase reporter vector. **B, C)** *In vitro* bioluminescence assay. Zebrafish PAC2 **(B)** and cavefish EPA **(C)** cells were cotransfected with 200ng of 15xD-box$_{cry1a}$-Luc heterologous construct and 1ng of the 6 zebrafish and 6 cavefish PAR factors expression vectors (x-axis) and kept in darkness for 48 hours before lysis. Fold inductions of relative bioluminescence compared to the control condition, ± SEM are plotted on the y-axis. Results are the means of three independent experiments. The β–galactosidase assay was used to normalize for transfection efficiency. Differences between zebrafish and cavefish transcription factors are compared via t-tests with Bonferroni correction. Detailed statistical analysis can be found in Table S6. p<0.5, p<0.01, p<0.001 are represented by *, **, and *** respectively.

Are the PAR–bZip factors able to activate the D-Box sequences previously identified in the hebp2 promoter? To answer this question, 1ng of each factor was transiently cotransfected

with 50ng of the hebp2-Luc reporter in PAC2 and EPA cells (Figure 3.64). Results reveal all factors except DBP-1 activate hebp2-Luc, albeit much less strongly than the heterologous 15xD-box$_{cry1a}$-Luc. Moreover, TEF-1, TEF-2, and HLF-2 are the strongest activators in PAC2 cells. The factors activate hebp2-Luc much less strongly in EPA cells.

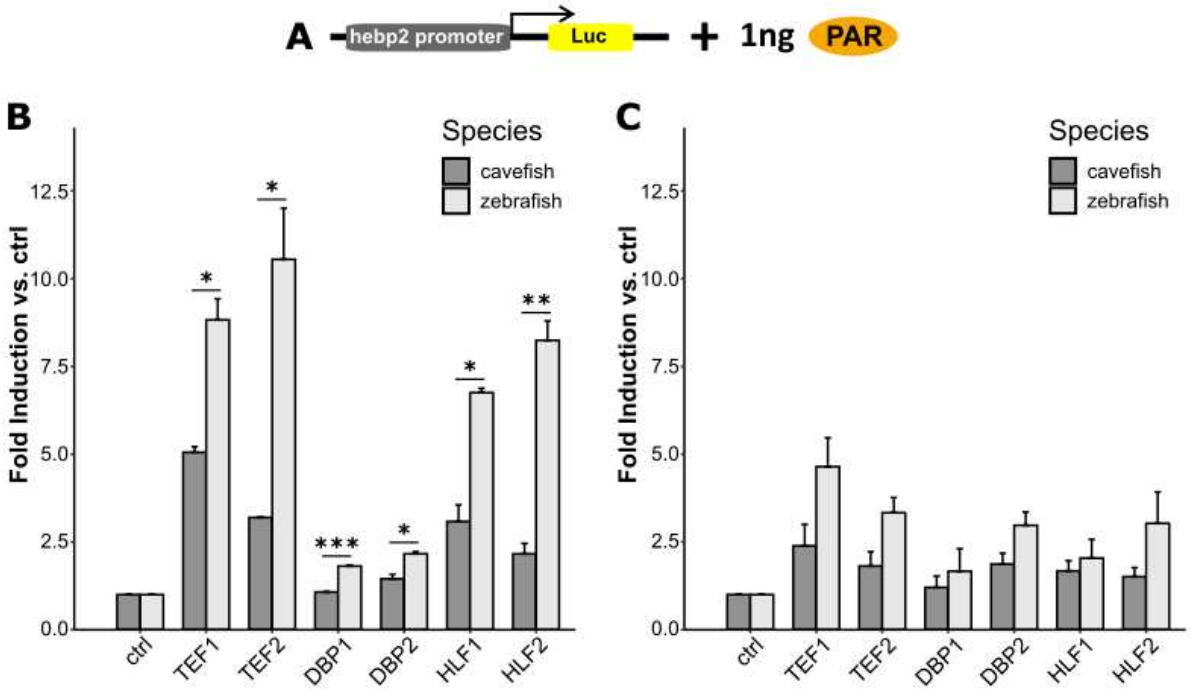

Figure 3.64. ***In vitro*** **bioluminescence assay in zebrafish (B) and cavefish (C) cells cotransfected with hebp2-Luc and the PAR factors. A)** scheme of the hebp2-Luc luciferase reporter vector. **B, C)** *In vitro* bioluminescence assay. Zebrafish PAC2 **(B)** and cavefish EPA **(C)** cells were cotransfected with 50ng of hebp2-Luc and 1ng of the 6 zebrafish and 6 cavefish PAR factors expression vectors (x-axis) and kept in darkness for 48 hours before lysis. Fold inductions of relative bioluminescence compared to the control condition, ± SEM are plotted on the y-axis. Results are the means of three independent experiments. The β–galactosidase assay was used to normalize for transfection efficiency. Differences between zebrafish and cavefish transcription factors are compared via t-tests with Bonferroni correction. Detailed statistical analysis can be found in Table S6. p<0.5, p<0.01, p<0.001 are represented by *, **, and *** respectively.

3.7.3 The N-terminal part of HLF-2 is important for the transactivation of hebp2-Luc

HLF-2 was chosen for further analyses aimed at unraveling the difference between the zebrafish and cavefish orthologs in the transactivation of the hebp2 promoter. Two hybrids of HLF-2 were genetically constructed by fusing the N-terminal of one protein and the C-terminal (defined as

the part of the protein containing the PAR, bZip, and basic domains) of the other. The resulting proteins were zc-HLF-2, containing the N-terminal of zHLF-2 and the domains of cHLF-2, and cz-HLF-2, containing the N-terminal of cHLF-2 and the domains of zHLF-2 (Figure 3.65 C). Their ability to transactivate the D-box in comparison to the wildtype zHLF-2 and cHLF-2 was tested by cotransfecting them with the hebp2-Luc reporter in PAC2 cells (Figure 3.65 B). Results point to the importance of the zebrafish N-terminal of the protein for transactivation: only zfHLF-2 and zc-HLF-2, containing the zHLF-2 N-terminal portion, can significantly activate hebp2-Luc.

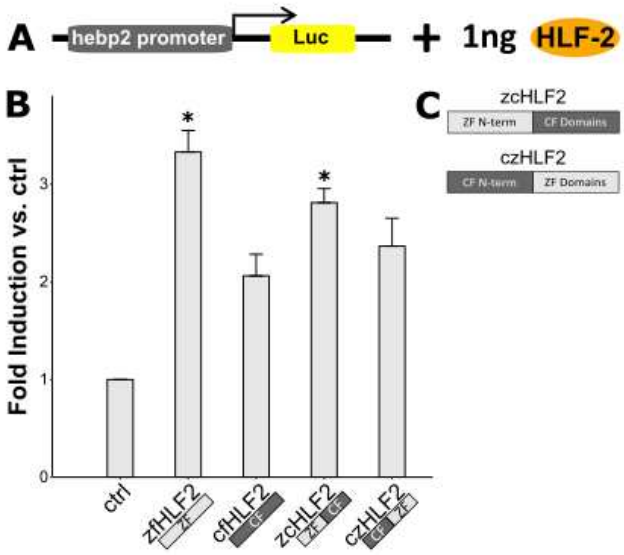

Figure 3.65. *In vitro* bioluminescence assay in zebrafish cells cotransfected with hebp2-Luc and the HLF2 hybrid factors. *In vitro* bioluminescence assay. Zebrafish cells were cotransfected with 50ng of hebp2-Luc and 1ng of zfHLF-2, cfHLF-2, and HLF-2 hybrid factors expression vectors (x-axis) and kept in darkness for 48 hours before lysis. Fold inductions of relative bioluminescence compared to the control condition, $\pm$ SEM are plotted on the y-axis. Results are the means of three independent experiments. The β–galactosidase assay was used to normalize for transfection efficiency. Differences between each of the transcription factors and the control condition are compared via t-tests with Bonferroni correction. Detailed statistical analysis can be found in Table S6. $p<0.5$, $p<0.01$, $p<0.001$ are represented by *, **, and *** respectively.

3.8 Changes to regulatory and total heme levels in zebrafish and cavefish cells

3.8.1 Total heme levels in zebrafish cells and larvae, and cavefish cells are not affected by blue light

In subsequent experiments, I aimed to determine whether heme levels change in response to light as a result of the regulation of heme-related genes in zebrafish cells. First, PAC2 and EPA cells were exposed to blue light (BL) for 24 hours, with controls kept in darkness (DD), and samples were collected every 6 hours. Total heme contents were measured with a modified version of the oxalic acid assay, and normalized per mg of protein. Results reveal no significant changes in total heme levels in cells exposed to blue light over 24 hours (Figure 3.66).

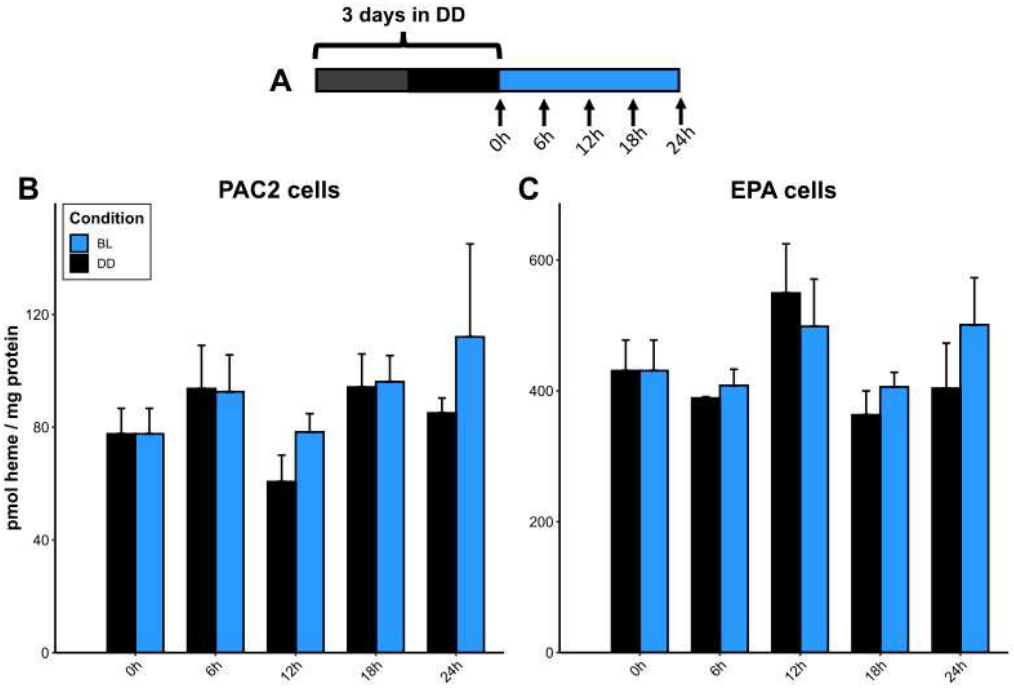

Figure 3.66. Total heme levels in zebrafish cells after exposure to blue light for up to 24 hours or darkness. Cells were kept for three days in darkness, then exposed to blue light (BL) or kept in darkness (DD), and harvested every 6 hours until the end of the light period (24 hours). Means + SEM (N=3) of total heme levels (pmol per mg of protein) are plotted on the y-axis. Protein contents were measured with the BCA assay and used for normalization.

Total heme levels were also measured in zebrafish larvae raised in darkness until the fifth day when they were exposed to blue light for 12 hours. Samples of 10 larvae each were collected

every two hours during the light period, and heme levels were compared to the respective controls of larvae kept in darkness. No changes in total heme levels could be observed (Figure 3.67).

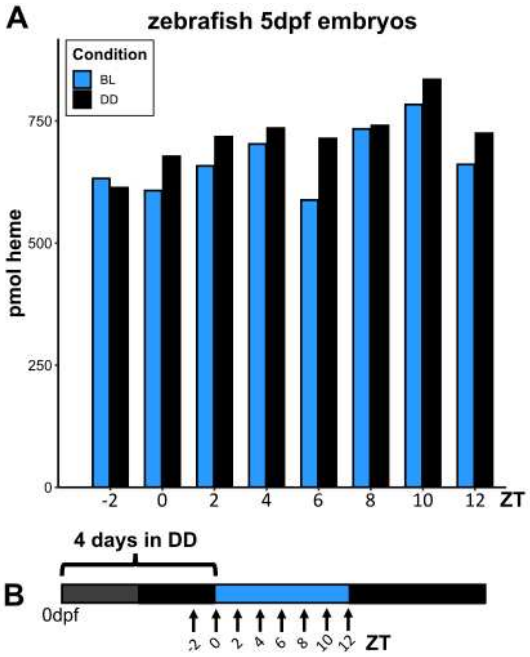

Figure 3.67. Total heme levels in zebrafish larvae during exposure to blue light or darkness. Cells were raised until 4dpf in darkness and treated with PTU from 1dpf. They were then exposed to blue light (BL) or kept in darkness (DD) and harvested every 2 hours until the end of the light period. Means of total heme levels (pmol) of samples of 10 larvae each are plotted on the y-axis.

3.8.2 Total heme levels in zebrafish and cavefish cells are not affected by exposure to light and dark cycles

The total amounts of heme did not significantly change in response to a single pulse of blue light. However, cells and tissues are cyclically exposed to light, and changes in heme levels may only become visible as a result of repeated exposure. Therefore I measured total heme levels after the cells were subjected to LD cycles or kept in darkness (DD) for seven days (Figure 3.68). No difference could be observed in the total amounts of heme in the two lighting conditions.

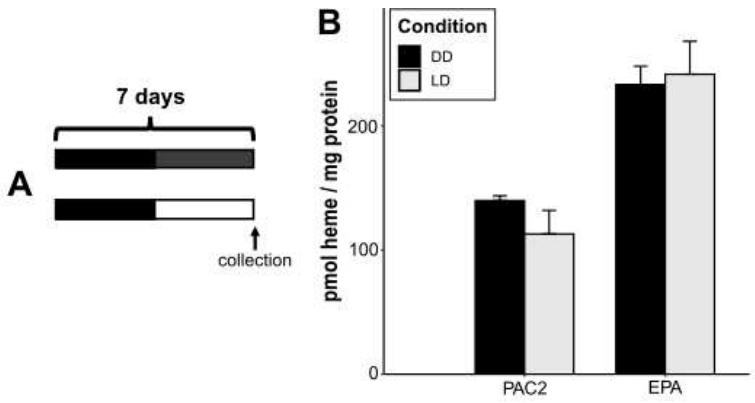

Figure 3.68. Total heme levels in zebrafish PAC2 and cavefish EPA cells after exposure to LD cycles or darkness (DD). Cells were kept for seven days in LD or DD and harvested at the end of the light period. Means + SEM (N=3) of regulatory heme levels (pmol per mg of protein) are plotted on the y-axis. Protein contents were measured with the BCA assay and used for normalization.

3.8.3 Regulatory heme levels in zebrafish and cavefish cells are not affected by exposure to light and dark cycles

Next, I measured "free" or regulatory heme levels based on the assumption that while total heme levels may not change, light may affect the amounts of heme available within cells for signaling and modulation functions. One complication for measuring the levels of intracellular heme in cell cultures is the presence of free heme in the FBS supplied in the cell medium. To minimize the effects on regulatory heme levels, PAC2 cells were cultured in varying concentrations of FBS (standard 15%, 1%, 0.5%, and 0%). After seven days of exposure to LD or DD, no change in regulatory heme levels was detected in either treatment group (Figure 3.69).

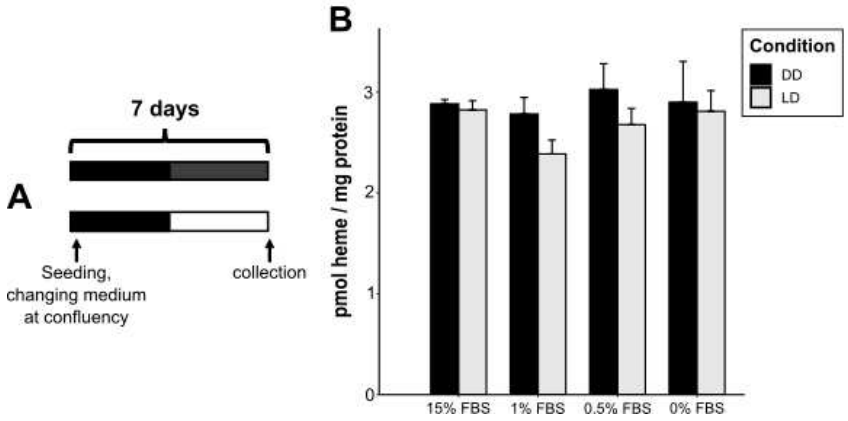

Figure 3.69. Regulatory heme levels in zebrafish cells after exposure to LD cycles or darkness (DD). Cells were seeded in medium with 15% FBS. At confluency, the medium was changed to 15%, 1%, 0.5%, or 0% FBS (x-axis). Cells were kept for seven days in LD or DD and harvested at the end of the light period. Means + SEM (N=3) of regulatory heme levels (pmol per mg of protein) are plotted on the y-axis. Protein contents were measured with the BCA assay and used for normalization.

The experiment was repeated with both PAC2 and EPA cells cultured in medium supplemented with 1%, 0.5%, and 0% FBS (Figure 3.70). While in EPA but not PAC2 cells the amounts of regulatory heme decreased with the amount of FBS supplied, no differences between the two lighting conditions were found in either cell type.

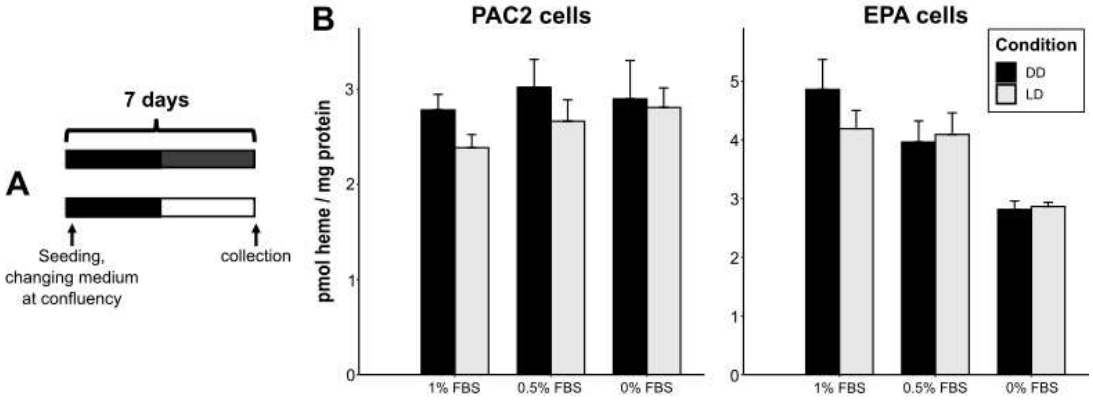

Figure 3.70. Regulatory heme levels in zebrafish PAC2 and cavefish EPA cells after exposure to LD cycles or darkness (DD). Cells were seeded in medium with 15% and 20% FBS, for zebrafish and cavefish cells, respectively. At confluency, the medium was changed to 1%, 0.5%, or 0% FBS (x-axis). Cells were kept for seven days in LD or DD and harvested at the end of the light period. Means + SEM (N=3) of regulatory heme levels (pmol per mg of protein) are plotted on the y-axis. Protein contents were measured with the BCA assay and used for normalization.

3.9 Mitochondrial function in cells exposed to blue light

The transcriptome analysis indicate that blue light exposure may trigger transcriptional changes potentially impacting mitochondrial structure and function. Furthermore, previous studies [43], [44] point to blue light being detrimental to mitochondrial activity and cellular survival. For this reason, I examined the effects of blue light on zebrafish and cavefish cells to determine whether the transcriptomic changes translate into altered cell metabolic activity and viability. The MTT assay was used to assess cell metabolic activity and viability following prolonged exposure to blue light. MTT is converted by mitochondrial reductases into formazan crystals, with the amount of formazan produced being directly proportional to mitochondrial activity levels. The experiment reveals a significant increase in metabolic activity after 24 hours of blue light exposure in PAC2 cells and a decrease in EPA after 18 hours (Figure 3.71). These preliminary results suggest that blue light exposure could differentially influence mitochondrial function and cell viability, however further investigation is needed to better understand the specific mechanisms involved and their implications for cellular health and survival.

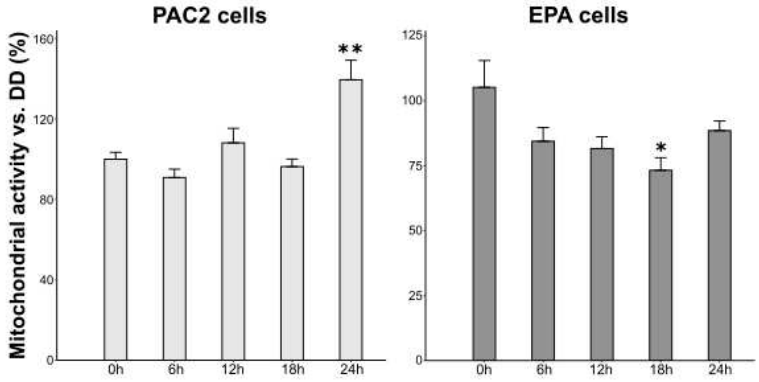

Figure 3.71. Metabolic activity assay of cells exposed to blue light (468nm) for up to 24 hours. Zebrafish and cavefish cells were kept for one day in darkness, then exposed to blue light or kept in darkness. MTT assay was performed every 6 hours (x-axis). On the y-axis, the percentage + SEM of metabolic activity of cells exposed to blue light with respect to cells kept in darkness at the same time point is plotted. Levels of mitochondrial activity are compared via ANOVA followed by Tukey's HSD post-hoc multiple comparison tests against unexposed cells at time zero (0h). Detailed statistical analysis can be found in Table S5. $p<0.5$, $p<0.01$, $p<0.001$ are represented by *, **, and *** respectively.

4. Discussion

In the present study, I investigated the transcriptomic impact of sunlight on cells, focusing on the evolutionary aspects of this response by comparing the transcriptomes of zebrafish and Somalian cavefish cells. I found that both the visible and ultraviolet components of sunlight induce the transcription of genes associated with heme metabolism and mitochondrial structure and function in zebrafish cells. This effect is seen not only in the isolated zebrafish embryonic cell line but also in whole zebrafish larvae exposed to blue light, indicating a systemic organism-wide response. Similarly to clock and DNA repair-related gene transcription, this response is lost in the cavefish cell line. The bioinformatic, *in vivo*, and *in vitro* analyses of *abcb6a* and *soul5* promoters, along with a more in-depth examination of the *hebp2* promoter supported the notion that in zebrafish the transcriptional upregulation of these genes is dependent on D-box enhancer sequences. This finding suggests that the D-box enhancer may play a broader role in light-induced gene expression than previously recognized. Additionally, I identified the cavefish PAR-bZip and Nfil3 transcription factors and compared their transcriptional regulation via the D-box sequence with that of their zebrafish orthologs, revealing a diminished ability to activate transcription in all cavefish factors. Although the transcriptomic analyses indicate possible changes to heme metabolism, no significant changes in heme levels were detected in response to various types of light exposure.

4.1 Blue light and UV-induced transcriptomes in zebrafish cells

The transcriptomic experiment revealed that exposure of zebrafish cells to blue light for up to six hours induced the upregulation of genes related to heme synthesis, transport, and degradation, as well as genes related to mitochondria structure and function. This response was confirmed via RT-qPCR analysis for the selected genes of interest *hebp2*, *abcb6a*, and *soul5*, which were determined to be regulated primarily by light exposure, with limited influence from the circadian clock. Notably, analyses of zebrafish larvae raised in complete darkness and exposed to blue light at 5dpf reveal the upregulation of these genes to be an organism-wide response to visible light, albeit with diminished amplitude of change compared to the cell line. Such variability could reflect the differential cellular sensitivities across the organism rather than issues with light penetration. In fact, it has been shown that blue light can penetrate up to 1 mm through human skin, which is sufficient to reach the entire body of the transparent, PTU-treated, thin-bodied zebrafish larvae at 5dpf [150]. Similarly, the upregulation of this class of mitochondrial and heme genes was observed in zebrafish cells 18 and 36 hours after exposure to a brief pulse of UV-C, as determined via transcriptomic and RT-qPCR analyses. However, when looking broadly at the transcriptomic changes produced by UV exposure, I found no significant enrichment of this class of genes. UV exposure represents an important stressor for cells and their response is directed to the upregulation of genes related to DNA repair, cellular structural organization, MAPK signaling, mRNA translation, and protein modifications, due to the direct and indirect damage of DNA, proteins, and membranes resulting from UV exposure. Additionally, the longer timeline of the UV experiment makes the attribution of transcriptomic changes to the treatment more complex. It is noteworthy to mention that UV irradiation did not upregulate the three genes of interest, nor the DNA repair gene *6-4 phr*, in zebrafish

larvae treated at 4dpf. In general, the longer the wavelength, the deeper the penetration of tissues [150] so it is possible that UV only reached the outer layers of the larvae, and the transcriptomic response was diluted and could not be detected via RT-qPCR. Furthermore, it has been shown that maternal gadusol present in zebrafish embryos and larvae successfully protects them from UV insults [118]. A significant increase in the expression of DNA repair and stress response genes can be detected only in the absence of gadusol. The same could be true for mitochondrial and heme-related genes. I determined that *de novo* transcription is a crucial factor in the expression changes of *abcb6a*, *hebp2*, and *soul5* driven by blue light and UV-C exposure. UV-driven expression changes of previously identified DNA repair genes such as *6-4 phr*, *ddb2*, *CPD photolyase*, and *xpc* were shown to rely on both transcriptional activity and mRNA stability [137], a dual dependency that underscores the complexity of cellular responses to UV stress [151], [152]. Interestingly, in the case of *hebp2*, *abcb6a*, and *soul5*, inhibition of transcription by Actinomycin-D treatment resulted in the complete loss of upregulation by UV suggesting their expression is tightly controlled at the transcriptional level. In the present study, *6-4 phr* expression was not significantly affected by transcriptional inhibition. The reason for this is unclear, as *6-4 phr* is upregulated strongly at all time points between 24 and 32 hours post UV exposure compared to the controls kept in darkness (data not shown). The efficacy of Actinomycin-D treatment is evidenced by the reduced expression of *c-myc*, a gene characterized by high mRNA turnover. Overall, this dual transcriptomic study of blue light and UV-C effects on zebrafish cell line and larvae provides deeper insights into the mechanisms of transcriptional response to sunlight, broadening the landscape of light-mediated gene expression beyond circadian clock entrainment and DNA repair.

4.2 The D-box: a wider mechanism of regulation in response to visible light, UV, and ROS

The timeline of transcriptional expression of 63 genes related to mitochondria and heme metabolism, as well as their independence from circadian rhythmicity, suggested a role of the D-box enhancer element in their upregulation in response to blue light and UV. The bioinformatic promoter analysis identified putative D-box sequences in 70% of these genes. Both *in vivo* and *in vitro* promoter analyses of the genes of interest *abcb6a* and *soul5*, and particularly the in-depth exploration of the *hebp2* promoter, further suggest the involvement of the D-box enhancer in light and ROS-mediated gene expression. This represents a novel role for the D-box, beyond its known functions in circadian rhythm entrainment and DNA repair regulation, possibly extending its regulatory scope within the zebrafish genome in response to sunlight and other stressors. The presence of E-box sequences in 48% of these promoters and the observed contribution of the E-box in the regulation of *hebp2* indicate a potential role of this element in light-mediated gene expression. My findings further couple light and circadian clock functions within cells, as D-box and E-box sites frequently appear together in many promoters across species [153], [154] and intact E-box and D-box sites have been shown to be vital for light-induced gene expression in zebrafish [123]. Notably, the results align with mammalian studies which found the clock-regulated D-box sites in genes related to xenobiotic metabolism [132], thyroid hormone production [134], and glucose and lipid metabolism [135], [136]. This suggests that these processes' regulation may have shifted between D-box and E-box control depending on the evolutionary context and the lighting environment.

4.2.1 Cavefish cells

The blind Somalian cavefish *P. andruzzii* has previously been studied as a natural knockout for light-mediated gene expression to elucidate the mechanisms underlying this response and understand how evolution in constant darkness has differentially shaped it [7], [85], [104], [137]. Unlike zebrafish, the Somalian cavefish do not exhibit the typical upregulation of genes related to the circadian clock and DNA repair in response to visible and ultraviolet light. In my study, the new class of genes related to mitochondria and heme, which was found to be induced by light in zebrafish cells and larvae, was determined to be non-responsive to light in cavefish cells. Previous reports have suggested that adaptation to the aphotic environment of dark caves may be responsible for the loss of clock and DNA repair light-induced gene expression [7], [85], [104]. It is plausible that similar adaptive mechanisms also led to the loss of gene expression related to mitochondrial function and heme metabolism. The zebrafish promoters of *hebp2*, *abcb6a*, and *soul5* do not exhibit light-induced activation when transfected in cavefish cells. Interestingly, the *abcb6a* gene partially retained the response to light in this cell line, suggesting specific elements within the cavefish *abcb6a* promoter might drive this response. Therefore, cloning and analyzing this promoter could offer insights into its regulatory mechanisms, for instance, whether other enhancers mediate or are necessary for its light-induced activation. Previously, the gene *ddb2*, a crucial element in the NER DNA repair pathway, was shown to be upregulated in cavefish cells in response to light, UV, and ROS due to the presence of an E2F binding site [137]. Only the cooperation between this site and the D-box present in the promoter enabled its expression, underscoring the importance of cooperation between different regulatory elements.

4.2.2 The role of ROS in light-induced gene expression

It has previously been shown that light-induced gene expression is at least in part dependent on ROS levels, which increase and peak after one hour of exposure to light and subsequently quickly decrease despite continued exposure [104]. Transcriptional regulation by H_2O_2 in the present and previous studies [104], [137] was noted as transient, peaking around three hours after the treatment, indicating that while H_2O_2 is crucial for initial gene upregulation, other signaling mechanisms likely contribute to sustained gene expression under continuous light exposure. Of note, the response of both *hebp2* and *soul5* promoters to 1 mM H_2O_2 is much weaker than that of previously identified genes such as cry1a, where a similar response is achieved by treatment with 300μM H_2O_2 [104]. Furthermore, H_2O_2 treatment activates the promoters of *hebp2* and *soul5*, but not *abcb6a*, and a transcriptomic study from my lab found it was not upregulated in zebrafish cells exposed to 300μM H_2O_2. A small increase in luciferase expression is seen around three hours after treatment, and in general, the baseline of expression is higher than that for the untreated control. While this is consistently seen throughout experiments, one cannot completely rule out the contribution of transfection efficiency of the reporter vectors. The intrinsic qualitative, not quantitative, connotation of *in vivo* luciferase experiments further limits the extent to which it can be inferred that the observed variations in the response of the *abcb6a* promoter are directly attributable to the H_2O_2 treatment. The *hebp2* promoter fragment was investigated in detail by mutating the D-box and E-box sites to study their isolated and synergistic functionality in response to light and ROS. Each of the D-box and E-box sites found upstream of the transcription start site contributes to the light and ROS-dependent regulation exhibited by the promoter fragment, exerting a synergistic effect when all sequences are intact. I proved that single D-boxes are sufficient for the response to light but not to 1 mM H_2O_2. This suggests that while the response to light is facilitated by

single D-boxes, multiple cooperating D-boxes are necessary to achieve a response to elevated ROS levels. Furthermore, while catalase overexpression decreases the activation of *hebp2* and *soul5* promoters during light exposure, it does not completely abolish it. On the other hand, the dominant negative form of ERK, competing with functional endogenous ERK, only slightly increases their activation. These results, while preliminary, suggest a complicated interplay of signaling mechanisms in response to light, which certainly encompasses ROS but also other pathways.

4.2.3 PAR-bZip transcription factors involvement in D-box mediated gene expression

The involvement of PAR-bZip and the Nfil3 factors in the regulation of gene expression via the D-box enhancer has now been demonstrated in a variety of cells and animals. The role of the D-box and of the transcription factors binding to it has changed in the course of evolution. It ranges from being the target of core clock proteins and in turn regulating clock output processes [132], [134], [136], to being the main regulator of the core clock mechanism in response to various external stimuli in fish. The presence of paralogs of the PAR-bZip and Nfil3 transcription factors in the teleost lineage, due to genome duplication events [155], supports their varied expression and functional differentiation across tissues and in response to light and circadian rhythms [149], [156], [157]. My *in vitro* analyses of the activation of *cry1a* and *hebp2* promoters, as well as those of other promoters such as *6-4 phr*, *per2*, and *xpc* (data from my lab), show the functions of the various PAR-bZip factors are not redundant. Transcription factors and their DNA binding sites are highly complex machinery. Within the human genome, the number of potential binding sites is over 200 times greater than the number of identified transcription factors [158]. On top of this, most factors recognize highly degenerate sequences with varying affinity. For instance, the binding site of PAR factors, the D-box itself was initially

identified as 5′–RTTAYGTAAY–3′ (where R is A or G, Y is C or T) [159]. Later research rapidly increased the pool of sequences recognized by these proteins. In my own studies, only one of the three D-box sequences identified in the *hebp2* promoter can be considered a canonical D-box (5'–GTGATGTAAC–3'), while the other two are slight variations of other known sequences (5'–GTTACTTAAC–3' and 5'–GTTATTTAAG–3'). Additionally, despite presenting high similarity, the PAR factors can have distinct preferences for binding sites. Differences in binding affinities have been proposed as a spatial and temporal regulatory mechanism [160]. The view of a single transcription factor recognizing single sequences has indeed long been demonstrated to be too simplistic. The cellular environment, the state of the protein and the DNA, and the presence of cofactors, among many others, are all important players in transcriptional activation [161]. The wide range of factors and D-box sequences potentially reflect a way to finely tune transcriptional regulation. For instance, one could speculate that light-induced clock genes present common D-box sequences and/or are all activated by one transcription factor, which are different in DNA repair and other classes of genes. Alternatively, differences in the stimuli, such as light, ROS, or UV in my case, could determine which factors and binding sites are preferentially targeted. However, the current status of research does not allow for the assessment of these hypotheses efficiently and reveals matters are probably much more complex. Cavefish and zebrafish orthologs share 74 to 93% similarity, particularly in the C-terminal regions responsible for DNA binding, dimerization, and transactivation. No truncation mutations are present in the cavefish factors that could explain the loss of D-box activation, in contrast with previous reports of truncations affecting the functionality of a series of cavefish proteins [7], [81], [162]. Functional assays show cavefish factors behave similarly to the zebrafish factors in both cell systems. The main difference lies in the lower levels of activated transcription mediated by the cavefish factors across different promoters. To elucidate

the mechanisms underlying the reduced transactivation by cavefish PAR factors, HLF-2 hybrids were engineered. My results suggest the N-terminal part of the zebrafish HLF-2 plays a key role in D-box activation. This is in line with previous findings in the lab (unpublished data) showing that the N-terminal portion of the TEF-1 protein is essential for transactivation. Mutations of putative phosphorylation sites in TEF-1 resulted in a complete loss of function in the activation of the regulatory target *xpc* promoter, containing three D-boxes and one E-box, similar to the *hebp2* promoter. Moreover, previous research showed that a human TEF/DBP fusion protein, incorporating the N-terminal domains of DBP, restored the ability of TEF to activate the D-box in the C7αH promoter, further pointing to the importance of the N-terminal region [157]. Overall, my findings suggest that while no single PAR-bZip factor is solely responsible for D-box-mediated light-induced gene expression, the transcription factors have retained their function in cavefish, and are alone not fully responsible for the species' diminished response to light. However, mutations or other alterations affecting all cavefish factors are likely impacting their ability to transactivate the D-box. These alterations could be related to differences in phosphorylation, protein affinity, binding efficiency, and cellular localization, which could all influence the functional dynamics of these transcriptional regulators. Importantly, in the present study, a key property of the PAR-bZip factors, their ability to hetero-dimerize, remains largely unexplored. These factors are endogenously expressed in the cells, so the activation of the D-box seen in the *in vitro* luciferase reporter experiments could depend on their availability and their potential heterodimerization with each transfected factor. One approach to investigating the role of heterodimerization in D-box transactivation would be the co-transfection of paired factors. Alternatively, knock-out models targeting individual PAR factors could be used, followed by the transfection of PAR factors to evaluate the contribution of the absent endogenous factor.

4.3 Biological meaning of transcriptomic changes induced by sunlight in zebrafish

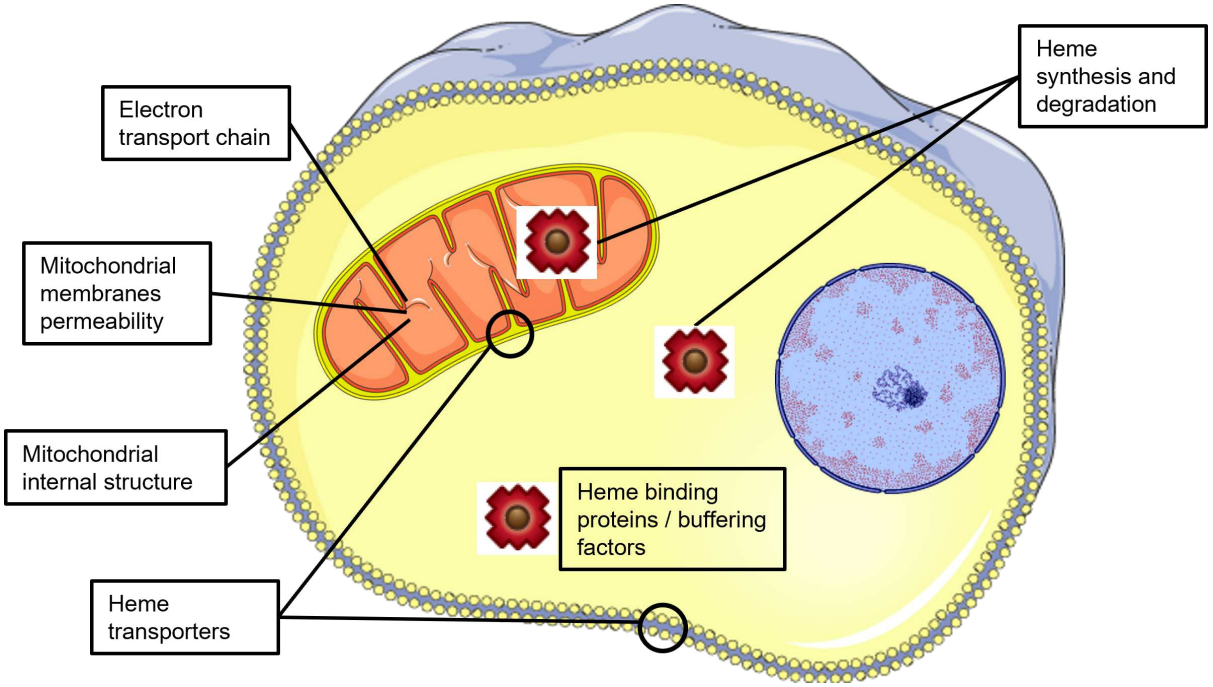

Figure 4.1. Schematic summary of the types of mitochondrial and heme genes upregulated in response to blue light and UV in zebrafish cells.

4.3.1 Adaptive mitochondrial responses to sunlight

The transcriptomic analysis revealed zebrafish cells exposed to blue light and to UV significantly upregulate genes associated with mitochondrial and heme functions, summarized in Figure 4.1. Specifically, genes such as *mff*, *adck1*, *rap1gds1*, *retsat*, and *tfr1a*, which regulate mitochondrial architecture and connectivity [163]–[166] were induced. This suggests potential changes both in the internal architecture of the organelle, which is crucial for their function, and to their morphology and connectivity [40], [167]. Additionally, the upregulation of genes encoding subunits of the ETC complexes, such as *sdha*, *sdhb*, *sdhaf1*, *sdhaf2*, *sdhaf3* [168] as well as those involved in their assembly, like *afg3l2*, *chchd4b* and *ttc19* [169]–[171] indicate possible changes in mitochondrial respiration and ATP production capacity. The genes

bbc3, *hebp2*, *retsat*, and *sirt4*, previously implicated in regulating mitochondrial activity and membrane permeability [72], [172], [173] were also light-induced. Notably, both HEBP2 and BBC3, by binding to the anti-apoptotic protein Bcl-xL of the Bcl-2 family, have been shown to promote necrotic cell death under stress conditions [69], [73], [172]. Bcl-gS, another Bcl-2 family member characterized as pro-apoptotic, is regulated by the PAR factors and by Nfil3 in cancer cells to promote apoptosis [174]. Taken together, these findings suggest the possibility of regulation of apoptosis mediated by the D-box via both direct and indirect effects on Bcl-2 proteins. The observed transcriptional changes may reflect an adaptive response aimed at maintaining or even enhancing mitochondrial efficiency upon exposure to light. Additionally, modifications to the ETC assemblies reflect a possible regulation of mitochondrial respiration and ATP production which could be necessary to support energy-demanding cellular processes such as DNA repair mechanisms. Notably, unlike photoreactivation, both BER and NER DNA repair systems require ATP to excise damaged nucleotides and to fill in the gaps [4]. It is established that the short wavelengths of visible light and UV radiation can compromise cellular integrity by impairing mitochondria and their functions [43], [44]. In zebrafish, which are particularly exposed to these wavelengths due to their natural shallow-water habitats and the filtering effects of water, these transcriptional changes could serve as a protective mechanism. This would resemble the adaptive response of photoreactivation, wherein photolyase enzymes, upregulated by sunlight, utilize their energy to repair DNA damage. Concurrently, the interaction of proteins such as HEBP2 and BBC3 with Bcl–xL and their roles in modulating cell death pathways suggest that necrotic processes may be initiated if the stress induced by sunlight exceeds physiological thresholds. In the present study, I found differing mitochondrial activity and cell viability in zebrafish and cavefish cell lines exposed to sustained blue light. A notable decrease in mitochondrial activity was observed in cavefish cells after 18 hours, but not

in the zebrafish cells, suggesting a possible protective effect that mitigates the effect of light on mitochondria. However, cavefish cells seem to recover afterward, suggesting the presence of an alternative mechanism of protection. The current findings underscore that the transcriptomic response to sunlight involves a broad spectrum of mitochondrial changes. Further studies are needed to understand the short-term and long-term implications to cellular health concerning energy and metabolism, for instance, focusing on ATP production or assessing the activity of the ETC complexes. Additionally, examining the effects on cavefish cells, which lack the described transcriptional response due to adaptation to dark environments, and even mammalian cells, can provide crucial controls for discerning the protective and pathological roles of the observed transcriptomic changes during sunlight exposure.

4.3.2 Heme: a connection to xenobiotic metabolism and oxidative stress regulation

Genes coding for enzymes involved in the metabolism and intracellular transport of heme were also found to be upregulated in response to blue light and UV. Specifically, among the elevated genes are *abcb6a*, *blvra*, *fech* and *slc40a1* (also known as *ferroportin 1*), involved in heme biosynthesis and metabolism [58], [175]–[177]. The genes *abcb6a*, *slc48a1a*, *tfr1a*, and *tspo* are implicated in the intracellular transport of heme and other porphyrins [163], [178]. Additionally, genes encoding heme-binding proteins and hemoproteins such as *tbxas1*, *cyb5a*, *cyp2ae1*, *hebp2*, and *soul5* were also upregulated [179], [180]. Heme biosynthesis predominantly occurs within the mitochondria where it serves as a crucial cofactor for numerous enzymes, particularly those involved in the ETC. Therefore, changes in heme levels and trafficking could be linked to the changes in mitochondrial function proposed above. Additionally, light exposure is known to increase ROS levels within cells, leading to oxidative stress that can damage proteins and DNA. Heme is pivotal in managing this oxidative stress as a prosthetic group for various

proteins involved in the cellular antioxidant defense such as catalase and peroxidases, which catalyze the breakdown of ROS molecules [8], [41]. Heme itself can influence ROS levels indirectly through its effect on mitochondrial function. In fact, at physiological levels, heme ensures that the electron flow through the ETC is tightly coupled, minimizing electron leakage and subsequent ROS formation [181]. Alterations to heme metabolism have instead been associated with various disorders linked to mitochondrial dysfunction [51], [182]–[184]. The upregulation of *hebp2* and antioxidant genes might serve as a primary defense mechanism to maintain homeostasis, counter oxidative stress, detoxify, and potentially mitigate the Fenton reactions that generate ROS when levels of free heme are high within cells [51]. In my study, no significant changes in either total or labile heme levels were detected upon exposure to blue light or upon cyclic exposure to white light. While this could correctly reflect the state of the cells, it cannot be excluded that the results are due to the nature of the assays used to measure total and labile heme. There are no commercial assays to quantify labile heme and very few are available for total heme, which usually require high amounts of the starting material. The assays used have been described in papers [47], [142], [143], and I applied multiple checkpoints to ensure their correct functioning, such as confirming my results align with previously reported amounts of total and labile heme within cells. However, I cannot exclude that either assay may lack the precision, sensitivity, and/or specificity required to detect the potential changes in heme levels following light exposure. Furthermore, intracellular heme trafficking and changes within cellular compartments should be studied, for instance, using heme biosensors [185] to better understand the effects of sunlight on heme *in vivo*. Intriguingly, a variety of genes implicated in xenobiotic metabolism were also found to be upregulated by light, including *porb*, *akr1b1* (alias *si:dkey-180p18.9*), *cbr1*, *nr1i2*, and *gss*. *Tbxas1* and *cyp2ae1*, which encode for cytochromes P450, are crucial in the metabolism of xenobiotics as they utilize the heme-bound oxygen

molecule to oxidize these compounds, facilitating their excretion [180], [186]. A previous study found many of the same genes upregulated by blue light to be regulated in response to benzo[a]pyrene/ethanol co–exposure in zebrafish larvae [65]. Their subsequent analyses revealed mitochondrial dysfunction and increases in iron and heme levels and proposed a role of Aryl hydrocarbon Receptor (AhR) signaling in transcriptional regulation. Furthermore, a triple knock-out of TEF, DBP, and HLF in mice revealed their prominent role in mediating the expression of genes associated with xenobiotic metabolism, as well as heme-related genes such as that coding for the rate-limiting enzyme for its synthesis, *alas1* [132]. Drug metabolism has been proven to be influenced by circadian rhythms [187], [188] so it would not be surprising if sunlight exposure directly influenced it through the D-box enhancer in zebrafish.

4.4 Conclusion

The present findings expand the known landscape of light-mediated gene expression and identify the D-box as part of a broader mechanism extending beyond circadian clock entrainment and DNA repair. The transcriptomic analysis suggests that light exposure triggers complex biochemical responses in zebrafish cells, influencing mitochondrial structure and function and heme metabolism and transport, which are integral to cellular energy dynamics and stress responses. However, further analyses are needed to elucidate the functional outcomes of the observed transcriptomic changes in relation to cellular and mitochondrial health and metabolic efficiency. The D-box enhancer element is progressively assuming a central role in the modulation of light, ROS, and UV-mediated gene expression. My work highlights the complex relationship with the PAR-bZip transcription factors, which presents challenges for the identification of the exact pathways of this transcriptional regulation in vertebrates. Finally, my results further offer new insights into the evolutionary adaptations made in response to the aphotic environments inhabited by cave-dwelling organisms.

5. References

[1] K. P. Able, "Skylight polarization patterns at dusk influence migratory orientation in birds," en, *Nature*, vol. 299, no. 5883, pp. 550–551, Oct. 1982, Publisher: Nature Publishing Group, ISSN: 1476-4687. DOI: 10.1038/299550a0.

[2] T. W. Cronin, N. Shashar, R. L. Caldwell, J. Marshall, A. G. Cheroske, and T.-H. Chiou, "Polarization Vision and Its Role in Biological Signaling1," *Integrative and Comparative Biology*, vol. 43, no. 4, pp. 549–558, Aug. 2003, ISSN: 1540-7063. DOI: 10.1093/icb/43.4.549.

[3] C. S. Pittendrigh, "Temporal Organization: Reflections of a Darwinian Clock-Watcher," en, p. 39, 1993.

[4] R. P. Sinha and D.-P. Häder, "UV-induced DNA damage and repair: A review," en, *Photochemical & Photobiological Sciences*, vol. 1, no. 4, pp. 225–236, Apr. 2002, ISSN: 1474-905X, 1474-9092. DOI: 10.1039/b201230h.

[5] N. N. Osborne, C. Núñez-Álvarez, S. del Olmo-Aguado, and J. Merrayo-Lloves, "Visual light effects on mitochondria: The potential implications in relation to glaucoma," en, *Mitochondrion*, vol. 36, pp. 29–35, Sep. 2017, ISSN: 15677249. DOI: 10.1016/j.mito.2016.11.009.

[6] Z. Ben-Moshe, S. Alon, P. Mracek, *et al.*, "The light-induced transcriptome of the zebrafish pineal gland reveals complex regulation of the circadian clockwork by light," en, *Nucleic Acids Research*, vol. 42, no. 6, pp. 3750–3767, Apr. 2014, ISSN: 1362-4962, 0305-1048. DOI: 10.1093/nar/gkt1359.

[7] H. Zhao, G. Di Mauro, S. Lungu-Mitea, *et al.*, "Modulation of DNA Repair Systems in Blind Cavefish during Evolution in Constant Darkness," en, *Current Biology*, vol. 28, no. 20, 3229–3243.e4, Oct. 2018, ISSN: 09609822. DOI: 10.1016/j.cub.2018.08.039.

[8] M. Rinnerthaler, J. Bischof, M. Streubel, A. Trost, and K. Richter, "Oxidative Stress in Aging Human Skin," en, *Biomolecules*, vol. 5, no. 2, pp. 545–589, Apr. 2015, ISSN: 2218-273X. DOI: 10.3390/biom5020545.

[9] U. Lagercrantz, "At the end of the day: A common molecular mechanism for photoperiod responses in plants?" *Journal of Experimental Botany*, vol. 60, no. 9, pp. 2501–2515, Jul. 2009, ISSN: 0022-0957. DOI: 10.1093/jxb/erp139.

[10] G. Serrano-Bueno, F. J. Romero-Campero, E. Lucas-Reina, J. M. Romero, and F. Valverde, "Evolution of photoperiod sensing in plants and algae," *Current Opinion in Plant Biology*, 37 Physiology and metabolism 2017, vol. 37, pp. 10–17, Jun. 2017, ISSN: 1369-5266. DOI: 10.1016/j.pbi.2017.03.007.

[11] W. E. Bradshaw and C. M. Holzapfel, "What Season Is It Anyway? Circadian Tracking vs. Photoperiodic Anticipation in Insects," en, *Journal of Biological Rhythms*, vol. 25, no. 3, pp. 155–165, Jun. 2010, Publisher: SAGE Publications Inc, ISSN: 0748-7304. DOI: 10.1177/0748730410365656.

[12] C. L. Partch, C. B. Green, and J. S. Takahashi, "Molecular architecture of the mammalian circadian clock," en, *Trends in Cell Biology*, vol. 24, no. 2, pp. 90–99, Feb. 2014, ISSN: 09628924. DOI: 10.1016/j.tcb.2013.07.002.

[13] T. Yoshikawa, S. Yamazaki, and M. Menaker, "Effects of Preparation Time on Phase of Cultured Tissues Reveal Complexity of Circadian Organization," en, *Journal of Biological Rhythms*, vol. 20, no. 6, pp. 500–512, Dec. 2005, ISSN: 0748-7304, 1552-4531. DOI: 10.1177/0748730405280775.

[14] S. Doyle and M. Menaker, "Circadian Photoreception in Vertebrates," en, *Cold Spring Harbor Symposia on Quantitative Biology*, vol. 72, no. 1, pp. 499–508, Jan. 2007, ISSN: 0091-7451. DOI: 10.1101/sqb.2007.72.003.

[15] M. Menaker, J. S. Takahashi, and A. Eskin, "The Physiology of Circadian Pacemakers," en, *Annual Review of Physiology*, vol. 40, no. Volume 40, 1978, pp. 501–526, Mar. 1978, Publisher: Annual Reviews, ISSN: 0066-4278, 1545-1585. DOI: 10.1146/annurev.ph.40.030178.002441.

[16] T. Dickmeis, "Glucocorticoids and the circadian clock," en, *Journal of Endocrinology*, vol. 200, no. 1, pp. 3–22, Jan. 2009, ISSN: 0022-0795, 1479-6805. DOI: 10.1677/JOE-08-0415.

[17] S. Gaddameedhi, C. P. Selby, W. K. Kaufmann, R. C. Smart, and A. Sancar, "Control of skin cancer by the circadian rhythm," en, *Proceedings of the National Academy of Sciences*, vol. 108, no. 46, pp. 18 790–18 795, Nov. 2011, ISSN: 0027-8424, 1091-6490. DOI: 10.1073/pnas.1115249108.

[18] P. J. Shiromani and W. J. Schwartz, "Towards a molecular biology of the circadian clock and sleep of mammals," eng, *Advances in Neuroimmunology*, vol. 5, no. 2, pp. 217–230, 1995, ISSN: 0960-5428. DOI: 10.1016/0960-5428(95)00011-p.

[19] J. C. Florez and J. S. Takahashi, "The Circadian Clock: From Molecules to Behaviour," *Annals of Medicine*, vol. 27, no. 4, pp. 481–490, Jan. 1995, Publisher: Taylor & Francis _eprint: https://doi.org/10.3109/07853899709002457, ISSN: 0785-3890. DOI: 10.3109/07853899709002457.

[20] C. A. Wyse, S. M. Biello, and J. M. R. Gill, "The bright-nights and dim-days of the urban photoperiod: Implications for circadian rhythmicity, metabolism and obesity," *Annals of Medicine*, vol. 46, no. 5, pp. 253–263, Aug. 2014, Publisher: Taylor & Francis _eprint: https://doi.org/10.3109/07853890.2014.913422, ISSN: 0785-3890. DOI: 10.3109/07853890.2014.913422.

[21] I. Heyde and H. Oster, "Differentiating external zeitgeber impact on peripheral circadian clock resetting," en, *Scientific Reports*, vol. 9, no. 1, p. 20 114, Dec. 2019, Publisher: Nature Publishing Group, ISSN: 2045-2322. DOI: 10.1038/s41598-019-56323-z.

[22] *Protecting your eyes from the sun's UV light | National Eye Institute*.

[23] R. Bonnett, A. A. Charalambides, E. J. Land, R. S. Sinclair, D. Tait, and T. G. Truscott, "Triplet States of Porphyrin Esters," vol. 76, pp. 852–859, 1980.

[24] R. Begum, M. B. Powner, N. Hudson, C. Hogg, and G. Jeffery, "Treatment with 670 nm Light Up Regulates Cytochrome C Oxidase Expression and Reduces Inflammation in an Age-Related Macular Degeneration Model," en, *PLoS ONE*, vol. 8, no. 2, A. Lewin, Ed., e57828, Feb. 2013, ISSN: 1932-6203. DOI: 10.1371/journal.pone.0057828.

[25] R. Albarracin and K. Valter, "670 nm Red Light Preconditioning Supports Müller Cell Function: Evidence from the White Light-induced Damage Model in the Rat Retina†," en, *Photochemistry and Photobiology*, vol. 88, no. 6, pp. 1418–1427, 2012, _eprint: https://onlinelibrary.wiley.com/doi/pdf/10.1111/j.1751-1097.2012.01130.x, ISSN: 1751-1097. DOI: 10.1111/j.1751-1097.2012.01130.x.

[26] S. Song, Y. Zhang, C.-C. Fong, C.-H. Tsang, Z. Yang, and M. Yang, "cDNA Microarray Analysis of Gene Expression Profiles in Human Fibroblast Cells Irradiated with Red Light," en, *Journal of Investigative Dermatology*, vol. 120, no. 5, pp. 849–857, May 2003, ISSN: 0022202X. DOI: 10.1046/j.1523-1747.2003.12133.x.

[27] K.-F. Hung, J. M. Sidorova, P. Nghiem, and M. Kawasumi, "The 6-4 photoproduct is the trigger of UV-induced replication blockage and ATR activation," *Proceedings of the National Academy of Sciences*, vol. 117, no. 23, pp. 12 806–12 816, Jun. 2020, Publisher: Proceedings of the National Academy of Sciences. DOI: 10.1073/pnas.1917196117.

[28] D. Pattison and M. Davies, "Actions of ultraviolet light on cellular structures," *EXS*, vol. 96, pp. 131–57, Jan. 2006, ISSN: 3-7643-7156-0. DOI: 10.1007/3-7643-7378-4_6.

[29] B. H. Mahmoud, C. L. Hexsel, I. H. Hamzavi, and H. W. Lim, "Effects of Visible Light on the Skin†," en, *Photochemistry and Photobiology*, vol. 84, no. 2, pp. 450–462, 2008, _eprint: https://onlinelibrary.wiley.com/doi/pdf/10.1111/j.1751-1097.2007.00286.x, ISSN: 1751-1097. DOI: 10.1111/j.1751-1097.2007.00286.x.

[30] A. Kammeyer and R. M. Luiten, "Oxidation events and skin aging," *Ageing Research Reviews*, vol. 21, pp. 16–29, May 2015, ISSN: 1568-1637. DOI: 10.1016/j.arr.2015.01.001.

[31] D. L. Narayanan, R. N. Saladi, and J. L. Fox, "Review: Ultraviolet radiation and skin cancer," en, *International Journal of Dermatology*, vol. 49, no. 9, pp. 978–986, 2010, _eprint: https://onlinelibrary.wiley.com/doi/pdf/10.1111/j.1365-4632.2010.04474.x, ISSN: 1365-4632. DOI: 10.1111/j.1365-4632.2010.04474.x.

[32] J. I. Lucas-Lledo and M. Lynch, "Evolution of Mutation Rates: Phylogenomic Analysis of the Photolyase/Cryptochrome Family," en, *Molecular Biology and Evolution*, vol. 26, no. 5, pp. 1143–1153, May 2009, ISSN: 0737-4038, 1537-1719. DOI: 10.1093/molbev/msp029.

[33] L. O. Essen and T. Klar, "Light-driven DNA repair by photolyases," en, *Cellular and Molecular Life Sciences*, vol. 63, no. 11, pp. 1266–1277, Jun. 2006, ISSN: 1420-682X, 1420-9071. DOI: 10.1007/s00018-005-5447-y.

[34] M. Christmann and B. Kaina, "Transcriptional regulation of human DNA repair genes following genotoxic stress: Trigger mechanisms, inducible responses and genotoxic adaptation," en, *Nucleic Acids Research*, vol. 41, no. 18, pp. 8403–8420, Oct. 2013, ISSN: 0305-1048, 1362-4962. DOI: 10.1093/nar/gkt635.

[35] D. Gavriouchkina, S. Fischer, T. Ivacevic, J. Stolte, V. Benes, and M. P. S. Dekens, "Thyrotroph Embryonic Factor Regulates Light-Induced Transcription of Repair Genes in Zebrafish Embryonic Cells," en, *PLoS ONE*, vol. 5, no. 9, B. B. Riley, Ed., e12542, Sep. 2010, ISSN: 1932-6203. DOI: 10.1371/journal.pone.0012542.

[36] B. D. Weger, M. Sahinbas, G. W. Otto, *et al.*, "The Light Responsive Transcriptome of the Zebrafish: Function and Regulation," en, *PLOS ONE*, vol. 6, no. 2, e17080, Feb. 2011, Publisher: Public Library of Science, ISSN: 1932-6203. DOI: 10.1371/journal.pone.0017080.

[37] E. M. Hemond and S. V. Vollmer, "Diurnal and nocturnal transcriptomic variation in the Caribbean staghorn coral, *Acropora cervicornis*," en, *Molecular Ecology*, vol. 24, no. 17, pp. 4460–4473, Sep. 2015, ISSN: 0962-1083, 1365-294X. DOI: 10.1111/mec.13320.

[38] M. Rinsky, E. Weizman, H. W. Ben-Asher, G. Eyal, B. Zhu, and O. Levy, "Temporal gene expression patterns in the coral *Euphyllia paradivisa* reveal the complexity of biological clocks in the cnidarian-algal symbiosis," en, *Science Advances*, vol. 8, no. 37, eabo6467, Sep. 2022, ISSN: 2375-2548. DOI: 10.1126/sciadv.abo6467.

[39] Q. Yuan, Z. L. Zeng, S. Yang, A. Li, X. Zu, and J. Liu, "Mitochondrial Stress in Metabolic Inflammation: Modest Benefits and Full Losses," en, *Oxidative Medicine and Cellular Longevity*, vol. 2022, e8803404, Nov. 2022, Publisher: Hindawi, ISSN: 1942-0900. DOI: 10.1155/2022/8803404.

[40] P. De Goede, J. Wefers, E. C. Brombacher, P. Schrauwen, and A. Kalsbeek, "Circadian rhythms in mitochondrial respiration," en, *Journal of Molecular Endocrinology*, vol. 60, no. 3, R115–R130, Apr. 2018, ISSN: 0952-5041, 1479-6813. DOI: 10.1530/JME-17-0196.

[41] A. Y. Andreyev, Y. E. Kushnareva, and A. A. Starkov, "Mitochondrial metabolism of reactive oxygen species," en, *Biochemistry (Moscow)*, vol. 70, no. 2, pp. 200–214, Feb. 2005, ISSN: 1608-3040. DOI: 10.1007/s10541-005-0102-7.

[42] J. C. Tsibris, D. B. McCormick, and L. D. Wright, "Studies on the Binding and Function of Flavin Phosphates with Flavin Mononucleotide-dependent Enzymes," en, *Journal of Biological Chemistry*, vol. 241, no. 5, pp. 1138–1143, Mar. 1966, ISSN: 00219258. DOI: 10.1016/S0021-9258(18)96813-4.

[43] N. N. Osborne, G.-Y. Li, D. Ji, H. J. Mortiboys, and S. Jackson, "Light affects mitochondria to cause apoptosis to cultured cells: Possible relevance to ganglion cell death in certain optic neuropathies," en, *Journal of Neurochemistry*, vol. 105, no. 5, pp. 2013–2028, Jun. 2008, ISSN: 0022-3042, 1471-4159. DOI: 10.1111/j.1471-4159.2008.05320.x.

[44] A. King, E. Gottlieb, D. G. Brooks, M. P. Murphy, and J. L. Dunaief, "Mitochondria-derived Reactive Oxygen Species Mediate Blue Light-induced Death of Retinal Pigment Epithelial Cells¶," en, *Photochemistry and Photobiology*, vol. 79, no. 5, pp. 470–475, 2004, _eprint: https://onlinelibrary.wiley.com/doi/pdf/10.1111/j.1751-1097.2004.tb00036.x, ISSN: 1751-1097. DOI: 10.1111/j.1751-1097.2004.tb00036.x.

[45] G. Padmanaban, V. Venkateswar, and P. Rangarajan, "Haem as a multifunctional regulator," en, *Trends in Biochemical Sciences*, vol. 14, no. 12, pp. 492–496, Dec. 1989, ISSN: 09680004. DOI: 10.1016/0968-0004(89)90182-5.

[46] A. E. Gallio, S. S.-P. Fung, A. Cammack-Najera, A. J. Hudson, and E. L. Raven, "Understanding the Logistics for the Distribution of Heme in Cells," *JACS Au*, vol. 1, no. 10, pp. 1541–1555, Oct. 2021, Publisher: American Chemical Society. DOI: 10.1021/jacsau.1c00288.

[47] H. Atamna, M. Brahmbhatt, W. Atamna, G. A. Shanower, and J. M. Dhahbi, "ApoHRP-based assay to measure intracellular regulatory heme," en, *Metallomics*, vol. 7, no. 2, pp. 309–321, 2015, ISSN: 1756-5901, 1756-591X. DOI: 10.1039/C4MT00246F.

[48] R. B. Piel, H. A. Dailey, and A. E. Medlock, "The mitochondrial heme metabolon: Insights into the complex(ity) of heme synthesis and distribution," *Molecular Genetics and Metabolism*, Recent advances in Heme Biosynthesis and the Porphyrias, vol. 128, no. 3, pp. 198–203, Nov. 2019, ISSN: 1096-7192. DOI: 10.1016/j.ymgme.2019.01.006.

[49] Y. Zhu, T. Hon, W. Ye, and L. Zhang, "Heme Deficiency Interferes with the Ras-Mitogen-activated Protein Kinase Signaling Pathway and Expression of a Subset of Neuronal Genes1," *Cell Growth & Differentiation*, vol. 13, no. 9, pp. 431–439, Sep. 2002, ISSN: 1044-9523.

[50] T. Shimizu, A. Lengalova, V. Martínek, and M. Martínková, "Heme: Emergent roles of heme in signal transduction, functional regulation and as catalytic centres," en, *Chemical Society Reviews*, vol. 48, no. 24, pp. 5624–5657, 2019, ISSN: 0306-0012, 1460-4744. DOI: 10.1039/C9CS00268E.

[51] D. Chiabrando, F. Vinchi, V. Fiorito, S. Mercurio, and E. Tolosano, "Heme in pathophysiology: A matter of scavenging, metabolism and trafficking across cell membranes," English, *Frontiers in Pharmacology*, vol. 5, Apr. 2014, Publisher: Frontiers, ISSN: 1663-9812. DOI: 10.3389/fphar.2014.00061.

[52] S. M. Mense and L. Zhang, "Heme: A versatile signaling molecule controlling the activities of diverse regulators ranging from transcription factors to MAP kinases," en, *Cell Research*, vol. 16, no. 8, pp. 681–692, Aug. 2006, ISSN: 1001-0602, 1748-7838. DOI: 10.1038/sj.cr.7310086.

[53] S. Kumar and U. Bandyopadhyay, "Free heme toxicity and its detoxification systems in human," *Toxicology Letters*, vol. 157, no. 3, pp. 175–188, Jul. 2005, ISSN: 0378-4274. DOI: 10.1016/j.toxlet.2005.03.004.

[54] R. K. Kutty, G. Kutty, B. Wiggert, G. J. Chader, R. M. Darrow, and D. T. Organisciak, "Induction of heme oxygenase 1 in the retina by intense visible light: Suppression by the antioxidant dimethylthiourea.," en, *Proceedings of the National Academy of Sciences*, vol. 92, no. 4, pp. 1177–1181, Feb. 1995, ISSN: 0027-8424, 1091-6490. DOI: 10.1073/pnas.92.4.1177.

[55] S. Raghuram, K. R. Stayrook, P. Huang, *et al.*, "Identification of heme as the ligand for the orphan nuclear receptors REV-ERBα and REV-ERBβ," en, *Nature Structural & Molecular Biology*, vol. 14, no. 12, pp. 1207–1213, Dec. 2007, ISSN: 1545-9993, 1545-9985. DOI: 10.1038/nsmb1344.

[56] J. Lee, S. Lee, S. Chung, *et al.*, "Identification of a novel circadian clock modulator controlling BMAL1 expression through a ROR/REV-ERB-response element-dependent mechanism," en, *Biochemical and Biophysical Research Communications*, vol. 469, no. 3, pp. 580–586, Jan. 2016, ISSN: 0006291X. DOI: 10.1016/j.bbrc.2015.12.030.

[57] P. M. Rogers, L. Ying, and T. P. Burris, "Relationship between circadian oscillations of Rev-erbα expression and intracellular levels of its ligand, heme," en, *Biochemical and Biophysical Research Communications*, vol. 368, no. 4, pp. 955–958, Apr. 2008, ISSN: 0006291X. DOI: 10.1016/j.bbrc.2008.02.031.

[58] P. C. Krishnamurthy, G. Du, Y. Fukuda, *et al.*, "Identification of a mammalian mitochondrial porphyrin transporter," en, *Nature*, vol. 443, no. 7111, pp. 586–589, Oct. 2006, ISSN: 0028-0836, 1476-4687. DOI: 10.1038/nature05125.

[59] S. A. Swenson, C. M. Moore, J. R. Marcero, A. E. Medlock, A. R. Reddi, and O. Khalimonchuk, "From Synthesis to Utilization: The Ins and Outs of Mitochondrial Heme," en, *Cells*, vol. 9, no. 3, p. 579, Feb. 2020, ISSN: 2073-4409. DOI: 10.3390/cells9030579.

[60] J. K. Paterson, S. Shukla, C. M. Black, *et al.*, "Human ABCB6 Localizes to Both the Outer Mitochondrial Membrane and the Plasma Membrane," en, *Biochemistry*, vol. 46, no. 33, pp. 9443–9452, Aug. 2007, ISSN: 0006-2960, 1520-4995. DOI: 10.1021/bi700015m.

[61] J. Lynch, Y. Fukuda, P. Krishnamurthy, G. Du, and J. D. Schuetz, "Cell Survival under Stress Is Enhanced by a Mitochondrial ATP-Binding Cassette Transporter That Regulates Hemoproteins," en, *Cancer Research*, vol. 69, no. 13, pp. 5560–5567, Jul. 2009, ISSN: 0008-5472, 1538-7445. DOI: 10.1158/0008-5472.CAN-09-0078.

[62] Y. Fukuda, P. L. Cheong, J. Lynch, *et al.*, "The severity of hereditary porphyria is modulated by the porphyrin exporter and Lan antigen ABCB6," en, *Nature Communications*, vol. 7, no. 1, p. 12 353, Aug. 2016, ISSN: 2041-1723. DOI: 10.1038/ncomms12353.

[63] H. Chavan, M. Oruganti, and P. Krishnamurthy, "The ATP-Binding Cassette Transporter ABCB6 Is Induced by Arsenic and Protects against Arsenic Cytotoxicity," *Toxicological Sciences*, vol. 120, no. 2, pp. 519–528, Apr. 2011, ISSN: 1096-6080. DOI: 10.1093/toxsci/kfr008.

[64] H. Chavan and P. Krishnamurthy, "Polycyclic Aromatic Hydrocarbons (PAHs) Mediate Transcriptional Activation of the ATP Binding Cassette Transporter ABCB6 Gene via the Aryl Hydrocarbon Receptor (AhR)," en, *Journal of Biological Chemistry*, vol. 287, no. 38, pp. 32 054–32 068, Sep. 2012, ISSN: 00219258. DOI: 10.1074/jbc.M112.371476.

[65] M. Imran, F. Chalmel, O. Sergent, *et al.*, "Transcriptomic analysis in zebrafish larvae identifies iron-dependent mitochondrial dysfunction as a possible key event of NAFLD progression induced by benzo[a]pyrene/ethanol co-exposure," en, *Cell Biology and Toxicology*, Apr. 2022, ISSN: 0742-2091, 1573-6822. DOI: 10.1007/s10565-022-09706-4.

[66] T. Mikasa, M. Kugo, S. Nishimura, S. Taketani, S. Ishijima, and I. Sagami, "Thermodynamic Characterization of the Ca2+-Dependent Interaction Between SOUL and ALG-2," en, *International Journal of Molecular Sciences*, vol. 19, no. 12, p. 3802, Dec. 2018, Number: 12 Publisher: Multidisciplinary Digital Publishing Institute, ISSN: 1422-0067. DOI: 10.3390/ijms19123802.

[67] B. Jacob Blackmon, T. A. Dailey, X. Lianchun, and H. A. Dailey, "Characterization of a human and mouse tetrapyrrole-binding protein," *Archives of Biochemistry and Biophysics*, vol. 407, no. 2, pp. 196–201, Nov. 2002, ISSN: 0003-9861. DOI: 10.1016/S0003-9861(02)00471-X.

[68] E. Sato, I. Sagami, T. Uchida, *et al.*, "SOUL in Mouse Eyes Is a New Hexameric Heme-Binding Protein with Characteristic Optical Absorption, Resonance Raman Spectral, and Heme-Binding Properties," *Biochemistry*, vol. 43, no. 44, pp. 14 189–14 198, Nov. 2004, Publisher: American Chemical Society, ISSN: 0006-2960. DOI: 10.1021/bi048742i.

[69] E. Ambrosi, S. Capaldi, M. Bovi, G. Saccomani, M. Perduca, and H. L. Monaco, "Structural changes in the BH3 domain of SOUL protein upon interaction with the anti-apoptotic protein Bcl-xL," en, *Biochemical Journal*, vol. 438, no. 2, pp. 291–301, Sep. 2011, ISSN: 0264-6021, 1470-8728. DOI: 10.1042/BJ20110257.

[70] M. J. Zylka and S. M. Reppert, "Discovery of a putative heme-binding protein family žSOULrHBP/ by two-tissue suppression subtractive hybridization and database searches," en, 1999.

[71] A. E. Fortunato, F. Langellotto, and P. Sordino, "Identification and expression of soul/p22HBP genes in zebrafish," en, *Gene Expression Patterns*, vol. 11, no. 5-6, pp. 360–369, Jun. 2011, ISSN: 1567133X. DOI: 10.1016/j.gep.2011.03.006.

[72] A. Szigeti, S. Bellyei, B. Gasz, *et al.*, "Induction of necrotic cell death and mitochondrial permeabilization by heme binding protein 2/SOUL," en, *FEBS Letters*, vol. 580, no. 27, pp. 6447–6454, Nov. 2006, ISSN: 00145793. DOI: 10.1016/j.febslet.2006.10.067.

[73] A. Szigeti, E. Hocsak, E. Rapolti, *et al.*, "Facilitation of Mitochondrial Outer and Inner Membrane Permeabilization and Cell Death in Oxidative Stress by a Novel Bcl-2 Homology 3 Domain Protein," en, *Journal of Biological Chemistry*, vol. 285, no. 3, pp. 2140–2151, Jan. 2010, ISSN: 00219258. DOI: 10.1074/jbc.M109.015222.

[74] K. Nakasone, Y. Nagahama, and K. Okubo, "Hebp3, a Novel Member of the Heme-Binding Protein Gene Family, Is Expressed in the Medaka Meninges With Higher Abundance in Females Due to a Direct Stimulating Action of Ovarian Estrogens," en, *Endocrinology*, vol. 154, no. 2, pp. 920–930, Feb. 2013, ISSN: 0013-7227, 1945-7170. DOI: 10.1210/en.2012-2000.

[75] T. W. Cronin and S. Johnsen, "Extraocular, Non-Visual, and Simple Photoreceptors: An Introduction to the Symposium," en, *Integrative and Comparative Biology*, vol. 56, no. 5, pp. 758–763, Nov. 2016, ISSN: 1540-7063, 1557-7023. DOI: 10.1093/icb/icw106.

[76] J. H. Pérez, E. Tolla, V. R. Bishop, *et al.*, "Functional inhibition of deep brain non-visual opsins facilitates acute long day induction of reproductive recrudescence in male Japanese quail," en, *Hormones and Behavior*, vol. 148, p. 105 298, Feb. 2023, ISSN: 0018506X. DOI: 10.1016/j.yhbeh.2022.105298.

[77] J. M. García-Fernández, R. Cernuda-Cernuda, W. I. L. Davies, *et al.*, "The hypothalamic photoreceptors regulating seasonal reproduction in birds: A prime role for VA opsin," *Frontiers in Neuroendocrinology*, Seasonal Changes in the Neuroendocrine System, vol. 37, pp. 13–28, Apr. 2015, ISSN: 0091-3022. DOI: 10.1016/j.yfrne.2014.11.001.

[78] A. Zoond and N. A. H. Bokenham, "Studies in Reptilian Colour Response: II. The Role of Retinal and Dermal Photoreceptors in the Pigmentary Activity of the Chameleon," *Journal of Experimental Biology*, vol. 12, no. 1, pp. 39–43, Jan. 1935, ISSN: 0022-0949. DOI: 10.1242/jeb.12.1.39.

[79] Y. Miyashita, T. Moriya, K. Yamada, *et al.*, "The Photoreceptor Molecules in Xenopus Tadpole Tail Fin, in which Melanophores Exist," *Zoological Science*, vol. 18, no. 5, pp. 671–674, Jul. 2001, Publisher: Zoological Society of Japan, ISSN: 0289-0003. DOI: 10.2108/zsj.18.671.

[80] J. H. Pérez, E. Tolla, I. C. Dunn, S. L. Meddle, and T. J. Stevenson, "A Comparative Perspective on Extra-retinal Photoreception," en, *Trends in Endocrinology & Metabolism*, vol. 30, no. 1, pp. 39–53, Dec. 2018, ISSN: 10432760. DOI: 10.1016/j.tem.2018.10.005.

[81] L. Calderoni, O. Rota-Stabelli, E. Frigato, *et al.*, "Relaxed selective constraints drove functional modifications in peripheral photoreception of the cavefish P. andruzzii and provide insight into the time of cave colonization," en, *Heredity*, vol. 117, no. 5, pp. 383–392, Nov. 2016, Publisher: Nature Publishing Group, ISSN: 1365-2540. DOI: 10.1038/hdy.2016.59.

[82] W. I. L. Davies, T. K. Tamai, L. Zheng, *et al.*, "An extended family of novel vertebrate photopigments is widely expressed and displays a diversity of function," en, *Genome Research*, vol. 25, no. 11, pp. 1666–1679, Nov. 2015, Company: Cold Spring Harbor Laboratory Press Distributor: Cold Spring Harbor Laboratory Press Institution: Cold Spring Harbor Laboratory Press Label: Cold Spring Harbor Laboratory Press Publisher: Cold Spring Harbor Lab, ISSN: 1088-9051, 1549-5469. DOI: 10.1101/gr.189886.115.

[83] M. F. Ceriani, T. K. Darlington, D. Staknis, *et al.*, "Light-Dependent Sequestration of TIMELESS by CRYPTOCHROME," *Science*, vol. 285, no. 5427, pp. 553–556, Jul. 1999, Publisher: American Association for the Advancement of Science. DOI: 10.1126/science.285.5427.553.

[84] A. M. Fernandes, K. Fero, A. B. Arrenberg, S. A. Bergeron, W. Driever, and H. A. Burgess, "Deep Brain Photoreceptors Control Light-Seeking Behavior in Zebrafish Larvae," en, *Current Biology*, vol. 22, no. 21, pp. 2042–2047, Nov. 2012, ISSN: 09609822. DOI: 10.1016/j.cub.2012.08.016.

[85] N. Cavallari, E. Frigato, D. Vallone, *et al.*, "A Blind Circadian Clock in Cavefish Reveals that Opsins Mediate Peripheral Clock Photoreception," en, *PLoS Biology*, vol. 9, no. 9, U. Schibler, Ed., e1001142, Sep. 2011, ISSN: 1545-7885. DOI: 10.1371/journal.pbio.1001142.

[86] W. Dröge, "Free Radicals in the Physiological Control of Cell Function," *Physiological Reviews*, vol. 82, no. 1, pp. 47–95, Jan. 2002, Publisher: American Physiological Society, ISSN: 0031-9333. DOI: 10.1152/physrev.00018.2001.

[87] C. E. Cross, B. Halliwell, E. T. Borish, *et al.*, "Oxygen Radicals and Human Disease," *Annals of Internal Medicine*, vol. 107, no. 4, pp. 526–545, Oct. 1987, Publisher: American College of Physicians, ISSN: 0003-4819. DOI: 10.7326/0003-4819-107-4-526.

[88] T. Finkel, "Signal transduction by reactive oxygen species," *Journal of Cell Biology*, vol. 194, no. 1, pp. 7–15, Jul. 2011, ISSN: 0021-9525. DOI: 10.1083/jcb.201102095.

[89] J. D. Lambeth, T. Kawahara, and B. Diebold, "Regulation of Nox and Duox enzymatic activity and expression," *Free Radical Biology and Medicine*, vol. 43, no. 3, pp. 319–331, Aug. 2007, ISSN: 0891-5849. DOI: 10.1016/j.freeradbiomed.2007.03.028.

[90] K. Bedard and K.-H. Krause, "The NOX Family of ROS-Generating NADPH Oxidases: Physiology and Pathophysiology," *Physiological Reviews*, vol. 87, no. 1, pp. 245–313, Jan. 2007, Publisher: American Physiological Society, ISSN: 0031-9333. DOI: 10.1152/physrev.00044.2005.

[91] Z. A. Wood, L. B. Poole, and P. A. Karplus, "Peroxiredoxin Evolution and the Regulation of Hydrogen Peroxide Signaling," *Science*, vol. 300, no. 5619, pp. 650–653, Apr. 2003, Publisher: American Association for the Advancement of Science. DOI: 10.1126/science.1080405.

[92] M. Nieborowska-Skorska, P. K. Kopinski, R. Ray, *et al.*, "Rac2-MRC-cIII–generated ROS cause genomic instability in chronic myeloid leukemia stem cells and primitive progenitors," *Blood*, vol. 119, no. 18, pp. 4253–4263, May 2012, ISSN: 0006-4971. DOI: 10.1182/blood-2011-10-385658.

[93] N. K. Tonks, "Redox Redux: Revisiting PTPs and the Control of Cell Signaling," English, *Cell*, vol. 121, no. 5, pp. 667–670, Jun. 2005, Publisher: Elsevier, ISSN: 0092-8674, 1097-4172. DOI: 10.1016/j.cell.2005.05.016.

[94] E. C. Cheung and K. H. Vousden, "The role of ROS in tumour development and progression," en, *Nature Reviews Cancer*, vol. 22, no. 5, pp. 280–297, May 2022, Publisher: Nature Publishing Group, ISSN: 1474-1768. DOI: 10.1038/s41568-021-00435-0.

[95] J. Hirayama, S. Cho, and P. Sassone-Corsi, "Circadian control by the reduction/oxidation pathway: Catalase represses light-dependent clock gene expression in the zebrafish," *Proceedings of the National Academy of Sciences*, vol. 104, no. 40, pp. 15 747–15 752, Oct. 2007, Publisher: Proceedings of the National Academy of Sciences. DOI: 10.1073/pnas.0705614104.

[96] N. Cermakian, M. P. Pando, C. L. Thompson, *et al.*, "Light Induction of a Vertebrate Clock Gene Involves Signaling through Blue-Light Receptors and MAP Kinases," en, *Current Biology*, vol. 12, no. 10, pp. 844–848, May 2002, ISSN: 09609822. DOI: 10.1016/S0960-9822(02)00835-7.

[97] M. L. Idda, C. Bertolucci, D. Vallone, Y. Gothilf, F. J. Sánchez-Vázquez, and N. S. Foulkes, "Circadian clocks," en, in *Progress in Brain Research*, vol. 199, Elsevier, 2012, pp. 41–57, ISBN: 978-0-444-59427-3. DOI: 10.1016/B978-0-444-59427-3.00003-4.

[98] Z. Travnickova-Bendova, N. Cermakian, S. M. Reppert, and P. Sassone-Corsi, "Bimodal regulation of mPeriod promoters by CREB-dependent signaling and CLOCK/BMAL1 activity," *Proceedings of the National Academy of Sciences*, vol. 99, no. 11, pp. 7728–7733, May 2002, Publisher: Proceedings of the National Academy of Sciences. DOI: 10.1073/pnas.102075599.

[99] Y. Son, Y.-K. Cheong, N.-H. Kim, H.-T. Chung, D. G. Kang, and H.-O. Pae, "Mitogen-Activated Protein Kinases and Reactive Oxygen Species: How Can ROS Activate MAPK Pathways?" en, *Journal of Signal Transduction*, vol. 2011, e792639, Feb. 2011, Publisher: Hindawi, ISSN: 2090-1739. DOI: 10.1155/2011/792639.

[100] M. Cargnello and P. P. Roux, "Activation and Function of the MAPKs and Their Substrates, the MAPK-Activated Protein Kinases," *Microbiology and Molecular Biology Reviews*, vol. 75, no. 1, pp. 50–83, Mar. 2011, Publisher: American Society for Microbiology. DOI: 10.1128/mmbr.00031-10.

[101] H. Dziema, B. Oatis, G. Q. Butcher, R. Yates, K. R. Hoyt, and K. Obrietan, "The ERK/MAP kinase pathway couples light to immediate-early gene expression in the suprachiasmatic nucleus," en, *European Journal of Neuroscience*, vol. 17, no. 8, pp. 1617–1627, 2003, _eprint: https://onlinelibrary.wiley.com/doi/pdf/10.1046/j.1460-9568.2003.02592.x, ISSN: 1460-9568. DOI: 10.1046/j.1460-9568.2003.02592.x.

[102] V. M. Porterfield and E. M. Mintz, "Temporal patterns of light-induced immediate-early gene expression in the suprachiasmatic nucleus," *Neuroscience Letters*, vol. 463, no. 1, pp. 70–73, Sep. 2009, ISSN: 0304-3940. DOI: 10.1016/j.neulet.2009.07.066.

[103] J. Hirayama, N. Miyamura, Y. Uchida, *et al.*, "Common light signaling pathways controlling DNA repair and circadian clock entrainment in zebrafish," en, *Cell Cycle*, vol. 8, no. 17, pp. 2794–2801, Sep. 2009, ISSN: 1538-4101, 1551-4005. DOI: 10.4161/cc.8.17.9447.

[104] C. Pagano, R. Siauciunaite, M. L. Idda, *et al.*, "Evolution shapes the responsiveness of the D-box enhancer element to light and reactive oxygen species in vertebrates," en, *Scientific Reports*, vol. 8, no. 1, p. 13 180, Sep. 2018, Publisher: Nature Publishing Group, ISSN: 2045-2322. DOI: 10.1038/s41598-018-31570-8.

[105] P. Mracek, C. Pagano, N. Fröhlich, *et al.*, "ERK Signaling Regulates Light-Induced Gene Expression via D-Box Enhancers in a Differential, Wavelength-Dependent Manner," en, *PLoS ONE*, vol. 8, no. 6, E. M. Mintz, Ed., e67858, Jun. 2013, ISSN: 1932-6203. DOI: 10.1371/journal.pone.0067858.

[106] K. Okano, S. Ozawa, H. Sato, *et al.*, "Light- and circadian-controlled genes respond to a broad light spectrum in Puffer Fish-derived Fugu eye cells," en, *Scientific Reports*, vol. 7, no. 1, p. 46 150, Apr. 2017, ISSN: 2045-2322. DOI: 10.1038/srep46150.

[107] P. Mracek, C. Santoriello, M. L. Idda, *et al.*, "Regulation of per and cry Genes Reveals a Central Role for the D-Box Enhancer in Light-Dependent Gene Expression," en, *PLoS ONE*, vol. 7, no. 12, S. Yamazaki, Ed., e51278, Dec. 2012, ISSN: 1932-6203. DOI: 10.1371/journal.pone.0051278.

[108] S. M. Reppert and D. R. Weaver, "Coordination of circadian timing in mammals," en, *Nature*, vol. 418, no. 6901, pp. 935–941, Aug. 2002, ISSN: 0028-0836, 1476-4687. DOI: 10.1038/nature00965.

[109] D. Whitmore, N. S. Foulkes, and P. Sassone-Corsi, "Light acts directly on organs and cells in culture to set the vertebrate circadian clock," en, *Nature*, vol. 404, no. 6773, pp. 87–91, Mar. 2000, ISSN: 0028-0836, 1476-4687. DOI: 10.1038/35003589.

[110] C. Chakraborty, C. H. Hsu, Z. H. Wen, C. S. Lin, and G. Agoramoorthy, "Zebrafish: A Complete Animal Model for In Vivo Drug Discovery and Development," *Current Drug Metabolism*, vol. 10, no. 2, pp. 116–124, Feb. 2009. DOI: 10.2174/138920009787522197.

[111] W. Norton and L. Bally-Cuif, "Adult zebrafish as a model organism for behavioural genetics," en, *BMC Neuroscience*, vol. 11, no. 1, p. 90, Aug. 2010, ISSN: 1471-2202. DOI: 10.1186/1471-2202-11-90.

[112] C. B. Kimmel, W. W. Ballard, S. R. Kimmel, B. Ullmann, and T. F. Schilling, "Stages of embryonic development of the zebrafish," en, *Developmental Dynamics*, vol. 203, no. 3, pp. 253–310, 1995, _eprint: https://onlinelibrary.wiley.com/doi/pdf/10.1002/aja.1002030302, ISSN: 1097-0177. DOI: 10.1002/aja.1002030302.

[113] K. Howe, M. D. Clark, C. F. Torroja, *et al.*, "The zebrafish reference genome sequence and its relationship to the human genome," en, *Nature*, vol. 496, no. 7446, pp. 498–503, Apr. 2013, Publisher: Nature Publishing Group, ISSN: 1476-4687. DOI: 10.1038/nature12111.

[114] G. E. Ackermann and B. H. Paw, "Zebrafish: A genetic model for vertebrate organogenesis and human disorders," *Frontiers in Bioscience-Landmark*, vol. 8, no. 4, pp. 1227–1253, Sep. 2003, Number: 4 Publisher: IMR Press, ISSN: 2768-6701. DOI: 10.2741/1092.

[115] A. Meyer, C. H. Biermann, and G. Orti, "The phylogenetic position of the zebrafish (Danio rerio), a model system in developmental biology: An invitation to the comparative method," *Proceedings of the Royal Society of London. Series B: Biological Sciences*, vol. 252, no. 1335, pp. 231–236, Jan. 1997, Publisher: Royal Society. DOI: 10.1098/rspb.1993.0070.

[116] R. Gerlai, "Using Zebrafish to Unravel the Genetics of Complex Brain Disorders," en, in *Behavioral Neurogenetics*, J. F. Cryan and A. Reif, Eds., Berlin, Heidelberg: Springer, 2012, pp. 3–24, ISBN: 978-3-642-27859-4. DOI: 10.1007/7854_2011_180.

[117] T. Tamai, V. Vardhanabhuti, N. S. Foulkes, and D. Whitmore, "Early Embryonic Light Detection Improves Survival," en, *Current Biology*, vol. 14, no. 5, p. 446, Mar. 2004, ISSN: 09609822. DOI: 10.1016/j.cub.2004.02.040.

[118] M. C. Rice, J. H. Little, D. L. Forrister, J. Machado, N. L. Clark, and J. A. Gagnon, "Gadusol is a maternally provided sunscreen that protects fish embryos from DNA damage," English, *Current Biology*, vol. 33, no. 15, 3229–3237.e4, Aug. 2023, Publisher: Elsevier, ISSN: 0960-9822. DOI: 10.1016/j.cub.2023.06.012.

[119] L. Ziv and Y. Gothilf, "Circadian time-keeping during early stages of development," *Proceedings of the National Academy of Sciences*, vol. 103, no. 11, pp. 4146–4151, Mar. 2006, Publisher: Proceedings of the National Academy of Sciences. DOI: 10.1073/pnas.0600571103.

[120] V. Di Rosa, E. Frigato, J. F. López-Olmeda, F. J. Sánchez-Vázquez, and C. Bertolucci, "The Light Wavelength Affects the Ontogeny of Clock Gene Expression and Activity Rhythms in Zebrafish Larvae," en, *PLOS ONE*, vol. 10, no. 7, N. S. Foulkes, Ed., e0132235, Jul. 2015, ISSN: 1932-6203. DOI: 10.1371/journal.pone.0132235.

[121] M. P. Dekens, C. Santoriello, D. Vallone, G. Grassi, D. Whitmore, and N. S. Foulkes, "Light Regulates the Cell Cycle in Zebrafish," en, *Current Biology*, vol. 13, no. 23, pp. 2051–2057, Dec. 2003, ISSN: 09609822. DOI: 10.1016/j.cub.2003.10.022.

[122] M. Hernández Fernández and E. S. Vrba, "Plio-Pleistocene climatic change in the Turkana Basin (East Africa): Evidence from large mammal faunas," *Journal of Human Evolution*, vol. 50, no. 6, pp. 595–626, Jun. 2006, ISSN: 0047-2484. DOI: 10.1016/j.jhevol.2005.11.004.

[123] G. Vatine, D. Vallone, L. Appelbaum, *et al.*, "Light Directs Zebrafish period2 Expression via Conserved D and E Boxes," en, *PLoS Biology*, vol. 7, no. 10, A. Kramer, Ed., e1000223, Oct. 2009, ISSN: 1545-7885. DOI: 10.1371/journal.pbio.1000223.

[124] N. B. Haas, C. A. Cantwell, P. F. Johnson, and J. B. E. Burch, "DNA-Binding Specificity of the PAR Basic Leucine Zipper Protein VBP Partially Overlaps Those of the C/EBP and CREB/ATF Families and Is Influenced by Domains That Flank the Core Basic Region," *Molecular and Cellular Biology*, vol. 15, no. 4, pp. 1923–1932, Apr. 1995, Publisher: Taylor & Francis _eprint: https://doi.org/10.1128/MCB.15.4.1923, ISSN: null. DOI: 10.1128/MCB.15.4.1923.

[125] D. W. Drolet, K. M. Scully, D. M. Simmons, *et al.*, "TEF, a transcription factor expressed specifically in the anterior pituitary during embryogenesis, defines a new class of leucine zipper proteins.," en, *Genes & Development*, vol. 5, no. 10, pp. 1739–1753, Oct. 1991, Company: Cold Spring Harbor Laboratory Press Distributor: Cold Spring Harbor Laboratory Press Institution: Cold Spring Harbor Laboratory Press Label: Cold Spring Harbor Laboratory Press Publisher: Cold Spring Harbor Lab, ISSN: 0890-9369, 1549-5477. DOI: 10.1101/gad.5.10.1739.

[126] S. Hunger, S. Li, M. Fall, L. Naumovski, and M. Cleary, "The proto-oncogene HLF and the related basic leucine zipper protein TEF display highly similar DNA-binding and transcriptional regulatory properties," *Blood*, vol. 87, no. 11, pp. 4607–4617, Jun. 1996, ISSN: 0006-4971. DOI: 10.1182/blood.V87.11.4607.bloodjournal87114607.

[127] I. G. Cowell, "E4BP4/NFIL3, a PAR-related bZIP factor with many roles," en, *BioEssays*, vol. 24, no. 11, pp. 1023–1029, Nov. 2002, ISSN: 0265-9247, 1521-1878. DOI: 10.1002/bies.10176.

[128] Z. Ben-Moshe, N. S. Foulkes, and Y. Gothilf, "Functional Development of the Circadian Clock in the Zebrafish Pineal Gland," en, *BioMed Research International*, vol. 2014, pp. 1–8, 2014, ISSN: 2314-6133, 2314-6141. DOI: 10.1155/2014/235781.

[129] Y. Sun, C. Liu, M. Huang, *et al.*, "The Molecular Evolution of Circadian Clock Genes in Spotted Gar (Lepisosteus oculatus)," en, *Genes*, vol. 10, no. 8, p. 622, Aug. 2019, ISSN: 2073-4425. DOI: 10.3390/genes10080622.

[130] C. Lamprecht and C. R. Mueller, "D-site Binding Protein Transactivation Requires the Proline- and Acid-rich Domain and Involves the Coactivator p300 *," English, *Journal of Biological Chemistry*, vol. 274, no. 25, pp. 17 643–17 648, Jun. 1999, Publisher: Elsevier, ISSN: 0021-9258, 1083-351X. DOI: 10.1074/jbc.274.25.17643.

[131] S. Mitsui, S. Yamaguchi, T. Matsuo, Y. Ishida, and H. Okamura, "Antagonistic role of E4BP4 and PAR proteins in the circadian oscillatory mechanism," en, *Genes & Development*, vol. 15, no. 8, pp. 995–1006, Apr. 2001, Company: Cold Spring Harbor Laboratory Press Distributor: Cold Spring Harbor Laboratory Press Institution: Cold Spring Harbor Laboratory Press Label: Cold Spring Harbor Laboratory Press Publisher: Cold Spring Harbor Lab, ISSN: 0890-9369, 1549-5477. DOI: 10.1101/gad.873501.

[132] F. Gachon, F. F. Olela, O. Schaad, P. Descombes, and U. Schibler, "The circadian PAR-domain basic leucine zipper transcription factors DBP, TEF, and HLF modulate basal and inducible xenobiotic detoxification," English, *Cell Metabolism*, vol. 4, no. 1, pp. 25–36, Jul. 2006, Publisher: Elsevier, ISSN: 1550-4131. DOI: 10.1016/j.cmet.2006.04.015.

[133] H. R. Ueda, S. Hayashi, W. Chen, *et al.*, "System-level identification of transcriptional circuits underlying mammalian circadian clocks," en, *Nature Genetics*, vol. 37, no. 2, pp. 187–192, Feb. 2005, Publisher: Nature Publishing Group, ISSN: 1546-1718. DOI: 10.1038/ng1504.

[134] H. Dardente, C. A. Wyse, M. J. Birnie, *et al.*, "A Molecular Switch for Photoperiod Responsiveness in Mammals," en, *Current Biology*, vol. 20, no. 24, pp. 2193–2198, Dec. 2010, ISSN: 09609822. DOI: 10.1016/j.cub.2010.10.048.

[135] F. Eileen, M. Lysiane, and S. Ueli, "DNA-Binding Specificity of PAR and C/EBP Leucine Zipper Proteins: A Single Amino Acid Substitution in the C/EBP DNA-Binding Domain Confers PAR-Like Specificity to C/EBP," en, *Biological Chemistry Hoppe-Seyler*, vol. 377, no. 12, pp. 797–810, Dec. 1996, Publisher: De Gruyter Section: Biological Chemistry, ISSN: 1437-4315. DOI: 10.1515/bchm3.1996.377.12.797.

[136] B. Staels, "When the Clock stops ticking, metabolic syndrome explodes," en, *Nature Medicine*, vol. 12, no. 1, pp. 54–55, Jan. 2006, ISSN: 1078-8956, 1546-170X. DOI: 10.1038/nm0106-54.

[137] H. Zhao, H. Li, J. Du, *et al.*, "Regulation of ddb2 expression in blind cavefish and zebrafish reveals plasticity in the control of sunlight-induced DNA damage repair," en, *PLOS Genetics*, vol. 17, no. 2, D. A. Gordenin, Ed., e1009356, Feb. 2021, ISSN: 1553-7404. DOI: 10.1371/journal.pgen.1009356.

[138] G. Vatine, D. Vallone, Y. Gothilf, and N. S. Foulkes, "It's time to swim! Zebrafish and the circadian clock," en, *FEBS Letters*, vol. 585, no. 10, pp. 1485–1494, May 2011, ISSN: 00145793. DOI: 10.1016/j.febslet.2011.04.007.

[139] D. Vallone, C. Santoriello, S. B. Gondi, and N. S. Foulkes, "Basic Protocols for Zebrafish Cell Lines," en, in *Circadian Rhythms: Methods and Protocols*, E. Rosato, Ed., Totowa, NJ: Humana Press, 2007, pp. 429–441, ISBN: 978-1-59745-257-1. DOI: 10.1007/978-1-59745-257-1_35.

[140] B. J. Haas, A. Papanicolaou, M. Yassour, *et al.*, "De novo transcript sequence reconstruction from RNA-seq using the Trinity platform for reference generation and analysis," en, *Nature Protocols*, vol. 8, no. 8, pp. 1494–1512, Aug. 2013, Publisher: Nature Publishing Group, ISSN: 1750-2799. DOI: 10.1038/nprot.2013.084.

[141] Y. Fu, M. C. Frith, P. M. Haverty, and Z. Weng, "MotifViz: An analysis and visualization tool for motif discovery," *Nucleic Acids Research*, vol. 32, no. suppl_2, W420–W423, Jul. 2004, ISSN: 0305-1048. DOI: 10.1093/nar/gkh426.

[142] S. Sassa, "Sequential induction of heme pathway enzymes during erythroid differentiation of mouse Friend leukemia virus-infected cells.," *Journal of Experimental Medicine*, vol. 143, no. 2, pp. 305–315, Feb. 1976, ISSN: 0022-1007. DOI: 10.1084/jem.143.2.305.

[143] P. R. Sinclair, N. Gorman, and J. M. Jacobs, "Measurement of Heme Concentration," en, *Current Protocols in Toxicology*, vol. 00, no. 1, May 1999, ISSN: 1934-9254, 1934-9262. DOI: 10.1002/0471140856.tx0803s00.

[144] S. Kim, K. Malhotra, C. Smith, J. Taylor, and A. Sancar, "Characterization of (6-4) photoproduct DNA photolyase.," en, *Journal of Biological Chemistry*, vol. 269, no. 11, pp. 8535–8540, Mar. 1994, ISSN: 00219258. DOI: 10.1016/S0021-9258(17)37228-9.

[145] F. Thoma, “Light and dark in chromatin repair: Repair of UV-induced DNA lesions by photolyase and nucleotide excision repair,” en, *The EMBO Journal*, vol. 18, no. 23, pp. 6585–6598, Dec. 1999, ISSN: 14602075. DOI: 10.1093/emboj/18.23.6585.

[146] W. Gehring and M. Rosbash, “The Coevolution of Blue-Light Photoreception and Circadian Rhythms,” en, *Journal of Molecular Evolution*, vol. 57, no. 0, S286–S289, Aug. 2003, ISSN: 0022-2844, 1432-1432. DOI: 10.1007/s00239-003-0038-8.

[147] D.-f. Huang, M.-y. Wang, W. Yin, *et al.*, “Zebrafish Lacking Circadian Gene per2 Exhibit Visual Function Deficiency,” English, *Frontiers in Behavioral Neuroscience*, vol. 12, Mar. 2018, Publisher: Frontiers, ISSN: 1662-5153. DOI: 10.3389/fnbeh.2018.00053.

[148] R. C. Sears, “The Life Cycle of C-Myc: From Synthesis to Degradation,” *Cell Cycle*, vol. 3, no. 9, pp. 1131–1135, Sep. 2004, Publisher: Taylor & Francis _eprint: https://doi.org/10.4161/cc.3.9.1145, ISSN: 1538-4101. DOI: 10.4161/cc.3.9.1145.

[149] S. Li and S. P. Hunger, “The DBP transcriptional activation domain is highly homologous to that of HLF and TEF and is not responsible for the tissue type-specific transcriptional activity of DBP,” en, *Gene*, vol. 263, no. 1, pp. 239–245, Jan. 2001, ISSN: 0378-1119. DOI: 10.1016/S0378-1119(00)00565-5.

[150] L. Finlayson, I. R. M. Barnard, L. McMillan, *et al.*, “Depth Penetration of Light into Skin as a Function of Wavelength from 200 to 1000 nm,” en, *Photochemistry and Photobiology*, vol. 98, no. 4, pp. 974–981, 2022, _eprint: https://onlinelibrary.wiley.com/doi/pdf/10.1111/php.13550, ISSN: 1751-1097. DOI: 10.1111/php.13550.

[151] C. Blattner, P. Kannouche, M. Litfin, *et al.*, “UV-Induced Stabilization of c- *fos* and Other Short-Lived mRNAs,” en, *Molecular and Cellular Biology*, vol. 20, no. 10, pp. 3616–3625, May 2000, ISSN: 1098-5549. DOI: 10.1128/MCB.20.10.3616-3625.2000.

[152] F. Bollig, R. Winzen, M. Kracht, *et al.*, “Evidence for general stabilization of mRNAs in response to UV light,” en, *European Journal of Biochemistry*, vol. 269, no. 23, pp. 5830–5839, Dec. 2002, ISSN: 0014-2956, 1432-1033. DOI: 10.1046/j.1432-1033.2002.03300.x.

[153] T. A. Liddle, T. J. Stevenson, and G. Majumdar, “Photoperiodic regulation of avian physiology: From external coincidence to seasonal reproduction,” en, *Journal of Experimental Zoology Part A: Ecological and Integrative Physiology*, vol. 337, no. 9-10, pp. 890–901, 2022, _eprint: https://onlinelibrary.wiley.com/doi/pdf/10.1002/jez.2604, ISSN: 2471-5646. DOI: 10.1002/jez.2604.

[154] E. Muñoz and R. Baler, “The Circadian E-Box: When Perfect Is Not Good Enough: REVIEW,” *Chronobiology International*, vol. 20, no. 3, pp. 371–388, Jan. 2003, Publisher: Taylor & Francis _eprint: https://doi.org/10.1081/CBI-120022525, ISSN: 0742-0528. DOI: 10.1081/CBI-120022525.

[155] J. H. Postlethwait, Y.-L. Yan, M. A. Gates, *et al.*, “Vertebrate genome evolution and the zebrafish gene map,” en, *Nature Genetics*, vol. 18, no. 4, pp. 345–349, Apr. 1998, Publisher: Nature Publishing Group, ISSN: 1546-1718. DOI: 10.1038/ng0498-345.

[156] Z. Ben-Moshe, G. Vatine, S. Alon, *et al.*, "MULTIPLE PAR AND E4BP4 bZIP TRANSCRIPTION FACTORS IN ZEBRAFISH: DIVERSE SPATIAL AND TEMPORAL EXPRESSION PATTERNS," en, *Chronobiology International*, vol. 27, no. 8, pp. 1509–1531, Oct. 2010, ISSN: 0742-0528, 1525-6073. DOI: 10.3109/07420528.2010.510229.

[157] P. Fonjallaz, V. Ossipow, G. Wanner, and U. Schibler, "The two PAR leucine zipper proteins, TEF and DBP, display similar circadian and tissue□specific expression, but have different target promoter preferences.," *The EMBO Journal*, vol. 15, no. 2, pp. 351–362, Jan. 1996, Num Pages: 362 Publisher: John Wiley & Sons, Ltd, ISSN: 0261-4189. DOI: 10.1002/j.1460-2075.1996.tb00365.x.

[158] Y. Pan, C.-J. Tsai, B. Ma, and R. Nussinov, "Mechanisms of transcription factor selectivity," English, *Trends in Genetics*, vol. 26, no. 2, pp. 75–83, Feb. 2010, Publisher: Elsevier, ISSN: 0168-9525. DOI: 10.1016/j.tig.2009.12.003.

[159] E. Falvey, F. Fleury□Olela, and U. Schibler, "The rat hepatic leukemia factor (HLF) gene encodes two transcriptional activators with distinct circadian rhythms, tissue distributions and target preferences.," *The EMBO Journal*, vol. 14, no. 17, pp. 4307–4317, Sep. 1995, Num Pages: 4317 Publisher: John Wiley & Sons, Ltd, ISSN: 0261-4189. DOI: 10.1002/j.1460-2075.1995.tb00105.x.

[160] J. Crocker, E. Preger-Ben Noon, and D. L. Stern, "Chapter Twenty-Seven - The Soft Touch: Low-Affinity Transcription Factor Binding Sites in Development and Evolution," in *Current Topics in Developmental Biology*, ser. Essays on Developmental Biology, Part B, P. M. Wassarman, Ed., vol. 117, Academic Press, Jan. 2016, pp. 455–469. DOI: 10.1016/bs.ctdb.2015.11.018.

[161] S. Inukai, K. H. Kock, and M. L. Bulyk, "Transcription factor–DNA binding: Beyond binding site motifs," *Current Opinion in Genetics & Development*, Genome architecture and expression, vol. 43, pp. 110–119, Apr. 2017, ISSN: 0959-437X. DOI: 10.1016/j.gde.2017.02.007.

[162] R. M. Ceinos, E. Frigato, C. Pagano, *et al.*, "Mutations in blind cavefish target the light-regulated circadian clock gene, period 2," en, *Scientific Reports*, vol. 8, no. 1, p. 8754, Dec. 2018, ISSN: 2045-2322. DOI: 10.1038/s41598-018-27080-2.

[163] A. Rajagopal, A. U. Rao, J. Amigo, *et al.*, "Haem homeostasis is regulated by the conserved and concerted functions of HRG-1 proteins," eng, *Nature*, vol. 453, no. 7198, pp. 1127–1131, Jun. 2008, ISSN: 1476-4687. DOI: 10.1038/nature06934.

[164] S. Gandre-Babbe and A. M. van der Bliek, "The novel tail-anchored membrane protein Mff controls mitochondrial and peroxisomal fission in mammalian cells," eng, *Molecular Biology of the Cell*, vol. 19, no. 6, pp. 2402–2412, Jun. 2008, ISSN: 1939-4586. DOI: 10.1091/mbc.e07-12-1287.

[165] W. Yoon, S.-H. Hwang, S.-H. Lee, and J. Chung, "Drosophila ADCK1 is critical for maintaining mitochondrial structures and functions in the muscle," eng, *PLoS genetics*, vol. 15, no. 5, e1008184, May 2019, ISSN: 1553-7404. DOI: 10.1371/journal.pgen.1008184.

[166] L. Ding, Y. Lei, Y. Han, Y. Li, X. Ji, and L. Liu, "Vimar Is a Novel Regulator of Mitochondrial Fission through Miro," eng, *PLoS genetics*, vol. 12, no. 10, e1006359, Oct. 2016, ISSN: 1553-7404. DOI: 10.1371/journal.pgen.1006359.

[167] R. J. Youle and A. M. van der Bliek, "Mitochondrial Fission, Fusion, and Stress," *Science*, vol. 337, no. 6098, pp. 1062–1065, Aug. 2012, Publisher: American Association for the Advancement of Science. DOI: 10.1126/science.1219855.

[168] G. H. Renkema, S. B. Wortmann, R. J. Smeets, *et al.*, "SDHA mutations causing a multisystem mitochondrial disease: Novel mutations and genetic overlap with hereditary tumors," en, *European Journal of Human Genetics*, vol. 23, no. 2, pp. 202–209, Feb. 2015, ISSN: 1018-4813, 1476-5438. DOI: 10.1038/ejhg.2014.80.

[169] S. Magri, V. Fracasso, M. Plumari, *et al.*, "Concurrent AFG3L2 and SPG7 mutations associated with syndromic parkinsonism and optic atrophy with aberrant OPA1 processing and mitochondrial network fragmentation," en, *Human Mutation*, vol. 39, no. 12, pp. 2060–2071, 2018, _eprint: https://onlinelibrary.wiley.com/doi/pdf/10.1002/humu.23658, ISSN: 1098-1004. DOI: 10.1002/humu.23658.

[170] E. Hangen, O. Féraud, S. Lachkar, *et al.*, "Interaction between AIF and CHCHD4 Regulates Respiratory Chain Biogenesis," en, *Molecular Cell*, vol. 58, no. 6, pp. 1001–1014, Jun. 2015, ISSN: 10972765. DOI: 10.1016/j.molcel.2015.04.020.

[171] D. Ghezzi, P. Arzuffi, M. Zordan, *et al.*, "Mutations in TTC19 cause mitochondrial complex III deficiency and neurological impairment in humans and flies," eng, *Nature Genetics*, vol. 43, no. 3, pp. 259–263, Mar. 2011, ISSN: 1546-1718. DOI: 10.1038/ng.761.

[172] A. V. Follis, J. E. Chipuk, J. C. Fisher, *et al.*, "PUMA binding induces partial unfolding within BCL-xL to disrupt p53 binding and promote apoptosis," eng, *Nature Chemical Biology*, vol. 9, no. 3, pp. 163–168, Mar. 2013, ISSN: 1552-4469. DOI: 10.1038/nchembio.1166.

[173] A. Fransson, A. Ruusala, and P. Aspenström, "Atypical Rho GTPases have roles in mitochondrial homeostasis and apoptosis," eng, *The Journal of Biological Chemistry*, vol. 278, no. 8, pp. 6495–6502, Feb. 2003, ISSN: 0021-9258. DOI: 10.1074/jbc.M208609200.

[174] A. Benito, O. Gutierrez, C. Pipaon, *et al.*, "A Novel Role for Proline- and Acid-rich Basic Region Leucine Zipper (PAR bZIP) Proteins in the Transcriptional Regulation of a BH3-only Proapoptotic Gene *," English, *Journal of Biological Chemistry*, vol. 281, no. 50, pp. 38 351–38 357, Dec. 2006, Publisher: Elsevier, ISSN: 0021-9258, 1083-351X. DOI: 10.1074/jbc.M607004200.

[175] M. D. Maines, B. V. Polevoda, T. J. Huang, and W. K. McCoubrey, "Human biliverdin IXalpha reductase is a zinc-metalloprotein. Characterization of purified and Escherichia coli expressed enzymes," eng, *European Journal of Biochemistry*, vol. 235, no. 1-2, pp. 372–381, Jan. 1996, ISSN: 0014-2956. DOI: 10.1111/j.1432-1033.1996.00372.x.

[176] H. A. Dailey, M. G. Finnegan, and M. K. Johnson, "Human ferrochelatase is an iron-sulfur protein," en, *Biochemistry*, vol. 33, no. 2, pp. 403–407, Jan. 1994, ISSN: 0006-2960, 1520-4995. DOI: 10.1021/bi00168a003.

[177] D.-L. Zhang, J. Wu, B. N. Shah, *et al.*, "Erythrocytic ferroportin reduces intracellular iron accumulation, hemolysis, and malaria risk," eng, *Science (New York, N.Y.)*, vol. 359, no. 6383, pp. 1520–1523, Mar. 2018, ISSN: 1095-9203. DOI: 10.1126/science.aal2022.

[178] D. Senyilmaz, S. Virtue, X. Xu, *et al.*, "Regulation of mitochondrial morphology and function by stearoylation of TFR1," eng, *Nature*, vol. 525, no. 7567, pp. 124–128, Sep. 2015, ISSN: 1476-4687. DOI: 10.1038/nature14601.

[179] J. V. Goldstone, A. G. McArthur, A. Kubota, *et al.*, "Identification and developmental expression of the full complement of Cytochrome P450 genes in Zebrafish," *BMC Genomics*, vol. 11, no. 1, p. 643, Nov. 2010, ISSN: 1471-2164. DOI: 10.1186/1471-2164-11-643.

[180] U. Hoch and P. R. O. d. Montellano, "Covalently Linked Heme in Cytochrome P4504A Fatty Acid Hydroxylases *," English, *Journal of Biological Chemistry*, vol. 276, no. 14, pp. 11 339–11 346, Apr. 2001, Publisher: Elsevier, ISSN: 0021-9258, 1083-351X. DOI: 10.1074/jbc.M009969200.

[181] S. Raha and B. H. Robinson, "Mitochondria, oxygen free radicals, disease and ageing," English, *Trends in Biochemical Sciences*, vol. 25, no. 10, pp. 502–508, Oct. 2000, Publisher: Elsevier, ISSN: 0968-0004. DOI: 10.1016/S0968-0004(00)01674-1.

[182] V. Fiorito, D. Chiabrando, and E. Tolosano, "Mitochondrial Targeting in Neurodegeneration: A Heme Perspective," en, *Pharmaceuticals*, vol. 11, no. 3, p. 87, Sep. 2018, Number: 3 Publisher: Multidisciplinary Digital Publishing Institute, ISSN: 1424-8247. DOI: 10.3390/ph11030087.

[183] H. Atamna, "Heme, iron, and the mitochondrial decay of ageing," *Ageing Research Reviews*, Iron in Ageing and Age-Related Diseases, vol. 3, no. 3, pp. 303–318, Jul. 2004, ISSN: 1568-1637. DOI: 10.1016/j.arr.2004.02.002.

[184] W. Xu, T. Barrientos, and N. C. Andrews, "Iron and Copper in Mitochondrial Diseases," en, *Cell Metabolism*, vol. 17, no. 3, pp. 319–328, Mar. 2013, ISSN: 15504131. DOI: 10.1016/j.cmet.2013.02.004.

[185] D. A. Hanna, R. Hu, H. Kim, O. Martinez-Guzman, M. P. Torres, and A. R. Reddi, "Heme bioavailability and signaling in response to stress in yeast cells," English, *Journal of Biological Chemistry*, vol. 293, no. 32, pp. 12 378–12 393, Aug. 2018, Publisher: Elsevier, ISSN: 0021-9258, 1083-351X. DOI: 10.1074/jbc.RA118.002125.

[186] F. Esteves, J. Rueff, and M. Kranendonk, "The Central Role of Cytochrome P450 in Xenobiotic Metabolism—A Brief Review on a Fascinating Enzyme Family," en, *Journal of Xenobiotics*, vol. 11, no. 3, pp. 94–114, Sep. 2021, Number: 3 Publisher: Multidisciplinary Digital Publishing Institute, ISSN: 2039-4713. DOI: 10.3390/jox11030007.

[187] J. P. DeBruyne, D. R. Weaver, and R. Dallmann, "The Hepatic Circadian Clock Modulates Xenobiotic Metabolism in Mice," en, *Journal of Biological Rhythms*, vol. 29, no. 4, pp. 277–287, Aug. 2014, Publisher: SAGE Publications Inc, ISSN: 0748-7304. DOI: 10.1177/0748730414544740.

[188] D. Lu, M. Zhao, M. Chen, and B. Wu, "Circadian Clock–Controlled Drug Metabolism: Implications for Chronotherapeutics," en, *Drug Metabolism and Disposition*, vol. 48, no. 5, pp. 395–406, May 2020, Publisher: American Society for Pharmacology and Experimental Therapeutics Section: Minireview, ISSN: 0090-9556, 1521-009X. DOI: 10.1124/dmd.120.090472.

6. Supplementary tables

Gene promoter	JASPAR enhancer	From bp	To bp	Strand	Sequence	Score
abcb6a	MA0043.3_HLF	982	995	-	ttattgtataagtc	6.96
	MA0025.2_NFIL3	982	994	-	ttattgtataagt	6.44
adck1	MA0819.2_CLOCK	17	26	+	acccacgtga	6.63
	MA0043.3_HLF	94	107	+	atcttatacaacaa	7.16
	MA0025.2_NFIL3	276	288	+	ttttatgcaaaaa	6.32
	MA0819.2_CLOCK	742	751	+	gaccatgtgt	7.17
	MA0819.2_CLOCK	744	753	-	ccatgtgtcc	8.35
	MA0819.2_CLOCK	1022	1031	-	gcacgttgcg	7.52
bbc3	MA0843.1_TEF	348	359	+	tgttatgtcacc	6.1
	MA0843.1_TEF	348	359	-	tgttatgtcacc	6.65
	MA0639.1_DBP	348	359	+	tgttatgtcacc	6.96
	MA0639.1_DBP	348	359	-	tgttatgtcacc	8.3
	MA0025.2_NFIL3	348	360	+	tgttatgtcaccg	6.14
bco1l	MA0043.3_HLF	648	661	+	tgattatgcaatta	9.03
	MA0025.2_NFIL3	649	661	+	gattatgcaatta	9.5
	MA0639.1_DBP	649	660	-	gattatgcaatt	6.1
	MA0043.3_HLF	708	721	+	tagttatgcaacaa	10.9
	MA0025.2_NFIL3	709	721	+	agttatgcaacaa	9.46
	MA0639.1_DBP	709	720	-	agttatgcaaca	6.63
	MA0639.1_DBP	709	720	+	agttatgcaaca	7.15
	MA0843.1_TEF	709	720	-	agttatgcaaca	6.55
	MA0639.1_DBP	997	1008	+	agttatataatg	7.03
	MA0639.1_DBP	997	1008	-	agttatataatg	6.86
	MA0843.1_TEF	997	1008	-	agttatataatg	6.65
	MA0819.2_CLOCK	1019	1028	+	gaccacgttc	6.14
blvra	MA0819.2_CLOCK	720	729	+	ccgcacatgg	6.46
	MA0819.2_CLOCK	722	731	-	gcacatggat	6.74
	MA0819.2_CLOCK	845	854	+	ccacacgtgc	10.3
	MA0819.2_CLOCK	847	856	-	acacgtgcga	7.73
	MA0819.2_CLOCK	972	981	+	aaacacgtgc	10.5
	MA0819.2_CLOCK	974	983	-	acacgtgcga	7.73
	MA0639.1_DBP	986	997	+	cgtgacgtcaga	6.43
	MA0819.2_CLOCK	997	1006	+	acgcacgcgc	6.69
	MA0819.2_CLOCK	999	1008	-	gcacgcgcgg	6.58
	MA0043.3_HLF	1083	1096	-	acgttgcgtaagaa	8.17
	MA0025.2_NFIL3	1083	1095	-	acgttgcgtaaga	7.27
	MA0843.1_TEF	1084	1095	-	cgttgcgtaaga	7.4
	MA0843.1_TEF	1084	1095	+	cgttgcgtaaga	7.43
	MA0639.1_DBP	1084	1095	-	cgttgcgtaaga	8.38
	MA0639.1_DBP	1084	1095	+	cgttgcgtaaga	8.78
cbr1	MA0025.2_NFIL3	734	746	-	aaattacataata	7.89
	MA0025.2_NFIL3	857	869	+	agttatgaaatac	7.1
	MA0819.2_CLOCK	951	960	+	atgcacgtga	6.01
	MA0819.2_CLOCK	953	962	-	gcacgtgata	6.87
	MA0025.2_NFIL3	966	978	-	accttacgtaagc	6.17
	MA0025.2_NFIL3	967	979	+	ccttacgtaagca	6.09
	MA0819.2_CLOCK	988	997	-	gcgcgtgcgc	7.16
chchd4b	MA0025.2_NFIL3	73	85	-	actttgcataacc	8.9
	MA0025.2_NFIL3	163	175	+	tattgtgcaagag	6.22
	MA0819.2_CLOCK	803	812	+	ctacacgtgg	9.15
	MA0819.2_CLOCK	805	814	-	acacgtggtt	8.91
cyb5a	MA0639.1_DBP	367	378	+	cctgacataact	6.36
	MA0639.1_DBP	367	378	-	cctgacataact	6.01
cyp2ae1	MA0819.2_CLOCK	532	541	+	aaacacatgt	7.37
	MA0819.2_CLOCK	534	543	+	acacatgtgc	7.31
	MA0819.2_CLOCK	534	543	-	acacatgtgc	6.79
	MA0819.2_CLOCK	570	579	+	ggccatgtgt	6.48
	MA0819.2_CLOCK	572	581	-	ccatgtgtgt	6.62
	MA0819.2_CLOCK	646	655	+	aaacacatgc	8.07
	MA0819.2_CLOCK	648	657	-	acacatgctg	6.31
	MA0819.2_CLOCK	822	831	+	aaacacgtgg	10.3
	MA0819.2_CLOCK	824	833	-	acacgtggat	8.14
	MA0819.2_CLOCK	929	938	+	ccacatgtgc	7.34
	MA0819.2_CLOCK	929	938	-	ccacatgtgc	7.24
	MA0639.1_DBP	1653	1664	-	cgtgacgtcatc	6.44
	MA0639.1_DBP	1653	1664	+	cgtgacgtcatc	6.11

Gene promoter	JASPAR enhancer	From bp	To bp	Strand	Sequence	Score
dhrs11b	MA0043.3_HLF	759	772	+	gtattgtgtaagcg	6.24
	MA0639.1_DBP	760	771	-	tattgtgtaagc	6.14
	MA0043.3_HLF	913	926	+	agtttatgtaactg	7.25
	MA0025.2_NFIL3	914	926	+	gtttatgtaactg	7.21
dhrs12	MA0025.2_NFIL3	90	102	-	aaattgcttaatt	6.02
	MA0639.1_DBP	164	175	+	gatgatgtaata	6.91
	MA0025.2_NFIL3	164	176	+	gatgatgtaataa	7.28
	MA0843.1_TEF	164	175	-	gatgatgtaata	6.26
	MA0043.3_HLF	683	696	+	aaattatgtaaatc	6.03
	MA0025.2_NFIL3	684	696	+	aattatgtaaatc	7
	MA0819.2_CLOCK	706	715	-	gcatgtgtat	6.97
	MA0819.2_CLOCK	967	976	-	gcacgtgatc	7.4
dhrs13a.1	MA0819.2_CLOCK	177	186	+	ccccacgtgt	8.43
	MA0819.2_CLOCK	179	188	-	ccacgtgttc	10.3
	MA0043.3_HLF	376	389	+	cttttatgcaatat	7.52
	MA0025.2_NFIL3	377	389	+	ttttatgcaatat	8.33
	MA0025.2_NFIL3	407	419	+	atttatgtaatat	7.47
dhrs13a.3	MA0025.2_NFIL3	997	1009	+	agttatgaaacaa	6.32
	MA0819.2_CLOCK	1037	1046	+	aaacacgcgt	7.42
	MA0819.2_CLOCK	1039	1048	-	acacgcgttc	7.45
	MA0043.3_HLF	1079	1092	+	cagttatgaaacaa	6.54
	MA0025.2_NFIL3	1080	1092	+	agttatgaaacaa	6.3
	MA0819.2_CLOCK	1120	1129	+	aaacacgcgt	7.42
	MA0819.2_CLOCK	1122	1131	-	acacgcgttc	7.47
dio1	MA0819.2_CLOCK	869	878	+	aaacatgtgc	8.05
	MA0819.2_CLOCK	1138	1147	+	cgacgcgtgc	8.4
	MA0819.2_CLOCK	1140	1149	-	acgcgtgcac	6.07
enpp1	MA0025.2_NFIL3	162	174	-	caatggcataact	6.99
	MA0025.2_NFIL3	430	442	-	atattacataaat	6.81
	MA0043.3_HLF	474	487	+	gtcttgtgcaataa	7.4
	MA0025.2_NFIL3	475	487	+	tcttgtgcaataa	6.86
	MA0043.3_HLF	521	534	-	ttgttgtataattt	6.7
	MA0043.3_HLF	607	620	+	gccttgtgcaacat	9.29
	MA0025.2_NFIL3	608	620	+	ccttgtgcaacat	7.2
	MA0819.2_CLOCK	895	904	+	gggcatgtgc	7.97
ephx1	MA0025.2_NFIL3	1114	1126	-	gagttacataaaa	7.17
	MA0025.2_NFIL3	1144	1156	+	ttttatgtaatga	7.28
fastkd1	MA0819.2_CLOCK	697	706	+	aaacacatgc	7.75
	MA0819.2_CLOCK	1167	1176	+	caacacgtgg	10.3
	MA0819.2_CLOCK	1169	1178	-	acacgtggag	8.2
	MA0639.1_DBP	1199	1210	-	cattatgtcatg	7.22
	MA0639.1_DBP	1199	1210	+	cattatgtcatg	6.3
gcdha	MA0819.2_CLOCK	201	210	-	ccccgtgtcc	6.14
	MA0819.2_CLOCK	207	216	+	gtccatgtgg	6.77
	MA0639.1_DBP	790	801	-	tgtgacataatc	6.86
	MA0639.1_DBP	790	801	+	tgtgacataatc	7.17
	MA0819.2_CLOCK	1030	1039	+	cgacacgttc	6.77
hebp2	MA0043.3_HLF	926	939	+	gagtgatgtaacat	6.89
	MA0843.1_TEF	927	938	-	agtgatgtaaca	6.05
	MA0025.2_NFIL3	927	939	+	agtgatgtaacat	6.63
	MA0639.1_DBP	927	938	+	agtgatgtaaca	7.11
	MA0819.2_CLOCK	1036	1045	-	gcgcgtgtgt	6.7
MFF	MA0639.1_DBP	393	404	-	cattatgtcata	6.41
	MA0843.1_TEF	719	730	-	tgtaatgtaata	6.53
	MA0843.1_TEF	729	740	-	tataatgtaatg	6.08
	MA0025.2_NFIL3	1047	1059	-	tgtttgcacaaca	6.18
	MA0043.3_HLF	1047	1060	-	tgtttgcacaacat	6.55
mmel1	MA0819.2_CLOCK	728	737	+	atacatgtgt	6.33
	MA0043.3_HLF	759	772	-	gtattacataatga	8.58
	MA0025.2_NFIL3	759	771	-	gtattacataatg	9.37
	MA0843.1_TEF	760	771	+	tattacataatg	9.38
	MA0843.1_TEF	760	771	-	tattacataatg	8.66
	MA0639.1_DBP	760	771	+	tattacataatg	9.16
	MA0639.1_DBP	760	771	-	tattacataatg	9.26
nfs1	MA0043.3_HLF	378	391	+	ttattatgtaattt	7.15
	MA0843.1_TEF	379	390	-	tattatgtaatt	8.2
	MA0025.2_NFIL3	379	391	+	tattatgtaattt	8.34
	MA0639.1_DBP	379	390	-	tattatgtaatt	8
	MA0639.1_DBP	379	390	+	tattatgtaatt	7.21
	MA0843.1_TEF	379	390	+	tattatgtaatt	6.44
	MA0025.2_NFIL3	781	793	-	aaattacataaac	7.33

Gene promoter	JASPAR enhancer	From bp	To bp	Strand	Sequence	Score
nr1i2	MA0043.3_HLF	873	886	-	cagttgcataacaa	11.6
	MA0025.2_NFIL3	873	885	-	cagttgcataaca	9.71
	MA0843.1_TEF	874	885	+	agttgcataaca	6.95
	MA0639.1_DBP	874	885	+	agttgcataaca	7.43
	MA0639.1_DBP	874	885	-	agttgcataaca	6.72
	MA0043.3_HLF	900	913	-	aaattgcataatgc	9.34
	MA0025.2_NFIL3	900	912	-	aaattgcataatg	9.49
	MA0639.1_DBP	901	912	+	aattgcataatg	6.34
pnpo	MA0025.2_NFIL3	537	549	-	atattgcatagtt	6.35
porb	MA0043.3_HLF	80	93	-	catttacataataa	6.58
	MA0025.2_NFIL3	80	92	-	catttacataata	7.24
	MA0025.2_NFIL3	663	675	-	tgattgcataacc	10.7
	MA0043.3_HLF	663	676	-	tgattgcataaccc	11.1
	MA0639.1_DBP	664	675	-	gattgcataacc	7.39
	MA0639.1_DBP	664	675	+	gattgcataacc	7.67
	MA0843.1_TEF	664	675	+	gattgcataacc	7.79
	MA0025.2_NFIL3	715	727	-	acgttgcatatgc	6.12
	MA0043.3_HLF	719	732	+	tgcatatgcaacat	6.53
	MA0025.2_NFIL3	720	732	+	gcatatgcaacat	6.21
prdx1	MA0043.3_HLF	636	649	-	catttacataacaa	7.24
	MA0025.2_NFIL3	636	648	-	catttacataaca	7.51
	MA0043.3_HLF	935	948	-	catttacataacaa	7.15
	MA0025.2_NFIL3	935	947	-	catttacataaca	7.46
RAP1GDS1	MA0043.3_HLF	759	772	+	atgttatacaaacg	6.53
	MA0043.3_HLF	821	834	+	atgttatacaaacg	6.53
	MA0843.1_TEF	910	921	+	tgtaacataact	6.03
	MA0043.3_HLF	1182	1195	-	atattacgtaatcc	6.33
	MA0043.3_HLF	1182	1195	+	atattacgtaatcc	6.18
	MA0025.2_NFIL3	1182	1194	-	atattacgtaatc	7.19
	MA0025.2_NFIL3	1183	1195	+	tattacgtaatcc	7.18
	MA0639.1_DBP	1183	1194	-	tattacgtaatc	10.3
	MA0639.1_DBP	1183	1194	+	tattacgtaatc	9.83
	MA0843.1_TEF	1183	1194	-	tattacgtaatc	10.4
	MA0843.1_TEF	1183	1194	+	tattacgtaatc	10.6
retsat	MA0819.2_CLOCK	317	326	+	caacacatgt	7.26
	MA0819.2_CLOCK	319	328	-	acacatgtat	6.31
	MA0043.3_HLF	636	649	-	ttgttgcatcatca	8.79
	MA0025.2_NFIL3	636	648	-	ttgttgcatcatc	8.4
	MA0639.1_DBP	637	648	-	tgttgcatcatc	6.25
rhot1b	MA0025.2_NFIL3	311	323	-	atgttgcataacc	10.1
	MA0043.3_HLF	311	324	-	atgttgcataaccc	12.1
	MA0639.1_DBP	312	323	-	tgttgcataacc	8.04
	MA0843.1_TEF	312	323	+	tgttgcataacc	8.03
	MA0639.1_DBP	312	323	+	tgttgcataacc	7.71
	MA0843.1_TEF	312	323	-	tgttgcataacc	6.58
rnls	MA0819.2_CLOCK	216	225	+	caacatgtgt	7.45
	MA0819.2_CLOCK	218	227	-	acatgtgtta	6.53
	MA0819.2_CLOCK	428	437	+	ctacacatgc	7
	MA0025.2_NFIL3	994	1006	-	ggctttcataata	6.48
scd	MA0819.2_CLOCK	378	387	-	gcacatgttt	7.88
	MA0639.1_DBP	687	698	+	catgatgtaatc	7.09
	MA0639.1_DBP	687	698	-	catgatgtaatc	6.69
	MA0025.2_NFIL3	687	699	+	catgatgtaatcg	7.31
	MA0025.2_NFIL3	891	903	+	cattatgaaatat	7.7
	MA0819.2_CLOCK	1195	1204	+	gtccacgtgt	7.9
	MA0819.2_CLOCK	1197	1206	-	ccacgtgttt	10
sdha	MA0043.3_HLF	994	1007	-	gcgttacatcacaa	6.95
	MA0025.2_NFIL3	994	1006	-	gcgttacatcaca	7.19
	MA0843.1_TEF	995	1006	+	cgttacatcaca	7.41
	MA0639.1_DBP	995	1006	+	cgttacatcaca	7.12
	MA0639.1_DBP	995	1006	-	cgttacatcaca	7.41
sdhaf1	MA0819.2_CLOCK	790	799	-	gaacgtgtct	7.02
sdhaf2	MA0843.1_TEF	598	609	+	agttacattaca	6.19
	MA0819.2_CLOCK	869	878	+	ttacacgtgc	9.73
	MA0819.2_CLOCK	871	880	-	acacgtgcca	8.82
	MA0043.3_HLF	1019	1032	-	cagttgcataaact	9.15
	MA0025.2_NFIL3	1019	1031	-	cagttgcataaac	8.36

Gene promoter	JASPAR enhancer	From bp	To bp	Strand	Sequence	Score
sdhaf3	MA0819.2_CLOCK	117	126	+	agacatgtgg	7.62
	MA0025.2_NFIL3	1091	1103	+	ttttatgtaatta	7.4
si:ch211-210c8.6	MA0043.3_HLF	134	147	+	atattatgtaagaa	7.29
	MA0843.1_TEF	135	146	+	tattatgtaaga	6.12
	MA0843.1_TEF	135	146	-	tattatgtaaga	7.7
	MA0025.2_NFIL3	135	147	+	tattatgtaagaa	7.45
	MA0639.1_DBP	135	146	+	tattatgtaaga	7.66
	MA0639.1_DBP	135	146	-	tattatgtaaga	7.44
	MA0025.2_NFIL3	631	643	-	atattgcataata	9.1
	MA0043.3_HLF	631	644	-	atattgcataataa	8.68
	MA0819.2_CLOCK	783	792	+	aaacacatgc	8.06
si:dkey-82o10.4	MA0025.2_NFIL3	252	264	-	ctcttacataaaa	6.59
	MA0043.3_HLF	1008	1021	-	ggattgcgcaactt	6.56
	MA0025.2_NFIL3	1008	1020	-	ggattgcgcaact	6.36
	MA0043.3_HLF	1008	1021	+	ggattgcgcaactt	7.15
	MA0639.1_DBP	1009	1020	+	gattgcgcaact	6.46
	MA0639.1_DBP	1009	1020	-	gattgcgcaact	6.47
sirt4	MA0819.2_CLOCK	418	427	+	gaacacatgg	7.93
	MA0025.2_NFIL3	610	622	+	agttctgcaatca	6.3
	MA0043.3_HLF	889	902	+	ggcatatgcaatac	6.57
	MA0025.2_NFIL3	890	902	+	gcatatgcaatac	7.27
	MA0025.2_NFIL3	920	932	-	tcattgcatagtt	6.45
slc48a1a	MA0025.2_NFIL3	1021	1033	-	gcattacataatc	9.28
	MA0843.1_TEF	1022	1033	+	cattacataatc	9.65
	MA0639.1_DBP	1022	1033	-	cattacataatc	8.61
	MA0639.1_DBP	1022	1033	+	cattacataatc	8.63
	MA0843.1_TEF	1022	1033	-	cattacataatc	7.17
soul5	MA0043.3_HLF	682	695	-	atcttacacaacac	6.25
	MA0843.1_TEF	683	694	+	tcttacacaaca	6.09
	MA0639.1_DBP	683	694	-	tcttacacaaca	6.24
	MA0639.1_DBP	683	694	+	tcttacacaaca	6.28
	MA0025.2_NFIL3	1885	1897	-	agatttcataaca	7.49
	MA0819.2_CLOCK	1929	1938	+	gcacacatgc	7.07
	MA0819.2_CLOCK	1939	1948	-	acacgtttcc	6.88
stim1b	MA0819.2_CLOCK	538	547	+	aaacacatgg	7.98
	MA0819.2_CLOCK	540	549	-	acacatggta	6.25
	MA0819.2_CLOCK	912	921	+	aaacacatgg	7.95
	MA0819.2_CLOCK	914	923	-	acacatggta	6.26
	MA0043.3_HLF	943	956	-	ttgttgcgtaaact	6.83
	MA0025.2_NFIL3	943	955	-	ttgttgcgtaaac	6.32
	MA0043.3_HLF	1317	1330	-	ttgttgcgtaaact	6.95
	MA0025.2_NFIL3	1317	1329	-	ttgttgcgtaaac	6.45
tbrg4	MA0043.3_HLF	880	893	-	atgttatataagca	6.06
	MA0843.1_TEF	881	892	-	tgttatataagc	6.32
	MA0639.1_DBP	881	892	+	tgttatataagc	6.97
	MA0639.1_DBP	881	892	-	tgttatataagc	7.18
tbxas1	MA0819.2_CLOCK	1018	1027	+	aaacacgggg	6.28
tfr1a	MA0043.3_HLF	56	69	-	tcattacataaaaa	6.05
	MA0025.2_NFIL3	56	68	-	tcattacataaaa	8.12
	MA0639.1_DBP	57	68	+	cattacataaaa	6.07
	MA0043.3_HLF	143	156	-	cggttgcataaaaa	9.3
	MA0025.2_NFIL3	143	155	-	cggttgcataaaa	8.43
	MA0819.2_CLOCK	294	303	+	ctgcatgtgc	7.23
	MA0819.2_CLOCK	721	730	+	ttccatgtgg	6.35
	MA0819.2_CLOCK	723	732	-	ccatgtgggc	7.69
	MA0043.3_HLF	865	878	+	tgattatataataa	6.49
	MA0043.3_HLF	865	878	-	tgattatataataa	6.39
	MA0025.2_NFIL3	865	877	-	tgattatataata	6.97
	MA0639.1_DBP	866	877	-	gattatataata	7.85
	MA0025.2_NFIL3	866	878	+	gattatataataa	6.85
	MA0843.1_TEF	866	877	+	gattatataata	7.63
	MA0639.1_DBP	866	877	+	gattatataata	8.28
	MA0843.1_TEF	866	877	-	gattatataata	7.74

Gene promoter	JASPAR enhancer	From bp	To bp	Strand	Sequence	Score
ttc19	MA0025.2_NFIL3	276	288	-	aggttgcatcgtt	6.56
	MA0639.1_DBP	394	405	+	tattatataagg	6.59
	MA0639.1_DBP	394	405	-	tattatataagg	6.46
	MA0043.3_HLF	1005	1018	-	ggcttgcgtcattg	7.78
	MA0025.2_NFIL3	1005	1017	-	ggcttgcgtcatt	7.46
	MA0639.1_DBP	1006	1017	-	gcttgcgtcatt	7.44
	MA0639.1_DBP	1006	1017	+	gcttgcgtcatt	6.04
	MA0043.3_HLF	1013	1026	-	tcattgcataatca	9.03
	MA0025.2_NFIL3	1013	1025	-	tcattgcataatc	10.1
	MA0639.1_DBP	1014	1025	-	cattgcataatc	6.96
	MA0639.1_DBP	1014	1025	+	cattgcataatc	6.9
	MA0843.1_TEF	1014	1025	+	cattgcataatc	7.07
zgc:110366	MA0819.2_CLOCK	257	266	-	gcatgtgtcg	7.89
	MA0043.3_HLF	953	966	-	gagttgcataactg	11.2
	MA0025.2_NFIL3	953	965	-	gagttgcataact	9.47
	MA0639.1_DBP	954	965	+	agttgcataact	6.44
	MA0639.1_DBP	954	965	-	agttgcataact	6.34

Table S1. D-box and E-box predictions of mitochondrial and heme genes based on MotifViz analysis.

ENSEMBL Gene ID	Gene name	log2FC	p.adj	Ont.	GO Terms	D-box	E-box
ENSDARG00000063297	abcb6a	2.54	5.35166E-96	BP, CC, MF	heme transport, mitochondrion, heme binding	yes	yes
ENSDARG00000104719	abcc1	1.42	1.29483E-84	BP	detoxification	no	no
ENSDARG00000058953	abcc4	1.39	1.6591E-126	BP	detoxification	no	no
ENSDARG00000062561	adck1	1.12	1.26971E-12	BP, CC	mitochondrial respiratory chain complex II assembly, mitochondrion	yes	yes
ENSDARG00000062272	afg3l2	1.07	4.40423E-70	BP, CC	mitochondrial protein processing, mitochondrion	no	no
ENSDARG00000069282	bbc3	1.25	4.8408E-05	BP, CC	mitochondrial respiratory chain complex II assembly, mitochondrion	yes	no
ENSDARG00000103659	bco1l	2.90	6.03587E-11	MF	oxidoreductase activity	yes	yes
ENSDARG00000027620	bco2l	1.49	4.07325E-11	MF	oxidoreductase activity	no	no
ENSDARG00000059857	blvra	2.71	3.2878E-108	BP, MF	regulation of mitochondrial mRNA stability, oxidoreductase activity	yes	yes
ENSDARG00000036587	cbr1	2.35	5.0606E-201	MF	oxidoreductase activity	yes	yes
ENSDARG00000040707	chchd4b	2.30	2.52096E-59	MF	oxidoreductase activity	yes	yes
ENSDARG00000098589	cyb5a	1.02	2.65619E-23	MF, BP	heme binding, oxidoreductase activity, detoxification	yes	no
ENSDARG00000013524	cyp2ae1	2.15	1.50516E-12	MF	heme binding, oxidoreductase activity	yes	yes
ENSDARG00000045257	decr2	1.12	5.18469E-10	MF	oxidoreductase activity	yes	yes
ENSDARG00000031299	dhrs11b	1.07	5.95584E-07	MF	oxidoreductase activity	yes	no
ENSDARG00000011770	dhrs12	2.04	1.2522E-127	MF	oxidoreductase activity	yes	yes
ENSDARG00000026322	dhrs13a.1	1.64	4.70039E-17	MF	oxidoreductase activity	yes	yes
ENSDARG00000041137	dhrs13a.3	1.58	7.72037E-52	CC, MF	mitochondrion, oxidoreductase activity	yes	yes
ENSDARG00000042112	dio1	1.81	2.10062E-06	MF	oxidoreductase activity	no	yes
ENSDARG00000102142	ECE2	1.66	4.37486E-18	BP	mitochondrial protein processing	no	no
ENSDARG00000005789	enpp1	1.33	1.30314E-82	BP	regulation of mitochondrial mRNA stability, cell redox homeostasis	yes	yes
ENSDARG00000042854	ephx1	1.29	7.14964E-45	BP	regulation of mitochondrial mRNA stability, detoxification	yes	no
ENSDARG00000029795	fam213b	3.49	0	MF	oxidoreductase activity, antioxidant activity	no	no
ENSDARG00000056128	fastkd1	1.06	2.10002E-23	BP, CC	mitochondrial RNA processing, regulation of mitochondrial mRNA stability, mitochondrion	yes	yes
ENSDARG00000003462	fech	3.75	2.2895E-116	CC, MF	mitochondrion, ferrochelatase activity	no	no
ENSDARG00000037057	gcdha	1.13	2.86559E-13	MF	oxidoreductase activity	yes	yes
ENSDARG00000042630	hebp2	5.39	0	MF	heme binding	yes	yes
ENSDARG00000105389	mmel1	3.70	1.41053E-10	BP	mitochondrial protein processing	yes	yes
ENSDARG00000062237	nfs1	1.20	1.2528E-104	CC	mitochondrion	yes	no
ENSDARG00000029766	nr1i2	1.11	6.26918E-05	BP	detoxification	yes	no
ENSDARG00000100462	paqr7a	2.64	5.87178E-14	BP	detoxification	no	no
ENSDARG00000017612	pnpo	1.23	3.39507E-06	MF	oxidoreductase activity	yes	no
ENSDARG00000059035	porb	1.33	2.8076E-120	MF	oxidoreductase activity	yes	no

ENSEMBL Gene ID	Gene name	log2FC	p.adj	Ont.	GO Terms	D-box	E-box
ENSDARG00000058734	prdx1	1.11	1.54899E-82	BP, MF	oxidoreductase activity, detoxification, cell redox homeostasis	yes	no
ENSDARG00000073741	RAP1GDS1	1.07	0.000283563	CC	mitochondrion	yes	no
ENSDARG00000018600	retsat	1.36	2.12895E-56	MF	oxidoreductase activity	yes	yes
ENSDARG00000103313	rhot1b	1.13	8.99253E-08	BP, CC	mitochondrial respiratory chain complex II assembly, mitochondrion	yes	no
ENSDARG00000012453	rnls	1.13	6.07425E-17	MF	oxidoreductase activity	yes	yes
ENSDARG00000033662	scd	1.17	1.60705E-28	BP, MF	oxidoreductase activity, detoxification	yes	yes
ENSDARG00000012194	scp2a	1.37	9.34584E-59	CC	mitochondrion	no	no
ENSDARG00000016721	sdha	1.30	3.3437E-169	MF	oxidoreductase activity	yes	no
ENSDARG00000092478	sdhaf1	1.80	1.28005E-29	BP, CC	mitochondrial respiratory chain complex II assembly, mitochondrion	no	yes
ENSDARG00000062971	sdhaf2	1.25	2.71765E-11	CC	mitochondrion	yes	yes
ENSDARG00000036092	sdhaf3	1.02	1.01181E-11	BP, CC	mitochondrial respiratory chain complex II assembly, mitochondrion	yes	yes
ENSDARG00000075768	sdhb	1.10	7.00232E-34	MF	oxidoreductase activity	no	no
ENSDARG00000017811	si:ch211-210c8.6	1.76	2.53745E-70	MF	oxidoreductase activity	yes	yes
ENSDARG00000097489	si:ch73-390p7.2	1.60	2.59361E-24	MF	oxidoreductase activity	no	no
ENSDARG00000045598	si:dkey-180p18.9	1.07	3.81433E-14	MF	oxidoreductase activity	no	no
ENSDARG00000101526	si:dkey-82o10.4	1.06	3.80672E-09	CC	mitochondrion	yes	no
ENSDARG00000010415	sirt4	1.96	8.41448E-74	CC	mitochondrion	yes	yes
ENSDARG00000000241	slc40a1	1.28	0.000797265	BP	heme transport	no	no
ENSDARG00000026907	slc48a1a	1.45	3.14845E-13	BP	heme transport	yes	no
ENSDARG00000056252	sort1b	1.37	2.76844E-05	BP	mitochondrial respiratory chain complex II assembly, detoxification	no	no
ENSDARG00000075015	soul5	6.21	0	MF	heme binding	yes	yes
ENSDARG00000061560	stim1b	1.17	3.22313E-06	BP	heme transport	yes	yes
ENSDARG00000074807	tbrg4	1.01	1.21437E-35	BP, CC	mitochondrial RNA processing, regulation of mitochondrial mRNA stability, mitochondrion	yes	no
ENSDARG00000002249	tbxas1	1.27	1.77423E-10	MF	heme binding	no	yes
ENSDARG00000101322	tfr1a	1.47	8.05451E-15	BP	heme transport	yes	yes
ENSDARG00000026655	tspo	2.82	0	CC	mitochondrion	no	no
ENSDARG00000074435	ttc19	1.25	8.08573E-30	BP, CC	mitochondrial respiratory chain complex II assembly, mitochondrion	yes	no
ENSDARG00000039203	zgc:110130/MFF	1.03	2.09205E-09	BP, CC	mitochondrial respiratory chain complex II assembly, mitochondrion	yes	no
ENSDARG00000004167	zgc:110366	1.27	9.2136E-77	MF	oxidoreductase activity	yes	yes
					total	44	30
					total %	69.8	47.6

Table S2. Mitochondria and heme-related genes extracted from the Gene Ontology analysis for zebrafish cells exposed to 6 hours of blue light vs. nonexposed controls.

Figure	Analysis	Cell	Gene	Comparison	Statistic	p-value	Sig.	N
PAC2 and EPA blue light exposure	One-way ANOVA	PAC2	hebp2		68.67	4.7322E-06	***	3
			per2		30.13	0.000104057	***	
			abcb6a		64.94	5.86187E-06	***	
			soul5		6.62	0.014683685	*	
	Tukey HSD multiple comparisons		hebp2	DD vs. 1h		p > 0.05	n.s.	
			hebp2	DD vs. 3h		0.005130977	**	
			hebp2	DD vs. 6h		7.61672E-06	***	
			per2	DD vs. 1h		p > 0.05	n.s.	
			per2	DD vs. 3h		0.001077184	**	
			per2	DD vs. 6h		0.000350244	***	
			abcb6a	DD vs. 1h		p > 0.05	n.s.	
			abcb6a	DD vs. 3h		0.000573092	***	
			abcb6a	DD vs. 6h		8.8776E-06	***	
			soul5	DD vs. 1-3h		p > 0.05	n.s.	
			soul5	DD vs. 6h		0.019183159	*	
	One-way ANOVA	EPA	hebp2		0.83	p > 0.05	n.s.	3
			per2		26.24	0.000171636	***	
			abcb6a		13.51	0.001693523	**	
	Tukey HSD multiple comparisons		hebp2	DD vs. 1-6h		p > 0.05	n.s.	
			per2	DD vs. 1-3h		p > 0.05	n.s.	
			per2	DD vs. 6h		0.00011801	***	
			abcb6a	DD vs. 1-3h		p > 0.05	n.s.	
			abcb6a	DD vs. 6h		0.002573623	**	
zebrafish larvae blue light exposure	one-way ANOVA		hebp2		5.36	0.025727712	*	3
			per2		59.86	8.00394E-06	***	
			abcb6a		10.99	0.003288024	**	
			soul5		10.44	0.003853493	**	
	Tukey HSD multiple comparisons		hebp2	DD vs. 1-3h		p > 0.05	n.s.	
			hebp2	DD vs. 6h		0.044831457	*	
			per2	DD vs. 1h		p > 0.05	n.s.	
			per2	DD vs. 3h		8.24952E-06	***	
			per2	DD vs. 6h		0.001195335	**	
			abcb6a	DD vs. 1h		p > 0.05	n.s.	
			abcb6a	DD vs. 3h		0.009121072	**	
			abcb6a	DD vs. 6h		0.013973391	*	
			soul5	DD vs. 1-3h		p > 0.05	n.s.	
			soul5	DD vs. 6h		0.006136988	**	

Table S3. ANOVA and Tukey HSD comparisons analyses for exposure to blue light of zebrafish PAC2 and cavefish EPA cells, and zebrafish larvae.

Figure	Analysis	Cell	Gene	Comparison	Statistic	p-value	Sig.	N
PAC2 UV-C exposure	Two-way ANOVA		hebp2	timepoint	14.97	0.000549328	***	3
				condition	27.35	0.000211241	***	
				timepoint*condition	7.43	0.007940363	**	
			6-4phr	timepoint	21.27	1.81629E-05	***	
				condition	31.11	2.7051E-05	***	
				timepoint*condition	14.95	0.000149653	***	
			abcb6a	timepoint	29.96	2.1562E-05	***	
				condition	16.26	0.001661983	**	
				timepoint*condition	5.83	0.017060303	*	
			soul5	timepoint	7.71	0.003807918	**	
				condition	2.32	p > 0.05	n.s.	
				timepoint*condition	2.69	p > 0.05	n.s.	
	Tukey HSD multiple comparisons		hebp2	DD vs. 18h UV		0.011550851	*	
			hebp2	DD vs. 36h UV		0.000333425	***	
			hebp2	18h DD vs. 18h UV		0.025528518	*	
			hebp2	36h DD vs. 36h UV		0.002001102	**	
			6-4 phr	DD vs. 18h UV		p > 0.05	n.s.	
			6-4 phr	DD vs. 36h UV		1.77807E-06	***	
			6-4 phr	18h DD vs. 18h UV		p > 0.05	n.s.	
			6-4 phr	36h DD vs. 36h UV		7.81012E-06	***	
			abcb6a	DD vs. 18h UV		0.040080778	*	
			abcb6a	DD vs. 36h UV		5.09588E-05	***	
			abcb6a	18h DD vs. 18h UV		p > 0.05	n.s.	
			abcb6a	36h DD vs. 36h UV		0.004339761	**	
			soul5	DD vs. 18h UV		p > 0.05	n.s.	
			soul5	DD vs. 36h UV		0.006689863	**	
			soul5	18h DD vs. 18h UV		p > 0.05	n.s.	
			soul5	36h DD vs. 36h UV		p > 0.05	n.s.	
zebrafish larvae UV-C exposure	Two-way ANOVA		hebp2	timepoint	5.20	0.023575649	*	3
				condition	0.39	p > 0.05	n.s.	
				timepoint*condition	1.41	p > 0.05	n.s.	
			6-4 phr	timepoint	0.14	p > 0.05	n.s.	
				condition	0.06	p > 0.05	n.s.	
				timepoint*condition	1.45	p > 0.05	n.s.	
			abcb6a	timepoint	4.52	0.034351847	*	
				condition	0.00	p > 0.05	n.s.	
				timepoint*condition	0.05	p > 0.05	n.s.	
			soul5	timepoint	5.98	0.015769601	*	
				condition	1.79	p > 0.05	n.s.	
				timepoint*condition	1.67	p > 0.05	n.s.	
	Tukey HSD multiple comparisons		hebp2	DD vs. 18h UV		p > 0.05	n.s.	
			hebp2	DD vs. 36h UV		p > 0.05	n.s.	
			hebp2	18h DD vs. 18h UV		p > 0.05	n.s.	
			hebp2	36h DD vs. 36h UV		p > 0.05	n.s.	
			6-4 phr	DD vs. 18h UV		p > 0.05	n.s.	
			6-4 phr	DD vs. 36h UV		p > 0.05	n.s.	
			6-4 phr	18h DD vs. 18h UV		p > 0.05	n.s.	
			6-4 phr	36h DD vs. 36h UV		p > 0.05	n.s.	
			abcb6a	DD vs. 18h UV		p > 0.05	n.s.	
			abcb6a	DD vs. 36h UV		p > 0.05	n.s.	
			abcb6a	18h DD vs. 18h UV		p > 0.05	n.s.	
			abcb6a	36h DD vs. 36h UV		p > 0.05	n.s.	
			soul5	DD vs. 18h UV		p > 0.05	n.s.	
			soul5	DD vs. 36h UV		0.036058717	*	
			soul5	18h DD vs. 18h UV		p > 0.05	n.s.	
			soul5	36h DD vs. 36h UV		p > 0.05	n.s.	

Table S4. ANOVA and Tukey HSD comparisons analyses for exposure to UV-C of zebrafish PAC2 cells and zebrafish larvae.

Figure	Analysis	Cell	Gene	Comparison	Statistic	p-value	Sig.	N
mRNA stability blue light exposure	One-way ANOVA	PAC2	hebp2	DD vs. BL	0.02	p > 0.05	n.s.	3
		PAC2	per2	DD vs. BL	0.16	p > 0.05	n.s.	
		PAC2	abcb6a	DD vs. BL	0.21	p > 0.05	n.s.	
		PAC2	soul5	DD vs. BL	0.74	p > 0.05	n.s.	
		PAC2	c-myc	DD vs. BL	0.00	p > 0.05	n.s.	
mRNA stability UV-C exposure	One-way ANOVA	PAC2	hebp2	DD vs. UV	0.05	p > 0.05	n.s.	3
		PAC2	6-4 phr	DD vs. UV	0.07	p > 0.05	n.s.	
		PAC2	abcb6a	DD vs. UV	1.58	p > 0.05	n.s.	
		PAC2	soul5	DD vs. UV	0.00	p > 0.05	n.s.	
		PAC2	c-myc	DD vs. UV	1.52	p > 0.05	n.s.	
metabolic activity assay (MTT)	One-way ANOVA	PAC2			8.16	0.000450062	***	5
	Tukey HSD multiple comparisons	PAC2		DD vs. 6h - 18h		p > 0.05	n.s.	
		PAC2		DD vs. 24h		0.004038357	**	
metabolic activity assay (MTT)	One-way ANOVA	EPA			3.03	0.041903281	*	5
	Tukey HSD multiple comparisons	EPA		DD vs. 6h - 12h,24h		p > 0.05	n.s.	
		EPA		DD vs. 18h		0.0246235	*	

Table S5. ANOVA and Tukey HSD comparisons analyses for mRNA stability assays of zebrafish PAC2 cells following exposure to blue light and UV-C, and MTT assay.

Figure	Analysis	Cell/factor	Comparison	Statistic	adj p-val	sig.	N
in vitro assay	t-test with	PAC2 zf factors	ctrl vs. TEF-1	10.03435325	0.009786097	**	3
15xD-box cry1a-Luc	Bonferroni		ctrl vs. TEF-2	11.15466593	0.007941261	**	
	Correction		ctrl vs. DBP-1	14.5172336	0.00471145	**	
			ctrl vs. DBP-2	22.02636119	0.002054822	**	
			ctrl vs. HLF-1	8.605683733	0.013235486	*	
			ctrl vs. HLF-2	11.35650744	0.007664695	**	
		PAC2 cf factors	ctrl vs. all		p > 0.05	n.s.	3
		PAC2	TEF-1 zf vs. cf	4.402446117	0.011668977	*	3
			TEF-2 zf vs. cf	8.022449178	0.003182011	**	
			DBP-1 zf vs. cf	1.769781814	p > 0.05	n.s.	
			DBP-2 zf vs. cf	4.404742208	0.03175854	*	
			HLF-1 zf vs. cf	2.839573089	0.048906654	*	
			HLF-2 zf vs. cf	6.340535798	0.003214013	**	
in vitro assay	t-test with	EPA zf factors	ctrl vs. TEF-1	4.966800842	0.038227224	*	3
15xD-box cry1a-Luc	Bonferroni		ctrl vs. TEF-2	11.53230152	0.00743538	**	
	Correction		ctrl vs. DBP-1	5.50328832	0.031468124	*	
			ctrl vs. DBP-2	3.110419518	p > 0.05	n.s.	
			ctrl vs. HLF-1	4.80035652	0.04076139	*	
			ctrl vs. HLF-2	12.32587579	0.006517818	**	
		EPA cf factors	ctrl vs. TEF-1	5.973488805	0.026899254	*	3
			ctrl vs. TEF-2	6.97669065	0.019932557	*	
			ctrl vs. HLF-1	4.961247253	0.038307997	*	
			ctrl vs. HLF-2	4.370352945	0.048573071	*	
			ctrl vs. DBP-1, DBP-2		p > 0.05	n.s.	
		EPA	TEF-2 zf vs. cf	8.74698254	0.006747813	**	3
			HLF-2 zf vs. cf	7.111339744	0.002624952	**	
			TEF-1, DBP-1, DBP-2, HLF-1 zf vs. cf		p > 0.05	n.s.	
in vitro assay	t-test with	PAC2 zf factors	ctrl vs. TEF-1	13.13023042	0.005750381	**	3
Hebp2-Luc	Bonferroni		ctrl vs. TEF-2	6.553491017	0.022500956	*	
	Correction		ctrl vs. DBP-1	41.58491898	0.000577766	***	
			ctrl vs. DBP-2	19.43494515	0.002637017	**	
			ctrl vs. HLF-1	47.07407884	0.000450965	***	
			ctrl vs. HLF-2	13.11617178	0.005762609	**	
		PAC2 cf factors	ctrl vs. TEF-1	25.27119558	0.001562176	**	3
			ctrl vs. TEF-2	218.3695781	2.09702E-05	***	
			ctrl vs. DBP-1	13.86762742	0.005159698	**	
			ctrl vs. HLF-1	4.361278087	0.04876086	*	
			ctrl vs. DBP-2, HLF-2		p > 0.05	n.s.	
		PAC2	TEF-1 zf vs. cf	6.110828302	0.018442362	*	3
			TEF-2 zf vs. cf	5.046055645	0.037094057	*	
			DBP-1 zf vs. cf	36.37198138	0.000311971	***	
			DBP-2 zf vs. cf	5.092144603	0.01662568	*	
			HLF-1 zf vs. cf	7.45062628	0.012346013	*	
			HLF-2 zf vs. cf	9.693647348	0.002112268	**	
in vitro assay	t-test with	EPA zf factors	ctrl vs. TEF-1	4.440218875	0.047162095	*	3
Hebp2-Luc	Bonferroni		ctrl vs. TEF-2	5.43369471	0.032240544	*	
	Correction		ctrl vs. DBP-2	5.256382153	0.034339694	*	
			ctrl vs. DBP-1, HLF-1, HLF-2		p > 0.05	n.s.	
		EPA cf factors	ctrl vs. all		p > 0.05	n.s.	3
		EPA	all, zf vs. cf		p > 0.05	n.s.	3
in vitro assay	t-test with		ctrl vs zfHLF-2	10.54666622	0.035483031	*	3
hebp2-Luc	Bonferroni		ctrl vs zcHLF-2	12.6611091	0.024721553	*	
HLF-2 hybrids	Correction		ctrl vs cfHLF-2 and czHLF-2		p > 0.05	n.s.	

Table S6. In vitro luciferase assays t-test analyses with Bonferroni corrections (adj p-val).